N d'ordre : 40857

ACADEMIE DE LILLE

UNIVERSITE LILLE 1

SCIENCES ET TECHNOLOGIES

THESE

présentée par

Monsieur Ammar ELQIDREA

pour obtenir le grade de

DOCTEUR

Spécialité : Molécules et Matière Condensée

Effect of irradiation on the monomer-liquid crystal systems

Effet du rayonnement sur des systèmes monomère-cristal liquide

Soutenue le 17 Juillet 2012 devant la commission d'examen

Laurent LECLERCQ	CR CNRS, Université Montpellier 1	Rapporteur
Jeroen BEECKMAN	Pr., Ghent University, Belgique	Rapporteur
Jihad-René ALBANI	MC, Université Lille 1	Président
Ulrich MASCHKE	DR CNRS, Université Lille 1	Directeur de thèse

ACKNOWLEDGEMENTS

I am deeply grateful to many people who supported me in this thesis. First, I would like to thank my supervisor, Dr. Ulrich Maschke for offering me the great challenge and support during the process of this research and development of this thesis.

I thank the management team of unit of materials and transformation UMET for the facilities and support which they gave me to successfully exploring this research project.
I extend my deepest thanks and appreciation to the staff of all laboratories and centers at Lille 1 university who offered me place to conduct part of the experiments during this study.

I would like to express my deepest thanks for Dr. A. Dimian for his special support and providing me the challenge and confidence during my master thesis at the University of Amsterdam. I am very grateful Prof. P. Hamersma for guiding me and his encouragements financially and academically to obtain my Master degree.

I would like to thank my colleagues Y. Derouiche and C. Beyens for having several useful discussions, and the polymer system engineering laboratory staff A. Malfait and F. Cazaux for the opportunities to conduct part of the experiments together.

In particular, I am grateful my family in the Netherlands, R. Feddema and M. Boulsma for providing me that wonderful and exceptional support during my graduates studies, they were always the most beautiful people in my life.

I express my deepest thanks and appreciation to my wife, whose unwavering support and sacrifices was essential for completion my studies. My children gave me the motivation to progress and carryout my objectives. I finally would like to thank my parents who always supported and encouraging me through all of my life's endeavors.

I wish to deeply thank the reviewers of this thesis for reviewing the manuscript and for their valuable comments and recommendations.

TABLE OF CONTENTS

LIST OF FIGURES

LIST OF TABLES

GENERAL INTRODUCTION

The composites of polymer and liquid crystal are known as polymer dispersed liquid crystal (PDLC) [1]. The interest of PDLC systems came from its wide applications in the technological devices ranging from displays, sensors, light valves and privacy windows. PDLC composites are composed of liquid crystal molecules dispersed in a polymer matrix [2,3,4]. A liquid crystal is a phase of material between solid crystal and isotropic liquid phase with certain degree of orientation between its molecules. Applications of liquid crystals are related to the electro-optical characteristics of these materials by applying external magnetic or electrical field. The response of liquid crystal in turn is related to the thermophysical parameters and phase properties at a given temperature and compositions [5]. The liquid crystal phase in the polymer matrix applies orientation to minimize the surface free energy. Growing attention has been given to control the phase behavior of polymer/liquid crystal films to achieve the required PDLC system for potential electronic devices. The form of composites known as crystal liquid gels formed by crosslinking or gelling agent network, it possess interesting properties to be suitable candidate for several applications such as displays, sensors, mechanical and electronic activators. Final properties and morphology of liquid crystal materials are strongly dependent on their preparation conditions.

The use of polymeric materials is common as substrates in LC devices due to ease of processing, surface control and mechanical stability, in addition to its physical and chemical properties compared to low molecular weight compounds. Moreover, dispersion of liquid crystal in polymer matrix results in drop in the phase transition temperature of the liquid crystal, while presence of the liquid crystal in the polymer matrix may affect glass transition temperature, which attracts the researchers to describe PDLC composites behavior at different polymer/liquid crystal concentrations.

Radiation curing has found increasing interests in the industrial applications in preparing polymer composites due to ease of control of the reaction rate, morphology and hence final properties of the polymer matrix.

The main objective of this thesis is to study the effect of preparation condition using ultraviolet (UV) and electron beam (EB) curing on the phase behavior of liquid crystal and the chemical structure of polymer matrix. We focus on understanding effect of irradiation dose, reaction rate and the liquid crystal concentration on architecture and molecular weight

distribution in the polymer matrix. This knowledge can be exploited to fabricate new highly selective electro-optical devices based on polymer/LC composites.

Radiation curing polymerization based on exposing the reactive mixture into radiation with sufficient energy to ionize atoms or molecules in the material through which and usually result in formation of radical species that initiate the reaction. Electromagnetic radiation can vary from long wavelength such as radio wave to short wavelength below 10 nm such as x-rays, γ-rays and electron beams. The radiation source can generate radioactive nuclides or particle accelerators. In this thesis, only UV and electron beam radiation will be used to study the polymerization process.

Motivation and organization of the Thesis

The motivation of this work is to investigate the effect of UV and electron beam EB irradiation on the structure and properties of the polymer composites prepared by free radical polymerization. The research interests in this field were mainly focused on the solution and emulsion polymerization of polymer composites using UV curing. Whereas in this work, we focus on presenting deeper understanding of the polymer liquid crystal interactions with detailed analysis of kinetics and mechanism of the polymerization reaction. On the other hand, physical and chemical properties of produced polymer matrix will be investigated and compared by both UV and EB curing. Main objective will be to study polymer matrix properties at variety of preparation conditions in microscopic level, by which optimization of process parameters can be achieved based on the required properties of the final product.

In the first chapter, a literature survey will be conducted; free radical photopolymerization models will be discussed, in addition to the molecular weight distribution of the polymer matrix under different reaction conditions. Applications of UV and EB curing will be presented, and effect of curing method on the polymer composites will be presented. Characteristics of liquid crystals and different preparation methods will be described. Then, we will present a models that describes the phenomena of phase transition and phase separation.

The second chapter will focus on the description and preparation of the polymer composite films. We will present detail description for the materials which have been used in this study (liquid crystal polymer, monomer, solvent and photoinitiator). At the end of this chapter, we describe in details characterization and analysis techniques used in this thesis.

The third chapter will be dedicated to the reaction kinetics of acrylate polymerization using IR spectroscopy, by elaboration effect of liquid crystal and photoinitiator concentrations on the reaction rate for both UV and EB curing. Change in the reaction mechanism of both UV and EB curing techniques will be studied under variety curing conditions and mixture compositions.

The main objective of the fourth chapter will be devoted to thermophysical analysis of polymer composites and establishing the phase separation using the polarized optical microscopy (POM) and differential scanning calorimetry (DSC). Thereafter, it will characterize composites morphology as a function of temperature. In parallel, we will analyze effects of morphology on the different phase transitions of liquid crystal. Furthermore, confinement dynamic and stability of liquid crystal in the polymer matrix will be studied during polymerization.

The purpose of the fifth chapter is to study the degree of branching and chain transfer reactions based on different preparation conditions. For this purpose, the composites will be examined by investigating branching in photopolymerized systems based on the nature of branching in radical photopolymerization of 2-ethylhexyl acrylate (2EHA) as a key factor that determine the final properties of polymer composites. The nuclear magnetic resonance NMR (^{1}H and ^{13}C NMR) analysis will be used to deeply describe the branching level and the presence of intermolecular or intramolecular chain transfer during radical polymerization. The behavior of chain transfer to liquid crystal and polymer will be examined under certain preparation conditions.

The sixth chapter will focus on analyzing molecular weight distribution of polymer composites using gel permeation chromatography (GPC). This technique will be appropriate to reveal the effect of liquid crystal, photoinitiator and irradiation dose on molecular weight distribution of polymer chains. Dynamic mechanical analysis (DMA) of the composites will be also investigated, by comparing the variation of these properties based on different preparation conditions. For this purpose, the composites will be examined by dynamic rheometer to determine the viscosity, storage modulus and loss modulus.

1 INTRODUCTION TO PHOTOPOLYMERIZATION AND POLYMER DISPERSED LIQUID CRYSTAL COMPOSITES

1.1 Introduction to polymer

Polymers are materials of high molecular mass formed from repetition of low relative molecular mass molecules bonded together to form large chains. The repeating units form the polymer chain is called monomer. A polymer with one type of monomer is known as homopolymer, while copolymers are formed from more than one type of repeating units. Exact structure and composition of network will determine its final properties.
Polymers are used in wide variety of materials and application ranging far exceeding any other known materials. Natural polymers are found in the form of proteins, starch and natural rubber. Synthetic polymers have been developed in the 18^{th} century [6,7]. Due to its wide industrial applications, polymer are highly growing field of materials. Applications include adhesives coatings, packaging materials, fibers, additives and structural plastics.

Polymers are divided into two main groups called thermoplastics and thermosets based on its internal structure and orientation. Thermosets have long chains with linear or branched architecture and cannot be reshaped. Thermoplastics are characterized with its intermolecular covalent bonds and interact with other polymer molecules by the weak Van der Waal's interactions, a property that makes thermosets easy to melt and to be shaped by temperature.

Polymers may also be classified based on the polymer network structure, which can be linear or nonlinear chains. Nonlinear polymers are classified into branched polymers with side chains attached to the backbone. The second type is the network polymers that joint all polymer chain together in the form of crosslinking.

An important property of polymer is the glass transition temperature T_g, at which the amorphous portion of polymer soften. Below the polymer glass transition temperature, only vibrational motions are possible, and the polymer is hard and glassy.

Describing the interrelationships among polymer structure, morphology, physical and mechanical behavior requires understanding molecular weight, molecular weight distribution and organization of the atoms in the polymer chain.

1.2 Photopolymerization

Polymerization reactions can be defined as the transformation of a liquid mixture into high molecular weight chain called polymer, the product shows more or less viscous solid material whose degree of crosslinking depends mainly on the number of functional group of the initial monomer. The nature of these active species is directly dependent on the functionality of the monomer. The creation of these active species occurs by direct excitation of the monomer in EB curing and by dissociation of the photoinitiator in UV curing [8,9,10,11].

The majority of polymers for commercial applications are prepared by photopolymerization technology [12]. Photoinitiated polymerization can result in a number of different reaction mechanisms including free radical, cationic, and living polymerizations. Detailed and comprehensive reviews have been published in the literature present the photopolymerization processes and techniques [13,14]. Photoinitiated polymerizations have found growing interests in the industrial applications due to their rapid polymerization rates, spatial and temporal control, chemical versatility and solvent-free processing [15,16,17,18].

Free radical polymerizations still the major industrial technique to produce acrylic resins, adhesives and coatings. According to the industrial requirements, there is increasing interest to produce polymers which are free of solvent with high degree of control. The free radical photopolymerization has been the method of choice to prepare wide range of polymer composites with highly selective properties at low reaction temperatures. Furthermore, photopolymerization supports controlling the polymerization rate and molecular structure of polymer that strongly affect properties of final polymer network. Detailed investigations of polymer structure, polymerization conditions and type of monomer molecules are essential to understand reaction mechanism and determine the kinetic parameters.

1.2.1 Advantages of the photopolymerization

Photopolymerization offers several interesting advantages over the conventional processes among which are summarized below:

- Polymerization is almost instantaneous; transformation of molecules into polymer material is carried out in a few seconds exposure time of irradiation, therefore, low energy consumption is expected;

- Selective crosslinking occurs only in well defined area which is exposed to light radiation, this allows for stereoscopic images with high resolution;
- The reaction can be initiated and terminated at a specific time by controlling the irradiation time;
- The intensity of the irradiation source can be controlled in a wide range, which allows high control of the initiation rate;
- Change the radiation intensity and / or the photoinitiator concentration offers ease of control for the depth of irradiation penetration into the film and thus the thickness of the polymer layer formed, which can vary from a few micrometers to several millimeters;
- Photoinitiated polymerizations are usually performed at room temperature, without solvent, which reduces emission of undesired pollutants;

Limitations of UV curing polymerization include low efficiency to polymerize dense or opaque material. While in EB curing, lack of selectivity, cost of equipment and possibility of polymer degradation due to high radiation energy are the main challenges.

1.2.2 Applications of photopolymerization

Photopolymerization covers wide range of industrial and technological applications with increasing potential for highly functional materials, among these applications:

- Coatings, paints and varnishes, as highly effective protective for materials in the field of plastics, textiles and metals[19,20];
- Graphics arts technology in the manufacturing of printing plates and printing inks products;
- Electronic devices and microelectronics in the creation of printed circuits sensors and processors [21];
- Medical applications include adhesives and curing of dental treatment [22];
- Nanotechnology in the preparation of PDLC's for high performance LCD screens that will be discussed in details in this study [23,24].

There are different types of photoinduced polymerization include radical, anionic and cationic polymerization, in this work we will focus on free radical photopolymerization using UV and EB irradiation.

1.2.3 Formation of polymer networks by photopolymerization

Polymerization is the formation of macromolecules in chains of repeating units usually referred to as monomers by a chemical reaction. Polymerization reactions can be classified based on the reaction mechanism into step and chain polymerization. In step polymerization the reaction occurs by successive reactions between the functional groups of pair of monomer [25]. In chain polymerization, addition of repeat units occurs at the active site of the end of a growing chain such as free radical, anionic and cationic polymerization.

Essential step in photopolymerization is the formation of sufficient radical species to initiate the photochemical reaction. Radical species can be formed either by addition of certain amount of photoinitiator to the monomer mixture, by exposure to UV irradiation the photoinitiator molecules absorb the UV light and produce radical species with high yield and the chain reaction starts. On the other hand, radical species can be formed by exposing monomer molecules to high irradiation dose enough for the monomer molecules to form the radical species; the electron beam EB is an effective technique to initiate the radical polymerization. Once initiated, the chain reaction develops as in the conventional polymerization. The main focus of these polymerization categories will be given to free radical polymerization, which is the main objective in this study.

The photocurable mixture in general must include a photoinitiator that under the influence of light source dissociate to form radical reactive and a monomer having one or more reactive functional groups.

Mixture composition is based on the industrial application to arrive at the desired matrix configuration. Various additives (stabilizers, dyes, pigments ...) may be added to improve the final properties of the polymeric material.

1.3 Photoinitiators

There are many photoinitiators which have been developed to effectively initiate photopolymerization process to achieve highest curing rates. Selection of the photoinitiator has to be based on the following characteristics:

- Good absorption in the domain of the light source;
- Short excited state lifetime to avoid its deactivation by oxygen or the monomer;
- High solubility in the reactive mixture;
- Colorless, odorless and not toxic.

There are two main types of the photoinitiators which generate radical species on ions by photolysis: radical and cationic photoinitiators [26].

1.3.1 Radical photoinitiators

Free radical photoinitiators are species capable of initiating a radical polymerization and can be classified into two main categories: the first includes photoinitiators that generates radical species by homolytic cleavage of σ bond in a compound containing a carbonyl group more often aromatic groups. The most used photoinitiators in this type are benzoin derivatives, the acetophenone, benzyl ketals, the hydroxyalkyl phenone, acylphosphine oxides and α-substituted aromatic amino ketones. The second type is the photoinitiators that generate radical initiators by a bimolecular process, hydrogen transfer or electron and proton transfer.

1.3.2 Cationic photoinitiators

Cationic photoinitiators can be classified into two categories: onium salts such as diaryliodonium salts and triarylsulfonium and organometallic salts (mainly salts of ferrocenium). In presence of hydrogen donors and UV radiation, these photoinitiators form a Bronsted acid which is capable of initiating cationic polymerization of monomers which cannot be polymerized by radical such as vinyl ethers or heterocyclic monomers (epoxides, lactones, cyclic ethers, epoxysilicones).

1.4 Free radical polymerization

Polymers may be synthesized by two major kinetic schemes, chain and stepwise polymerization. The most important chain polymerization methods is called free radical polymerization, in which reaction proceeds by growth of polymer chain at the free radical active sites at the chain. Methyl, Ethyl and 2-ethylhexyl acrylate are produced on industrial scale, other esters as tert-butyl, isobutyl, or dodecyl acrylates are also produced on smaller scales. Homopolymers of acrylates are usually too soft and tacky with extremely low glass transition temperature. Free radical polymerization has three major kinetic steps are initiation, propagation, and termination. Radical sources such as peroxides or azo-compounds are used as photoinitiators [21]. In addition to the other two reactions are known as chain transfer reactions and inhibition that may occur during the polymerization process.

Polymerization starts by absorption of light by the photoinitiators, the reaction proceeds by a typical chain-growth mechanism [27]. In free radical system, polymerization terminates with

the elimination of UV light. To describe the kinetic of free radical photopolymerization, it is required to evaluate the values of propagation rate constant k_p and termination rate constant k_t to present the kinetic model of the process. Several studies have been done to determine the kinetic parameters of free radical polymerization and present a classical polymerization model.

1.4.1 Steady state kinetics

Based on steady state assumption for monomer and initiator radicals, initiation, propagation and termination are considered in the kinetic study. Formation of a single chemical bond between two monomers is formed by opening the double bond between the two carbons of acrylate group. Free radical polymerization rate can be derived based on steady state assumption [28], the reaction mechanism and rate equation are presented by equations 1.1 and 1.2 for solution polymerization:

$$2fk_dI = k_t[P]^2 \tag{1.1}$$

$$R_p = \frac{k_p}{k_t^{0.5}}(2fk_d)^{0.5}[I]^{0.5}[M] \tag{1.2}$$

Polymerization rate is first order in monomer concentration while the reaction order of initiator is 0.5. This presents ideal polymerization rate law and can be used to obtain $k_p/k_t^{0.5}$ using simple techniques such as gravimetry and dilatometry.

The basic steps in free radical polymerization are summarized as follow:

Initiation	$I \xrightarrow{k_d} 2R$ $R + M \xrightarrow{k_i} P_1$	$R_i = 2fk_d[I]$
Propagation	$P_n + M \xrightarrow{k_p} P_{n+1}$	$R_p = k_p[P][M]$
Termination	$P_n + P_m \xrightarrow{k_t} Polymer$	$R_t = k_t[P]^2$

with R_p= propagation rate, R_i= initiation rate, R_t= termination rate, k_t= termination rate constant. k_p= propagation rate constant, k_d=initiator dissociation constant, f= fraction of

photoinitiator, [M] = monomer concentration, n = monomer units number and [P] = polymer concentration.

Propagation chain reactions result in decreasing the monomer concentration, which leads to slower growth of the chains. Furthermore, mobility of radicals and monomers is increasingly limited due to the gelation of the medium, which reduces their probability of forming new chain. On the other hand, the termination reactions may occur by reaction of the growing chain with another radical or by a transfer reaction. In this work the kinetic measurements will be determined based on steady state assumption conditions.

1.4.2 Non-steady state kinetics

In steady state kinetic, rate coefficients can be determined by experimental measurements of the rate of initiation and propagation. Individual rate coefficients can be determined based on non-steady state conditions. This involves polymerization of the system by altering the radiation to dark and light periods with known exposure time. Kinetic measurements in non-steady state can be performed by determining radical species concentrations at each cycle of light and dark period. Polymerization rate can be represented as a function of the time cycle in the system.

Polymerized systems are also subjected to oxygen inhibition. Oxygen molecule in the ground state has highly effective inhibitory properties, where it has a high affinity for free radicals and converts them into radical peroxides.

This drawback effect of oxygen on radical polymerization is also observed by its interactions with the radical species that gives rise to the radical species formed during polymerization in which growing chains can be transformed into peroxide radicals, which reduce the propagation reactions.

Presence of oxygen has a negative effect on the polymerization rate. Compared to a polymerization carried out under an inert atmosphere, presence of oxygen causes a decrease in polymerization rate and conversion rate. It can be observed at the beginning of the irradiation time. This inhibition effect of oxygen is being reflected in the polymerization by low degree of reticulation to the film surface which results in poor final properties of the polymer matrix. Negative effect of oxygen can be reduced by increasing the initiator concentration or intensity of radiation that overcomes the loss part of the growing chains [29].

1.5 Cationic polymerization

Cationic photopolymerization is usually applied for monomers with epoxy or vinyl ether functional group. Vinyl ethers and propenyl are considered the highly reactive monomer in cationic polymerization.

Monomers having epoxy or vinyl ether functions are typically used in cationic photopolymerization. Polymerization leads to crosslinked polymers with physical and chemical properties that mainly depend on the chemical structure and polymer chain length.

1.6 Formation of acrylate composites

Low temperature homopolymerization of acrylic esters was conducted in the early 60s to study the effect of the nature of ester group on the reaction rate [30,31].

Polymerization rate of acrylates is very high due to the high reactivity of acrylate functional group. Change from liquid to solid phase is almost instantaneous under intense irradiation. Whereas, in case of methacrylate monomers the chain reaction propagate slowly because of the low reactivity of the methacrylates compared to acrylates. Accordingly, vast majority of radiation curing systems currently used in the industrial applications is based on acrylate monomers.

Polymerization of triacrylates monomers have the disadvantage of formation highly crosslinked polymers, which make them unsuitable for several flexible industrial applications. In addition, formation of three-dimensional network result in reducing the molecular mobility of the reactive species as it trapped in the dense environment and causes termination the growth of polymer chains. Thus, photocured triacrylate polymer films contain a number of unreacted acrylates monomers. Presence of unreacted species in the final product leads to reducing the mechanical properties stability of crosslinked polymers for potential industrial applications. Diacrylates monomers are considered to offer the best requirements and are usually used as reactive diluents in the curing networks.

Different studies reveal that polymerization rate is characterized by monomer first order reaction rate law and a 0.5 exponent of photoinitiator concentration but sometimes slightly deviates from 0.5. Estimation of propagation rate constant k_p and termination rate constant k_t are critical parameters during the polymerization modeling and simulation. The reaction rate constants usually based on the conversion rate and molecular weight distribution data.

Selection of photopolymerized systems used in industrial applications is usually based on acrylate monomers. There are a wide range of functionalized acrylates whose network

structure is made up of various chemical structures, such as polyurethanes, polyesters or polyethers [32].

1.6.1 Crosslink Density

In free radical polymerization of multifunctional acrylates, presence of acrylate double bonds result in crosslinked polymer network. The degree of crosslinking is reflected in the chemical and physical properties of the polymer matrix. Highly crosslinked polymer is usually hard and chemical resistant while low crosslinked is flexible and soft. Crosslinked density can be defined as the weight per double bond. The weight per double bond can be estimated by dividing the average molecular weight of the formulation by the average functionality of the polymer.

1.6.2 Cure dose

Cure dose is the dose at which the desired polymer composite properties are obtained. The desired polymer properties vary based on the end use of the polymer composite. In most curing technology the double bond of acrylates is not totally consumed during the process, since formation of polymer network limit the mobility of radical species during polymerization. The term cure speed can be defined as the weight per double bond of the initial mixture, in other word, the more acrylate double bond in the molecules the higher the cure speed required achieving the highest conversion. The cure dose is largely affected by the oxygen inhibition of polymerization due to high reactivity of oxygen with the radical species to form epoxy radicals and finally reduce polymer properties. The cure dose is a major factor during polymerization of thick films, in which the dose has to penetrate the surface of formulation deeply into the material to initiate the reaction. In UV curing, the photoinitiator absorbs considerable amount of the UV dose. Effective curing process can be achieved at lower concentration of the photoinitiator. This can be controlled by the selection of the effective UV lamp based on the composition of the initial mixture.

1.7 Molecular weight distribution

of the molecular weight distribution analysis produced during photopolymerization of acrylic esters can be used to determine the reaction kinetics [33]. Chain transfer including chain transfer to monomer and possible intramolecular chain transfer has a considerable effect on the reaction rate measurements.

Molecular weight can be controlled by several techniques. Low polymer molecular weight can be achieved by increasing the concentration of photoinitiator relative to monomer. Another method to control the molecular weight of polymer using chain transfer agents in the reactive mixture. In addition, the molecular weight can be controlled by conducting the polymerization at high temperatures, which have drawback in terms of energy consumption and volatility of reactive molecules.

1.8 Chain transfer reactions

The term chain transfer in radical polymerization refers to termination of one growing chain and initiation of another [34]. Chain termination occurs when two radical species react to form one or two new molecules. On the other hand, chain transfer occurs when a radical reacts with a non-radical species on the C=C double bond of the propagating polymer chain to produce a new radical. The chain end radical usually attacks the weak bond and a monomer is then transferred to the chain end. Chain transfer leads to shorter chains in competition with the chain growth and termination reactions.

Chain transfer to polymer during free-radical polymerization can lead to formation of highly branched polymers with significant consequences on the properties. Polymer chain branching occurs in many important polymers such as polyethylene, polyacrylics and starch [35]. For the polyethylene, poly(vinyl acetate) and poly(alkyl acrylates) produced by radical polymerization, one may distinguish between short-chain branching (SCB) produced by intramolecular transfer to the polymer and long-chain branching (LCB) produced by intermolecular chain transfer to polymer [36,37]. Presence of intramolecular chain transfer has an effect on the melting point, glass-transition temperature and hardness as well as the degree of crystallinity of polymers. In contrast, intermolecular branching affects the rheological properties such as sedimentation behavior, viscosity and elasticity of polymer melt. Long chain branching may also directly affect the final application properties such as the adhesive nature of pressure-sensitive adhesives [38,39].

The main methods commonly discussed in the literature to determine the degree of branching are ^{13}C NMR spectroscopy, gel permeation chromatography (GPC) and IR spectroscopy [40]. The use of ^{13}C NMR spectroscopy for quantification branching level and the intermolecular chain transfer is well developed for some polymers, such as polyolefins. Whereas, NMR spectra of poly(alkylacrylates) are more complex and thus only the total degree of branching can be quantified [41] . In contrast, GPC and rheology are more sensitive to LCB [42]. Thus

in order to fully describe the molecular architecture, information from spectroscopic, chromatographic and rheological techniques must be combined [43].

1.8.1 Intermolecular Chain Transfer

Intermolecular chain transfer to polymer and random intramolecular transfer to polymer lead to the formation of long-chain branches (LCB) of various lengths. Furthermore, gel formation occurs due to the intermolecular chain transfer to polymer followed by termination by combination. Intermolecular chain transfer to polymer is related to the reaction kinetics, that increases with polymer concentration and hence with conversion rate.

1.8.2 Intramolecular chain transfer

Presence of intramolecular radical transfer, also termed backbiting, has been studied extensively in the polymerization of ethylene [44]. To account for high monomer and initiator orders of acrylate polymerizations, intramolecular chain transfer has received increasing attention due to the availability of characterization tools to describe the level of intramolecular chain transfer during polymerization. Intramolecular chain transfer proceeds mainly through backbiting leading to short-chain branches (5CB).

1.9 Photopolymerization curing techniques

The growing interests using photopolymerization curing in several industrial applications due to ease of control and high selectivity of monomers to achieve polymeric systems that have good physical and chemical properties. There are many radiation curing techniques to initiate the reactions based on the monomer mixture and the desired polymer composite. UV and EB curing are among the most interesting curing methods in producing high quality polymer resins. Efficiency of irradiation source is usually related to the absorption degree of the active substance and emission of the radiation source.

1.10 UV curing

UV curing has become a well established technology with large number of industrial applications, mainly in the fast drying of printing inks, curing of functional and protective coatings, the manufacture of adhesives and microelectronics. Rapid development of UV curing technology came from its distinct commercial, technical and environmental advantages [45]. In UV curing, a liquid monomer mixture is transformed into polymer by exposure to UV

light. UV equipment is a lamp curing unit on a fixed or moving speed conveyor with variable power sources to control the speed and the input energy. Conventional UV sources available on the market have an emission spectrum located in the near (300-400 nm) region in which monomers can slightly absorb. It is therefore necessary to incorporate a reactive material that can efficiently absorb this radiation and produce active species, a substance which is known as the photoinitiator.

The mixture consists of monomer and photoinitiators for initiation of the photopolymerization. The photoinitiator package plays a key role in the quality of the curing process. It determines the cure speed and the morphology of polymer.

The basic principle of photoinitiator includes two main steps, absorption of the incident photons associated with an electronic excitation of the initiator molecule and generation of initiating radicals from the excited states with a high yield. Common light source in UV curing is the mercury arc lamp. Consequently, most initiators are tuned to its spectrum. In contrast, most curing resins, e.g. acrylates, do not or only weakly absorb in this spectral domain.

Two main types of UV curing are based on free radical and cationic initiators. Many monomers and oligomers can be polymerized by free radical initiators, whereas limited numbers of monomers are used in cationic polymerization. Cationic systems are not subjected to oxygen inhibition as in case of free radical systems.

1.11 Electron beam curing

EB curing has advantages of high curing efficiency, no need to photoinitiator and effective curing of highly pigmented materials. Curing process initiated by the high speed accelerated electron beam bombarded onto the double bond of the monomer to create free radicals, which react with other double bonds and chain reaction is propagated to form the polymer network. As oxygen inhibits the polymerization reaction, the EB curing process is conducted under inert atmosphere using nitrogen.

1.11.1 Mechanism of EB polymerization

EB interaction with the monomer molecules produces excited states which undergo secondary reactions to produce free-radical intermediate species. Resulting chemical reactions are caused by the excited species and formation of reactive intermediates [46]. Excitation result in

electron transfer to higher energy orbital. Photons may be formed by the return of the excited electrons to the ground state. Positive ions are formed due to the ejection of the electrons from the atom. The ejected electrons may interact with other atoms until they lose the acceleration energy. Combination of the positive ions with the electrons may occur to once again to give a neutral atom. The radiation produces excited molecules and secondary reactions through the following mechanism:

$$A{:}B \xrightarrow{EB\ radiation} (A{:}B)^{*}\ (exited\ state)$$

$$(A{:}B)^{*} \longrightarrow (A\cdot B)^{\cdot+}\ (radical\ ion) + e^{-}\ (electron\ ejection)$$

$$(A\cdot B)^{\cdot+} \longrightarrow A^{+}\ (ion) + B^{\cdot}\ (free\ raical)$$

$$(A{:}B)^{*} + (C{:}D) \longrightarrow (A{:}B) + (C{:}D)^{*}\ (energy\ transfer)$$

$$(A\cdot B)^{+} + e^{-} \longrightarrow (A{:}B)^{*}\ (electron\ capture)$$

$$C{:}D + e^{-} \longrightarrow (C{:}D)^{-}\ (electron\ capture)$$

$$(A\cdot B)^{+} + (C{:}D)^{-} \longrightarrow (A{:}B)^{*} + (C{:}D)^{*}\ (charge\ neutralization)$$

$$(A{:}B)^{*} \longrightarrow A^{\cdot} + B^{\cdot}\ (molecular\ dissociation)$$

Highly accelerated electron may undergo deceleration due to its interaction with the electrons of the atoms and molecules of the material which lead to dissipation of kinetic energy. The distance travelled by the electrons in the material before losing energy based on the beam intensity and material thickness. Thus, a calibration and adjustment of the radiation source is required to achieve maximum ionization of the molecules in the material during the curing process.

Further exposure of produced material to EB radiation may result in change of polymer internal structure due to crosslinking and degradation reaction mechanisms. Crosslinking reaction mechanisms on polymer usually involve removal of hydrogen atoms to form chain radical intermediates. These radical intermediates can then combine to form a single macromolecule. This combination results in increase in average molecular weight of the starting polymer. Crosslinking reactions in the polymer can be schematically presented as follow:

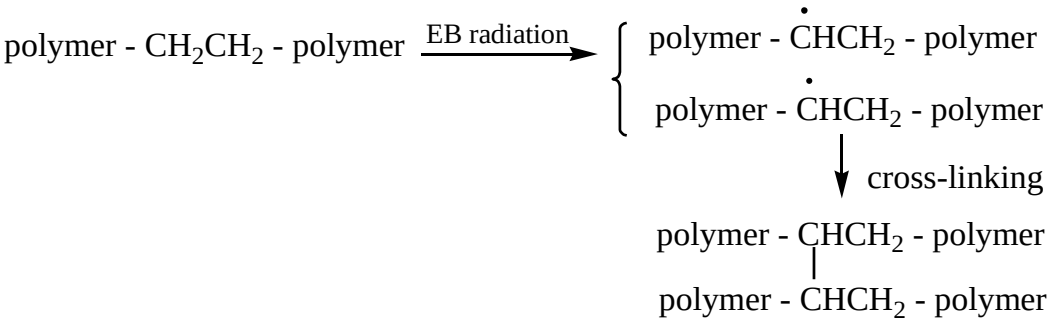

Continuous EB radiation on the polymer will result in larger macromolecules with huge molecular weights and different physical properties which are characterized by low solvent solubility and higher melting point from the original polymer. Rapid propagation reaction increases possibility of coupling reactions to form large amounts of gel [47,48]. EB radiation can also induce degradation reactions, the average molecular weight of the polymer decreases due to chain scission [49].

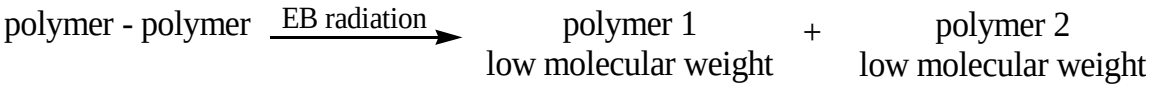

1.11.2 Radiation chemical yield (G-value)

The yield from the chemical reaction can be expressed by quantum yield as the ratio of number of molecules produced divided by the amount of absorbed radiation. This is usually referred to as G-value and can be given in units (molecules/100 eV), which is equivalent to 1.036×10^{-7} mol J^{-1} in SI units [50]. G-value is considered as essential parameter for optimization and comparison of chemical effect of radiation dose, G-value can be expressed by:

$$G - value = \frac{M}{N} \times \frac{100}{\mathrm{E}} \qquad (1.3)$$

where, M is the number of consumed molecules, N is the number of ion pairs formed, and E is the ionization energy per ion pair.

1.11.3 Radiation dose

To understand the behavior of species formation during EB curing, one should evaluate the amounts of species that are formed at a given irradiation rate. The absorbed dose can be

defined as the radiation energy used per unit mass of material. The SI unit of absorbed dose is expressed in gray (Gy) and is equivalent to J kg^{-1}. Dosimetry represents the dose absorbed by material. Radiation chemical yield is directly related to the absorbed dose by which the product chemical yield can be evaluated.

Radiation dose can be represented by the energy absorbed per unit time, which influence reaction kinetics and product final properties. In addition, radiation curing may accelerate development of heat inside the material and affect reaction kinetics, but this variable can be neglected in this study due to the curing of thin films with about 100µm thickness.

Excitation and ionization of molecules in the material occur within a very short time of irradiation by the formation of highly reactive radical species, which makes the electron beam curing very fast, thus it is required to optimize the preparation conditions as a control tool of the reaction rate.

1.12 Advantages and limitations of UV and EB curing

Advantages and disadvantages of UV and EB curing are discussed briefly in the literature, main advantages include: solvent free, low energy consumption, low temperature requirements, fast drying time, ease of reaction control and good physical properties. Limitations to UV and EB curing: higher material costs, curing thick materials by UV and high investment and costs of EB equipments. UV curing has also limitation in thick and unclear films to allow UV light to reach the material to be cured. However EB does not have this restriction in case of dense and highly pigmented materials due to the penetration of electron beam into the system. EB has another advantage: it doesn’t require photoinitiators to initiate the reaction, which gives EB products the advantages of low odor and low migration performers.

1.13 Polymer dispersed liquid crystal PDLC

1.13.1 Liquid crystal

Liquid crystals LC are molecules of rod like structure with strong dipole and possible polarized substituent. In contrast to liquid phase, LC molecules have the ability to align along a common axis. The orders of liquid crystals exist between the liquid phase and the highly ordered solid phase. Shapes of the solid, liquid crystal and liquid phases are shown in the following schematic diagram in figure 1.1:

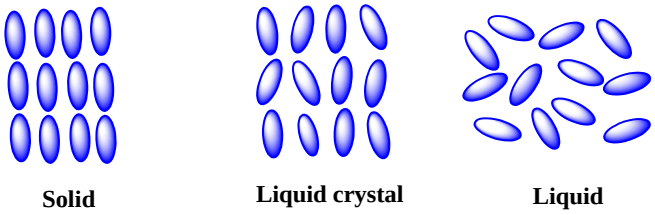

Figure 1.1 : Shapes of solid, liquid crystal and liquid phase.

Liquid crystals are classified as anisotropic materials; the electro-optical properties of anisotropic materials depend on direction of measurements. This property gives the LC a double identity to behave as crystal and liquid. Molecular order of liquid crystal is the main factor that determines its anisotropic properties. Molecular orientation is the reason of the optical properties of liquid crystals, which are of major interest in the research studies due to its applications in optical and electro-optical devices [51].

1.14 Classification of liquid crystal

Mesomorphic state has intermediate properties between solid crystal and liquid with molecules ranging between highly ordered to low order orientation. Liquid crystal has variety of mesophases with different symmetry. One can distinguish between thermotropic, lyotropic, polymeric and colloidal liquid crystal.

1.14.1 Thermotropic liquid crystal

Liquid crystal phases appear by varying the temperature. The phase can be separated into enantiotropic and monotropic liquid crystals. Enantiotropic liquid crystal can reach its liquid crystal phase by increasing or decreasing temperature, while monotropic phase can reach the liquid crystal phase by separately heating or cooling process.

Generally, there are two types of thermotropic liquid crystals: first whose molecules have a rod like shape and have an anisotropic geometry and the other have disc like shape which consist of aromatic body. Thermotropic mesophases have basically anisotropic dispersion forces (Van der Waals, polar, hydrogen bonds) between molecules.

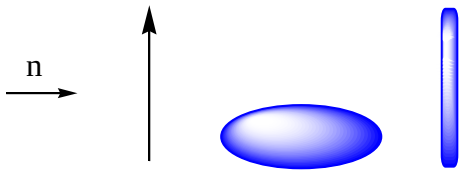

Figure 1.2: Configuration of thermotropic liquid crystal and the director.

Beside these molecules of low molecular weight, we also find a second major group of liquid crystal known as polymer liquid crystals, which are composed of polymer chain with mesogenic molecules and show thermotropic properties during melt state. These materials have properties of liquid crystals and the viscoelastic properties of polymer backbone. There are different types of polymer liquid crystal with linear mesogenic attached to each other by polymer chain. Polymer liquid crystals are consisting of polymer chains grafted by the mesogenic spaces. Both types of polymer liquid crystals are schematically presented in figure 1.3.

Combo polymer liquid crystal Linear polymer liquid crystal

Figure 1.3: Types of polymer liquid crystals

1.14.2 The lyotropic liquid crystal

Lyotropic liquid crystals are obtained by interaction of liquid crystal with a solvent and not by changing temperature. This phase has amphophilic behavior where the lyophilic parts direct themselves toward the solvent and the lyotropic parts are repelled by the solvent.

1.15 Phases of liquid crystal

Liquid crystal molecules behave in more than one phase in the liquid crystalline state. There are several types of liquid crystals based on degree of order between the molecules.

1.15.1 The nematic phase

Nematic liquid crystal phase is the well known and are widely found, this phase is characterized by molecules with medium tendency to align along the director (n) as shown in figure 1.4. Physical properties of this phase can be determined by the degree of alignment along the director. High degree of alignment means the material is anisotropic, while low degree of alignment presents isotropic phase.

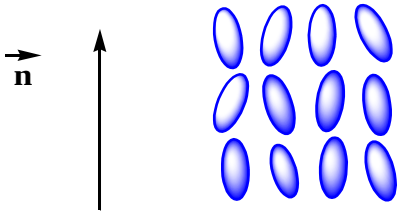

Figure 1.4: The alignment of nematic liquid phase with the director.

1.15.2 The smectic phase

Molecules in the smectic state have the same orientational order of nematic phase but they tend to align in layers or planes. This orientation restricts motion and flow of layers, as a result, separation of planes is observed to flow over each other. Several forms of smectic phase are known, the most distinct phases are smectic A and smectic C phases. In smectic A mesophase, the director is perpendicular to the plan while in the smectic C mesophase it forms an angle with the plan as given in figure 1.5.

Figure 1.5: Types and configuration of smectic phases.

1.15.3 The chiral nematic phase

Is composed of nematic mesogenic molecules containing a chiral center which produces intermolecular forces that tend the alignment of molecules at a slight angle to one another. In this phase, the directors are formed in a continuous helical structure, this leads to the formation of a structure of nematic-like plans with the layers twisted with respect to each other as shown in figure 1.6.

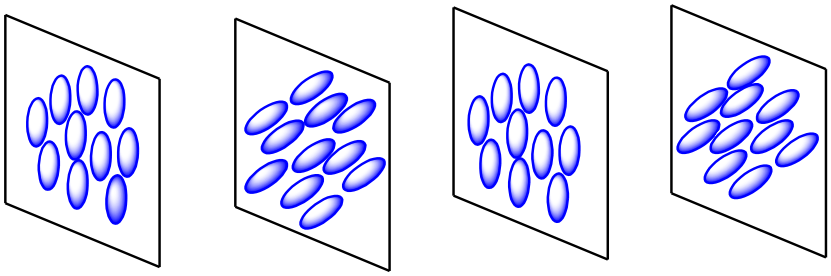

Figure 1.6: Schematic illustration of the chiral nematic phase.

1.15.4 The smectic C chiral phase

The smectic C phase has a chiral state in which the axis of helix is perpendicular to the layers at a constant angle with the direction of the molecules. The rotation of the director of the smectic C phase between layers will form a helix as presented in figure 1.7. The smectic C phase of the chiral molecules shows a continuous polarization perpendicular to the plane of inclination of the molecules [52].

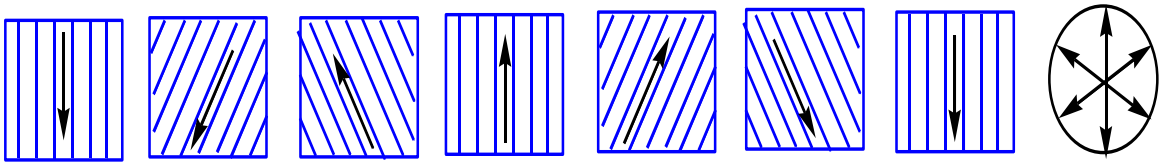

Figure 1.7: Schematic representation of a smectic C chiral phase.

1.16 Liquid crystal in polymer matrix

liquid crystals dispersed in a polymer matrix are known as Polymer Dispersed Liquid crystal PDLC. Its applications mainly are based on electronic displays. Another commercial

application is connected with the private windows industry, these windows can be opaque or transparence according to the user intention by changing the electric field across the window.

PDLC's consist of a polymer matrix with droplets of liquid crystals with diameter of few microns. Transparency will be based on the refraction and the orientation of polymer and liquid crystal in the matrix. The droplets of the liquid crystal are anisotropic with different refractive indices based on the direction of measurements (parallel or perpendicular) to the axis. Refractive indices of the polymer and liquid crystal are temperature dependant. In figure 1.8, shown electro-optical cell represents the configuration of liquid crystal droplets in the polymer matrix. The droplets are randomly oriented with respect to each other when the eclectic field is off and therefore difference in the refractive indices causes random distribution and the cell appears opaque. On the other hand, applying sufficient electric field across the cell, the droplets turned to align in the direction of director at which the refractive indices between the droplets is the same and the cell appears transparent. PDLC matrix has to be placed between two glass plates made of indium tin oxide (ITO).

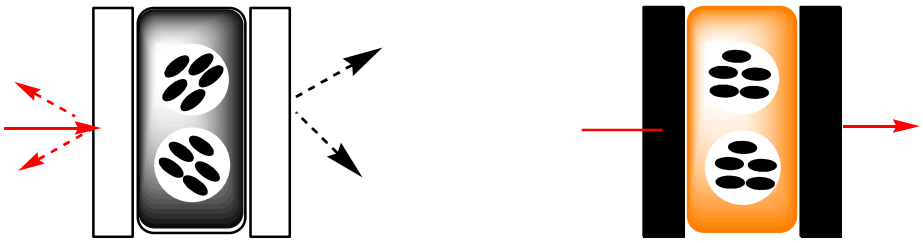

Figure 1.8: Schematic illustration for the operation of electro-optical cell.

PDLC display screens are based on the fact that liquid crystals are oriented in the matrix in a way to allow the light components to pass through the director without being diffracted, while others are strongly diffracted where refractive indices no longer coincide. Examples for a spherical drop of liquid crystal are illustrated in figure 1.9.

Figure 1.9: The configuration of liquid crystal droplet.

1.16.1 Liquid crystals and gel

Polymer/liquid crystal gels are prepared by polymerization of small amounts of monomer solutes in a liquid crystalline solvent. Importance of these polymer/LC gel systems are of increasing interest due to its many selective properties and applications namely stability in chiral nematic devices. The performance and applications of the polymer/liquid crystal gels are based on preparation conditions and composition of the systems.

Gels are materials consisting of network of molecules called gelling agent or polymer swelled by a liquid [53]. Different forms of gels are presented in figure 1.10. The molecules are connected together by ionic, Van der Waal or hydrogen bonds, in the form of intermolecular or intramolecular bonds.

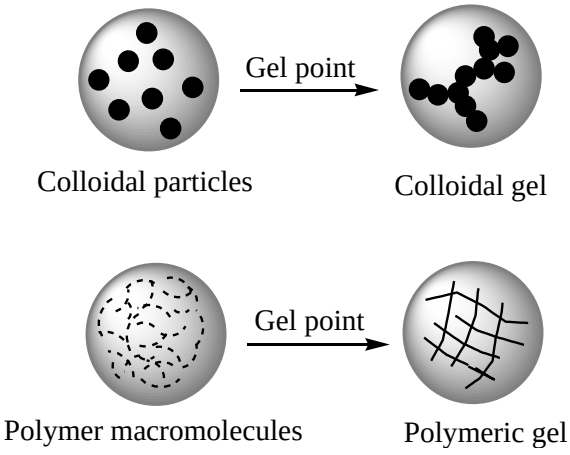

Figure 1.10: Preparation of different forms of gel.

Interest of liquid crystal gel was due to its potential applications in the refractive displays technology and the development of mechanicaly stable ferroelectric LC displays [54,55]. The mesogenic orientation can be stabilized by adding few percents of additive to the mesogenic material of low molecular weight, which will lead to a changes in dynamic and electro-optical characteristics of the mesogenic material [56,57]. Interactions of gel network with the mesogenic orientation may influence the material and lead to the coupling of size and shape on microscopic level, specially the characteristics of anisotropic swelling of gels [58]. In recent years, attention is given to the physical gelation of organic solvents by the fibrous aggregation of small molecules (gelling agent) in a thermotropic liquid crystal environment [59,60,61]. Phase segregation and orientation of the two components by hydrogen bond between the polymer and liquid crystal result in the generation of LC physical gel [62]. Orientation may also affect topology and network structure.

1.17 Preparation of PDLC systems

Recently, many methods have been developed to prepare functional PDLC films. The polymer dispersed liquid crystals are materials composed of a quantity of low molar mass liquid crystal and polymer. PDLC are films with properties and morphology that are based on the method of preparation. Polymerization process may be initiated by heat or by irradiation source based on the monomer used in the PDLC film. Two main methods are used for preparation of PDLC's: emulsion or encapsulation and phase separation. Selection of monomer and liquid crystal under certain preparation conditions would largely determine PDLC final properties. During preparation, several parameters have to be considered to achieve the desired properties [63,64]:

i. Birefringence of the liquid crystal, a high birefringence increases the difference between polymer refractive index and the average refractive index of liquid crystal, and therefore leads to more scattering. The use of lower birefringence liquid crystal mixtures leads to a lower opacity;
ii. Film thickness, where increasing the film thickness increases scattering degree;
iii. Liquid crystal droplet diameter, optimum scattering of white light can be achieved with droplet diameter of 1-2μm. At smaller diameters shorter wavelengths become scattered and the film becomes unclear. Droplet diameter can be controlled by the rate of phase separation during the process;
iv. Amount of liquid crystal phase separated out of the polymer matrix;
v. Clarity of the film in the on-state can be optimized by matching polymer refractive index and ordinary refractive index of liquid crystal.

The operating voltage of PDLC cell is usually in the range of 20 – 80 volts, whereas low voltage films for active matrix use can also be applied. The voltage required to switch a PDLC film is dependent upon many different factors, including film thickness, dielectric anisotropy of the liquid crystal, dielectric properties of the film, liquid crystal droplet size and the shape and configuration of the nematic director within the droplets.

Morphology of PDLC films depend on the concentration of a liquid crystal fraction in the polymer matrix, preparation conditions and method used [65]. Optical and electro-optical properties of this material are mainly determined by the orientational ordering of the director inside the LC droplets, which, in turn, depends on boundary conditions, droplet morphology and exposure time [66].

1.18 Encapsulation

Emulsion or encapsulation has been widely used for PDLC preparation. It consists of liquid crystal dispersion in a non-solvent containing polymer in the presence of surfactant to improve the distribution of liquid crystal [67,68]. Emulsion is then allowed to dry and covered with the second transparent substrate. The formed composite after evaporation of solvent presents high polydispersity based on the level of liquid crystal inclusion.

1.19 Phase separation

1.19.1 Polymerization induced phase separation PIPS

PIPS is considered one of the most practical methods to prepare efficient PDLC films, in which the polymer causes the liquid crystal to phase separate in the form of discrete droplets. In this method, phase separation is induced by polymerization. A homogenous mixture of the liquid crystal and monomer is prepared in the presence of photoinitiator. As the reaction proceeds, liquid crystal starts to disperse in the polymer matrix, solubility between the liquid crystal and the polymer chain decreases until the miscibility range. In the same time the molecules start to join each other to form droplets of liquid crystals. Material concentration and polymerization temperature are key factors that influence size and density of liquid crystals in the polymer matrix. Polymerization temperature may affect polymerization rate, polymer viscosity, solubility and the distribution of liquid crystal in the polymer matrix. The polymer matrix is the continuous phase while the mesogene form the dispersion phase. At high mesogene concentration, the continuous phase may be the liquid crystal in with a dispersion of polymer beads and the composite presents its final morphology [69]. This technique offer good control of polymerization, as it can be employed for a whole range of monomers and liquid crystals. Thus, development of polymer composite films by PIPS has become important methods for the preparation of PDLC due to the ability to control various parameters during the process.

1.19.2 Temperature induced phase separation TIPS

TIPS is based on controlling phase separation process by temperature or thermally induced phase separation, this method is usually applied in the thermoplastics which melt below their decomposition temperature. At high temperature, liquid crystal is soluble in the molten polymer matrix, temperature is gradually decreased until polymer glass transition T_g, liquid crystal will begin to form droplets that will continue to grow until the polymer become rigid. Droplet size and cooling rate are inversely proportional in this method.

Dispersion of diameter and droplets size can be controlled by the ratio of polymer to liquid crystal concentration in the initial mixture. Increasing liquid crystal concentration result in

fast dispersion in the matrix, while lowering the concentration accelerates formation of regular and fixed size drops [70].

1.19.3 Solvent induced phase separation SIPS

This method is based on the solvent evaporation, liquid crystal molecules form growing droplets by evaporation until complete solvent evaporation. At high evaporation rate, droplets will not have enough time to grow and small droplets are being formed. On the other hand, at low evaporation rate, molecules have time to grow and larger droplets are formed [71,72].

Influence of viscosity on the size variation of liquid crystal at different molar mass of polymer has been investigated by several research groups. Change in polarity of copolymer by introducing polar or non-polar monomer in the polymer chain will influence size of liquid crystal, the droplets size increases by increasing the interaction between the copolymer and liquid crystal [73].

Polymerization rate increases in less ordered liquid crystal phase for many polymers of different structure and liquid crystal properties; this can be explained by the segregation of monomer molecules into the liquid crystal phase. As a result, local concentration of the double bonds increases and the polymerization rate increases [74]. Variations in the polymerization rate and degree of segregation play a vital role in preparation of PDLC systems, which affect formation of polymer network structure and accordingly the performance of composite materials.

1.20 Phase diagram

The phase diagram is considered as a good tool to understand the phenomena that occur during phase separation. Several parameters affect the mixing process, which includes polymer/liquid crystal interfacial interactions, diffusion, molecular relaxation and confinement effect. Previous experimental and theoretical approaches on the phase diagram of PDLC have been performed. The characteristic behavior of the upper critical solution temperature (UCST) of PDLC have been described based on the application of thermodynamic theory of Flory, Ronca, and Maier and Saupe on the results of optical microscopy [75,76,77]. Furthermore, studies on the mean-field paradigm have also proved useful development of calorimetric methods to determine the solubility limits of LC in the polymer matrix.

1.20.1 The binodal analysis

The objective of phase diagram analysis of a mixture of liquid crystal and polymer is to characterize the thermodynamic equilibrium in the isotropic phase. Establishment of the theoretical diagram based on a combination of the Flory-Huggins theory of isotropic mixing and Maier-Saupe theory of nematic order. In the theoretical model, free energy density is given by the sum of the two terms:

$$f = f_{(i)} + f_{(n)} \tag{1.4}$$

The first term $f_{(i)}$ is given by the Flory-Huggins model:

$$\frac{f_{(i)}}{k_B T} = \frac{\varphi_1}{N_1} ln\varphi_1 + \frac{\varphi_2}{N_2} ln\varphi_2 + x\varphi_1\varphi_2 \tag{1.5}$$

where k_B is the Boltzmann constant, T is the absolute temperature, φ_1 and φ_2 are the volumetric fractions of LC and the polymer respectively, N_1 and N_2 are the number of repeating units of liquid crystal and the polymer respectively and x is the interaction parameter of Flory-Huggins and which is temperature dependant:

$$x = A + \frac{B}{T} \tag{1.6}$$

A and B are adjusting parameters, in case of a mixture of polymer/liquid crystal the behavior of the phase diagram is typically UCST [78,79].

The second term $f_{(n)}$ of the equation is given by the Maier-Saupe model:

$$\frac{f_{(n)}}{k_B T} = \frac{\varphi_1}{N_1}\left[-lnZ + \frac{v\varphi s^2}{2}\right] \tag{1.7}$$

where Z is the partition nematic function, v the interaction parameter which is inversely proportional to T:

$$v = 4{,}54\ \frac{T_{NI}}{T} \tag{1.8}$$

T_{NI} is the nematic-isotropic transition temperature, s is the nematic order parameter and can be given by:

$$s = \frac{1}{2}[3\langle cos^2\theta\rangle - 1] \tag{1.9}$$

θ is the angle of the director of liquid crystal, θ is taken as average with respect to the angular distribution.

In case of phase separation induced by PIPS, these formulas are also in agreement with experimental results. Nevertheless, it does not reflect the multiple parameters involved in the process like the mass distribution of polymer chains. Interaction and the morphology of polymer chain are likely the significant elements that contribute significantly to the final morphology of liquid crystal domains and thus ultimately to electro-optical properties.

1.21 Theories of spinodal decomposition

1.21.1 Cahn-Hilliard Theory

Dynamic behavior phenomena of phase separation in the binary system within the unstable region of the phase diagram can be described using the Cahn-Hilliard theory [80,81].

To understand the thermal movement of molecules, several theories have been used successfully to describe the dynamics of spinodal decomposition and morphological evaluation in binary systems of small molecules and polymers [82,83,84,85].

The linear theory of Cahn-Hilliard is considered the basis of the total free energy of a binary inhomogeneous solution:

$$F = \int (f + k\|\nabla\varphi_1\|^2)dV \tag{1.10}$$

k is constant, the first term of the equation represents the free energy density and the second term show the total free energy increases due to concentration gradients. These two contributions can be obtained from the Taylor series expansion of the free energy that depends on the concentration. The free energy density of Flory-Huggins can be used as a

homogeneous density of free energy for binary systems ranging from simple binary solutions in mixtures and polymer solutions. Cahn-Hilliard theory is derived by applying continuous flow equation:

$$j = -m\nabla\frac{\delta F}{\delta\varphi_1} = -m\nabla\left(\frac{\delta f}{\sigma\varphi_1} - 2k\nabla^2\varphi_1\right) \tag{1.11}$$

m is the mobility at an instant j in the continuous equation, the Cahn-Hilliard equation can be expressed as follow:

$$\frac{\delta\varphi_1}{\delta t} = \nabla\left[m\nabla\left(\frac{\delta f}{\delta c} - 2\mathrm{k}\nabla^2\varphi_1\right)\right] \tag{1.12}$$

Within short time, concentration fluctuations become small and equation 1.12 can be liberalized, this result shows that m and k can be considered constant:

$$\frac{\delta\varphi_1}{\delta t} = m\left[\left(\frac{\delta^2 f}{\delta f^2}\nabla\varphi_1 - 2\mathrm{k}\nabla^4\varphi_1\right)\right] \tag{1.13}$$

Phase separation is often followed by light scattering, X-ray or neutron scattering. The scattering spectrum consists of a ring distribution. Over time, intensity increases, while the distribution moves to smaller angles corresponding to growth in the size of the segregated zones. Although this ring is the mark of spinodal decomposition, numerical results for the structure factor profiles are usually compared to time-resolved intensity of dispersion. Quantitative information is obtained from the intensity profile of the diffusion on time resolution I (q, t), where q is the scattering vector. The digital equivalent of this profile is the structure factor S (k, t) [86].

$$I(q,t) \propto \mathrm{S}(q,t) = \|\mathrm{A}(\mathrm{q},\mathrm{t})\|^2 \tag{1.14}$$

$\mathrm{A}(\mathrm{q},\mathrm{t})$ is one of the general solutions in Fourier equation. Furthermore, the light intensity I(q,t) contains information on the lifetime of fluctuations within the concentration and length scales.

1.21.2 Dependence of the molar mass on mobility and interfacial parameters

The mobility m and the interfacial parameter k depend on the molecular mass M, using the PIPS method the molecular mass of polymer increase during the polymerization.

Dependency of molecular mass on the mobility m approximated using the Stokes-Einstien relation of the polymer blend. The Stokes-Einstein equation:

$$D' = \frac{k_B T}{\varepsilon} = \frac{k_B}{6\pi\mu_0 R} \tag{1.15}$$

ε is the friction coefficient of a sphere of radius R undergoing shear flow in a polymer solvent and μ is the solvent viscosity, D' is the diffusion constant which characterizes the thermal motion. The first equality is the expression of Einstein relation and the expression of Stokes relation ε and μ_0 is given by the second equality. In the theory of Flory-Huggins v is the volume occupied by a segment and with $m = v/\varepsilon$, equation (1.15) can be rewritten as a function of the mobility m:

$$m = \frac{v}{6\pi\mu_0 R} \tag{1.16}$$

These equations are given in the literature connecting the viscosity of the mixture of polymer on a number of atoms which form the polymer network [87,88]. The next relation is given by the auto condensation of a trifunctional monomer during previous steps of the spinodal decomposition:

$$m = \frac{m_o}{N_2} \tag{1.17}$$

$$m_0 = \frac{v}{12\pi R k_L} \tag{1.18}$$

k_L is a constant presenting the solvent viscosity μ_0. The dependence of m with respect to N_2 is appropriated for the systems of infinite networks, until the movement is restricted by

molecular crosslinking. Limitation occurs to products at the gelation ($N_2 \rightarrow \infty$) or the viscosity is infinite and therefore no molecular motion (m = 0) is allowed. An expression has been derived for k which is appropriate for the polymer mixture [89]. This expression contains enthalpic term as output of Flory interaction parameter $\mathbf{x}$ and the square of the interacton length between the molecules I_i^2. The entropic term is a function of the Kuhn length and the solvent volumetric fraction φ. In the polymer solution, the length I_i corresponds to the gyration radius R_g [90]. The enthalpic term is three orders of magnitude larger than the entropic term for typical molecular dimensions in polymer solutions [91]. Consequently, the entropy term can be neglected for polymer solution. In addition, for small molecular systems, k is assumed to be constant which means there is no entropy term. Therefore, only the enthalpic term is used in PIPS method because the evolution of a binary solution initially contains small molecules, or N_1 = N_2 = 1, in polymer solution N_1= 1 and N_2> 1. Since gyration radius is smaller for a non-linear polymer than a linear polymer of same molecular weight, the following expression can be written for k:

$$k = k_0 N_2 \tag{1.19}$$

This equation presents the interaction phenomena with the solvent and the growing polymer chain.

1.21.3 Kinetics of molecular size distribution

In the PIPS method, pure polymers react to form an infinite network. Consider the case of polycondensation and its expression kinetics. A monomer A of functionality f which will be called as Af:

$$\frac{dP}{dt} = k_1(1 - P)^n \tag{1.20}$$

where P is the reaction progress, $k_1$is the rate constant at time t. The condensation reaction is bimolecular (n=2), equation (1.20) can be solved analytically using the initial conditions $p(t$=0):

$$p = \frac{k_1 t}{1 + k_1 t} \tag{1.21}$$

Distribution function of the molecular size has been derived by Stockmayer and Flory [92,93] taking into account that there is no intramolecular reaction and fairly reactive functional groups.

The phase behavior of monofunctional acrylate 2EHA and low molecular weight nematic liquid crystals is given in Figure 1.11 (a) and (b). The system shows the 2EHA monomer with the eutectic LC mixture E7 and 5CB. The experimental phase diagrams are established using polarized optical microscopy and analyzed using a theoretical formalism which combines the Flory–Huggins theory of isotropic mixing and the Maier–Saupe theory of nematic order [94].

It can be observed that because of high degree of miscibility of 2EHA and liquid crystals, there is no isotropic-isotropic miscibility gap while the critical points are located at low temperatures [95].

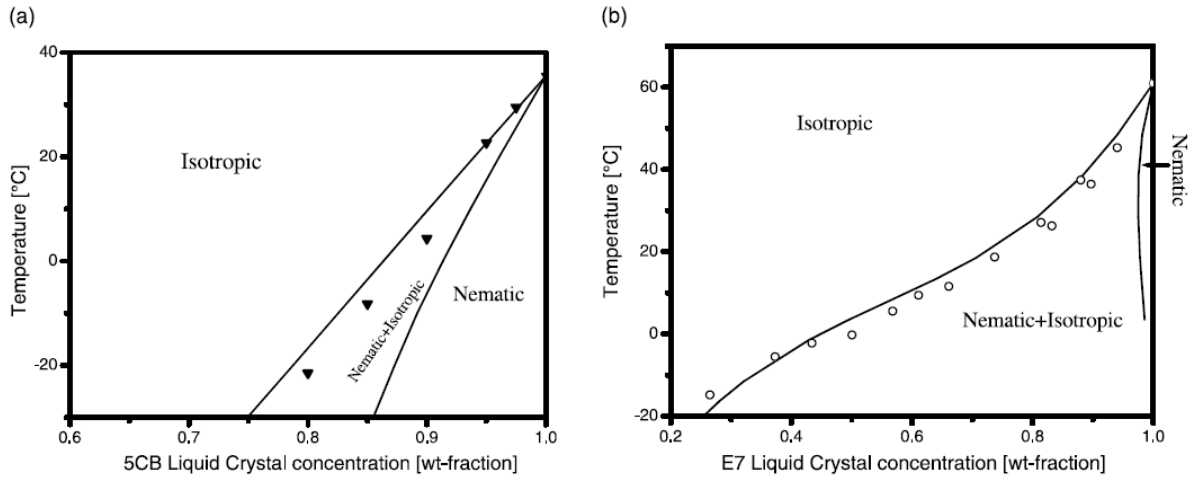

Figure 1.11: The phase diagram of the monomeric 2-EHA/LC systems. The symbols are POM data while the curves are theoretical binodal (solid) and spinodal (dashed) predictions.

The characterization of the miscibility of E7 and 5CB with polymeric 2EHA systems are presented in figure 1.12 (a) and (b). The symbols are data obtained by POM, while the continuous curves represent the theoretical binodal and spinodal predictions with solid and dashed lines respectively.

In case of polymeric state interactions, miscibility of 2EHA polymer in liquid crystal phase is quite low while the limit of solubility of 5CB at 30°C is no more than 60%. In the upper temperature region, the liquid crystals do not exhibit a nematic phase and larger difference is found between these two systems.

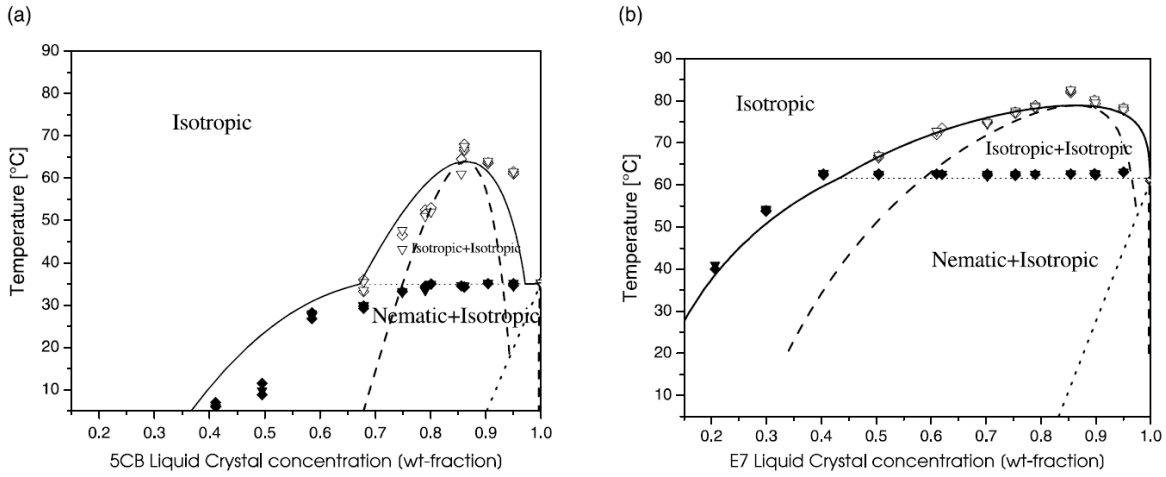

Figure 1.12: The phase diagram of the polymeric 2EHA/LC systems. The symbols are POM data while the curves are theoretical binodal (solid) and spinodal (dashed) predictions.

1.22 The gel content of acrylic polymers

Acrylic polymers find many applications in adhesives and coatings [96,97]. During polymerization, highly branched polymers are formed usually characterized by their degree of solubility in a given solvent. Insoluble fraction of these polymers is known as gel [98]. Applications of acrylic polymers depend on the glass transition temperature T_g, gel fraction and the molecular weight distribution. The mechanism offormation of gel can be described by the intramolecular and intermolecular chain transfer to polymer followed by termination by combination. Previous studies on gel fraction during polymerization of acrylates show that gel fraction decreases by increasing concentration of chain transfer agent [99], Whereas, addition of crosslinking agents led to a substantial increase of the gel content with deceasing in the molar mass [100]. Increasing gel fraction is usually accompanied by decreasing the polymer molecular weight [101].

Polymer architecture has strong impact on the end use properties of the polymer composites network. Gel fraction can be controlled by varying the preparation conditions during radical polymerization as irradiation dose, the choice between UV and EB curing and photoinitiator concentration.

1.23 Rheological properties of acrylic polymers

Rheological properties would offer detailed information about the structure of the polymer matrix. The rheological measurements are based on exposing the sample to shear stress that causes deformation of polymer particles [102,103]. Degree of deformation depends on the applied stress and the internal structure of the polymer matrix. In case of poly(2EHA), the produced polymer is softer and easily deformable compared to diacrylate or crosslinked polymers, which offer the viscoelastic properties to the monoacrylate polymers. The viscoelastic term is used to describe liquids which behave as ideal liquids and under stress they behave as solid with elastic properties.

We study the rheological behavior of the polymer matrix as a function of the internal structure of polymer. Applying shear stress τ and measure the degree of deformation γ and the phase angle δ, the viscoelastic properties of the material can be described using the storage shear modulus G' and the loss shear modulus G''.

The storage shear modulus G' is given by:

$$G' = \frac{\tau_0}{\gamma_0}\cos\delta \tag{1.22}$$

where τ_0 and γ_0 are amplitude of shear stress and shear strain respectively. G' represents a measure of the strain energy stored in the substance and characterizes the elastic behavior of the material.

The loss modulus is given by:

$$G'' = \frac{\tau_0}{\gamma_0}\sin\delta \tag{1.23}$$

The loss modulus is a measure of energy lost in the form of heat. Therefore, G'' characterizes the viscous behavior of the material.

The loss factor is defined as:

$$tan\delta = \frac{G''}{G'} \tag{1.24}$$

This quantity is proportional to the ratio between the viscous modulus and elastic modulus.

Based on these measurements the dynamic viscosity η can be defined as:

$$\eta = \frac{G''}{2\pi v} \tag{1.25}$$

where v is the applied frequency.

The viscoelastic behavior can be described in terms of temperature dependence. At low temperatures, polymer is glassy with low thermal energy for the chain rotation and translational motion. Increasing temperature, the amplitude of molecular vibration is sufficient to start a segmental motion. Above the glass transition temperature, modulus drops dramatically until reaching a rubbery state where segmental and translational motions occur rapidly. Maximum energy dissipation (loss factor) usually seen to occur in the transitional region between the glassy and rubber states [104].

1.24 Conclusion

In this literature review, a comparison between UV and electron beam EB curing methods have been made as the widely used techniques for free radical polymerization.

Detailed description of the polymer dispersed liquid crystal PDLC composites has been presented with different methods of preparation. We demonstrated the dependence of the morphology of polymer/liquid crystal composites on the method of preparation (PIPS, TIPS, SIPS), in addition to effect of temperature on the morphology of polymer composite. Formation of polymer/liquid crystal composites have been discussed, in terms of liquid and monomer structure with the evolution of the polymer network in liquid crystal medium. To describe the behavior of the PDLC, we briefly discussed the main theories which describe phase diagram based on the thermodynamics of polymer/liquid crystal blends. The mobility of molecules and its effect on the molar mass distribution was also demonstrated.

Gel formation during curing polymerization has been presented with effect of gel contents on the performance and applications of the PDLC films. To understand the gel behavior in the polymer composites, the viscoelastic properties of the polymer materials have been presented as a tool to describe the internal structure and interactions between the polymer and the liquid crystals in of the polymer composite.

Kinetics models of the polymerization reaction have been presented. The relation between polymer structure and kinetic of polymerization was briefly discussed. The molecular weight distribution of polymer networks has been outlined based on the preparation conditions, the curing method and monomer structure.

Optimization and characteristics of PDLC film can be achieved by choosing the appropriate preparation conditions during the curing process and understanding the monomer/liquid crystal interaction during the process.

1.25 References

[1] P. S. Drzaic, Liquid Crystal Dispersions, World Scientific:Singapore (1995).
[2] J. W. Doane, Polymer Dispersed Liquid Crystal Displays, in: Liquid Crystals: Their Applications and Uses, B. Bahadur, Ed. World Scientific, Singapore (1990).
[3] G. P. Crawford, S. Zumer, Liquid Crystals in Complex Geometries, Taylor & Francis, London (1996).
[4] U. Maschke, X. Coqueret, C. Loucheux, J. Appl. Polym. Sci. 56, 1547 (1995).
[5] T. Bouchaour, F. Benmouna, F. Roussel, J.-M. Buisine, X. Coqueret, M. Benmouna, U. Maschke, Polymer, 42, 1663-1667 (2001).
[6] Plastics, Materials and Processing, Second Edition, Ed. A. B. Strong, Prentice Hall, New Jersey (2000).
[7] Resins for Coatings: Chemistry, Properties and Applications, Ed. D. Stoye and W. Freitag, Hanser/Gardner Publications, Inc., Cincinnati (1996).
[8] C. Decker, Progr. Polym. Sci., 21, 593 (1996).
[9] C. Roffey, Photodegradation of reactive species for UV curing, John Wileng, Chichester (1997).
[10] D.J. Lougnot, chap.5, collection Electra. Dopee, 85, Paris, 245 (1992).
[11] C. Decker, Materials Science and Technology. Vol. 18, Meiser, VCH Verlay Weinheim (1997).
[12] R. Peiffer, In photopolymerization Fundamentals and Applications; American Chemical Society: Washington D.C.,Vol. 637 (1997).
[13] A. Reiser, Photoreactive Polymers: The Science and Technology of Resists; Wiley-Interscience (1989).
[14] J.-P. Fouassier, Photoinitiation, Photopolymerization, and Photocuring Fundamentals and Applications, Hanser Gardner: New York (1995).
[15] R. S. Benson, Nuclear Instruments and Methods in Physics Research B 2002, 191, 752.
[16] K. S. Anseth, J. A. Burdick, MRS Bulletin, 27, 130 (2002).
[17] K. S. Anseth, V. R. Shastri, C. T. Laurencin, R. Langer, Abstracts of Paper of the American Chemical Society, 211, 228 (1996).
[18] K. S. Anseth, D. C. Svaldi, C. T. Laurencin, R. Langer, Photopolymerization, 673, 189 (1997).

[19] E. Andrzejewska, Progress in Polymer Science, 26 ,4, 65 (2001).

[20] H. J. Assumption, L.J. Mathias, Polymer, 44, 18, 5131 (2003).

[21] J. P. Fouassier, X. Allonas, D. Burget, Progress in Polymer Coatings, 47, 16 (2003).

[22] A.M. Horton, Radiation Curing : Science and Technology, Vol. 4, J.-P. Fouassier and J.F. Rabek, Plenum Press, 1 (1992).

[23] S.A. Bateman, K.M. Dean, R. Simons, Polymer, 48, 8, 2231 (2007).

[24] C. Decker, L. Keller, K. Zahouily, S. Benfarhi, Polymer, 46, 6640 (2005).

[25] G. Odian, Principles of Polymerization. 3rd Ed. ed. New York: John Wiley & Sons, Inc (1991).

[26] C. Decker, in Engineering techniques, Plastic and composites treatment, Article AM3044 (2000).

[27] J. Kindernay, A.Blazkova, J. Ruda, V. Jancovicova, Z. Jakubikova, Journal of Photochemistry and Photobiology a-Chemistry, 151, 229 (2002).

[28] S. L. Rosen, Fundamental principles of polymeric materials, 2nd Ed., Wiley Interscience (1993).

[29] A. Rachini, PhD thesis, Nanocomposite films polymerization and charechterization (2006).

[30] Subrahmanyam, B.; S. D. Baruah, M. Rahman, J. N. Baruah and N. N.Dass, J. Polym. Sci., Par A: Polym. Chem., 30(12), 2531-40 (1992).

[31] M. A. Dube, K. Rilling, A. Penlidis, J. Appl. Polym. Sci., 43, 11, 2137-45 (1991).

[32] C. Decker, K. Moussa, Macromol. Chem., 189, 2381 (1988).

[33] P. M. Johnsona, T. B. Reynoldsb, J. W. Stansbury, C. N. Bowman, Polymer 46, 3300–3306 (2005).

[34] S.L. Rosen. Fundamental principles of polymeric materials. New York: Wiley (1982).

[35] W. Burchard, Adv Polym. Sci,143,113 (1999).

[36] C. Plessis, G. Arzamendi, J.M. Alberdi, A.M. van Herk, J.R. Leiza, J.M. Asua. Macromol Rapid Commun., 24,173 (2003).

[37] M. Gaborieau, J. Nicolas, M. Save, B. Charleux, J-P. Vairon, R.G. Gilbert, et al., J. Chromatogr. A, 1190,215 (2008).

[38] S. Filipe, I. Vittorias, M. Wilhelm, Macromol. Mater. Eng., 293, 57 (2008).

[39] C. Plessis, Modeling of molecular weight distribution of polyacrylic latexes, Ph.D. thesis, University of the Basque Country, Donasta – San Sebastian, Spain (2000).

[40] M. Helmstedt, J. Stejskal, W. Burchard, Macromol. Symp.,162, 63 (2000).

[41] F. Heatley, P.A. Lovell, T. Yamashita, Macromolecules,34, 7636 (2001).

[42] I. Vittorias, M. Wilhelm, Macromol. Mater. Eng., 292, 935 (2007).

[43] I. Vittorias, M. Parkinson, K. Klimke, B. Debbaut, M. Wilhelm, Rheol. Acta., 46, 321 (2007).

[44] E. F. McCord, W. H. Shaw, R. A. Hutchinson, Macromolecules, 30, 2, 246-256 (1997).

[45] R. Mehnert, A. Pincus, I. Janovský, UV & EB Curing Technology & Equipment, Vol. 1, Wiley-SITA, London (1998).

[46] J. W. T. Spinks and R. J. Woods, An Introduction to Radiation Chemistry, John Wiley & Sons, Inc., New York (1964).

[47] G. Alder, Science, 141, 321 (1963).

[48] G. Odian and B. S. Bernstein, Nucleonics, 21, 80 (1963).

[49] V.S. Ivanov, Radiation Chemistry of Polymers. Utrecht, The Netherlands: VSP BV (1992).

[50] C.G. Jones, Ph.D. thesis, University of Maryland, College Park (2001).

[51] L. Bouteiller, P. Le Barny, liquid crystals, 21, 2, 157 (1960).

[52] R.B. Meyer, L. Liebert, L. Strzeleck, P. Keller, J. phys. Let., 36, 169 (1975).

[53] E. Collins, Billmeyer, Experiments in Polymer Science, John Willey & Sons. New York (1980).

[54] R.A.M. Hikmet, Liq. Cryst., 9, 405 (1991); D.K. Yang, L.C. Chien, J.W. Doane, Appl. Phys. Lett., 60, 3102 (1992).

[55] J. Li, W. Zhao, K. Ma, X. Huang, Mol. Crys. Liq. Cryst., 321, 395 (1998) ; J. Li, X. Huang, Ferroelectics, 271, 85 (2002).

[56] R. Meziane, M. Bremer, U Maschke, R. Zentel, Soft matte, 4, 1237 (2008).

[57] Y. Zhao, L. Guan, liquid crystal, 30, 1, 81 (2003).

[58] A. Matsuyama, T. Kato, Phys. Rev. E., 64, 010701 (2001); A. Matsuyama, T. Kato, J. chem.. Phys., 114, 3817 (2001); A. Matsuyama, T. Kato, J. Chem. Phys. 116, 8175 (2002).

[59] T. Kato, 2002,Science, 295, 2414 (2002).

[60] D.J. Abdallah, R.G. Weiss, Adv. Mater., 12, 1237 (2000).

[61] H. Abe, H. Kikuchi, T. Kajiyama, K. Hanabusa, T. Kato, Liq. Cryst., 29, 1503 (2002).

[62] T. Kato, T Kutsuna, K. Hanabusa, M. Ukon, Adv. Mater., 13, 1307 (2001).

[63] D. Coates, S Greentield, Sage and G Smith, Liquid Crystal Mixtures tor Polymer Matrix Displays, SPIE Proceedings, 1257, 39 (1990).

[64] E Ginter, E Leuder, T Kalifass, S Huttelmaier, M Dobler, V Hochholzer, D Coates and M Tillin, Optimised PDLC for Active Matrix Addressed Light Valves in Projection Systems, Eurodisplay, 105 (1993).

[65] S. A. Carter, J. D. Le Grange, W. White, et al., J. Appl. Phys. 81, 5992 (1997).

[66] O. O. Prishchepa, A. V. Shabanov, and V. Ya. Zyryanov, Pis'ma Zh. Eksp. Teor. Fiz. 79, 315 (2004).

[67] J.L. fergason, SID Int. Symp. Dig. Tech. Pap., 16, 68 (1985).

[68] P.S. Drzaic, Jour. Appl. Phys., 60, 2142 (1986).

[69] J. Ding, H. Zhang, J. Lu, Japan Jour. Appl. Phys., 34, 4A, 1928 (1995).

[70] Y. Hirai, S. Niiyama, H. Kumai, T. Gunjima, Proc. SPIE 1257, Liquid Crystal Displays and Applications (1990)

[71] B.G. Wu, J.L. West, J.W. Doane, J. Appl. Phys., 62, 3925 (1987).

[72] B.K. Kim, Y.S. Ok, C.H. Choi, Jour. Polym. Sci., Part B: Polym. Phys., 33, 707 (1995).

[73] S.J. Im, J.H. Sung, W.Y. Park, D.S. Sakong, Synth. Met., 71, 2203 (1995).

[74] C.A. Guymon, E. N. Hoggan, N.A. Clark, T.P. Rieker, D.M. Walba, C.N. Bowman, Science, 275, 57 (1997).

[75] M. Ballauff. Mol. Cryst. Liq. Cryst., Lett., 15 (1986).

[76] J.R. Dorgan, D.S. Soane, Mol. Cryst. Liq. Cryst., 188, 129 (1990).

[77] W. Maier, A. Saupe, Z. Naturforchung, 15A, 287 (1960).

[78] P.C. Hiemenz, Polymer Chemistry: The basic concepts, Marcel Dekker, Inc., NY (1984).

[79] T. Nishi, Jour. Macromol., Sci.-Phys., B17, 517 (1980).

[80] J.W Cahn, J. Chem. Phys., 42, 93 (1964).

[81] J.D. Gunton, M. San Miguel, P.S. Shahni, Phase Transitions and Critical Phenomena, edited by C. Domb and J.L. Lebowitz, Academic Press, New York, Vol.8 (1983).

[82] H.E. Cook, Acta. Metall., 18, 297 (1970).

[83] G. Brown, A. Chakrabarii, Phys. Rev. E, 48, 3705 (1993).

[84] P.K. Chan, A.D. Rey, Macromolecules, 29, 8934 (1996).

[85] B.T. Jiang, P.K. Chan, Macromol. Theory Simul., 16, 690 (2007).

[86] K.B. Rundman, JE. Hilliard, Acta. Metd., 15, 1025 (1967).

[87] J.M.G. Cowie, Polymer: Chemistry and Physics of modern Materials, 2nd ed., Chapman and Hall: New York, (1991).

[88] L.H. Sperling, Introduction to Physical Polymer Science, 2nd ed., John Wiley: New York, (1992).

[89] P.G. de Gennes, J. Chem. Phys., 72, 4756 (1980).

[90] P. Debye, J. Chem. Phys., 31, 680 (1959).

[91] J. Lal, R. Bansil, Macromolecules, 24, 290 (1991).

[92] W.H. Stockmayer, J. Chem.Phys., 11, 45, (1943).

[93] P.J. Flory, Princiles of Polymer Chemistry, Comell University Press, Ithaca (1953).

[94] S . K. Slimane, U. Maschke, X. Coqueret, M . Benmouna, European Polymer Journal 38, 461–466 (2002).

[95] S.K. Slimane, F. Roussel, U. Maschke, Journal of Polymer Science: Part B: Polymer Physics, 45, 18-27 (2007).

[96] P.A. Lovell, M.S. El-Aasser, editors. Emulsion polymerization and emulsion polymers. New York: Willey (1997).

[97] J. C. Daniel, C. Pichot, Les latex synthétiques: élaboration, propriétés, applications'', Lavoisier, Paris (2006).

[98] C. Plessis, G. Arzamendi, J. R. Leiza, H. A. S. Schoonbrood, D. Charmot, J. M. Asua, Macromolecules, 33, 4 (2000).

[99] L. Bouvier-Fontes, R. Pirri, G. Arzamendi, J.M. Asua, J.R. Leiza, Macromol. Symp., 206,149–64 (2004).

[100] L. Bouvier-Fontes, R. Pirri, S. Magnet, J.M. Asua, J.R. Leiza, Macromolecules, 38, 2722–9 (2005).

[101] C. Plessis, G. Arzamendi, J. M. Alberdi, M. Agnely, J.R. Leiza, J.M. Asua, Macromolecules, 34, 6138–6143 (2001).

[102] H.A. Barnes, Colloids and Surfaces, 9, 89 (1994).

[103] M. Osterhold, W. Schubert, W. Schlesing, J. Rheol., 36, 45 (1992).

[104] Paul B. Foreman, National Adhesives, Bridgewater, NJ.

2 PREPARATION OF MATERIALS AND CHARACTERIZATION TECHNIQUES

2.1 Materials

In this work we study the effect of UV and electron beam EB irradiation on structure and morphology of the PDLC films. Liquid crystal used was 4-cyano-4'-n-pentyl-biphenyl known as (5CB). monomer used to prepare the PDLC films were monofunctional acrylate 2-ethylhexyl acrylate (2EHA) and difunctional acrylate tripropylene glycol diacrylate (TPGDA). In UV curing 2-hydroxy-2-methyl-1-phenylpropan-1-one (Darocur1173) was used as a photoinitiator to initiate the polymerization reaction.

2.1.1 The liquid crystal

During this study, 4-cyano-4'-n-pentyl-biphenyl (5CB) was used as liquid crystal represented in figure 2.1 provided by Merck Eurolab GmbH (Darmstadt, Germany), 5CB have been a subject of several polymer dispersed liquid crystal studies to understand the smectic - nematic phase transitions. Nematic LC molecules show up the same orientation in space without spatial ordering. 5CB molecule is about 20 Å long. In the nematic and isotropic phases, 5CB molecules form dipole bound dimers with about 2.3 nm long and 0.5 nm thick [1]. The nematic liquid crystal 5CB, have its solid crystal – nematic ($T_C - T_N$) phase transition at 22 C, and nematic–isotropic ($T_N - T_I$) liquid phase transition at 35.5 C. Studies conducted on 5CB by dielectric measurement show that dielectric constant in 5CB has a considerable influence at the isotropic-nematic transition and an abrupt decrease at the crystallization point [2].

5CB molecules behave as rodlike shape on the microscopic level; these molecules are aligned in the solid state. In the liquid crystal phase, the molecules are free to move and can rotate to form different alignment but remain with a certain level of orientation. Alignment gives the liquid crystal their unique properties. Transformation from solid to liquid crystal involves breaking of intermolecular bonds between the molecules which known as endothermic transition.

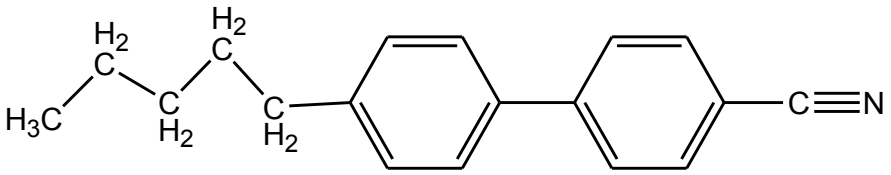

Figure 2.1 : 5CB molecule model containing CN group, an aliphatic chain of 5 carbons and two aromatic rings.

2.2 Monomers and polymers

2.2.1 The monomers

Acrylic esters such as ethyl are industrially important in synthesis of acrylic resins and polymer dispersed liquid crystal films because of their optical clarity, good mechanical properties and chemical stability. The first monomers used in this work have an acrylic functionality. 2-ethylhexyl acrylate (2EHA) exhibits no crystal phase or mesophase. The structure is given in Figure 2.2. It has been provided by Aldrich. The choice of our polymer has been made based on several criteria:

- Obtain a thermoplastic polymer after polymerization.
- Show no order (crystalline, mesophase).
- Not having a glass transition Tg found in the domain of the study and has to be lower that range (25 C – 75 C).
- Have known polymerization mechanisms

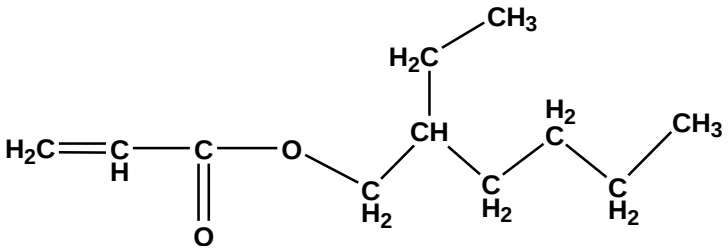

Figure 2.2 : Chemical structure of 2-ethylhexyl acrylate (2EHA)

Cross-linked acrylate polymers are generally characterized by their physical and mechanical properties, such as high mechanical strength and resistance to many chemical compounds like water, oil and alcohol. The unique properties of the diacrylates are largely influenced by molecular weight distribution of viscoelastic chains between networks, chemical composition, conversion and network structure.

The chemical structure of the difunctional acrylate used in this study is Tripropylene glycol diacrylate (TPGDA) given in figure 2.3. Monomer was provided by (UCB, Belgium).

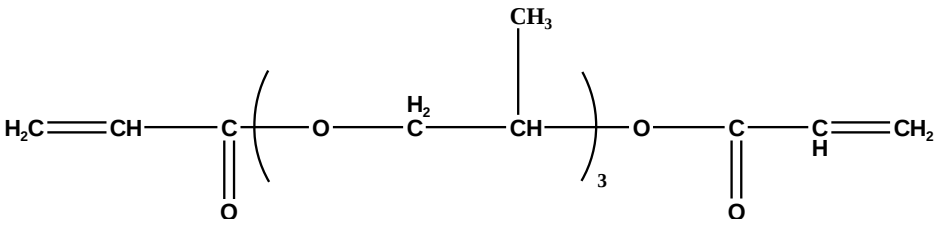

Figure 2.3: Chemical structure of TPGDA

TPGDA is clear liquid with low viscosity, low volatility high reactivity and good flexibility. Poly(TPGDA) has a glass transition temperature T_g of about 42 C.

2.2.2 The photoinitiator

Radical photopolymerization of acrylic monomers have been conducted by EB or UV irradiation; the UV curing reaction has been initiated by 2-hydroxy-2-methyl-1-phenylpropan-1-one photoinitiator also known as Darocur 1173. The structure is given in Figure 2.4. The photoinitiator was obtained from CIBA (Rueil Malmaison, France).

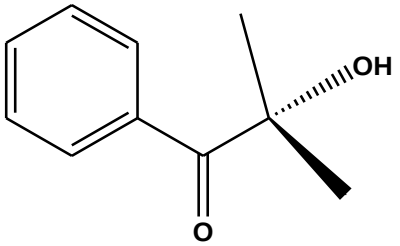

Figure 2.4: Chemical structure of the photoinitiator Darocur 1173

2.2.3 The solvents

i. Tetrahydrofuran (THF):

THF was used as solvent for preparation, extraction of polymer/liquid crystal and for gel permeation chromatography (GPC) analysis.

ii. Deuterated Chloroform ($CDCl_3$):

$CDCl_3$ was used as a solvent for all ^{1}H and ^{13}C NMR spectroscopic analysis.

iii. Methanol (CH_3OH)

Methanol was used as a solvent to extract the liquid crystal from the polymer matrix during preparation of NMR spectroscopy samples.

2.3 Preparation of polymer/liquid crystal composite

Mixtures of monomer and (Darocur 1173) are initially prepared; quantity of 5CB is ten added based on the required composition. The mixture is mechanically stirred for 12 hours ensuring that the final solution is homogeneous. It is known that oxygen presence has an inhibitory action on the radical polymerization under ambient atmosphere. However, tests carried out previously in our own laboratory showed that oxygen in the air had a negligible effect on the polymerization when the mixture is used between two glass slides. During FTIR analysis, samples were placed on NaCl crystals and rolled to a uniform thickness using wire rods, the whole is covered with a flat PET film to prevent oxygen inhibition. This slide is then fixed in a cassette and then exposed to UV or EB irradiation. Weight percents of the photoinitiator and the intensity of the irradiation doses have been varied to study the reaction mechanism and the internal structure of the polymer composites based on the selected reaction conditions.

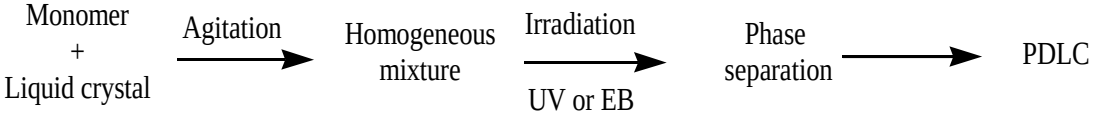

To insure normalized preparation and polymerization conditions for all measurements, photopolymerized samples for other analysis during this work have been prepared by placing several drops of the monomer/liquid crystal mixtures on a glass slide and rolled to a uniform thickness of about 100 µm and covered with a PET film as shown in figure 2.5.

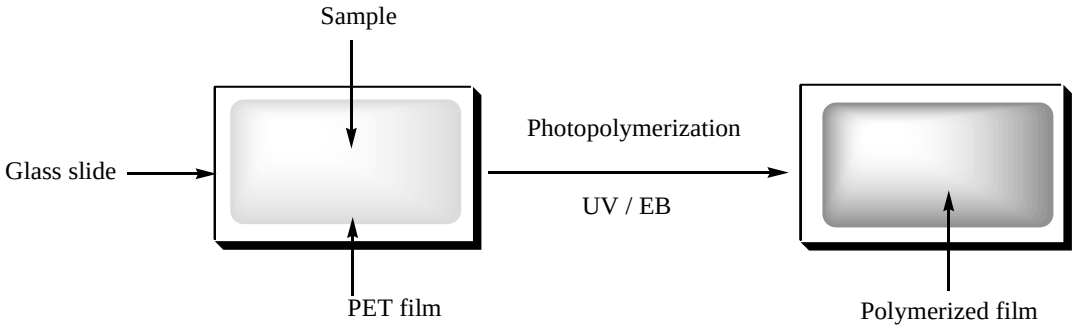

Figure 2.5: Preparation of the photopolymerized films

Different compositions of the monomer/liquid crystal samples used for the analysis of photopolymerization have been prepared based on mass percents of each component on the reactive mixture. No photoinitiator has been added to the mixture for EB cured samples.

2.4 The irradiation devices

Over the last few decades, many types of radiation curing devices have been developed to perform the photopolymerization process. Performance of the curing equipments largely depends on irradiation intensity, monomer type and desired application of the polymer film. To achieve highest curing efficiency, type and intensity of light exposure is critical. In UV curing, most curing films are accomplished using light ranging from about 200-450 nm. The wavelengths below 400 nm are considered UV, while output from 400-500 nm is visible. For a successful cure, the absorbance of the adhesive's photoinitiators must match the output of the selected light source. Furthermore, radiation curing includes other forms of radiant energy, including gamma, infrared, microwaves and electron beam. In electron beam curing, high irradiation intensity is capable of initiating the polymerization reaction by formation of radical species when attacking the double bond of the acrylate monomer, the generated radical species form reactive sites to form polymer films.

2.4.1 The UV irradiation device

Ultraviolet light is of 200 – 400 nm of electromagnetic spectrum and divided into three groups, UV with 200 – 280 nm, UV with 281 – 315 nm and UV with 316 – 400 nm. UV light from mercury lamp has the highest UV output at 224 nm.

UV irradiation device is Minicure MC4-300 Primarc UV Technology shown in figure 2.6, equipped with two medium pressure mercury lamp was used. Mixtures were fixed in a tray

which was passed under irradiation source using a conveyor belt. UV doses on the sample were adjusted by controlling the speed of the conveyor belt of the UV device. The machine is equipped with two UV mercury lamps fixed on the top of the conveyer belt. Irradiation dose was measured by UV dosimeter to select the required intensity. Power supply can be used to control the irradiation dose in case of working at very low irradiation doses. The reactive mixture is placed on a glass slide with about 100 µm and covered with PET film to prevent exposure to oxygen. The glass slide is fixed in a cassette and allowed to pass under UV light on the conveyer belt. Exposure time for each passage under UV light is estimated based on the conveyor belt speed when the sample passes under UV light.

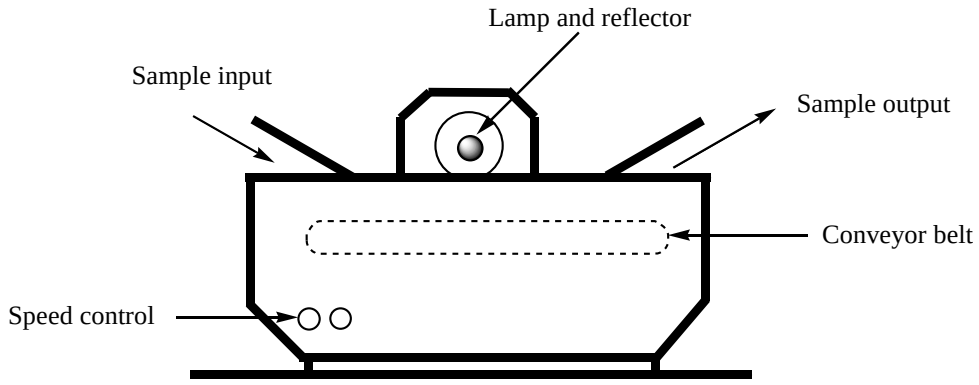

Figure 2.6: The UV irradiation device.

2.4.2 The EB irradiation device

Electron beams are an extremely efficient form of energy for industrial processes especially radiation curing to produce polymer films. Advantages of electron beam curing came from the low energy consumption and less harmful chemicals that lower the physical and chemical properties of the products. Electron beam is considered more environmentally friendly than thermal methods

Principle of electron beam consists mainly of power supply and electron beam acceleration tube. Power supply increases and rectifies line current and the accelerator tube generates and focuses the beam and controls the electron scanning. The beam is produced when high voltage energizes causing electrons to be produced at high rates. These fast electrons are concentrated to form high energy beam and are accelerated to full velocity inside the electron gun. EB unit used Electrocurtain vacuum gauge model CB 150 (Energy Sciences, Inc.), consists of high (175 kV) voltage electron tube that provides a continuous energetic electrons from a linear

filament or cathode, which is on the axis of symmetry of the system. The cylindrical electron gun directs and processes the electron beam in a grid-controlled structure. The opening is covered with a thin metal foil, usually titanium, which allows electrons to pass but maintains the high vacuum required for high free-path lengths. The stream is then accelerated across a vacuum gap to a metal window where it emerges directly into air and passes on the sample as presented in figure 2.7.

The unit parameters of the power, current and dose rate are 175 kV, 0.2-8 mA and 1 – 10 kGy respectively, where kGy =1 J/g per unit mass of material. Conveyer speed of the machine can be varied 50-500 feet/min.

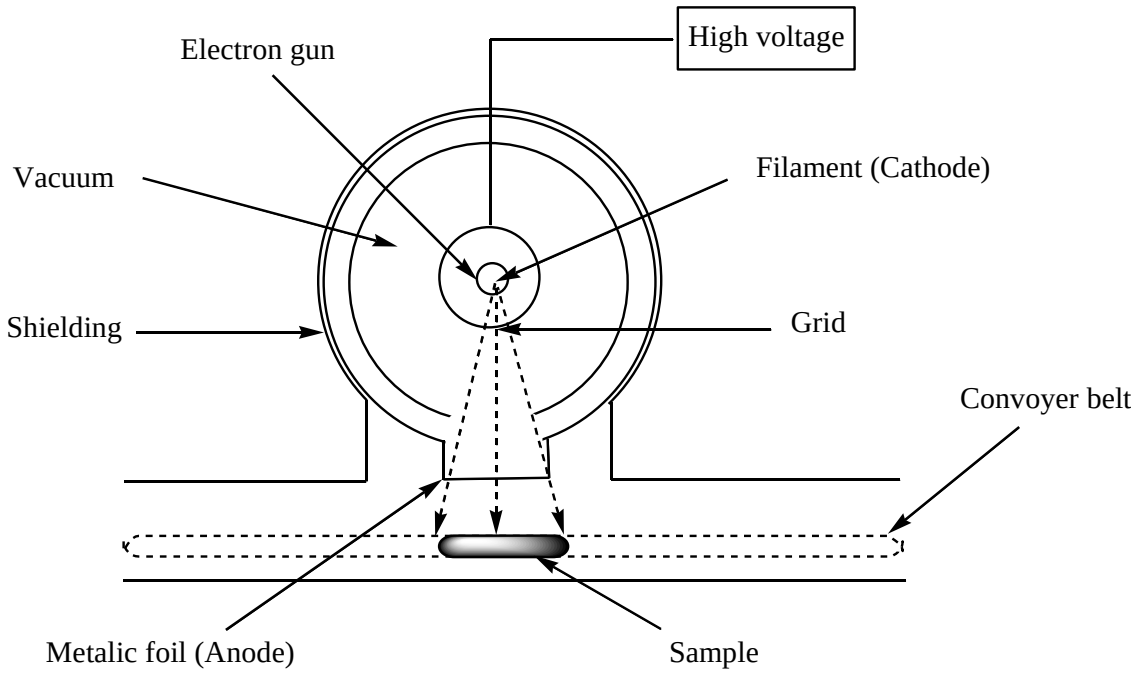

Figure 2.7: Schematic diagram of the mechanism of EB generation.

The energetic electrons from the processor penetrate the sample, where they create initiating free radicals. Polymerization process propagates until growing chains are terminated. Energetic electrons can penetrate many different types of materials and are capable of producing polymer composites. The power of the electrocurtain has a maximum-curing-film thickness range of 0.025 – 0.36 mm thickness.

Although electron beams have several advantages over potential alternatives curing systems, they have some disadvantage that traditional systems are very large, expensive and regular maintenance. In particular, electron beam systems require vacuum pumping equipment, high voltage power supplies and complex shielding, as well as engineering and maintenance

expertise. As a result, it faces difficulties to integrate the electron beams devices into industrial equipments.

2.4.3 Radiation Dosimetry

In order to determine the amount of UV radiation absorbed by the samples, UV dosimeter was calibrated and used to measure the UV dose during the preparation of all UV cured films.

EB device was calibrated using the operation parameters based on the applied current, volt intensity and the conveyer speed to determine dose intensity by units of kGy.

2.5 FTIR spectroscopy

IR spectroscopy is an important technique in organic chemistry analysis. It is considered as a good method to identify presence of certain functional groups in a molecule. Furthermore, this technique can be used to identify pure compound or to detect the conversion of specific group in the mixture based on the unique absorption bands of these groups.

IR spectroscopy is known for years as a powerful tool for the characterization of polymers [3]. It is based on the absorption of infrared radiation by the analyzed material. Recently, this technique is used to study the polymer dispersed liquid crystals systems [4,5]. There are two kinds of information that can be obtained from the FTIR spectra:

i. Qualitative analysis: the wavelengths which the sample absorbs are characteristics of chemical groups present in the analyzed material. Absorbance of different chemical groups is assigned in tables to identify the composition of the material.

ii. Quantitative analysis: intensity of the absorption wavelength is related to the concentration of the chemical group in the sample, this relation can be expressed by Beer-Lambert law:

$$A = -\log\left[\frac{I_t}{I_0}\right] = \varepsilon \,.\, c \,.\, L \qquad (2.1)$$

where A is the absorbance, I_0 is the incident intensity, I_t the transmitted intensity by the sample, ε is the molar extinction coefficient (L mol^{-1} cm^{-1}), L is the optical path length corresponding to the crossed thickness (cm) and c is the concentration of absorbing species (mol / L).

FTIR spectra were measured in the range between 400 – 4000 cm^{-1} region with 16 scans and a resolution of 4 cm^{-1}. By measuring the IR absorbance corresponding to the double bond (C=C) conversion of acrylate group at 810 cm^{-1} before and after polymerization, we can calculate the monomer conversion rate by comparing the peaks obtained from the IR spectra as shown in figure 2.8.

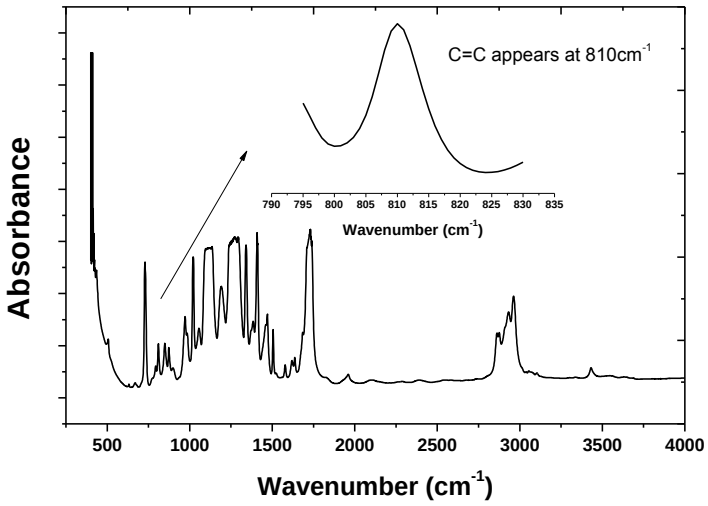

Figure 2.8: The IR plot of pure 2EHA monomer

Disappearance of characteristic peak by applying UV dose can be used to evaluate conversion percents using equation (2.2) to construct the kinetic curves:

$$\% \text{ Conversion} = \left[\frac{1-H_1}{H_0}\right] \times 100 \qquad (2.2)$$

The experiments carried out in this study are of two types:

i. Kinetic study: to study the polymerization under UV radiation for 2EHA with different photoinitiator percents (0.5, 1, 2, 4 and 6 wt %), the experiments were performed using an infrared spectrometer Fourier transform model Perkin Elmer 2000. This technique is mainly applied to study thin film samples (100 µm), monomer is sandwiched between NaCl slides and covered with flat PET film figure 2.9.

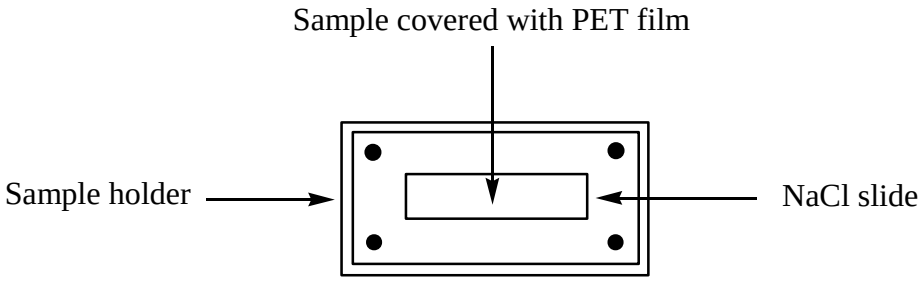

Figure 2.9: Sample preparation used in FTIR spectrometer.

ii. Polymer/Liquid crystal interaction: to study effect of different weight percents of liquid crystal on reaction kinetics, reaction rate measurements were performed at 30, 50 and 70 wt % of 5CB in the polymer matrix. Anther parameters can be elaborated from FTIR analysis like molecular configuration and interactions of polymer liquid crystals molecules.

2.6 Gel permeation chromatography GPC

GPC is a mode of liquid chromatography in which components of a mixture are separated on the basis of molecular size. Large molecules elute from the column with low elution time, followed by smaller molecules. It is an important tool for polymers analysis. The essential results are molecular weight data and molecular weight distribution curves. GPC is mainly used for samples with a molecular weight above 2000 g mol^{-1}, and also for separations of oligomers. Column packing is usually a rigid or semi-rigid totally porous material with pores of known size called stationary phase with a size distribution of pores of a few tens to thousands of Angstrom, which separates macromolecules according to their hydrodynamic volume. Figure 2.10 illustrates the mechanism of separation.

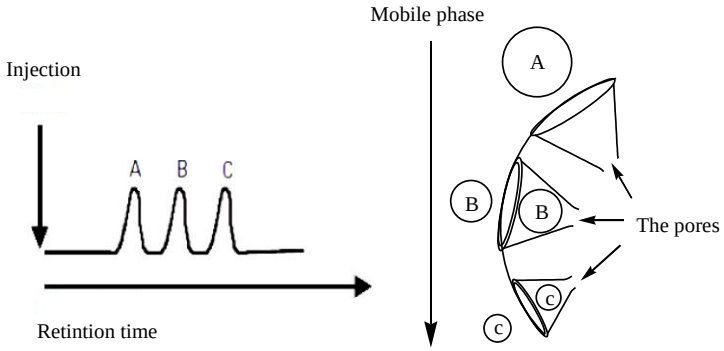

Figure 2.10: GPC separation mechanism in the column.

At the column exit, components are analyzed by a detector that measures the index difference between the reference (THF) and the sample to produce signals proportional to the polymer concentration. Molecular weight is represented by calibration curve and the elution volume is approximately linear function of molecular weight logarithm. Obviously, this function depends mainly on the pore size distribution of gel that is generally unknown. Consequently, the curve should be determined experimentally. This curve is then fitted with a polynomial equation to determine the characteristics of the calibration curve as shown in figure 2.11.

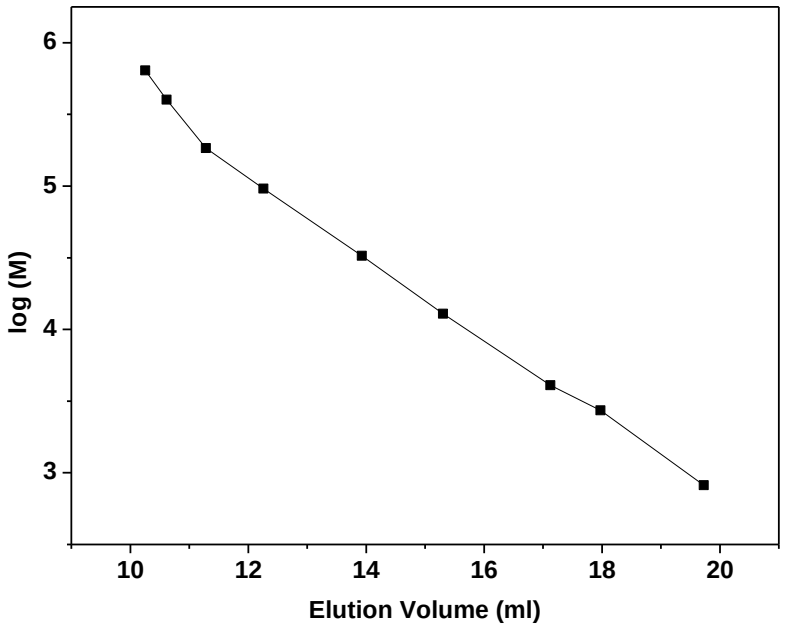

Figure 2.11: The calibration curve given by polynomial equation.

To summarize, GPC is a technique sensitive to the hydrodynamic size of polymer and generates a signal proportional to the amount of molecules, it therefore allows determining the molecular weight of polymers from standards and provides the conversion rate of monomer on the chromatogram.

Chromatographic analysis technique has the advantage to determine molar masses of polymer and its polydispersity, thus, we can follow the polymerization process according to the amount of irradiation dose applied and the composition of the reactive mixture. On the other hand, disadvantage of this technique is the needs to use standards (polystyrene) to be able to determine the molar mass of polymer, the detector is a differential refractometer; therefore the difference in refractive index between polystyrene and the polymer can generate some errors.

After polymerization, two series of samples were prepared for the GPC analysis. The samples have been prepared by dissolving about 30 mg of polymer in 10 mL of solvent (THF). Measurements of the molar masses by GPC were performed at T =25 C using a Waters apparatus and polystyrene standards were used for calibration. Each experiment elapsed nearly 1 hour with a flow rate of 1 mL/min. The different peaks obtained from the GPC measurements were compared and analyzed to evaluate the molar masses and polydispersity of polymer chains. Operation of the GPC instrument can be schematically represented in the following diagram:

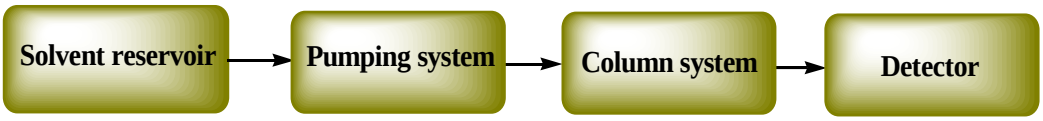

Figure 2.12: Schematic representation of the GPC device.

Thus, molar masses calculation of the polymer chains become possible by considering that the height h_i with an elution volume V_e corresponds to the concentration C_i. We can write:

$$Mn = \frac{\sum_i N_i M_i}{\sum_i N_i} = \frac{\sum_i C_i}{\sum_i C_i/M_i} = \frac{\sum_i h_i}{\sum_i h_i/M_i} \quad (2.3)$$

$$Mw = \frac{\sum_i N_i M^2{}_i}{\sum_i N_i M_i} = \frac{\sum_i C_i M_i}{\sum_i C_i} = \frac{\sum_i h_i M_i}{\sum_i h_i} \quad (2.4)$$

with M_n is the number average molecular weight, M_w is the weight average molecular weight, N_i is the number of molecules in volume and M_i is the mass number of the species in volume.

Molecular weights were determined at 25 C in THF (HPLC grade) at 1 mL/min rate using polystyrene standards on a Waters e2695 Autosampler GPC, a Waters 2414 Refractive Index Detector.

2.7 Thermal analysis characterization techniques

Thermogravimetric analysis (TGA) offers knowledge about thermal decomposition of polymer. On the other hand, differential scanning calorimetry (DSC) technique presents information about phase behavior and phase transitions in the polymer matrix. More insight about polymer network internal structure can be determined by thermal analysis: TGA, DSC and thermomechanical analysis (TMA). These techniques give useful information about

physical properties of the polymer, such as glass transition temperature T_g, melting point and thermal stability

2.7.1 Thermo gravimetric analysis TGA

TGA has been used to study the thermal stability of the polymer networks prepared by EB and UV curing. TGA measures mass change rate of a sample as a function of temperature in a controlled atmosphere. TGA analysis can analyze polymer materials that exhibit either mass loss due to decomposition, oxidation or loss of volatiles such as moisture. The experiments were conducted using a TGA-Q600 instrument (Perkin Elmer) using an amount of about 6 mg of polymer sample. The starting temperature was 40°C with a heating rate 10°C/min and the end temperature was 600°C. The basic instrumental requirements are: a precision balance, a programmable furnace and recorder, schematic diagram of the TGA device is shown in figure 2.13. In addition, provisions are made for surrounding sample with air, nitrogen or an oxygen atmosphere based on the required experimental conditions.

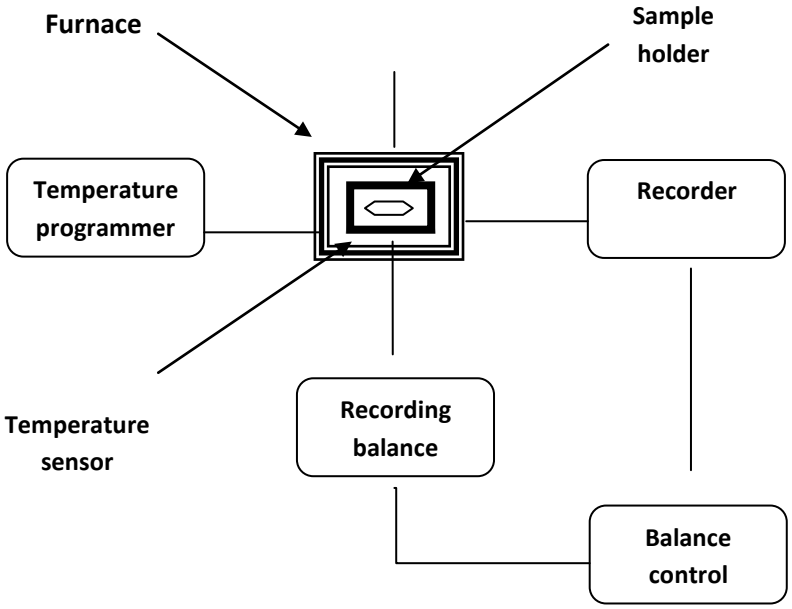

Figure 2.13: The basic components of TGA instrument.

2.7.2 Differential Scanning Calorimetry DSC

DSC is widely used to characterize thermophysical properties of polymer composites, in which the difference in the amount of heat required to increase the temperature of a sample

and the reference is measured as a function of temperature. Both sample and reference are maintained at very nearly the same temperature throughout the experiment. Generally, temperature program for a DSC analysis is designed such that the sample holder temperature increases linearly as a function of time. Reference sample should have a well-defined heat capacity over the range of temperatures to be scanned. The basic principle underlying this technique is that, when the sample undergoes a physical transformation such as phase transitions, more (or less) heat will need to flow to it than the reference to maintain both at the same temperature.

DSC measurements were performed on a Seiko DSC 220C instrument equipped with a liquid nitrogen system. The cell was purged with nitrogen at a rate of 50 mL min^{-1}. The heating–cooling ramp was used for DSC measurements in the temperature range -70 to 100°C. Polymer glass transition temperature was determined from the midpoint of the transition range. Enthalpy changes associated with crystalline–nematic (ΔH_{C-N}) and nematic–isotropic (ΔH_{N-I}) transitions are expressed as J g^{-1}. Calorimeter is calibrated with indium standards. The DSC program presented in figure 2.14 consisted first in cooling the sample followed by three heating and cooling cycles at a rate of 10°C min^{-1}.

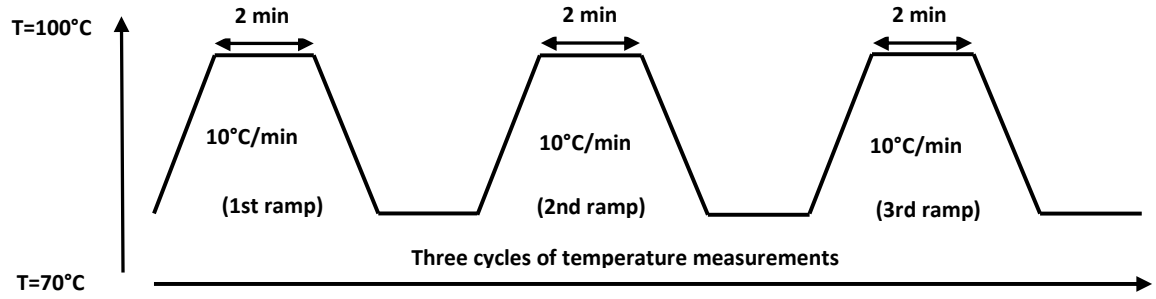

Figure 2.14: Temperature program applied during the DSC analysis.

2.7.3 Characterization by polarized light microscopy POM

Optical light microscopy (POM) is an ideal tool to determine phase transition and morphology of the composites. Determination of transition temperatures depending on composition of the PDLC can then be used to plot the corresponding phase diagram.

Thermo-optical device helps to determine the transition temperatures and morphology of the samples is represented in Figure 2.15.

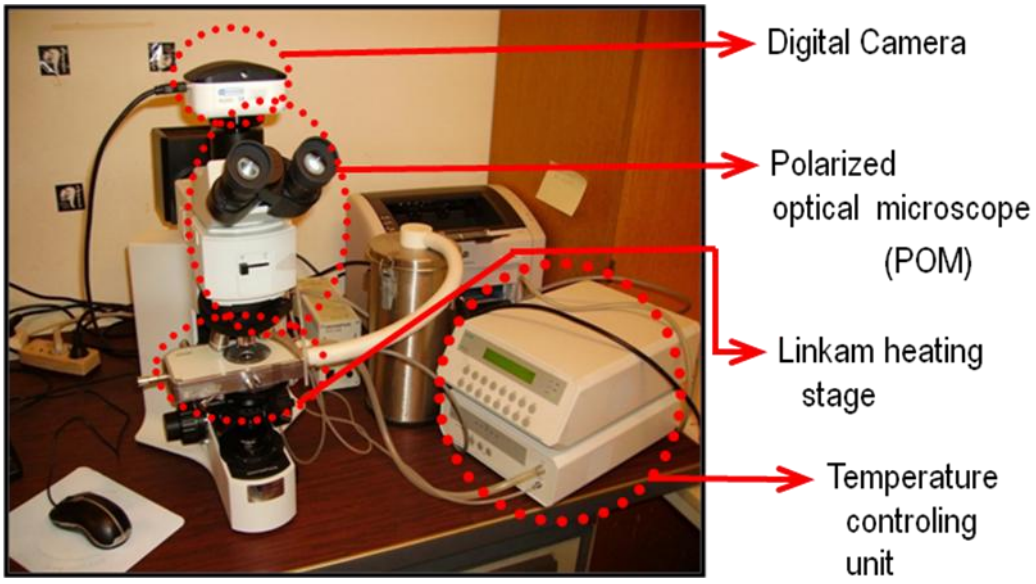

Figure 2.15: Schematic diagram of the optical microscope.

The composite mixtures were submitted to a heating ramp of 5 °C/min from room temperature to 15°C above transition temperature (first ramp up) and left for 5 min in isotropic state. Afterward, they were cooled below room temperature at a rate of -5 °C/min (first ramp down). This procedure was followed after 5 min by a second heating ramp at a rate of 1 °C/min (second ramp up) and left for 5 min in isotropic state. Subsequently, samples were cooled at a rate of -1 °C/min (second ramp down). The second heating/cooling cycle was repeated (third ramp up and third ramp down). Differences between maxima and minima of temperature exceeded 50°C in order to cover a large domain of the phase diagram. Transition temperatures were recorded during three successive heating and cooling ramps. The sample is then ready for microscopic analysis. In order to verify the reproducibility of results, three samples were prepared independently for the same composition. All samples exposed to the same heat treatment shown in Figure 2.16. They undergo three cycles of rise and fall in temperature during which measurements are made.

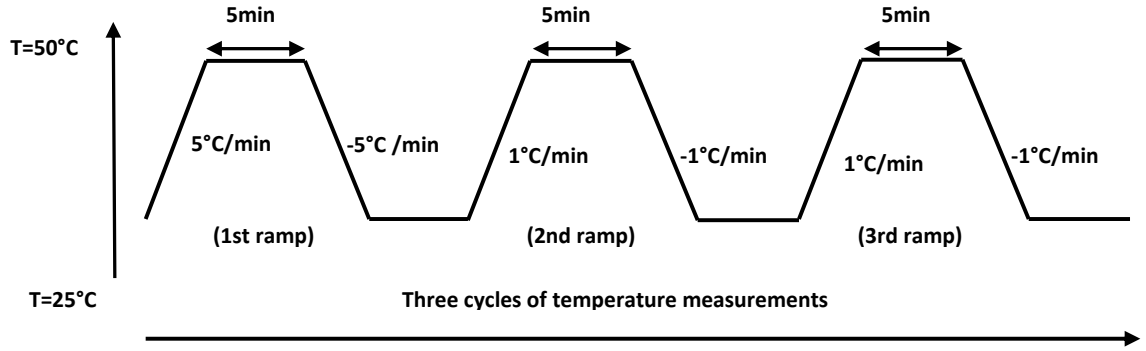

Figure 2.16: The temperature program applied during the POM analysis.

2.8 Dynamic mechanical analysis DMA

Viscoelastic properties of a polymer solution depend on concentration and molecular weight of polymer. Measuring these mechanical properties give idea about molecular weight of polymer chains, mechanical behavior of the acrylate polymers and describe the internal morphology of the polymer blend based on the variation of these properties. Viscoelastic properties of the material can be usually described by the storage shear modulus G' and the loss shear modulus G".

A rheometer is a typical instrument that measures the viscosity over a wide range of shear rates, and determines the viscoelasticity of fluids, semi-solids and solids.

Dynamic mechanical properties of the UV and EB curable films were conducted using Rheometrics dynamic mechanical analyzer type Physica MCR 301 instruments shown in figure 2.17. Temperature dependence of the viscoelastic properties such extension storage moduli E' =3G' or shear storage moduli G', extension loss moduli E" =3G" or shear loss moduli G", and dynamic loss tangent tanδ were measured at 1 Hz and 5°C/min heating rate. An amount of 0.5 g polymer sample was used to perform the analysis.

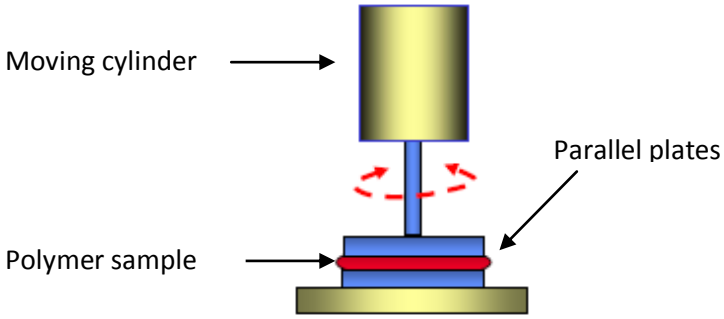

Figure 2.17: Schematic diagram for rheometrics dynamic mechanical analyzer.

Recognize that a rheometer is considered a highly sensitive device to quantify the viscoelastic properties of polymers, and can be used to determine apparent properties under a wide range of testing conditions, which can be used as a material benchmark.

2.9 Gel fraction measurements

During photopolymerization of acrylic monomers, formation of short and long chain branches during the process leads to insoluble fraction of the polymers usually called polymer gel. A possible mechanism for formation of gel due to intermolecular and intramolecular chain transfer to polymer followed by termination by combination leads to such morphology of polymer chains.

Gel fraction was determined using extraction with THF as a solvent at room temperature. 20 mL of THF was added and mixed with 50±5 mg of polymer sample in 25 mL vials. The mixtures were held at room temperature for 24 hours in triplicate.

Insoluble gel phase was separated from the sample by filtration. The separated gel phases were dried in the oven at 80 C for 3 hours followed by drying under vacuum at 50 C for 24 hours. The gel content was calculated as the ratio between dried weight and the initial weight. The swollen weight was determined by the difference between the weight of original sample and weight of collected gel.

A filter (weight W_1) was dried overnight at room temperature. This filter with the dried polymer was weighed (W_2) before performing extraction. After extraction, the filter contained the non-soluble polymer gel, was dried at room temperature during one night and weighed again (W_3). The amount of gel was calculated as:

$$Gel\ content = \frac{W_3 - W_1}{W_2 - W_1} \quad (2.5)$$

Swelling of polymer samples was calculated as the ratio between weight of swollen gel polymer and dry weight of gel polymer.

2.10 Nuclear Magnetic Resonance (NMR) spectroscopy

Proton nuclear magnetic resonance (^{1}H NMR) and Carbon nuclear magnetic resonance (^{13}C NMR) spectra were performed at room temperature using a Varian Associates Unity 300 spectrometer operating at 125.8 MHz with 10 mg/cm^3 solutions of polymer in $CDCl_3$. Chemical shifts were referenced to the solvent resonance which was taken at 77.0 ppm. In order to maximize the signal-to-noise ratio in a given time, spectra were run with continuous proton decoupling using a pulse interval of 0.5s and a flip angle of 45 . Under these conditions, relative intensities do not necessarily reflect relative abundance of each type of carbon because of differential relaxation times and nuclear Overhauser enhancements (NOE) [6]. Intensities of primary and quaternary carbons are underestimated relative to CH and CH_2 carbons. A critical peak in this work is observed at 48 ppm representing quaternary carbon, arising from a branch point generated by the chain transfer to polymer.

Characterization of internal polymer structures and degree of branching in the polymer matrix were analyzed based on:

1) Chemical shifts of the different carbons and intensities of the peaks in the ^{13}C NMR spectrum recorded on the selected polymer samples;

2) Multiplicity of carbons was determined by the technique of distortionless enhancement by polarization transfer (DEPT) for some samples, and the obtained spectra of the polymerized samples were compared with the original pure monomer sample.

3) Chemical shift of the different hydrogen in the samples have been obtained by ^{1}H NMR spectra were obtained for the polymer samples.

4) Correlations between carbons and their neighboring carbons and hydrogen were analyzed by comparing spectra of the polymer samples based on preparation conditions and composition of the polymer composites.

5) All samples were prepared and purified under normalized conditions for comparison purposes to insure the quality of analysis.

After free radical photopolymerization, samples have been collected by dissolving polymer composite in tetrahydrofuran THF as a suitable solvent. THF is then removed by evaporation under vacuum. The recovered residue contains a mixture of polymer and 5CB. The residue was washed five times with methanol to remove any traces of 5CB and dried in vacuum oven at 60°C.

In order to conduct the NMR analysis, 10 mg of the purified polymer is dissolved in 1 mL $CDCl_3$. Proton ^{1}H and carbon ^{13}C analysis have been conducted for each sample of our concentration domain (P2EHA, 70, 50 and 30 wt % 2EHA/5CB) prepared at different preparation conditions under UV and EB curing.

2.11 References

[1] G. Luckhurst, R. Stephans, R. Phyppen. Liq. Cryst, 8, 451 (1990).

[2] K. Abe, A. Usami, K. Ishida, Y. Fukushima, T. Shigenari, Journal of the Korean Physical Society, 46, 1 (2005).

[3] J.L. Koeing, Spectroscopy of polymers, Second edition, Elsevier Science (1999).

[4] W. Bentley, J.L. Koenig, Appl. Spectroscopy, 51, 1453 (1997).

[5] R. Barghava, W. Shi-King, J.L. Koenig, Macromolecules, 32, 8989 (1999).

[6] N. M. Ahmad et al, Macromol. Rapid Commun., 30, 2002–2021(2009).

3 KINETICS STUDY OF FREE RADICAL POLYMERIZATION OF ACRYLATES

3.1 Introduction

Kinetics of acrylates free radical polymerization has a major influence on structure and properties of the acrylic polymer. During polymerization, it is highly important to study the effect of polymerization conditions and the internal structure of the monomer on the reaction kinetics. Advantages UV and EB cured polymerization are ease of reaction control and the reactions can be carried out under different conditions. In this chapter, effect of the polymerization conditions on kinetics of free radical polymerization will be discussed. Complete understanding of the mechanisms of curing process is important to improve materials development and polymer composites with desired characteristics. Therefore, influence of irradiation dose, the photoinitiator concentration, liquid crystal concentration and the type of functional group will be investigated. In addition, kinetics of UV and EB will be briefly discussed. Fast polymerization rate can be translated into a minimum exposure time and low radiation intensity [1].

Exposure of acrylate monomer to EB radiation leads to formation of radical species by attacking the monomer vinyl group, the reaction proceeds by free radical polymerization. Whereas, UV curing reaction is initiated by dissociation of photoinitiator to form radical species, initiators in radical photopolymerization play a major role in radiation curing to achieve desired polymer network. Efficiency of the photoinitiator can be determined by its sensitivity to UV irradiation to form radical species. A remarkable effect of atmospheric oxygen on the photoinitiator as a result of reaction with carbon based radicals to form epoxy radicals that are less reactive toward the monomer double bond. Thus, photoinitiated reaction of acrylic monomer in this study was carried out by covering the reactive mixture with PET film to eliminate the influence of oxygen during the reaction. Effect of liquid crystal on kinetics of radical photopolymerization will be investigated under different concentrations of monomer/LC composites. On the other hand, irradiation rate in the radical polymerization enhances the cleavage of photoinitiator in UV curing, while in EB curing, irradiation rate increases the cleavage of the monomer double bond, which leads to higher reaction rates during polymerization.

3.2 Mechanism of free radical polymerization

Overall structure of free radical photopolymerization is based on four main steps: initiation, propagation, termination and chain transfer. Only initiation, propagation and termination are considered in the kinetic study based on steady state assumption for the monomer and initiator radicals. Formation of a single chemical bond between two monomers is formed by opening the double bond between the two carbons of acrylate group. This is caused by reaction with radicals, radical polymerization reaction can be described by reaction mechanisms during polymerization that include, initiation, propagation, termination, chain transfer, inhibition and autoacceleration.

3.2.1 Initiation

Initiation step consists of two stages, the first is formation of radicals that are organic molecules containing an unpaired electron. Radicals are generally considered unstable species because of their very short lifespan. Decomposition of an initiator I is common way to produce a pair of radicals R. This decomposition can be thermal or photochemical (usually done by UV radiation but also with EB).

$$I \xrightarrow{h\nu} 2R^{\cdot} \qquad 3.1$$

In this study, 2-hydroxy-2-methyl-1-phenylpropan-1-one (Darocur 1173) as photoinitiator; the decomposition mechanism is presented in figure 3.1:

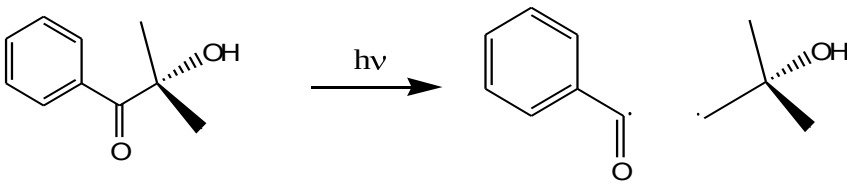

Figure 3.1: Decomposition of the photoinitiator (Darocur1173).

The second step of initiation involves the addition of the initiator radical $R^{\cdot}$ to the first monomer molecule to produce the "real" chain initiating species $M_1^{\cdot}$:

$$R^{\cdot} + M \xrightarrow{k_i} M_1^{\cdot} \qquad 3.2$$

where k_i is the rate constant for the initiation step.

In case of monoacrylate monomer (2EHA), addition of radical occurs at the double bond result in producing a new chain radical.

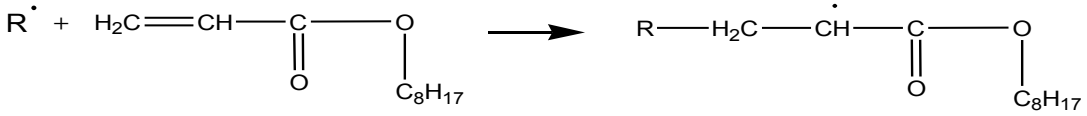

Figure 3.2 : The formation of 2EHA radicals.

While TPGDA undergoes addition of radical on both functional groups to form diradical species, followed by formation of crosslinked network where propagation reaction take place as given in figure 3.3.

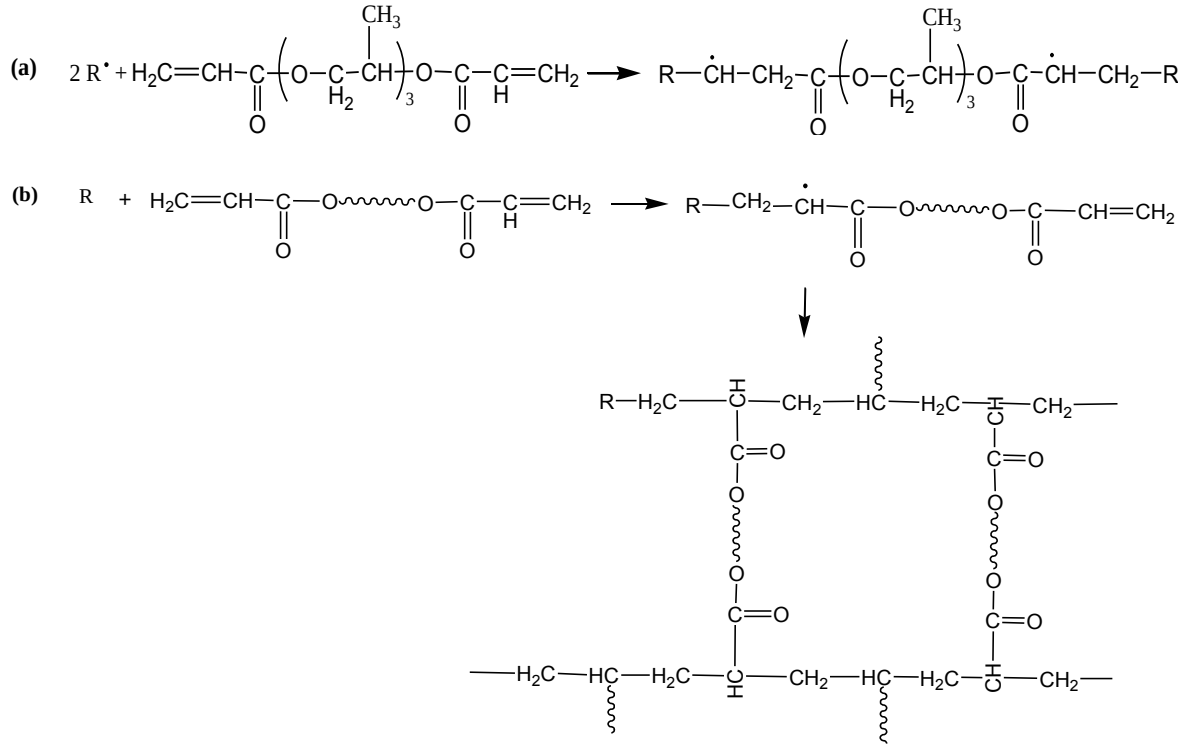

Figure 3.3: Polymerization mechanism of TPGDA, (a) the formation of radical species and (b) the propagation reaction and crosslinking.

3.2.2 Propagation

Propagation step is considered the main step in radical polymerization. Generated radical attacks the monomer double bond to form a new radical. The process involves radical growth of polymer by successive addition of a large number of monomer molecules which known as the chain reaction. As propagation continues, the radical has the same identity as the radical before except that it is larger by one unit:

$$M_n^{\cdot} + M \xrightarrow{k_p} M_{n+1}^{\cdot} \qquad 3.3$$

with k_p is the rate constant of the propagation steps. Chain growth to higher molecular weight polymer takes place very rapidly. During chain reaction, the decrease in monomer concentration leads to slower growth of the polymer chains that result in reducing mobility of monomer molecules due to increase of viscosity of reactive mixture.

3.2.3 Termination

At a certain point during propagation reactions, polymer chain stop growing and the reaction terminates. Termination of radical centers occurs by bimolecular reaction between two radicals. They react with each other by coupling or by disproportionation. Both modes of termination can be expressed by:

Coupling $$M_x^{\cdot} + M_y^{\cdot} \xrightarrow{k_{tr}} M_{x+y} \qquad 3.4$$

Disproportionation $$M_x^{\cdot} + M_y^{\cdot} \xrightarrow{k_{td}} M_x + M_y \qquad 3.5$$

where k_{tr} and k_{td} are the rate constants for termination by coupling and disproportionation, respectively.

Termination reactions may occur by the reaction of growing chain with another radical or by a transfer reaction. Furthermore, radical species may trap in the polymer network and terminate propagation reaction at this end radical.

3.2.4 Chain transfer

Kinetic mechanism for chain transfer occurs at low monomer concentration in the reactive mixture usually at the end of a radical polymerization when almost all monomer has been consumed. Chan transfer takes place with monomer independent of the reaction rate whereas, chain transfer to solvent takes place at higher polymerization rate. Detailed mechanism and kinetics of chain transfer is presented in chapter 5 of this study.

3.2.5 Inhibition

Inhibition is a common reaction in radical polymerization that may take place by side reactions under exposure of radiation to form new reactive radicals which attach the unsaturated sites of the acrylate monomer and result in new undesired compounds that terminate the propagation reaction.

The most common inhibition reactions occur by presence of oxygen during polymerization. The acrylate radicals may react with oxygen to form low reactive peroxy radicals.

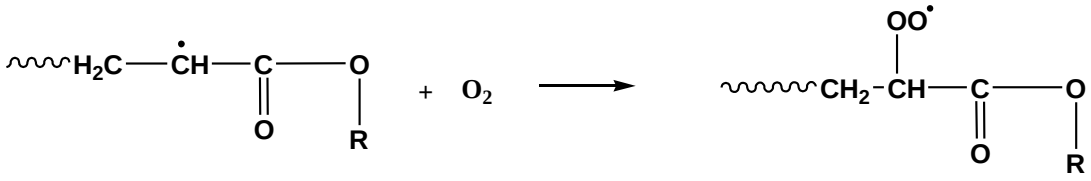

Figure 3.4: Formation of peroxy radicals in the presence of oxygen.

Thus, presence of oxygen may lead to side products which change morphology of the polymer matrix and affect polymerization rate. Samples in this study have been prepared under inert gas or covered with PET film to avoid the inhibition effect of oxygen.

3.2.6 Autoacceleration

Autoacceleration is observed at high initiator concentration above 2 wt % mostly in difunctional and multifunctional systems, which result in sharp increase in the polymerization rate. Formation of polymer networks reduces mixture viscosity, which decrease the diffusion of growing chains and radical species that leads to increase termination by combination. Autoacceleration makes polymerization reaction further out of control, thus lower radiation dosed and initiator concentration are usually applied to control the polymerization rate.

3.3 Kinetic of free radical UV polymerization

UV light initiates the reaction by the activation of initiator to produce radical species. These radical attacks the double bond of monomer to form chain radical site. Efficiency of UV curing process is related to the quantum yield of the photoinitiator, which can be defined as the amount of initiated radicals per absorbed photon. The quantum yield of photoinitiator is dependent on the initiator concentration and UV light intensity.

Different reaction in radical polymerization can be considered by establishing the kinetic equations, as first order for all reactive species. Certain approximations are made In order to derive kinetic equations for these reactions. Firstly, initiation rate R_i is the same as initiator decomposition rate R_d. Relation between the initiation rate UV light intensity can be expressed based on equations (3.1) and (3.2):

$$R_i = \Phi I_a \qquad 3.6$$

$$R_p = k_p[M_n^{\cdot}][M] \qquad 3.7$$

$$R_t = k_t[M_n^{\cdot}]^2 \qquad 3.8$$

where Φ indicates the initiation quantum yield, I_a the light intensity effectively absorbed by the sample.

The second assumption that propagation rate constant K_p is independent of degree of polymerization. Since all the monomer molecules are consumed during propagation, R_p can represent overall polymerization rate:

$$-\frac{d[M]}{dt} = R_p = k_p[M_n][M^{\cdot}] \qquad 3.9$$

Kinetic equations for the termination rate can be expressed by:

$$R_{tc} = 2\,k_{tc}[M\,\square]^2 \qquad 3.10$$

$$R_{td} = 2\,k_{td}[M\,\square]^2 \qquad 3.11$$

It was assumed experimentally that number of chains remains constant during reaction, and concentration of free radicals quickly reaches a value which does not substantially change. This assumption is kinetically known as steady state assumption, which can be expressed as $d[M\,\square]/dt = 0$ and $R_i = R_t$:

$$[M\,\square] = \sqrt{\left(\frac{\Phi I_a}{k_t}\right)} \qquad 3.12$$

Combination of equations 3.9 and 3.12, the propagation rate becomes:

$$R_p = k_p[M]\ \sqrt{\left(\frac{\Phi I_a}{k_t}\right)} \qquad 3.13$$

Therefore, polymerization rate is dependent on monomer concentration, square root of irradiation rate and initiator quantum yield. Furthermore, kinetic chain length K_{CL} and quantum yield of photopolymerization may decrease with increasing radiation rate.

$$K_{CL} = \frac{R_p}{R_i} \qquad 3.14$$

Polymerization quantum yield can be expressed in terms of effective irradiation rates as:

$$\Phi_p = \frac{R_p}{I_a} \qquad 3.15$$

Experimentally, polymerization quantum yield is not strongly influenced by irradiation rate and the kinetic chain length leads to the conclusion that, higher UV rate accelerate bimolecular termination mechanism over chain propagation [2].

Polymerization rate given in equation 3.13 is limited when describing polymerization kinetics of multifunctional monomer.

3.4 Kinetics of free radical EB polymerization

EB interaction with monomer produces excited states which undergo secondary reactions to produce free-radical intermediate species. Resulting chemical reactions are caused by the excited species and the formation of reactive intermediates [35].

Initiation rate of EB radiation polymerization can be expressed by:

$$R_i = G\rho \mathrm{I} \qquad 3.16$$

where G is radiation yield of radicals, ρ is monomer density in (g cm^{-3}), and I is dose rate $\mathrm{Gy\ s^{-1}}$. Combination of equations 3.12 and 3.14 based on steady state assumption, polymerization rate of EB polymerization can be given by:

$$\mathrm{R_p = k_p[M]}\sqrt{\left(\frac{\mathrm{G\rho I}}{\mathrm{k_t}}\right)} \qquad 3.17$$

As shown in equation 3.15, polymerization rate of EB reactions is derived to be proportional to the square root of the radiation dose.

The major termination reaction in radical polymerization of acrylates is mainly occurring by bimolecular combination of the propagating chains [3]. During polymerization reaction, radical species undergo propagation or termination. Termination rate is found to be dependent on the diffusion of species, at which termination rate is decreasing by increasing conversion rate that lead to low mobility chains. Mechanism of termination and propagation depend on concentration of radical species that can be determined by several parameters from which the radiation intensity and monomer structure.

EB radiation produce excited molecules and secondary reactions through the following mechanism shown in figure 3.5:

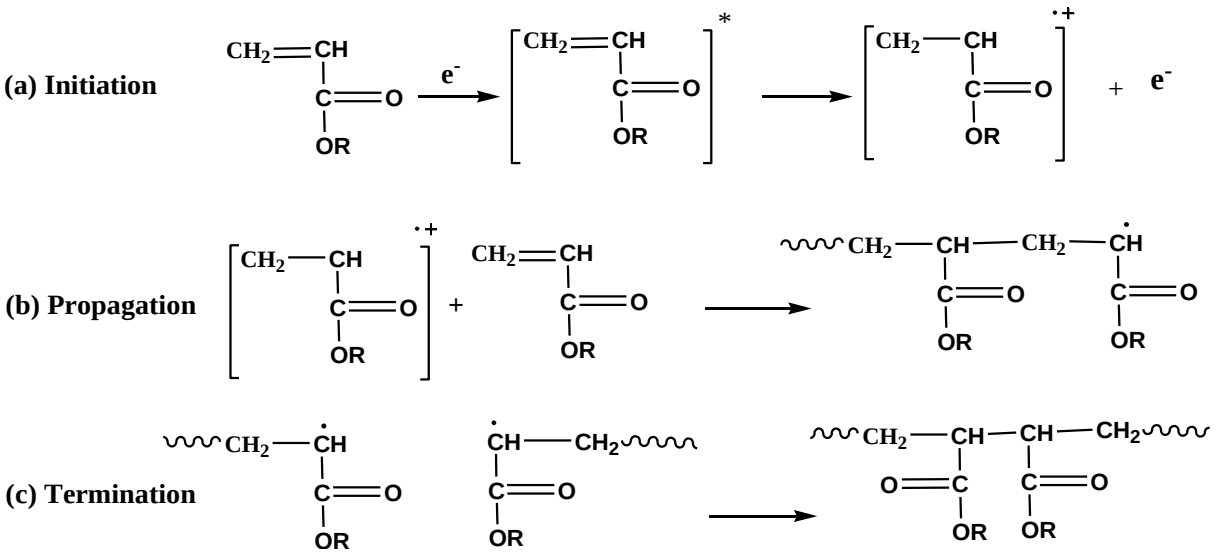

Figure 3.5: Polymerization mechanism of 2-ethylhexyl acrylate (a) initiation, (b) propagation, (c) termination under EB irradiation. R= 2-ethylhexyl.

The first step involves formation of primary radicals and exited species upon exposure to EB radiation. The monomer forms a radical anion which reacts with the monomer double bond to form stable neutral free radical that initiates the radical polymerization reaction. This step is expected to take place extremely fast. Monomers add to the radical species in the propagation step on growing chains. Reaction termination occurs by combination of two polymer chain radicals [4,5].

Further EB exposure of polymer may result in change of internal structure due to cross-linking and degradation reaction mechanisms. Cross-linking reaction mechanisms on polymer usually involve formation of bonds between chain radical of growing chains. These radical intermediates can then combine to form a single macromolecule. This combination results in increasing average molecular weight of starting polymer. Continuous EB radiation on the polymer will result in larger macromolecules with huge molecular weights having different physical properties with low solvent solubility and higher melting point from original polymer. High reaction rate may lead to increases the possibility coupling reactions to form large amounts of gel.

Species produced during propagation and termination step can be identified by kinetic curve. Detailed analysis of molecular weight distribution (MWD) of the polymer chains followed by

NMR spectroscopy to study the structure and morphology of polymer matrix will be discussed in chapters 5 and 6 of this thesis.

3.5 Monofunctional and multifunctional systems

Monofunctional acrylates usually follow elementary free radical polymerization kinetics which includes initiation, propagation chain transfer and termination. While, multifunctional systems show different features due to presence of multi-radical species in the reactive system and the reaction kinetics become more complicated than the simple monofunctional systems.

In monofunctional systems, chain transfer and bimolecular combination lead to reaction termination which results in losing reactive radicals. Termination is diffusion controlled, where termination rate depends on the motion of species during polymerization and would vary with conversion. Accordingly, termination rate constant is a function of radical chain length [6]. In addition, length of monomer group affects both polymerization rate and polymer final properties. Thus, high molecular weight monomer may polymerize slower. The hardest materials are obtained with short chain monomer, while monomers of long aliphatic chain lead to poor mechanical properties.

3.5.1 Effect of monomer structure on conversion rate

Effect of monomer structure on the kinetics of polymerization has been a subject of several research interests. Higher degree of functional groups in difunctional and multifunctional acrylates lead to increase the polymerization rate. However, dense polymer matrix reduces mobility of monomer molecules which leave many monomer molecules unreacted. Furthermore, length and type of chain connected to the functional group play a considerable role in the polymerization kinetics. Short chain monomers may lead to lower homogeneity in the polymer network. While on the other hand, long chain monomers have high conversion rate due to less cyclization of the polymer chains [7]. Spacer in the monomer molecules also affects the polymerization rate, this behavior was observed in ethylene glycol dimethacrylate and alkilenediol dimethacrylate [8].

3.6 Polymerization rate vs. polymer/LC interactions

Polymeric/LC composites have been a subject of many research interests that showed the unique behavior of polymerization kinetics in ordered liquid phase media. Presence of liquid crystal will alter the alignment of monomer molecules during curing process. Accordingly,

this will affect polymerization rate and will have a significant impact on structure and properties of the polymer/LC networks. In different mono and difunctional acrylates, a significant increase in polymerization rate has been observed for monomer/LC composites [9,10].

Exposing a homogenous monomer/LC precursors to irradiation source, chemical response of the initial mixture will change as polymerization process proceeds, which will lead to reducing miscibility of liquid crystal and growing polymer chains in the reactive mixture, at certain limit of miscibility, a phase separation occurs [11]. Liquid crystal phase separation results in forming droplets, as reaction proceeds, these droplets continue to grow until end of reaction. Liquid crystal phase shows a discontinuous Swiss-cheese morphology [12]. On the other hand, polymer chains separates in the form of particles connected to each other where liquid crystal phase occupies the gaps in the polymer structure to form polymer morphology referred to as polymer ball morphology [13].

3.7 Experimental study of the conversion rate

Maximum irradiation dose required to achieve highest conversion of monomer can be determined by FTIR spectroscopy. IR measurement has been used to conduct series of measurement without affecting produced polymer that enables us to track the actual evolution of the monomer during polymerization.

In fact, several studies reported effect of polymerization condition during formation of PDLC's on the polymerization kinetics. Structure of both monomer and LC in the initial mixture largely determines segregation of liquid crystal phase. Ordered liquid crystal phase leads to increase local concentration of double bond, therefore, polymerization rate increases [14,15].

3.7.1 Composition of reactive mixture

Reactive mixture used in this study for UV curing include 2EHA as monofunctional monomer, Darocur 1173 as photoinitiator and different weight percents of 5CB were added between 10-100 monomer to liquid crystal weight ratio. The same mixtures have been prepared for the diacrylate (TPGDA) systems. EB polymerization has been performed without photoinitiator. All mixtures have been prepared at normalized conditions, and each

measurement has been repeated three times to insure reproducibility of measurements. Preparation of polymer films is schematically presented in figure 3.6.

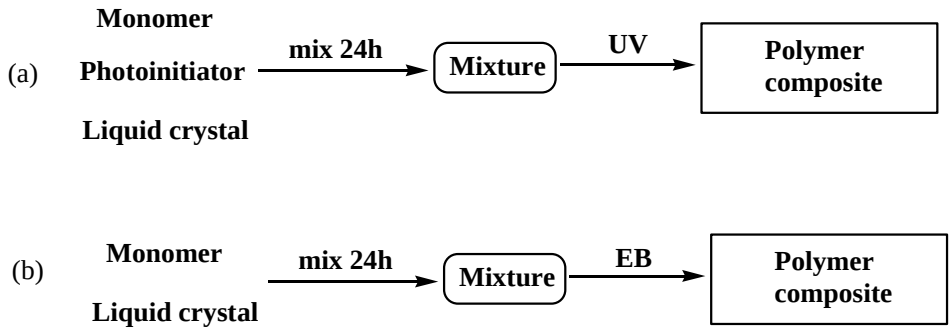

Figure 3.6: Preparation of polymer composites by (a) UV curing and (b) EB curing.

3.7.2 Reaction rate of pure monomer

Double bond (C=C) band appears at 810 cm^{-1} in FTIR spectroscopy presented in figure 3.7. This signal has been selected because it has no interaction with other liquid crystal signals. It is clearly observed evolution of this band during the polymerization by successive UV doses until the disappearance of the double bond band in the spectra as given in figure 3.8.

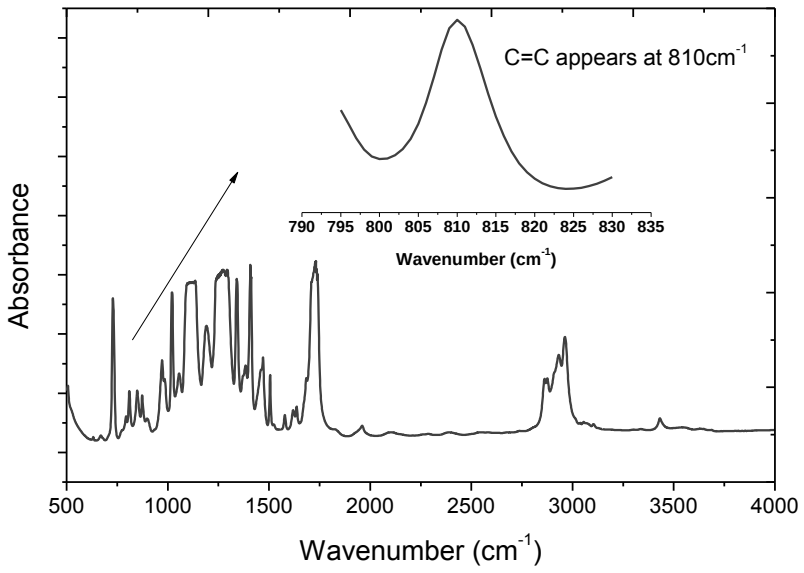

Figure 3.7: FTIR spectra of pure 2EHA before polymerization.

FTIR measurements have been conducted at a wave number between 400 and 4000 cm-1 with 16 scans. Samples were covered with PET films (23 µm) to prevent inhibition effect of atmospheric oxygen during polymerization.

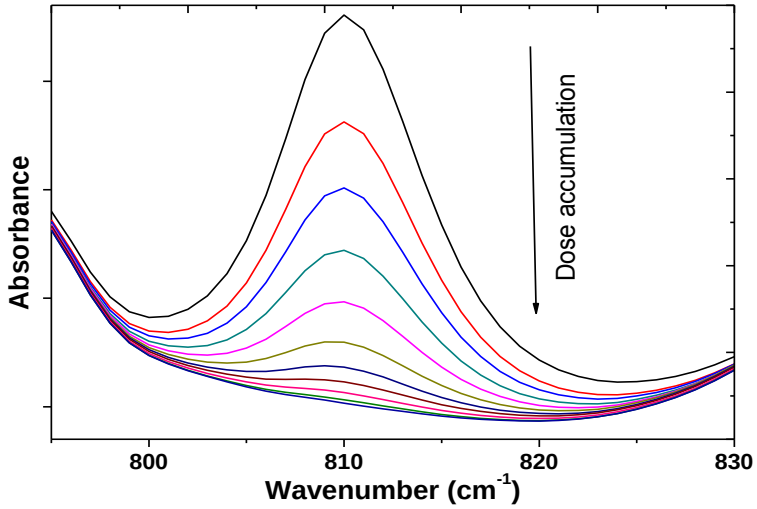

Figure 3.8: FTIR spectra for disappearance of C=C band at 810 cm^{-1} of 2EHA under UV irradiation.

UV irradiation dose was 120 mJ/cm^2 at a fixed speed of conveyer belt, which is equivalent to about 2 seconds exposure time, total exposure time was estimated to be 20 seconds to reach a plateau state as indication to complete consumption of the monomer molecules.

Using relation 3.18, conversion rate can be evaluated which leads to the results presented in Figure 3.8. All further kinetic measurements have been done based on this relation.

$$\% \text{ Conversion} = \frac{(H_0 - H_t)}{H_0} * 100 \qquad 3.18$$

where H_0 is the height of the C=C bond before irradiation and H_t is the height of the C=C bond after time t of exposure to irradiation.

3.7.3 Kinetic measurements

Exposure time of each passage during polymerization has been controlled based on speed of the conveyer belt of the instrument and the instrument parameters. Polymerization was performed by passing samples on the conveyer belt several times until maximum conversion is achieved. Samples have been analyzed after each passage using FTIR spectroscopy to

follow double bond conversion during polymerization. Exposure time of the UV instrument was estimated to be 1.45 seconds at a conveyer speed of 10 m/min which corresponds to a UV irradiation dose of 120 mJ/cm^2, while for the EB device, exposure time was estimated to be 0.4 seconds at a conveyer speed of 12 m/min, and this corresponds to EB dose of 8 kGy. Conveyer speed has been varied during the process as a control tool to adjust UV doses for the kinetic measurements. Kinetic measurements were repeated twice and average of these results was estimated to construct the kinetic curves. Conversion rate of 2EHA as a function of passage number is presented in figure 3.9 at different initiator concentrations.

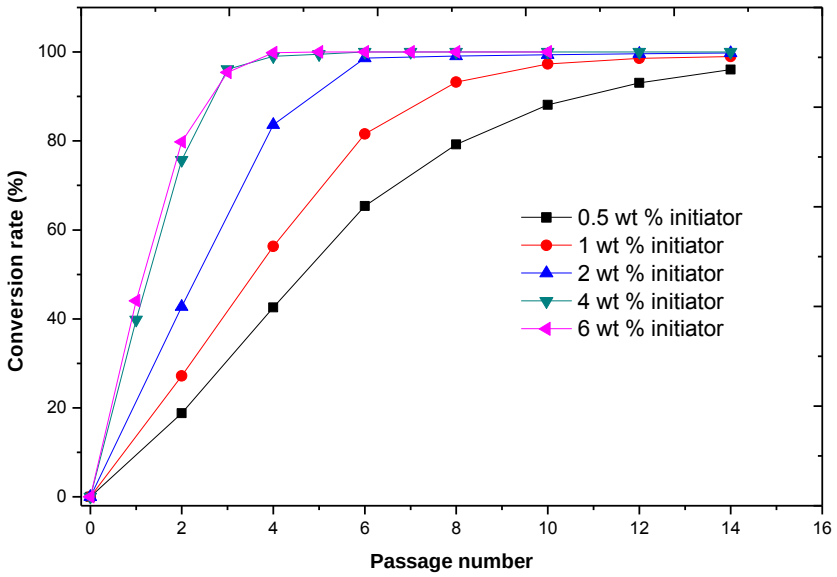

Figure 3.9: Conversion rate as a function of passage number for 2EHA at different initiator concentrations, UV dose is 120 mJ/cm^2

It is observed that kinetic curves are superimposed at higher initiator concentrations (4 and 6 wt % initiator) with sharp increase of conversion rate. Whereas, at lower initiator concentrations, a steep increase of the conversion rate at the beginning of the reaction until maximum double bond conversion is observed, then kinetic curves show plateau region. The conversion rate reaches its maximum with 2 and 4 wt % of photoinitiator after 6 passages, while about 16 passages are required to reach maximum conversion for sample of 0.5 wt % photoinitiator. This high reactivity can be explained by formation of large amount of dissociated initiator radicals at higher initiator concentration as a result of exposure to UV light, which may lead to high initiation rate. Several extra passages have been made to insure total double bond conversion.

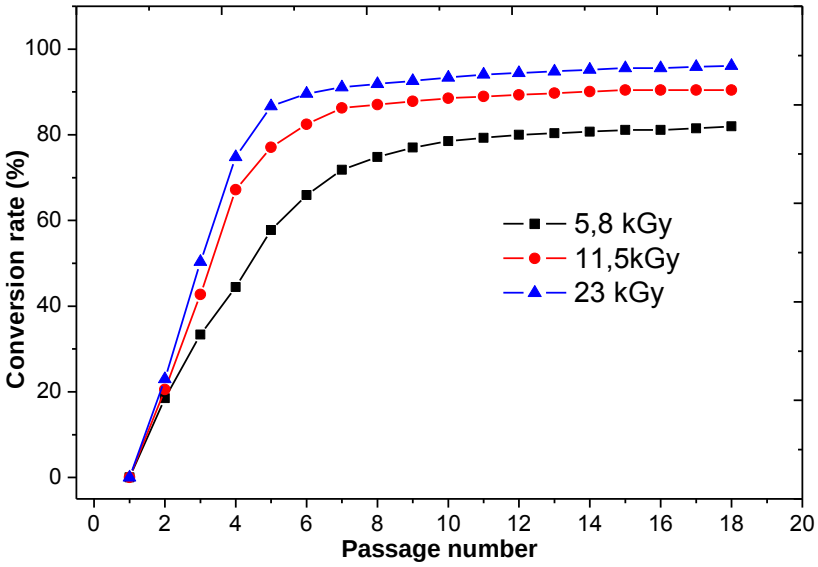

Figure 3.10: Conversion rate of 2EHA as a function of the number of passages.

In EB curing systems, conversion rate is presented in figure 3.10 as a function of passage number at different EB doses between 5.8 to 23 kGy. Kinetic curves for double bond conversion at 11.8 and 23 kGy are similar where maximum conversion rate achieved after about 16 passages under irradiation, which corresponds to a total of 6 seconds exposure time. Fast conversion rate is attributed to higher dissociation of monomer double bond under the intense EB irradiation. These results show high performance of EB irradiation to arrive at high and fast conversion of acrylate monomer within short exposure time.

3.8 Conversion rate as a function of initiator concentration

Reaction rate is proportional to square root of initiator concentration and effective radiation rate as previously given in equations 3.13 and 3.17. Polymerization rate has been studied at different initiator weight percents straining from low o high concentrations. Effect of photoinitiator concentration on kinetic curves is presented in figure 3.11. Each data point corresponds to an average value measured on two different samples.

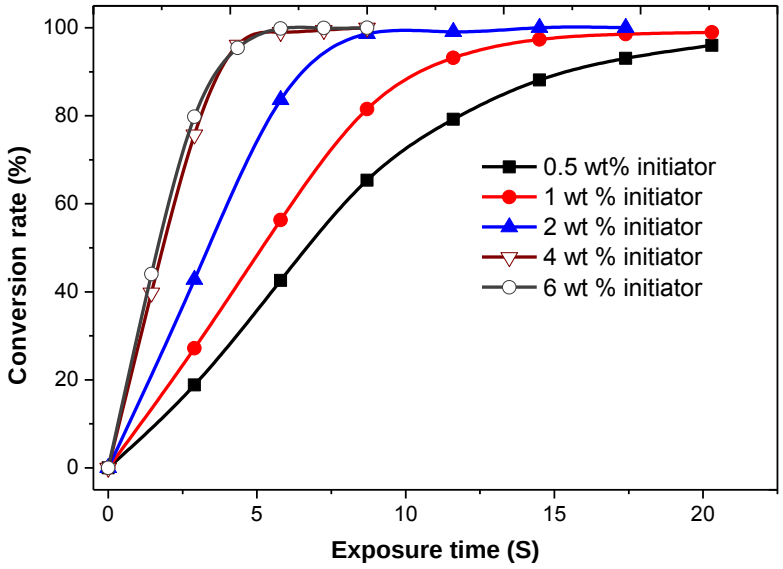

Figure 3.11: Effect of photoinitiator concentration on polymerization of 2EHA. UV intensity = 120 mJ/cm^2 per passage.

Kinetic results are summarized in Figure 3.12 show that initial polymerization rate is directly proportional to the square root of the photoinitiator concentration, according to classical kinetic equation 3.13. Therefore, these results support the kinetic equation that the polymerization rate is dependent the square root of the initiator concentration.

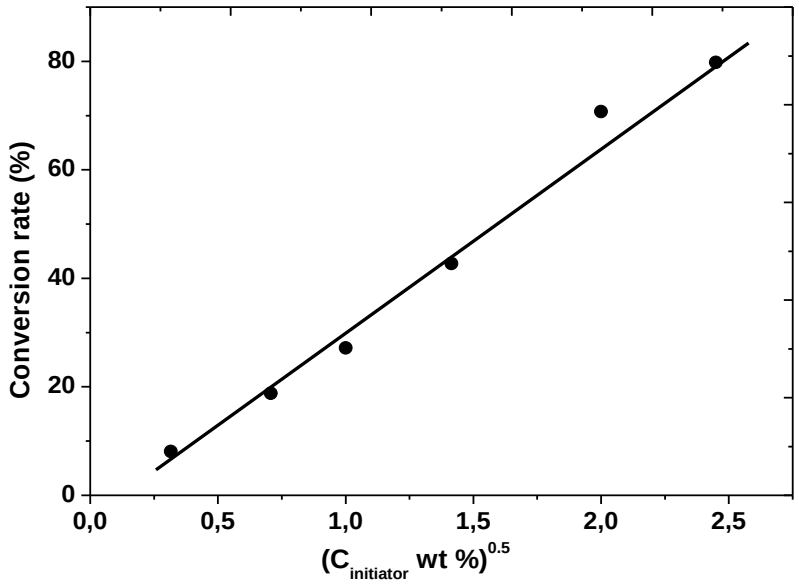

Figure 3.12: Dependence of the rate of polymerization on the square root of the photoinitiator concentration initiator.

It is assumed that photoinitiator is well distributed in the monomer mixture, the polymerization is initiated at each site were radicals exist in which both sites of the photoinitiated are active to initiate a further polymerization until the reaction is terminated.

Maximum rate is reached in the shortest exposure time at highest photoinitiator concentration. Initial part of the kinetic curves show high conversion rate, doubling the amount of the initiator from 2 to 4 wt % resulted in increasing the conversion of about 35%, whereas, further increase of initiator concentration from 4 to 6 wt % lead to very slight effect on reaction rate. These results show limitation of kinetic equation at very high photoinitiator concentration. A maximum of 4 wt % of the photoinitiator was sufficient to achieve complete polymerization for the given values of the polymerization conditions.

3.9 Effect of liquid crystal on conversion rate

Effect of liquid crystal concentration on the polymerization has been investigated by varying liquid crystal concentration in the initial mixture. Presence of liquid crystal in the reactive mixture will affect molecular order during polymerization due to the interactions between liquid crystal and monomer molecules. Most interesting parameter during preparation of PDLC composites is the interaction and alignment between the polymer matrix and dispersed liquid crystal. Study of the medium may give information about nature of interactions between monomers and liquid crystal molecules. It largely determines the reaction rate and molecular weight distribution of polymer chains.

Free radical polymerization under UV and EB irradiation has been studied at several 2EHA/5CB compositions (30, 50 and 70 wt % of 5CB). Wide range of 5CB concentrations has been chosen to cover the whole of the phase separation.

3.9.1 Effect of liquid crystal on conversion rate under UV curing

Kinetic study of polymerization of the above composites was carried out under normalized experimental conditions and the kinetic curves are shown in figure 3.13.

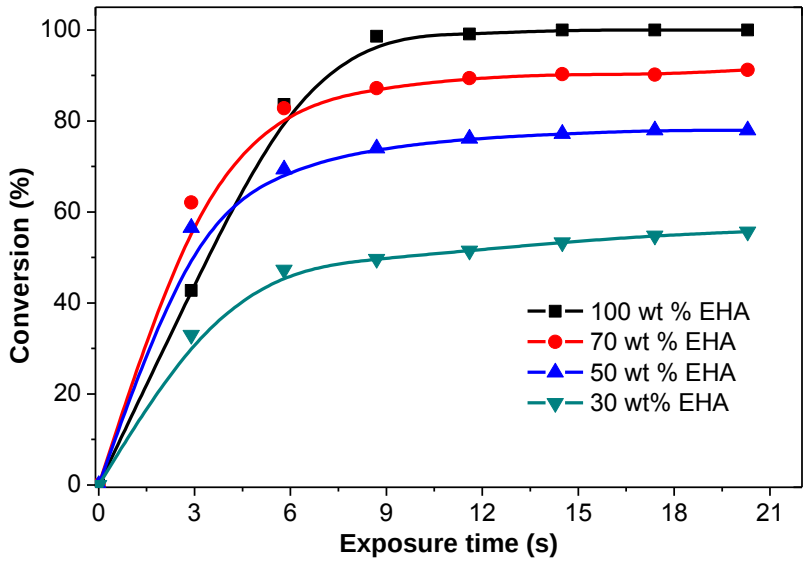

Figure 3.13: Kinetic curves of of 2EHA/5CB composites at 2 wt % initiator. The UV irradiation intensity = 120 mJ/cm^2 per passage.

Time required to reach maximum conversion is low for pure monomer compared to monomer/LC composite mixtures. At low 5CB concentration, higher conversion rate is observed at beginning of the reaction compared with the pure monomer, this occurs as a result of the dilution effect of liquid crystal since 5CB acts as a solvent to monomer and enhancing to some extent molecular interactions between monomer molecules. In addition, increasing reaction rate at initial phase of the reaction can be explained by decrease of polymerization termination rate in more ordered LC media.

Furthermore, increasing liquid crystal concentration in the reactive mixture leads to decreasing maximum conversion compared to pure monomer mixture, maximum conversion for 30/70 wt % of 2EAH/5CB composition does not exceed 60% conversion, this can be explained by trapping monomer molecules between liquid crystal molecules, which reduce mobility of monomer molecules to join the propagating polymer chains.

3.9.2 Effect of liquid crystal on conversion rate under EB curing

EB curing of 2EHA/5CB composites at different weight percents of the liquid crystal is presented in figure 3.14. Samples have been exposed to EB irradiation of 11.5 kGy per passage and analyzed using IR spectroscopy to estimate the conversion rate after each passage under EB irradiation.

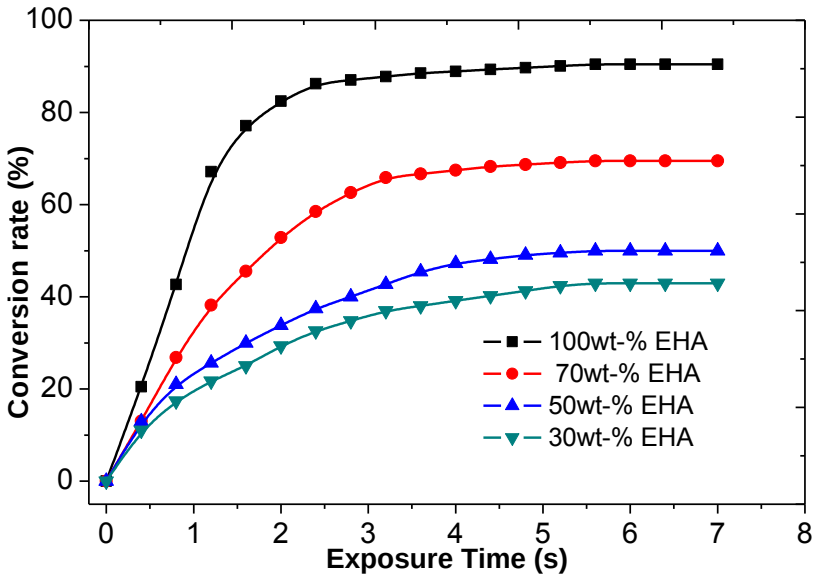

Figure 3.14: Kinetic curves of 2EHA/5CB composites. The EB intensity = 11.5 kGy per passage.

In EB curing, time required to reach maximum conversion is about 6 seconds which is low compared to the UV curing. Increasing the liquid crystal concentration in the initial composite mixture leads to considerable decrease of conversion rate due to dilution effect of the liquid crystal molecules, which reduces movement of monomer molecules and radical species toward the polymer chains. Furthermore, no remarkable increase of conversion rate at beginning of the reaction as case of UV curing is observed. This can be explained by the low effect of molecular order during EB curing, which can be explained by formation of initiating radical directly on the monomer molecules due to the absence of photoinitiator in EB curing.

Based on the above discussion it can be implied that during UV curing, gel contents of 2EHA rich composite may occur faster than with those with low 2EHA contents to form highly viscous gel structure, which reduce the mobility of monomers and long chain radicals. Accordingly, radical termination rate decreases and the polymerization rate increases rapidly.

3.10 Effect of irradiation rate on conversion rate

Kinetic investigations were conducted in the presence of photoinitiator under UV irradiation and without photoinitiator in case of EB curing. Effect of radiation dose has been determined by comparison of conversion rate for samples using UV and EB irradiation in a domain ranging from low to high doses. Reaction rate of photoinitiated polymerization at different

irradiation intensity has been studied by FTIR spectroscopy on composite mixtures of monomer and a liquid crystal.

3.10.1 Effect of UV irradiation rate on conversion rate

Kinetic measurements for polymerization of 2EHA under variety of UV irradiation rates are presented in figure 3.15 at the same concentration of photoinitiator.

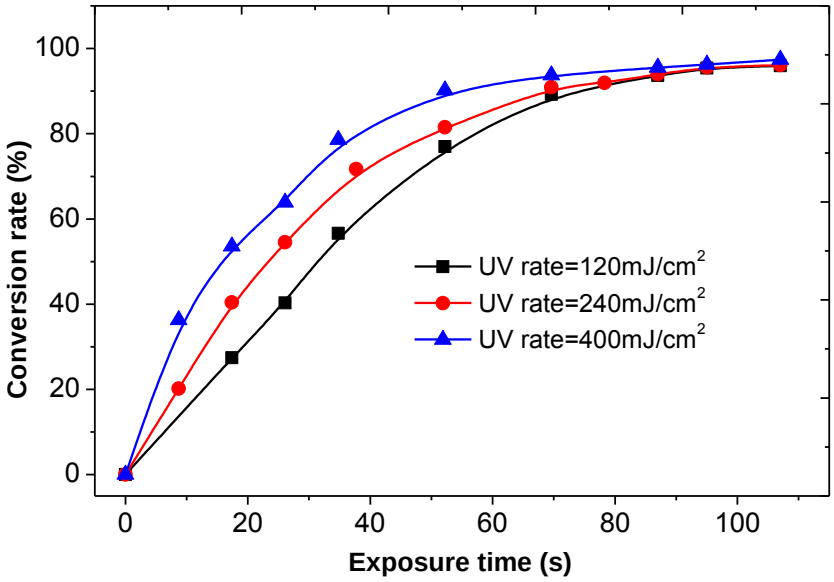

Figure 3.15: Conversion rate as a function of UV irradiation rate for 2EHA at 0.1 wt % initiator.

Values of the conversion rate were found to be increased by increasing irradiation dose from low to relatively high rates between 120 – 400 mJ/cm^2. Kinetic curve shows that doubling irradiation dose results in increasing conversion rate with relatively low rate, and further doubling the irradiation dose shows increasing conversion rate with not more than 10% conversion. For further investigation to this kinetic behavior, we conducted the measurements at higher photoinitiator weight percent as shown in figure 3.15.

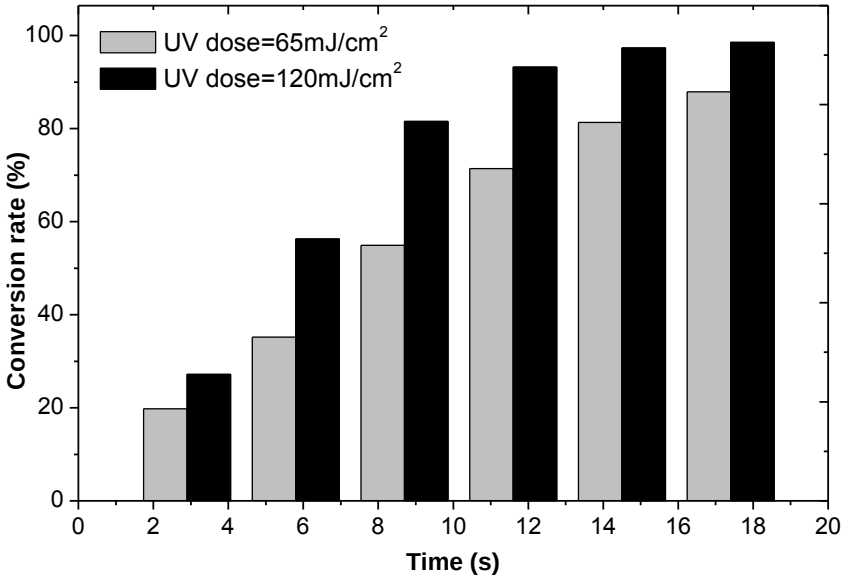

Figure 3.16: Conversion rate as a function of UV irradiation rate for 2EHA.

As shown in figure 3.16, by increasing initiator weight percent to 1 wt % in the reactive mixture, the conversion rate of UV cured photopolymerization increases with about 15% by doubling the irradiation dose from 65 – 120 mJ/cm^2. These results are similar to the values obtained in previous kinetic measurement in figure 3.10. In which we observe limitation of irradiation rate on the conversion rate. These results confirm the kinetic equation of monoacrylate polymerization in equation 3.15 that effective quantum yield is not largely affected by irradiation rate.

3.10.2 Effect of EB dose on conversion rate

The kinetic curve for 2EHA under EB irradiation is given in figure 3.17, shows variation of conversion rate as a function of EB dose, at 5.8 kGy it is observed that maximum conversion rate reached was about 80% conversion without further conversion, while increasing EB dose to 11.5 kGy, conversion rate reach about 90%. Doubling EB dose to reach 46 kGy, results in increasing conversion rate by 5% to reach about 95% conversion. In all EB kinetic measurements, exposure time required to reach a maximum conversion is about 6 seconds which is considered relatively small compared with the kinetic curve of UV cured photopolymerization.

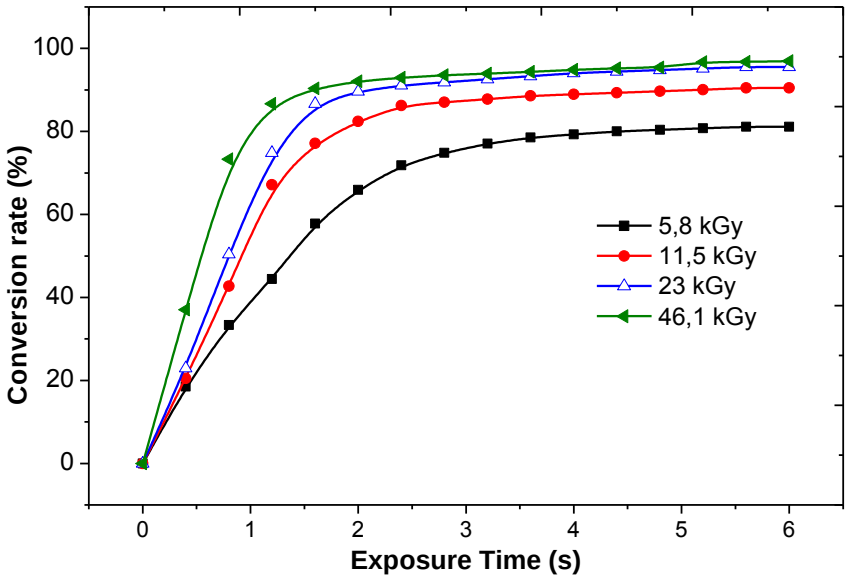

Figure 3.17: Conversion rate as a function of the EB irradiation rate for 2EHA.

3.11 Polymerization kinetics of difunctional acrylates

In this part of the kinetic analysis, kinetic behavior of difunctional acrylates will be described and compared with monoacrylate system. TPGDA monomer has been chosen to perform measurements. Previous studies on relation between monomer structure and double bond conversion show that increasing monomer functional groups leads to higher reaction rate as a result of presence of higher concentration of double bonds. Furthermore, higher functionality is accompanied with increasing crosslinking and formation of gels due to termination by combination, however, high networks density may reduce double bond conversion due to the limited movement of monomer molecules toward propagating radical species. Chain length of polymer largely affects reaction kinetics, in which short length chains accelerate gel contents and result in less homogenous polymer networks [16,17].

3.11.1 Effect of radiation rate on the polymerization kinetics

Figure 3.18 describes the polymerization kinetics of TPGDA under EB curing at different irradiation doses between 5.8 and 23 kGy. Kinetic polymerization curves indicate existence of two polymerization stages, first stage with a sharp increase in conversion rate at early exposure time, followed by slow conversion rate profile.

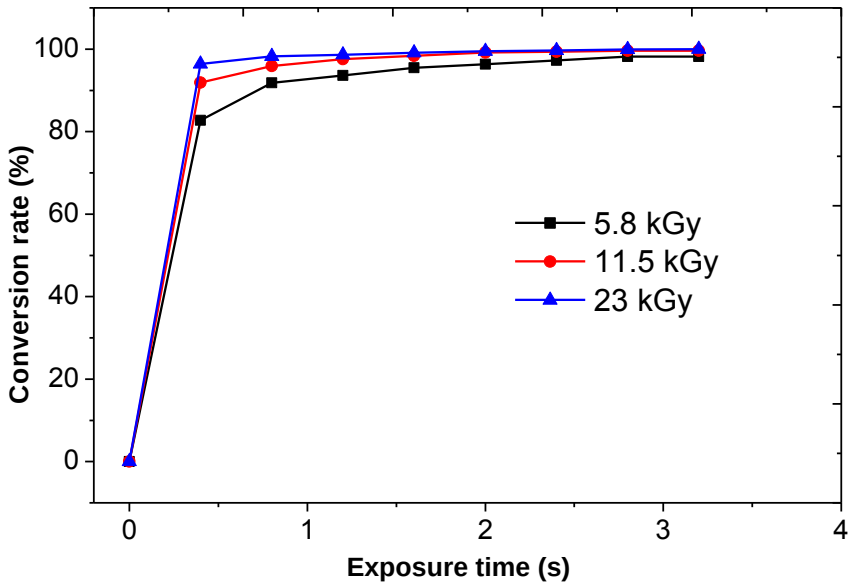

Figure 3.18: Conversion rate of TPGDA monomer as a function of the EB rate.

A sharp increase of conversion rate is observed in the kinetic curve due to fast crosslinking of TPGDA monomers. Conversion rate exceeds 80% after the first passage of monomer under EB irradiation and within about one second conversion rate reaches more than 90%. Furthermore, effect of EB dose on the conversion rate is limited as the difference of conversion rate is only observed at initial phase of the reaction and very small different of conversion rate is observed as a function of radiation dose. This corresponds to high reactivity of the radical species and presence of high density of difunctional TPGDA monomer. The characteristic feature of all these curves is high initial conversion rate followed by a steep rise and after this autoacceleration a significant drop in polymerization rate is observed.

3.11.2 Effect of liquid crystal content on the polymerization kinetics

It is highly important to study effect of liquid crystal concentration on reaction kinetics as the liquid crystal molecules affect the alignments of the monomer molecules and the dilution effect at higher liquid crystal concentrations. TPGDA has high degree of crosslinking and presence of liquid crystal molecules will determine the architecture of polymer chains.

In this work, kinetic parameters of UV cured TPGDA/5CB films is investigated as a function of initial composition. In this part, we limit our investigations to kinetic measurements whereas the thermophysical parameters will be studied and presented in chapter 4. Figure 3.19 shows the variation of conversion rate a function of the liquid crystal concentration.

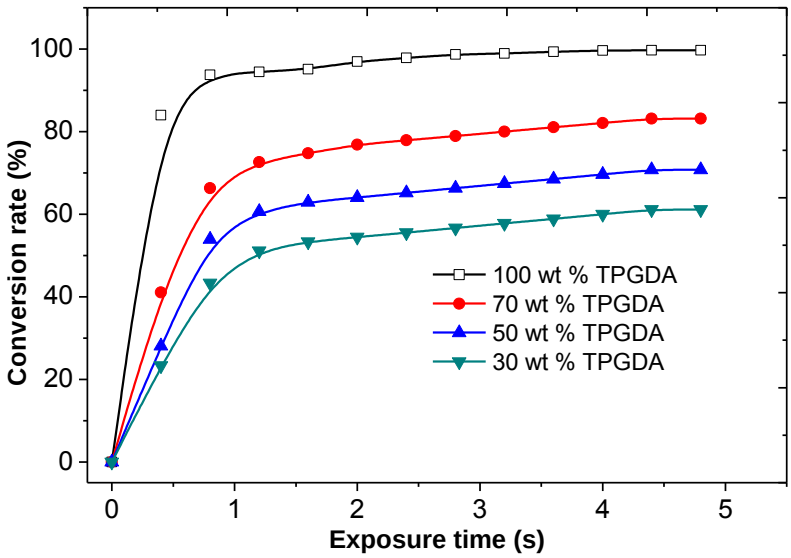

Figure 3.19: Kinetic curve of TPGDA polymerization as a function of 5CB concentration under EB rate of 11.8 kGy.

It can be observed in figure 3.19 a sharp increase of conversion rate of pure TPGDA monomer which reaches maximum conversion in about 3 to 4 seconds exposure time under EB irradiation with a dose rate 11.8 kGy. This can be explained by the high density of double bond in TPGDA as difunctional acrylate. Increasing liquid crystal concentration in the reactive mixture to 30 wt %, results in decreasing conversion rate of TPGDA to about 80% conversion. Further increase of 5CB concentration in the mixture results in a considerable decrease of conversion rate to not more than 60% conversion of the monomer. In all case of TPGDA/5CB, maximum monomer conversion rate does not reach conversion of pure TPGDA, which can be explained by movements limitation of monomer molecules in the mixture due to presence of liquid crystal molecules that prevent monomer molecules to join the propagating polymer chains during polymerization. Furthermore, trapped monomer and radical species in the formed crosslinking polymer matrix affect maximum conversion rate.

As reaction proceeds, higher crosslinking level apparently limits the mobility of monomers and radical species, which means that propagation reaction, is controlled by diffusion of radicals in the mixture. As a result, reactive species are trapped in the crosslink network and polymerization rate starts to decrease till reaction finally stops. This implies that the double bonds trapped in crosslinked structure could hardly take part in further polymerization

reaction [18], whereas, lower double bonds density may reduce conversion rate for samples with low TPGDA content, thus prevent formation of more crosslinked network systems. As a result, there are fewer double bonds trapped in the crosslink network that could take part in further polymerization; On the other hand, monomers and radical species which are trapped between the liquid crystal molecules lead to decrease the reaction rate at high liquid crystal concentration.

3.11.3 Monofunctional vs. difunctional acrylates

An interesting behavior during photopolymerization reaction is the reaction rate of mono and difunctional acrylate under normalized conditions to investigate the effect of higher density of the functional groups of TPGDA on the reaction kinetics. A comparison of polymerization rate between monoacrylate 2EHA and difunctional acrylate TPGDA is given in figure 3.20.

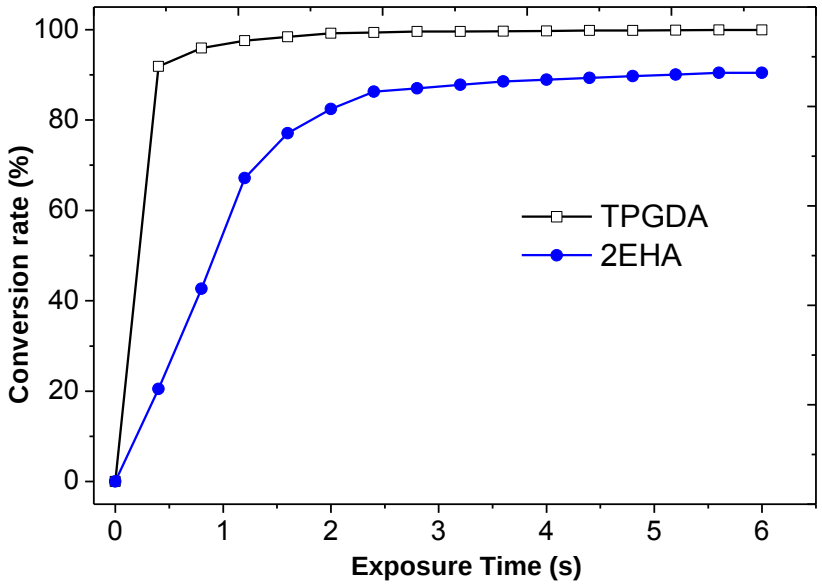

Figure 3.20: The kinetic curve for the polymerization of 2EHA and TPGDA under EB curing, the irradiation rate is 11,5 kGy.

As shown in figure 3.20, conversion rate of difunctional acrylate TPGDA is higher than the conversion rate of monofunctional acrylate 2EHA. In addition TPGDA reaches maximum conversion in about 2 seconds of exposure time while on the other hand, double bond conversion of 2EHA does not exceed 90% conversion. This phenomenon can be explained by the previous discussion that concentration of the double bond of TPGDA is much higher than that of 2EHA. Accordingly, possibility of termination by combination in 2EHA

polymerization is higher than the TPGDA system, which can reduce mobility of monomers and radical species toward the polymer chains that means decreasing in propagation reaction. As a result, reactive species are restricted between the polymer networks and reaction rate decreases and no further increase in the conversion rate is observed [19].

3.12 Conclusion

Polymerization rate was found to increase with increasing irradiation rate according to a nearly square root law. In UV curing, reaction rate increases up to a maximum limit for irradiation rate of 300 – 400 mJ/cm^2 per passage. While in EB curing, increase of reaction rate reaches a maximum limit of about 115 kGy of EB dose. This maximum limit effect can be related to the consumption of photoinitiator under intense irradiation for the UV curing and the consumption of monomer molecules in the EB curing.

FTIR spectroscopy has been successfully used to determine conversion profile of samples under UV and EB photopolymerization. A strong correlation exists between reaction rate increases and composition of the mixture, concentration of photoinitiator and irradiation rate. The reaction rate increases with increasing the initiator concentration and irradiation rate, while the reaction rate shows a decrease by increasing the liquid crystal concentration in the composite mixture.

Behavior of polymerization rate in the composites system could be explained by considering that interactions between the monomer and the LC produce phase separation, where a lower molecular mobility cause a decrease in polymerization rate; on the other hand, at initial stage of photopolymerization the presence of LC direct the monomer molecules toward each others, which cause an increase in the polymerization rate.

Polymerization of difunctional TPGDA acrylate shows a very fast response to irradiation rate to form crosslinking network due to presence of two functional group of TPGDA. A similar behavior to the monofunctional 2EHA acrylate is also observed for addition of liquid crystal to the mixture, in which increasing liquid crystal concentration results in decreasing the reaction rate due to the crosslinking density and liquid crystal molecules that prevent propagation of the polymer chains.

3.13 References

[1] K.A. Berchtold, C. N. Bowman, Macromolecules, 37, 9, (2004).

[2] V. S. Ivaniv, Radiation chemistry of polymers, VSP, Utrecht (1992).

[3} M. Buback, et al., Journal of Polymer Science Part a-Polymer Chemistry, 30, 5, 851-863 (1992).

[4] H.X. Feng, et al., Journal of Polymer Science Part a-Polymer Chemistry, 41,1, 196-203 (2003).

[5] D.E. Weiss and D.S. Dunn, Radiation Physics and Chemistry, 65,3, 281-288 (2002).

[6] O.F. Olaj, A. Kerherr, G Ziffere, Macromolecules, 32, 6 (1999).

[7] K. Dusek, London: Blackie Academic and Professional, 64-92 (1998).

[8] A.B. Scranton, C.N. Bowman, J . Klier, N.A. Peppas, Polymer, 33, 1686-9, (1992).

[9] D.J. Broer, B.N. Mol, Makromol. Chem., 190, 19, (1989).

[10] C. E. Hoyle, T. Watanabe, J. B. Whitehead, Macromolecules, 1994, 27, 6581.

[11] U. Maschke X. Coqueret, C. Loucheux , Nucl. Inst. and Meth. in Phys. Res., 105, 262 – 266, (1995).

[12] N.A. Vaz, G.W. Smith and G.P. Montgomery, Mol. Cryst. Liq. Cryst., 146, 1, 17. (1987).

[13] N.A. Vaz, Proc. SPIE, 1080, 2, (1989).

[14] C. A. Guymon, C. N. Bowman, Macromolecules, 30, 5271 (1997).

[15] C.A. Guymon, E.N. Hoggan, N.A. Clark, T. P. Rieker, D. M. Walba, C. N. Bowman, Science, 275, 57 (1997).

[16] J.P. Fouassier, J.F. Rabek, editors, Rad. curing in polymer science and technology, vol. I-IV. London: Elsevier Applied Science (1993).

[17] J.G. Kloosterboer, Adv. Polym. Sci., 84, 1,61 (1988).

[18] Z.G. Huang, W.F. Shi, European Polymer Journal 43, 4, 1302–1312, (2007).

[19] H. Wang, S. Xu, W. Shi, Progress in Organic Coatings 65, 417–424, (2009).

4 FORMATION OF PDLC MATRIX BY PHOTOINDUCED PHASE SEPARATION.

4.1 Introduction

Morphology of polymer composites has been a subject of many research studies to provide control of distribution of composition and morphology of product material. The industrial applications of PDLC materials in the electronic devises based on preparing thin film of between conducting substrates, applying electric field across the material result in the on orientation of liquid crystal droplets in the direction of electric field and show on-state. The electrooptical properties of liquid crystal droplets depend on the thermophysical and phase properties of the composite martial [1]. One way to study the PDLC composites based on understanding the dispersion of the liquid crystal particles in the polymeric material which offer overview of the configuration and interactions in the matrix. Confinement and interactions of liquid crystal in the polymer matrix largely determines phase changes and final thermophysical properties for potential technological applications. Different configurations may be achieved by varying reactive mixture composition and preparation condition during polymerization. Phase transition control is directly related to the orientation and morphology of polymer matrix.

Bulk alignment of liquid crystal determines the physical properties and anisotropic phase transition of liquid crystal in the polymer matrix. In absence of external forces, favored alignment of liquid crystal is to minimize surface energy which known as anchoring. Anchoring is the key factor to be considered in the preparation of liquid crystal for electronic devices. Anchoring effect can be controlled using a polymer matrix with certain configuration which also provides both low voltage operations and mechanical stability [2].

In this part, main focus is given to study the physical and chemical properties of the PDLC matrix, in addition, to study effect of preparation condition on phase transition of polymer composite and understanding the microscopic mechanism for such transitions. A comparison of UV and EB curing on properties of polymer composite will be highlighted at different irradiation rates, to understand the relation between the polymer matrix composition and phase transition of liquid crystal. Effect of irradiation rate on the physiochemical properties

and stability of pure 5CB will be studied under high electron beam doses and long UV exposure time.

4.2 Physical properties of nematic phase

4.2.1 Orientation order

Alignment of director can be described by the tilt angle θ and azimuthal angle α with respect to the axis [3]. The average orientation of the molecules can be described by the orientation order parameter S in a liquid crystal volume v_0 as:

$$S = (< 3\cos^2\theta - 1 >)/2 \tag{4.1}$$

Order parameter of nematic phase of low molecular weight liquid crystal is usually in the domain between 0.4 and 0.6. Several physical properties are related to the order parameter. Order parameter decreases with increasing temperature and drop dramatically at a temperature close to nematic-isotropic phase transition.

4.2.2 Liquid crystal anisotropic properties

Optical properties of nematic phase give the liquid crystal its anisotropic behavior. When polarized light passes through the nematic phase it scattered into both ordinary ray at the smallest value of n_0 and extraordinary ray at the highest value of n_e in which each ray have specific refractive index. Based on the angle between the direction of polarized light and the optical axis of the nematic phase [4], the extraordinary ray which is known as the effective refractive index can be evaluated by:

$$\text{Effective refractive index } n_{eff.} = \frac{n_e n_0}{\sqrt{n_0 cos^2\alpha + n_e sin^2\alpha}_{tc}} \tag{4.2}$$

The difference between the largest and smallest values of refractive index is known as the birefringence of the liquid phase.

Liquid crystal molecules prefer the parallel alignment in the orientational order. In fact, the molecules deform slightly to show the nematic phase as splay, twist and bend shapes [5].

4.3 Polymer dispersed liquid crystal composites

Polymer/liquid crystal composites can be classified based on their applications into: polymer dispersed liquid crystals; liquid crystal dispersed in colloidal cavities; polymer filled liquid crystal; liquid crystal/polymer membrane; liquid crystal gels; polymer dispersed ferroelectric liquid crystals; liquid crystal/crystalline polymer blends and phase separated composite films.

In liquid crystal/polymer composites, concentration of liquid crystal in the composite may vary in a range between 20 and 80 wt % based on the required application. PDLC composites may classified into two types based on the concentration of components. The first with PDLC of 50 – 80 wt % of the liquid crystal droplets are dispersed in the polymer matrix. The second are polymer stabilized liquid crystals in which about 25% of polymer is distributed in the continuous liquid crystal phase [6].

Polymer matrix in the PDLC supports formation of film, mechanically stabilize the dispersed liquid crystal phase and control liquid crystal configuration in the matrix [7]. Furthermore, degree of miscibility between the liquid crystal and polymer network affect properties of each phase in the composite based on the composition and condition of preparation. Mechanical properties of polymer are influenced by presence of the liquid crystal phase, such as drop in the glass transition temperature. A drop in the phase transition of the liquid crystal is usually observed by the addition of polymer or monomer to the composite system [8].

4.3.1 Preparation of PDLC films

In this work, main focus will be given to prepare PDLC films by polymerized induced phase separation PIPS method using UV and electron beam EB irradiation, since the polymerization phase separation has the advantages of fast curing, less impurities, high conversion and easily controlled compared with TIPS or SIPS. Polymerization rate can be controlled by varying the irradiation rate or the initiator concentration in UV curing, by which size of the liquid crystal droplets can also be controlled that higher polymerization rate accelerates formation of smaller droplets size [9,10].

4.3.2 Morphology of photopolymerized films

Distribution of LC droplets in the polymer matrix determines final morphology of the PDLC film. Preparation conditions affect both size and shape of LC phase and morphology of polymer matrix. That leads to significant effect on the electrooptical properties. On the other

hand, difunctional acrylates have higher polymerization rate which result in formation of polymer networks at early stages of the reaction which may lead to smaller droplet size, as the droplets grow much more rapidly than the monofunctional acrylates [11,12]. In this work, we study effect of preparation condition on the thermal and mechanical properties of the PDLC film and the phase transitions in the polymer matrix. Thus, several monomer/LC mixtures are prepared by UV or EB at different irradiation rates and initiator concentration. Size of LC droplets in the film can be controlled by varying LC concentration in the initial mixture, where droplet size increases by increasing the liquid crystal concentration [13]. Previous experiments in our laboratory on the phase diagram of linear polymer with 5CB show broader phase separation with increasing polymerization rate, which is related decreasing in the mixing entropy between the two phases [14].Pure 5CB shows nematic phase, whereas, pure P2EHA matrix shows isotropic phase. Adding LC with certain composition will offer color to the composite mixture due to the orientation of molecules as presented in figure 4.1.

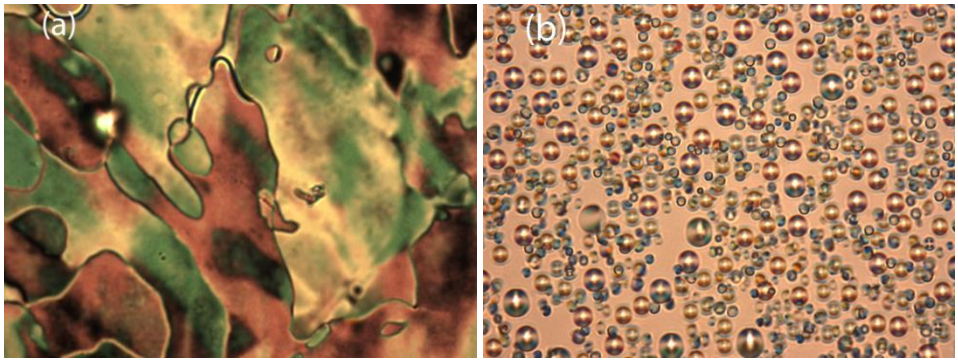

Figure 4.1: POM pictures of (a) pure 5CB and (b) UV polymerized 60/40 5CB P2EHA.

We can distinguish between several areas in the matrix, where liquid crystal confined in droplets or circular objects, recognized by the focal texture of nematic phase. Non colored parts correspond to polymer. In the isotropic phase, liquid crystal loses its birefringence and becomes transparent.

Phase diagram of this system can be constructed by analyzing the phase transitions (crystalline – nematic C – N, nematic – isotropic N – I and isotropic – isotropic I – I) for each composition, the composites undergo a steady temperature drop by increasing the amount of monomer in the initial mixture as previously discussed.

Phase transitions are directly related to mixture composition. This change could be due to the phase inversion as shown in figure 4.2. At high concentrations of 5CB, liquid crystal would

not be confined in the polymer matrix. A portion of the polymer agglomerates to reduce surface contact with the liquid crystal to minimize interactions between the polymer and mesogene. Thus, transition temperature of the composite mixture would be close to that of pure liquid crystal.

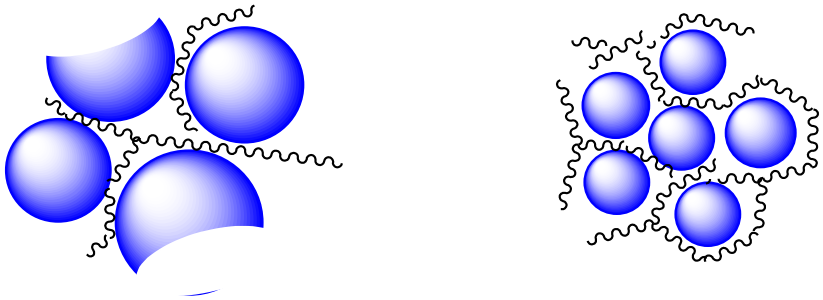

Figure 4.2: Schematic representation of (a) confined LC within the polymer matrix and (b) arrangement of restricted polymer in LC phase.

System of 5CB/P2EHA shows interesting behavior at high LC concentration above 70 wt %. Morphology of the mesogenic domains is varied by increasing temperature. Large area domains are formed in smaller dimensions to form an interconnection network. Inclusion of LC in the matrix is not really circular. Transformation into isotropic phase can be explained by the unification of several domains to form larger size areas to reach homogenous phase. Before forming isotropic phase, LC domains coexist in the matrix. It seems that two phenomena are in competition, first is the dissolution of small objects in the polymer matrix and the formation of macro areas by grouping before dissolving into the solution. This phenomenon has been described by the model of Ostwald-Ripening [15,16], when two clusters touch or collide and merge to form one bigger cluster to minimize system interface toward formation of isotropic phase. Behavior of LC droplets growth described by the mechanism of Ostwald-Ripening can be extended to describe the morphological evolution of 5CB in the matrix as a function of composition under different preparation conditions.

Distribution of liquid crystal droplets as a function of mixture composition for UV photopolymerized films is shown in figure 4.3, performed by POM. High liquid crystal concentrations in the initial mixture result in increasing the droplets size. Presence of higher ratio of the polymer chains make more viscous surrounding polymer matrix and accelerate phase separation that reduces growing of liquid crystal droplets.

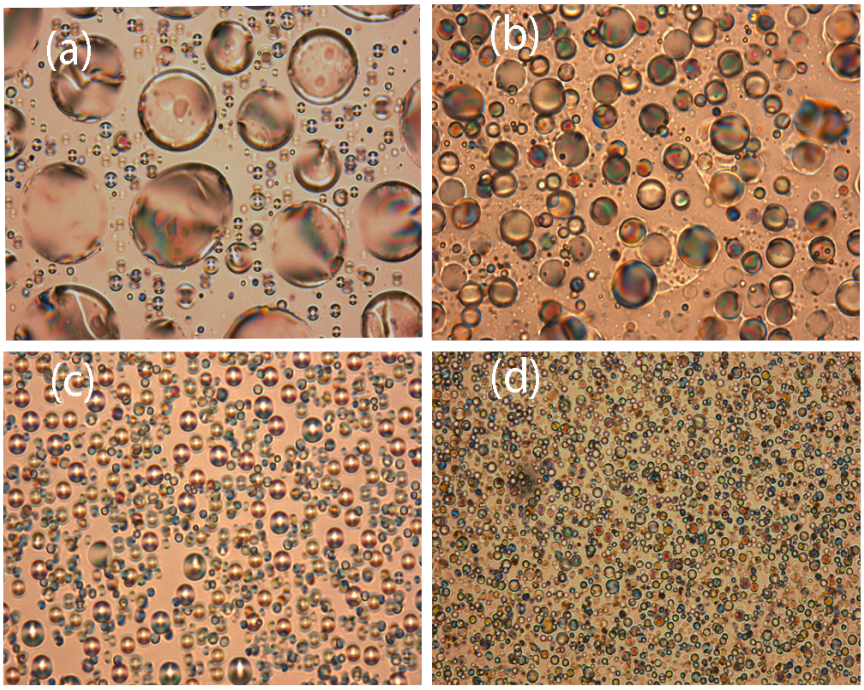

Figure 4.3: POM pictures of the phase separation of liquid crystal droplets size as a function of mixture composition (a) 90, (b) 80, (c) 70 and (d) 60 wt % 5CB.

Furthermore, liquid crystal phase can be dispersed in regular cellular morphology at high LC concentration. Low liquid crystal concentration lead to shift toward irregular droplets shape, where liquid crystal droplets fill the spaces in the polymer matrix [17].

Increasing amount of liquid crystal in the mixture results in larger droplets size. Another remark can be made on the density of objects corresponding to the composite formed at low LC contents shows more space between each homogeneous droplet. Whereas, when the sample is composed of higher LC content, density of inclusions increases sharply. Furthermore, composite mixture above 70 wt % 5CB, density is accompanied by an increase in the droplets diameter.

An interesting behavior of polymer network is the formation of continuous phase even at low weight percents of polymer in the initial mixture. Viscosity of the polymer phase usually supports formation of continuous phase to stabilize the dynamic asymmetry between the polymer and the liquid crystal molecules [18]. High polymerization rate result in formation of small droplets size, as the high propagation rate of polymer chains reduce the possibility of further growth of liquid crystal droplets. In figure 4.4, morphology of liquid crystal phase is

presented at different polymerization rate prepared at different weight percents of the initiator concentration.

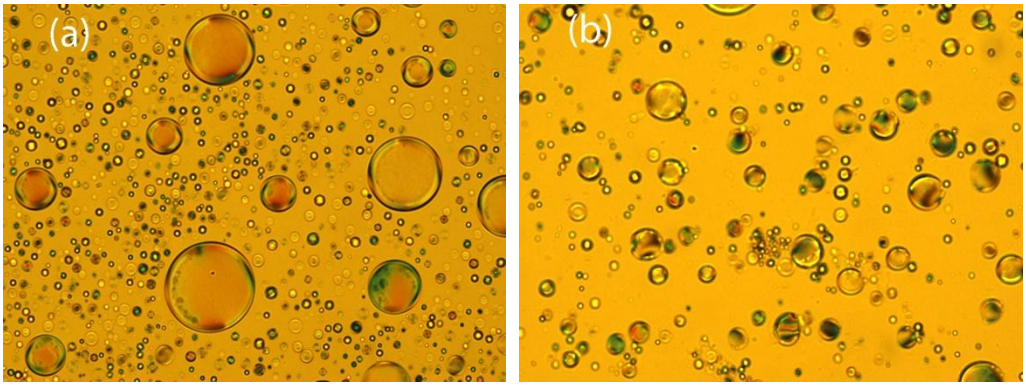

Figure 4.4: POM pictures of liquid crystal droplets size as a function of the polymerization rate (a) 0.5 and (b) 2 wt % photoinitiator.

A comparison between the distribution of LC droplets in the monoacrylate and diacrylate system is given in figure 4.5, non-polymerized mixture has been prepared with 80/20 of 5CB to monomer percent ratio and the POM image were captured at 9°C.

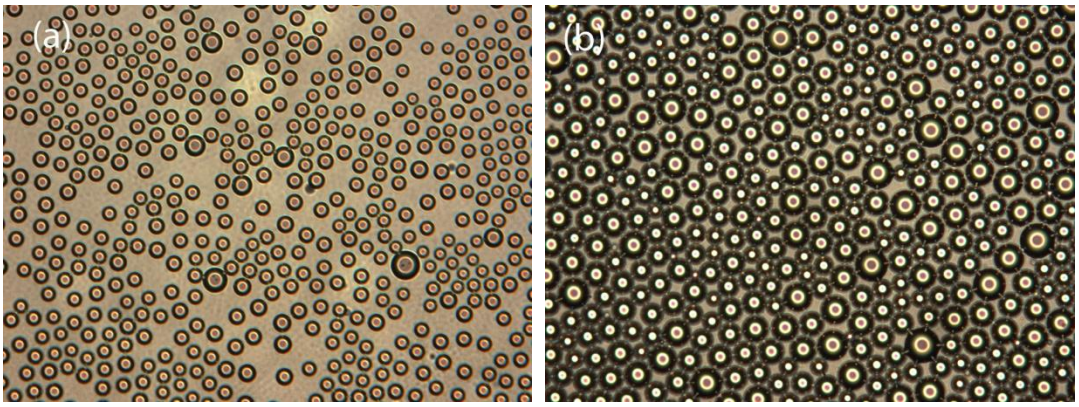

Figure 4.5: POM pictures of liquid crystal droplets in non-polymerized mixture 80/20 5CB with (a) monoacrylate 2EHA and (b) diacrylate TPGDA.

It can be clearly observed the difference between the droplets size and configurations in both systems, were droplets size in the diacrylate system are larger and highly oriented compared with the monoacrylate system which has smaller droplets size and less oriented configuration in the nematic phase. In addition, phase transition from nematic to isotropic phase of monoacrylate system occurs at 14°C compared to the diacrylate system which occurs at 16°C.

This behavior can be explained by high degree of mixing between LC and monoacrylate monomer which results in more homogeneous system with smaller droplets size.

4.4 Morphology characterization of the PDLC composites

4.4.1 Characterization using FTIR spectroscopy

Morphology of the PDLC can be described by the FTIR spectroscopy to present the configuration and interactions between mixture components. FTIR is considered ideal tool to study the interfacial interactions between molecules, and identify existence of liquid crystal intermolecular interactions. Figure 4.6 shows the FTIR spectrum of pure 2EHA monomer at room temperature. Spectral assignments for each band are shown in table 4.1.

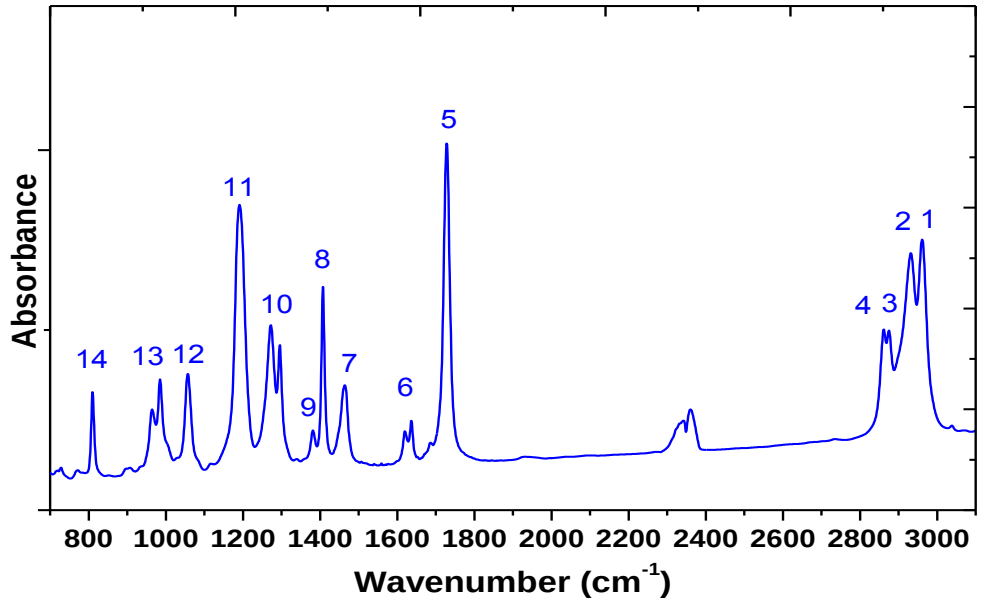

Figure 4.6: FTIR spectrum of 2-ethylhexyl acrylate monomer.

Table 4.1: FTIR spectral assignments for pure 2-ethylhexyl acrylate monomer.

Peak no.	Wavenumber (cm^{-1})	Assignment
1	2960	ν_{as} (CH_3) asymmetric stretch
2	2930	ν_{as} (CH_2) asymmetric stretch
3	2877	ν_s (CH_3) symmetric stretch
4	2875	ν_s (CH_2) symmetric stretch
5	1730	ν_s (C=O) symmetric stretch

6	1640, 1620	ν (C=C) stretch
7	1470	δ (CH_2) bend
8	1410	δ (=CH_2) bend
9	1380	δ (CH_3) bend
10	1300, 1270	(=CH) rock
11	1185	ν (C-O) stretch
12	1060	(=CH_2) rock
13	990, 960	(trans-CH) wag and (=CH_2) wag
14	810	(=CH_2) twist

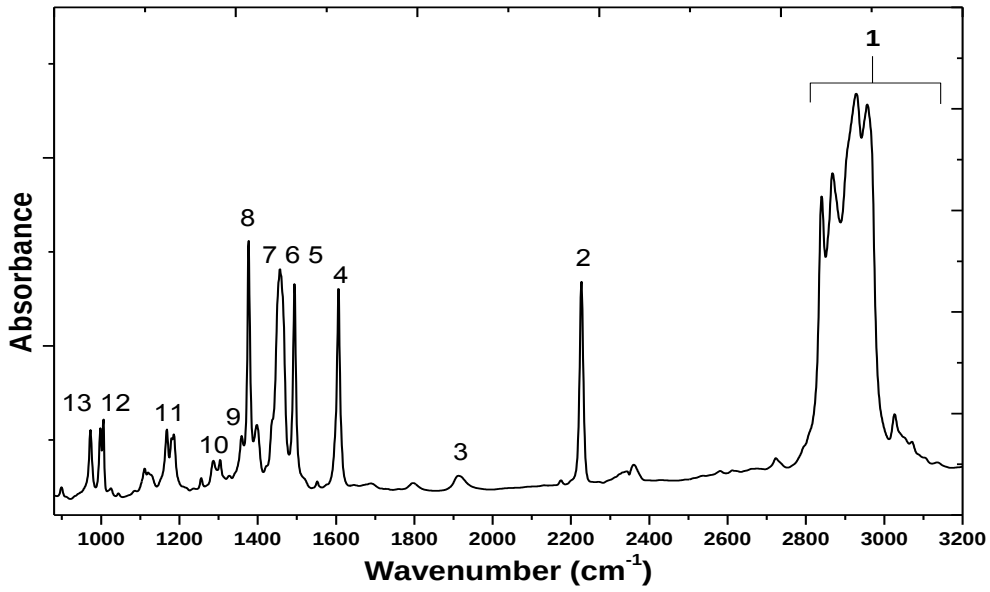

Figure 4.7: FTIR spectrum of pure 5CB liquid crystal.

Figure 4.7 shows the FTIR spectrum of pure liquid crystal 5CB at room temperature. The spectral assignments for each band in the spectrum are shown in table 4.2.

Table 4.2: FTIR spectral assignments of pure 5CB liquid crystal.

Peak no.	**Wavenumber (cm^{-1})**	**Assignment**
1	3072, 3053, 3041, 3029	ν (C-H) aromatic stretch
2	2226	ν (C≡N) cyanide stretch

3	1941	Combination band
4	1607	ν (C=C) stretch
5	1494	ν (C=C) phenyl stretch
6	1468	δ_s (CH_2) symmetric deformation
7	1458	δ_s (CH_3) symmetric deformation
8	1399	δ (C-H) lateral chain deformation
9	1380	δ_s (CH_3) symmetric deformation
10	1291	ν (C=C) biphenyl stretch
11	1181	δ (C-H) aromatic plan deformation
12	1007	δ (C-H) aromatic plan deformation
13	968	ρ (CH_3) aromatic plan deformation

Vibration band of CN group of 5CB appears large and fine at 2226 cm^{-1}, and is therefore considered a good indicator to describe the configuration of the liquid crystal in its environment. This band is often used in this type of analysis by IR spectroscopy. Thus, several authors have discussed liquid crystal confinement and show that band change occurs due to its containment through a process of spatial rearrangement or surface/liquid crystal interactions [19].

Evolution of the CN vibration band is given as a function of composition in figures 4.8 and 4.9 for non-polymerized and polymerized systems respectively. In isotropic state, 5CB band at 2226 cm^{-1} is visible regardless of LC concentration of in the mixture. Nevertheless, this band does not seem to suffer any significant shift regardless of the containment without significant deformation. Same observations can be obtained when in the nematic state of 5CB. These remarks suggest that segregation of LC can be described by graphical representations while the CN group is the least influenced by the confinement. However, in view of the spectra, each isolated band presents the same characteristics regardless of mixture composition. Different phase's behavior can be obtained by varying temperature of the mixture in which the liquid crystal groups are sensitive to temperature.

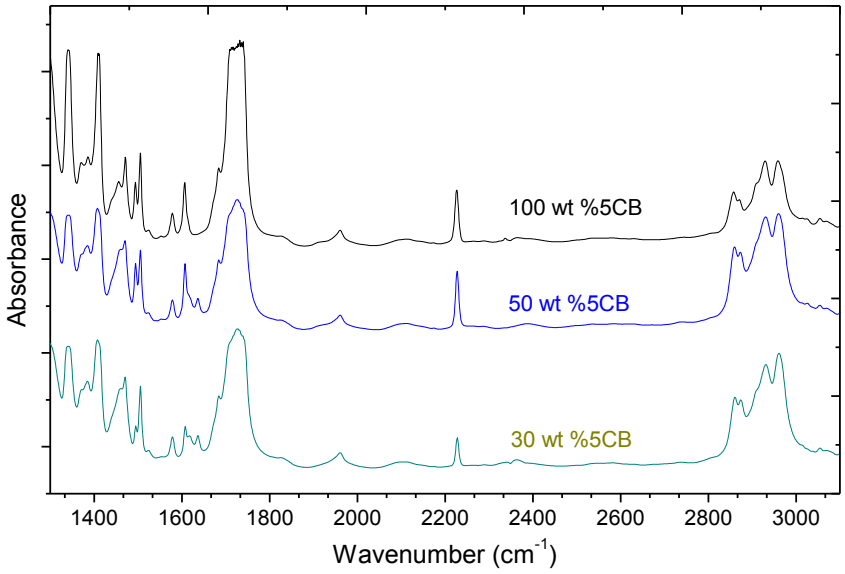

Figure 4.8: IR spectrum of un-polymerized 2EHA/5CB as a function of LC concentration.

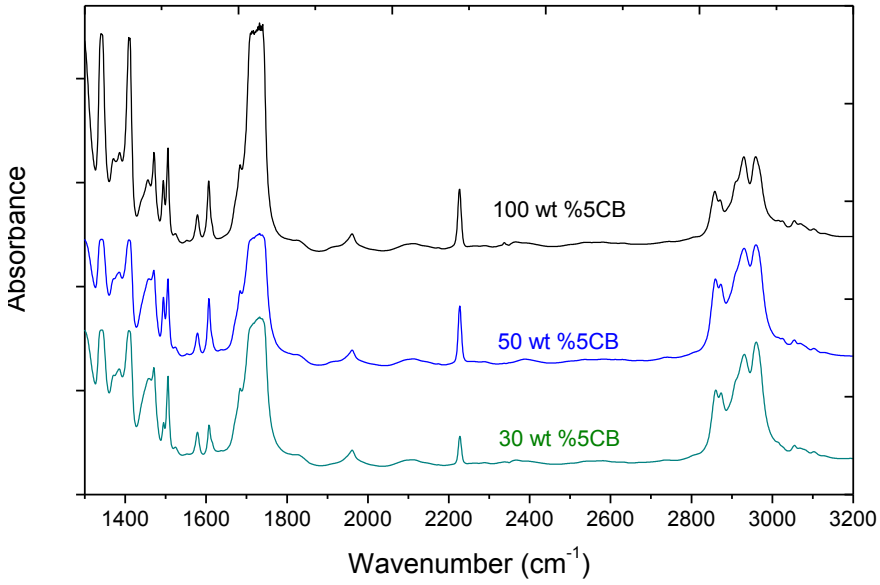

Figure 4.9: IR spectrum of UV cured P2EHA/5CB as a function of LC concentration.

Interaction between the monomer, polymer and liquid crystal molecules may vary based on the composition of the mixture. Figure 4.10 shows an overlay of the IR spectra of 2EHA and 5CB. The similarity in the spectra between the alkyl groups of pure monomer and the liquid crystal suggests that the conformation of the alkyl groups is not affected by the introduction of 5CB molecules into the system.

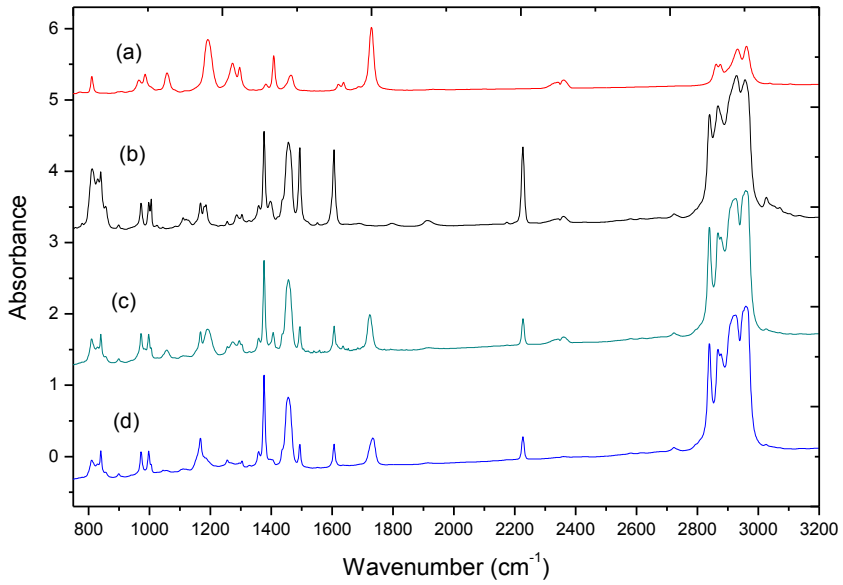

Figure 4.10 : The IR spectrum of (a) pure 2EHA, (b) pure 5CB, (c) un-polymerized 70 wt %5CB and (d) polymerized 70 wt %5CB systems.

The peak in the spectra located near 1730 cm^{-1} corresponds to carbonyl group (C=O) stretching of the 2EHA monomer and polymer. Overlapping between aromatic (C-H) of 5CB and the aliphatic (CH_3) band is observed in the region between 2960 –3072 cm^{-1}. There are four characteristic alkene absorbance shown in the spectrum: the stretching bands at 1637 and 1622 cm^{-1}, an olefinic bending absorbance at 1407 cm^{-1} and an olefinic twisting absorbance at 810 cm^{-1} [20]. However, a quantitative analysis of these bonds leads to evaluate the conversion rate at given preparation conditions.

During polymerization of 2EHA, a continuous drop of the double bond (C=C) peaks at 810 and 1630 cm^{-1} involves breakage of double bond until maximum conversion. Addition of 5CB into the system affects the IR band spectra, where interaction between liquid crystal molecules occurs with the double bond band. Total number of double bonds in the system should therefore decrease with irradiation dose and conversion into polymer, this process has been studied by IR spectroscopy in details in chapter 3 of this study. The cyano group (CN) at 2226 cm^{-1} appears sharply by the addition of liquid crystal to the system without overlap or interactions with the monomer or polymer matrix in the system. Notice that absence of overlap for the absorption bands of aromatic (C-H) plan and biphenyl stretch in the 1100 – 1800 cm^{-1} region of the two component system.

Furthermore, 5CB can be distinguished by the absence of frequency displacement (C=C) bon bands. While, 2EHA reveals several interactions by the alkyl chain and benzene due to possibility of combination bands at 1815 and 1960 cm^{-1} that are characteristics of (C-H) aromatic band as shown in figure 4.9. Thus, interactions of biphenyl of 5CB cycle and 2EHA are barely visible in this configuration of the containment area of the mixture. This can be explained by very small surface contact compared to the amount of 5CB that is not in contact with the polymer [21,22]. It is obvious that 5CB has no effect on the intermolecular bonds which lead to long-range constraints on the polymer configuration. This observation explains why only (C-H) bonds of the alkyl chain and the biphenyl of 5CB groups suffer frequency displacement of vibration bands which is especially true as the repulsive effect increases with amount of liquid crystal in the composite mixture.

4.5 Confinement dynamic of 5CB in the polymer matrix

Alignment of mesogenes in the polymer matrix is of high interest in determining the performance and switching speed of PDLC films. Interaction of the mesogene layer with the amorphous phase is a major factor for the potential technological applications. Several studies revealed that the 5CB molecules in different states can be characterized by the nature of their corresponding relaxation behaviors. Moreover, an additional relaxation located in the lower frequency side of them was observed in all phase regions, which strongly depends on phase transition and has a different relaxation mechanism in different phase region based on mixture composition [23].

First phenomena that take place in this system are the exposure to relaxation mechanisms leading to final architecture of segregated liquid crystal. It was shown in the previous section of this chapter that the main effect exists in the matrix is the repulsion between the mesogenic molecules and polymer. As presented in figure 4.11, evolution of infrared spectra as a function of time can be used to determine the dynamics of this phenomenon for a system prepared by UV curing.

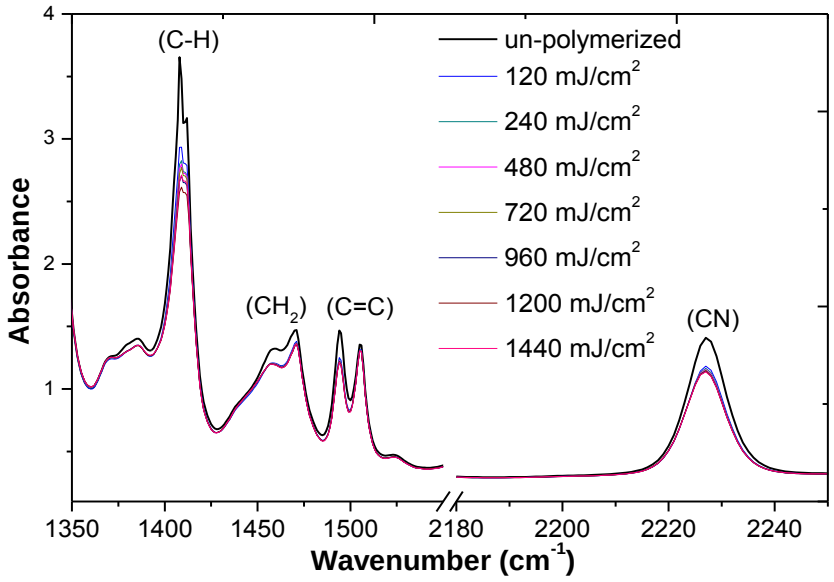

Figure 4.11: The evolution of the FTIR spectra of 70 wt %5CB/ 30 wt %2EAH system prepared by UV curing.

In this analysis, focus will be given to the vibration band ν(C=C) at 1495 cm^{-1} and cyano at 2226 cm^{-1} of 5CB. They have the advantage of not overlap other bands which are crucial for the interactional analysis between the liquid crystal and the polymer. Moreover, this slight change in the intensity versus irradiation time on the molecular diffusion marking the miscibility of 5CB in the matrix by polymerization. That can be explained by the diffusion of 5CB form a homogenous phase.

4.6 PDLC phase transitions

In this section, phase transition of liquid crystal will be studied using differential scanning calorimetry (DSC) by varying initial mixture concentrations under UV and EB curing. PDLC system has different thermodynamic properties related to the interactions between the liquid crystal molecules and the polymer matrix which influence phase transitions. Phase separation process and the phase behavior are widely influenced by the morphology of PDLC films. In which size, shape and distribution of liquid crystal droplets affect the electrooptical properties of the PDLC films [24].

The theoretical considerations that describe thermodynamic properties of PDLC systems are mostly based on lattice model. Interactions between molecules are related to mass fraction of the system, where polymers undergo size reduction at the isotropic to nematic transition state [25]. P2EHA/5CB films appear cloudy at room temperature because of system

inhomogeneity. Upon heating above the T_N-T_I transition temperature of 5CB, the film turns transparent as the mixture becomes homogeneous to form a single phase. However, the system reverts to a two-phase state upon cooling showing a thermal reversibility of the system.

In the phase diagram, a coexistence of nematic and isotropic phase can be expected in an intermediate region. Upon increasing the polymer content in the composite mixture, a depression of the N – I occurs which can be observed by DSC. While, below the T_N – T_I transition temperature the phase separates into polymer-rich and nematic liquid crystal domains. The nematic-isotropic transition is known to be as first order transition. The experimental difficulty in this case aims at distinguishing the nematic phase at low quantities of 5CB. Characteristics of PDLC films have been known to depend on the domain size, the shape and the dispersion of the composite, it is important to understand the kinetics of phase separation and phase growth.

Several authors have studied the effect of confinement on the N – I transition [26,27]. Roussel et al. [28] conducted a study at the liquid crystal confined in poly (2-ethylhexyl acrylate) matrix. They showed that the order of parameter of the nematic phase increases with decreasing droplet size of liquid crystal. Moreover, due to the interactions between the aliphatic chain of the polymer and 5CB molecule, the order of parameter beyond the N – I transition exist in low intensity demonstrating a pretransitional phenomenon.

Many techniques have been developed to offer reliable and precise control of liquid crystal alignment in the polymer matrix and understanding the interfacial phenomena between polymer and liquid crystal molecules [29]. In this section, we focus on the dynamic of phase separation and phase transition of the PDLC films prepared under different conditions using UV and electron beam curing, analysis and comparison of the systems will be performed by DSC technique.

The parameters that affect the T_{N-I} of PDLC film include irradiation intensity, irradiation time, initiator and liquid crystal concentration. In order to compare the different phase transition data from different polyacrylate systems, the above mentioned parameters can be varied to study the PDLC films based on maximum conversion for all samples to avoid the effect of monomer on the phase transition during measurements.

4.6.1 Effect of irradiation dose

In order to establish the relation between the intensity of UV and EB irradiation dose on the phase transition and properties in the PDLC film, the irradiation rate has been varied from low to high dose and phase transition have been recorded by DSC at each irradiation dose.

Effect of UV irradiation rate on the transition behavior of polymer dispersed liquid crystal. PDLC films are studied at different UV doses between 120 and 400mJ/cm^2. A series of samples were used as polymer matrices of the PDLC films as shown in figure 4.13.

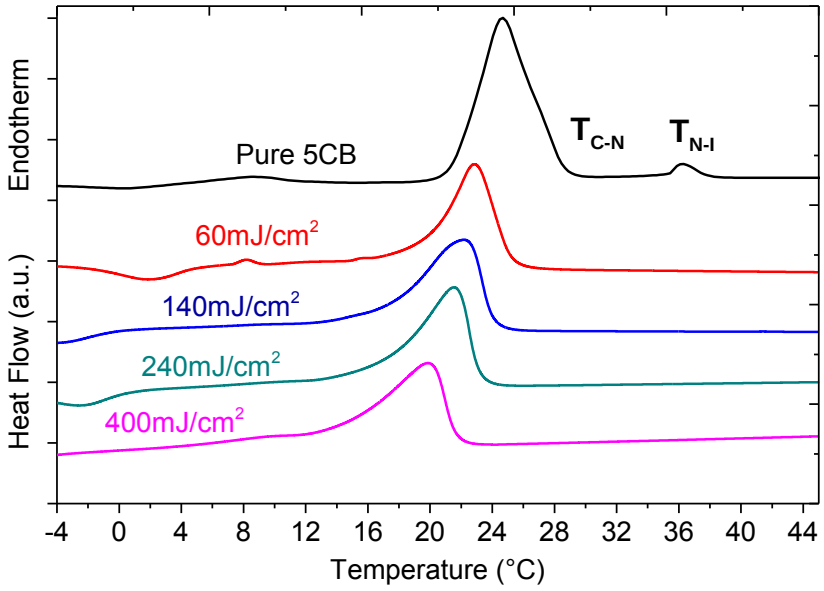

Figure 4.12: Effect of UV irradiation rate on transition temperature, for a system of 30wt% 2EHA/70 wt % 5CB.

The effect of EB irradiation rate on the transition behavior of PDLC films were studied at different EB doses between 46 and 115 kGy. A series of samples were used as polymer matrices of the PDLC films as shown in figure 4.14.

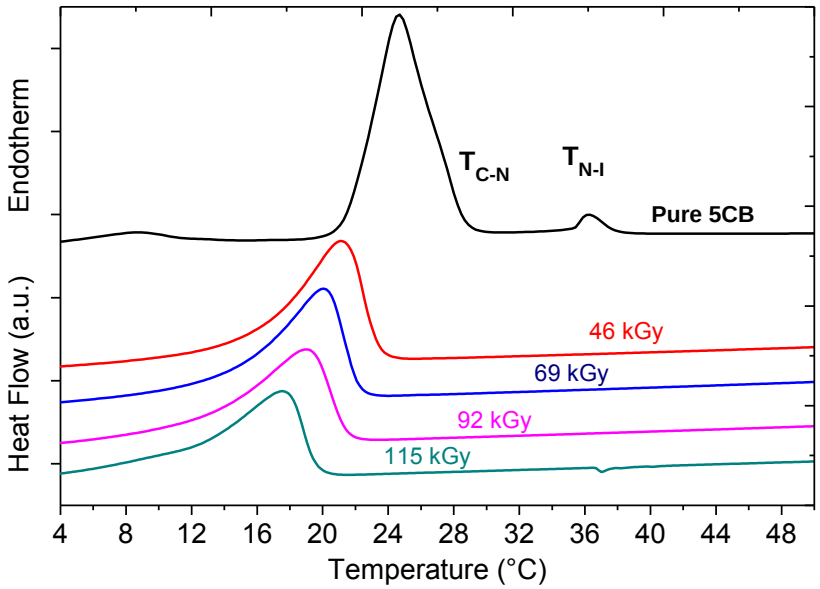

Figure 4.13: Effect of EB irradiation rate on transition temperature, for a system of 30/70 wt % 2EHA/5CB.

The mass ratio of 5CB/2EHA in the initial mixture is 70/30 for all samples. The liquid crystal 5CB has a uniform phase transitions from crystalline to nematic C – N at 23°C and nematic to isotropic N – I at 35.5°C. The isotropic-isotropic transition cannot be detected by DSC analysis since this transition is accompanied by a small enthalpy change.

Increasing the UV irradiation dose results in remarkable drop of the phase transition at 60 mJ/cm^2 dose occurs at 22°C and drops to about 19°C upon increasing the dose to 400 mJ/cm^2. In order to explain these observations, the interfacial interaction model is considered in which the interaction between the side chains of polyacrylates and the alkyl chain of LC molecules control the enthalpic drive for phase transition [30]. Furthermore, the alkyl side chains of polyacrylate in contact with the nematic molecules at the interface are partially ordered under transition conditions.

On the other hand, the phase transition is driven by entropy of molecules on the surface and possible order transition of the side chains of polymer matrix in contact with nematic fluid. These two driving forces are competitive and reach a balance at the transition temperature [31,32]. We suggest that the behavior of phase transition is related to the chain length of the polymer that is being formed at different irradiation doses. At low irradiation rate, formation of long chains polymer is preferred, while at higher irradiation doses shorter chains are formed which offer more mobility for the nematic molecules to adopt phase transition at

lower temperature. Polymer chain has a strong impact on the liquid crystal molecular configurations which give rise to direction of liquid crystal alignment.

4.6.2 Effect of initiator concentration

Effect of initiator concentration on the transition behavior of PDLC films were studied at different weight percents of photoinitiator (Darocur 1173) between 1 and 4 wt %. A series of samples were used as polymer matrices of the PDLC films as shown in figure 4.15.

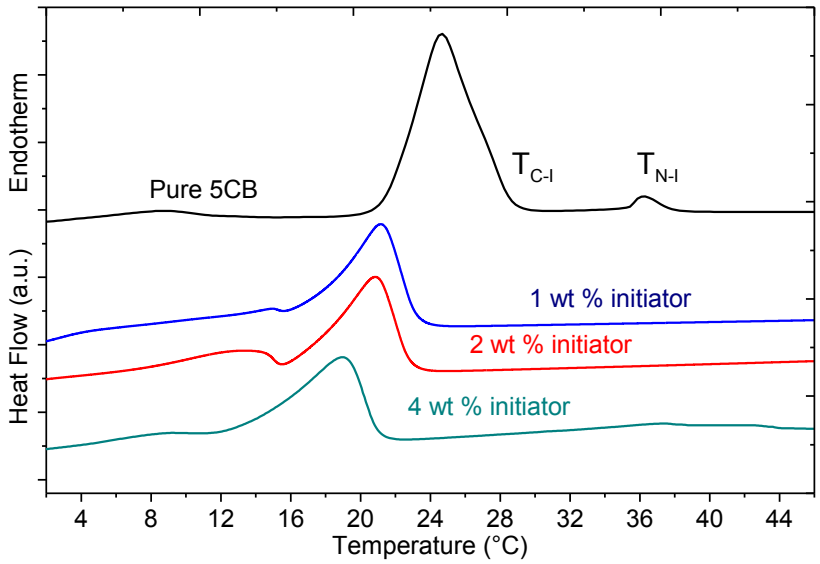

Figure 4.14: Effect of initiator concentration on transition temperature, for a system of 30/70 wt % 2EHA/5CB.

5CB has a uniform phase transition from crystalline to nematic C – N at 23.5°C and from nematic to isotropic N – I at 36°C. Increasing the initiator concentration from 1 to 4 wt % results in remarkable drop of the phase transition where phase transition at 1 wt % initiator at 22°C and drops to about 18°C upon increasing the initiator concentration to 4 wt % concentration. This behavior can be explained by formation of long chain polymer at low concentration of photoinitiator while shorter chains are formed at higher initiator concentrations, short chain polymer network has low interaction with nematic phase were the nematic phase may undergoe phase transition at lower temperature compared with the long chain polymer matrix.

All curves show similar behavior, with a strong dependence on the length of polymer chain, which can be controlled by varying the preparation condition of the PDLC films.

Effect of initiator concentration on the phase behavior of difunctional acrylate (TPGDA) is given in figure 4.16 for a series of samples prepared under UV curing using UV lamps exhibiting a wavelength of 365 nm and an intensity I_0=1.5W/cm^2. The exposure time was measured based on maximum monomer conversion for each sample. A gradual drop of the phase transition temperatures are observed by increasing the initiator concentration in the initial mixture, where increasing the initiator concentration from 1 to 4 wt % result in decreasing the C – N temperature from 22°C to about 20°C, which is also accompanied by drop of the N – I phase transition from 31°C to 28°C. These observations support the idea of formation of different PDLC morphology dmains, where increasing the initiator concentration leads to formation of low molar mass polymer networks during radical polymerization. Furthermore, no significant change in the LC glass transition is observed as revealed from the DSC thermogram.

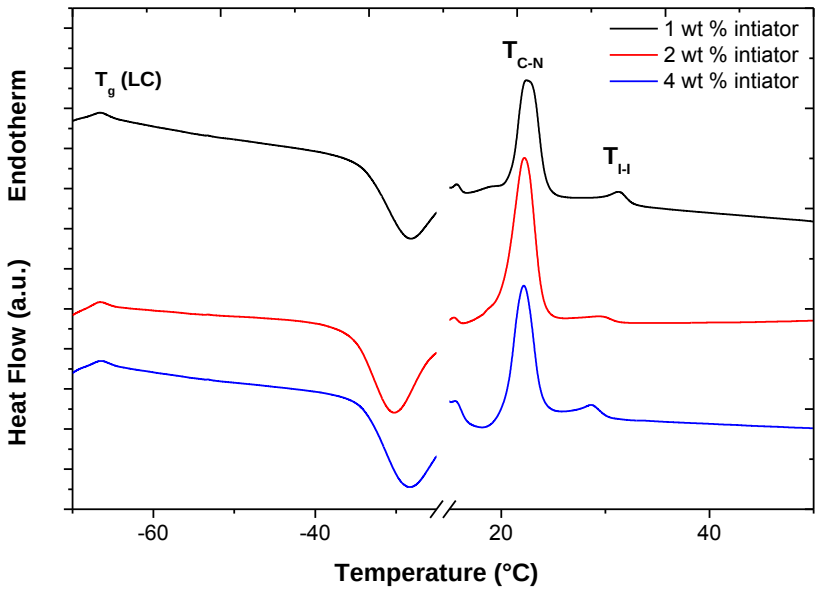

Figure 4.15: Effect of initiator concentration on the phase transition temperature, for a system of 40/60 wt % TPGDA/5CB.

Morphology of PDLC films as a function of the initiator concentration was also elaborated using the POM technique. The distribution of LC droplets in the polymer matrix is given in figure 4.17.

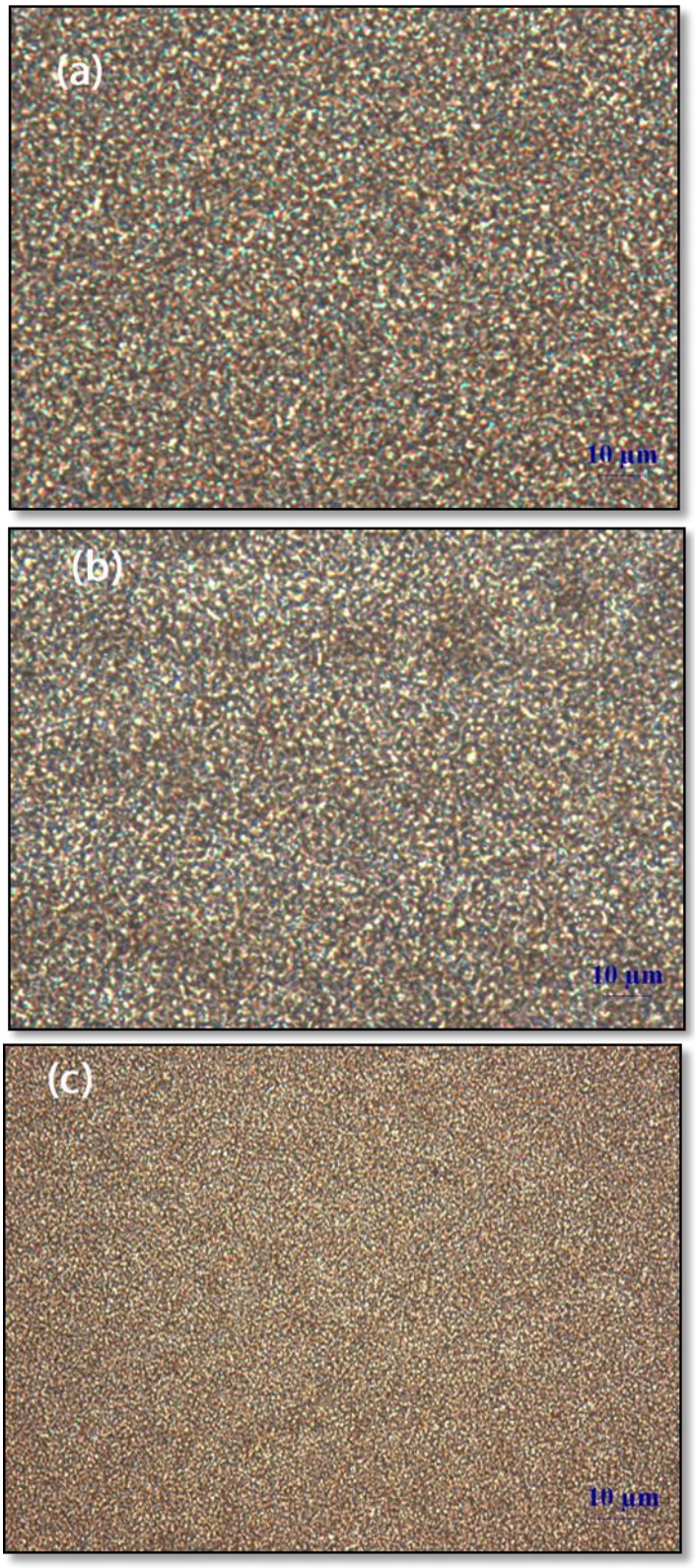

Figure 4.16: POM images of liquid crystal droplets size as a function of the initiator concentration (a) 1 wt % (b) 2 wt % and (c) 4 wt % photoinitiator.

Increasing the initiator concentration in the polymerized mixture leads to significant drop of the liquid crystal droplets size, this behavior can be explained based on the reaction kinetics, where higher amount of initiator concentration results in higher reaction rate, hence, smaller LC droplets size and polymer networks are favored at high polymerization rates.

The phase transition temperature for the TPGDA/5CB PDLC films are given in figure 4.18. A gradual drop of the N – I and I – I transition temperatures are observed by increasing the initiator concentration. This can be explained by the formation of smaller LC droplets at higher reaction rate by increasing the initiator concentration.

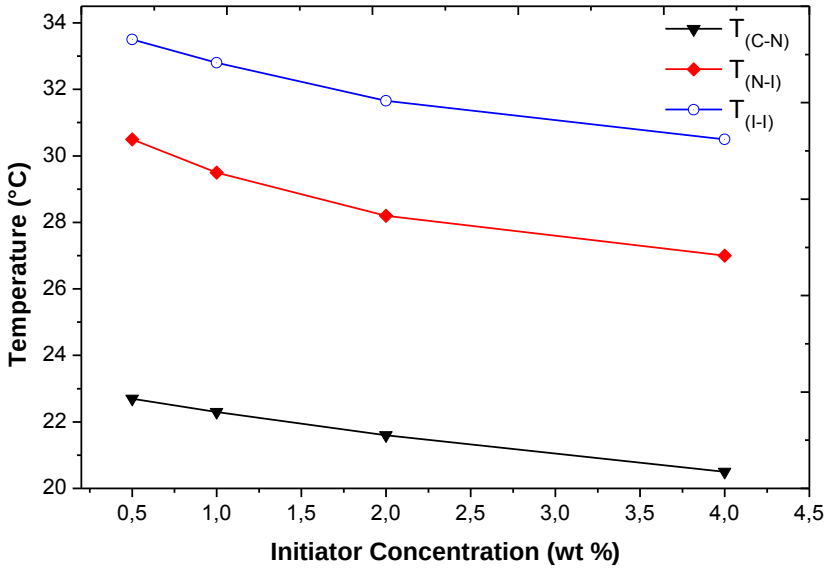

Figure 4.17: Phase transition temperatures as a function of the initiator concentration. The results are obtained by combined POM and DSC techniques.

4.6.3 Effect of liquid crystal concentration

Effect of liquid crystal concentration on the transition behavior of PDLC films were studied at different weight percents of liquid crystal in the initial mixture between 40 and 90 wt % 5CB/2EHA ratio. A series of samples were used as polymer matrices of the PDLC films prepared under the same UV curing dose as shown in figure 4.19 given by the DSC technique.

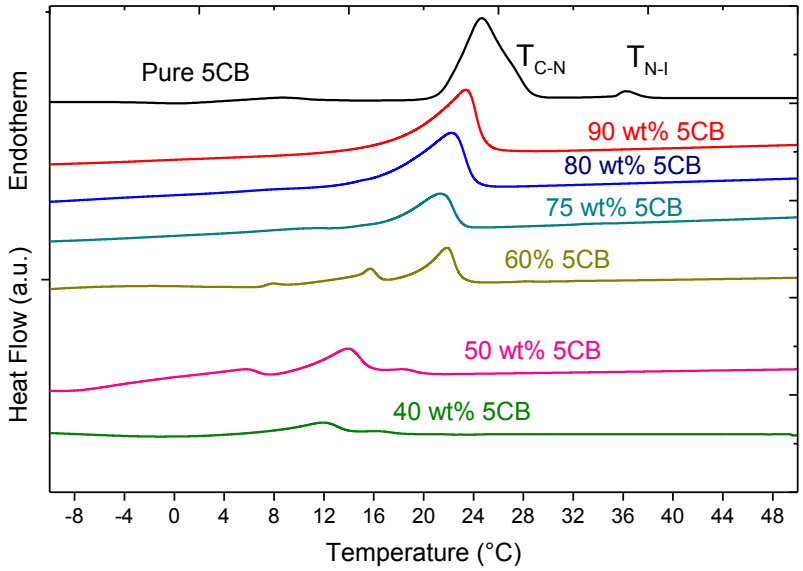

Figure 4.18: Effect of liquid crystal concentration on transition temperature of the PDLC prepared by UV curing.

In the case of the films prepared from 2EHA/5CB show a substantial drop of the phase transition by increasing weight percent of 2EHA in the initial mixture, from about 23°C at 90 wt % to about 12°C at 40 wt % of liquid crystal contents. At low LC content ranging between 40 to 50 wt % concentration, nematic to isotropic transition becomes diffuse and shows a baseline shift which can be explained by increasing the specific heat of mixing of the polymer and liquid crystal that lead to overlapping phase transition.

Effect of liquid crystal concentration on the transition behavior of PDLC films prepared using EB curing were studied at different weight percents of liquid crystal in the initial mixture between 40 and 90 wt % 5CB/2EHA. PDLC films prepared under at the same EB curing dose as shown in figure 4.20.

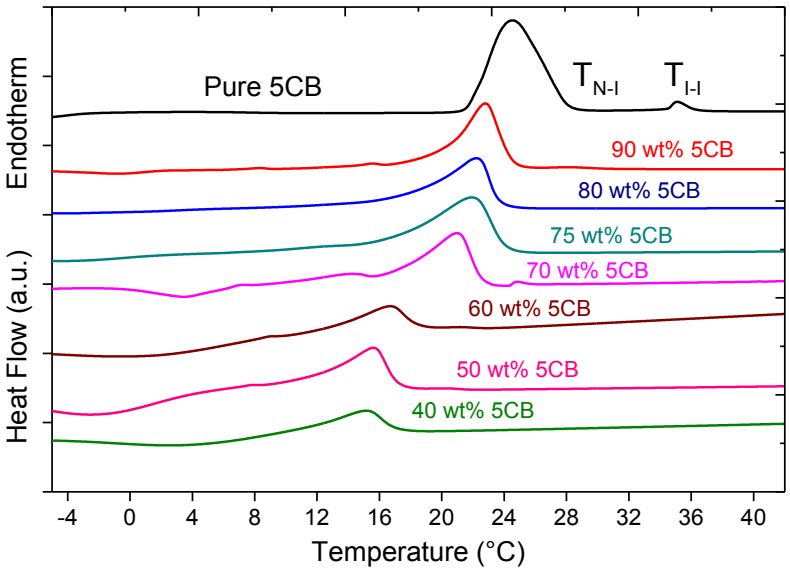

Figure 4.19: Effect of liquid crystal concentration on transition temperature of the PDLC prepared by EB curing.

Influence of increasing acrylate contents into the PDLC films on phase transition can be understood in terms of the interaction with nematic orientation mentioned above.

It could be clearly noted that the peak width of the phase transition at lower concentrations of the liquid crystal in the PDLC mixture is larger than the composites with higher concentrations of 5CB; this shows the structure heterogeneity of these composites and presence of spatial regions with different arrangements of LC structure under various mixture composition. In this system, long polymer chains at the interface may form ordered domains that favor order of nematic molecules. Addition of 2EHA in the mixture through polymerization presumably support the distribution of order of these domains due to increasing the density of polymer chains in the PDLC composite compared with that of low monomer contents This reduces the tendency of nematic molecules alignment and hence lowers the phase transition.

At lower LC contents, nematic to isotropic transformation becomes diffuse and exhibits a positive baseline shift. This shift can be explained by an excess specific heat of mixing ΔC_{pmix} of polymer and LC overlapping with the nematic to isotropic transition. The results obtained for linear polymer/nematic LC are therefore consistent with the previously published work. The (I+I)-(I) transition cannot be observed by DSC analysis since this transition is accompanied by a very small enthalpy change [33,34].

On the other hand, increasing ratio of monomers in the initial mixture may not totally represent composition of polymer at the polymer – LC interface which is related to the kinetic of polymerization process. During polymerization by induced phase separation, reaction rate of 2EHA is high and may segregate from the mixture during the early stages of the polymerization. As the polymerization proceeds to high conversion, the polymer is represented in the interfacial region with the liquid crystal at the end of polymerization. A concentration gradient can be formed in which the amount of 2EHA decreases upon proceeding from the film surface to the interface with the LC [35]. Detailed mechanisms of interactions between polymer and liquid crystal molecules have been presented in the previous section using IR spectroscopic analysis.

4.7 Stability of the nematic liquid crystal 5CB

Liquid crystal stability is of primary concern for the preparation of technological devices with long lifetime operation. In the liquid crystal displays, the lamp is extremely bright to offer the highest performance display, irradiated dose from this lamp may gradually affect liquid crystal molecules in the form of partial degradation to the material. That will cause change in the electrooptical properties of the PDLC film.

To compare stability of the 5CB in the preparation of PDLC films, a pure 5CB has been used to study effect of radiation doses on the molecular structure and phase transition of the liquid crystal. 5CB contain two-ring structures with an alkyl side chain and a polar cyano group, and have a nematic phase at room temperature.

In spectral analysis of stability of 5CB under high radiation source, several characteristic IR bands were selected to conduct this analysis. The characteristic bands for 5CB are those assigned to stretching vibrations of cyano group at 2226 cm^{-1}, stretching band of phenyl group at 1607 cm^{-1} and deformation of benzene ring at 1186 cm^{-1}. These IR bands were selected because of high sensitivity of their spectral parameters to variation of intermolecular interactions, also because of the absence of overlap of these bands in the IR spectra with the monomer or polymer bands. A comparison of the IR spectra of 5CB at different EB irradiation dose is presented in figure 4.21.

The spectral analysis of the 5CB peaks shows no considerable variation of the peak bands before and after irradiation at high EB dose of 115 kGy at a total exposure time of about 5 seconds. The peak positions of these bands are the same for all samples.

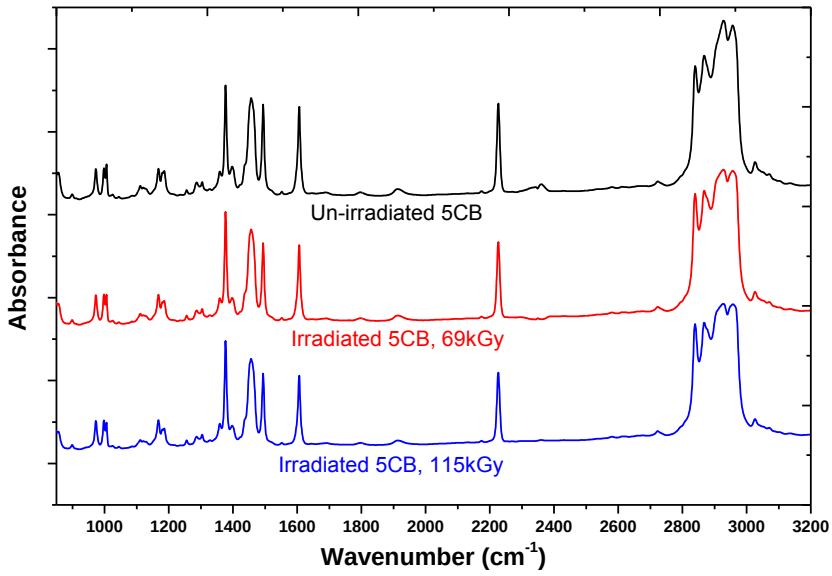

Figure 4.20: IR spectra of EB irradiated pure 5CB.

To verify effect of radiation exposure time on the liquid crystal, a further analysis of the stability of 5CB under long exposure time of UV irradiation has been studied by exposing the liquid crystal to high UV dose with 223 nm lamp. A comparison of irradiated 5CB is given in figure 4.22 at different exposure time. According to the spectral comparison of radiated 5CB at high UV doses, no change in the group intensities or displacement is observed in the obtained IR spectra which support the long lifetime stability of 5CB under high irradiation doses.

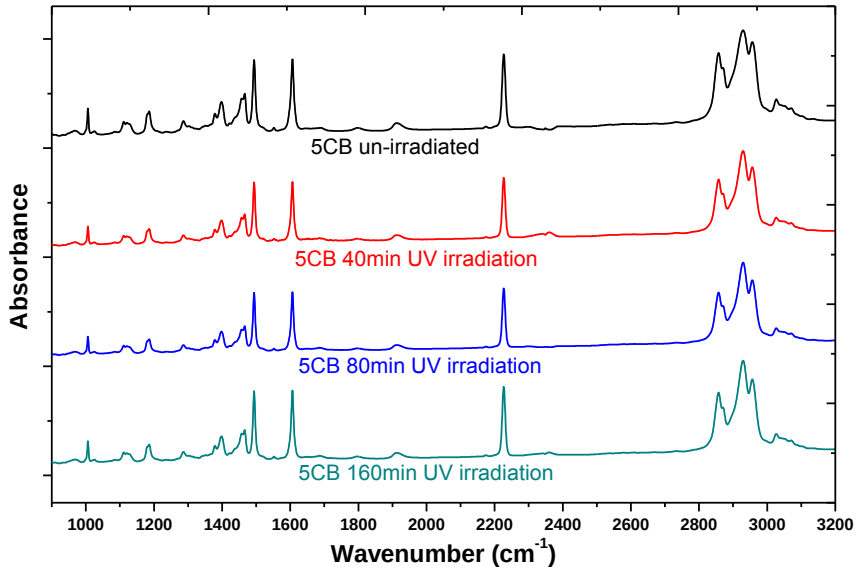

Figure 4.21: IR spectra of UV irradiated pure 5CB.

DSC technique is considered a useful tool to perform the thermodynamic measurements of the nematic liquid crystal to provide information on the phase transitions such as transition temperature, enthalpy, heat capacity and specific heat. 5CB molecules are roughly aligned and free to rotate to certain extent below the nematic transition. When the liquid crystal finally melts, the molecules lose its orientation to transform into isotropic phase.

The same liquid crystal sample which has been exposed to high EB dose has been analyzed by DSC technique to study the effect of high radiation rate on the thermophysical or stability of the liquid crystal. DSC measurements are shown in figure 4.23.

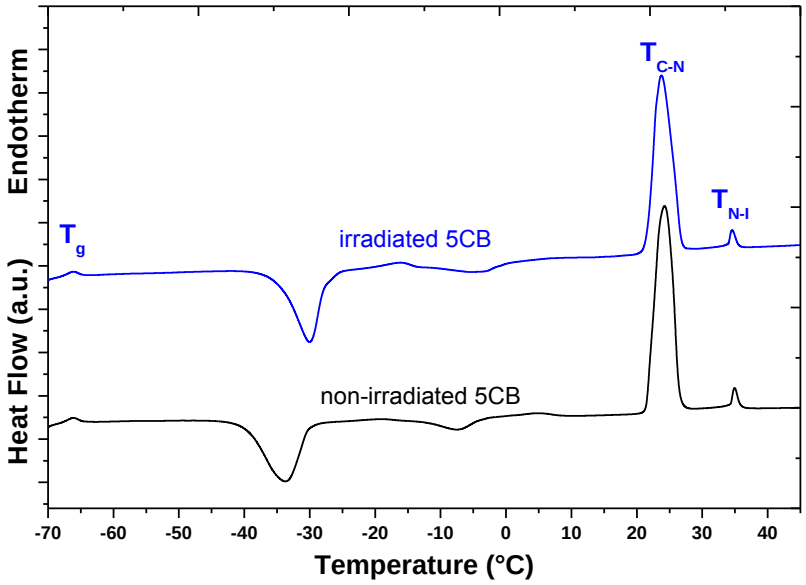

Figure 4.22: DSC thermogram of non-irradiated and irradiated 5CB sample under EB irradiation rate 115 kGy.

A typical thermogram in Figure 4.23 shows the crystalline-LC transition was endothermic with more energy than the LC-liquid transition. For both non-irradiated and irradiated samples, the glass transition temperature T_g, the crystalline to nematic (T_C-N) and the nematic to isotropic T_{N-I} transition are almost identical as further proof for the thermophysical stability of 5CB at high irradiation dose. In addition, the samples show small shift in the crystallization phase due to the equipment calibration that may affect variation in cooling and heating rates during measurements.

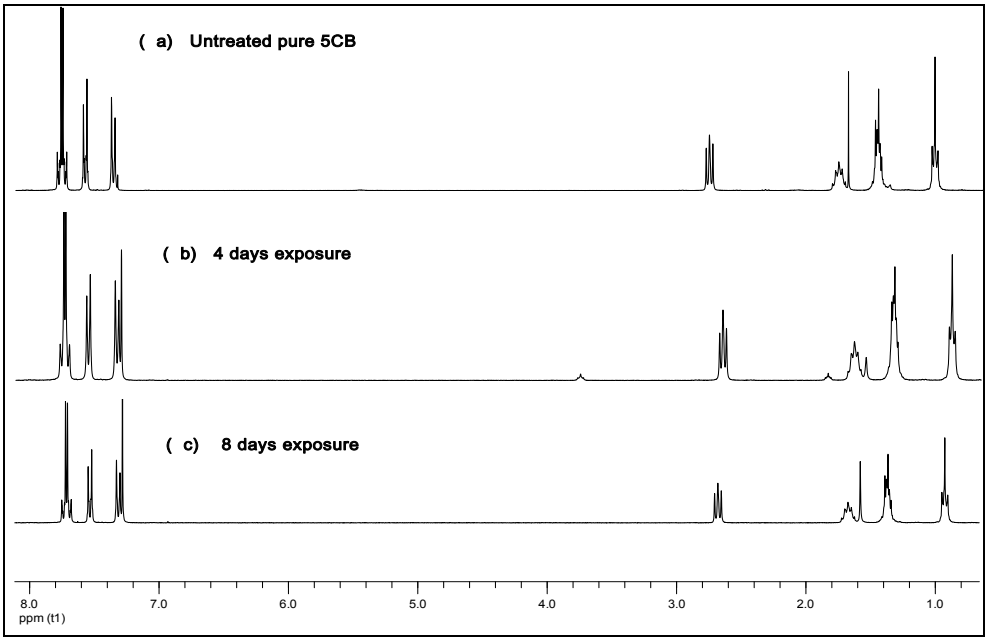

Figure 4.23: ^{1}H NMR spectra for 5CB structure as a function of the UV exposure time.

Molecular configuration of the liquid crystal molecules can also be analyzed by NMR spectroscopy to follow the response of the 5CB molecules to continuous UV irradiation dose. A series of liquid crystal samples have been exposed to longtime UV radiation (365 nm) up to 10 days to investigate the stability of 5CB under continuous irradiation. These results would be interested in the selection of liquid crystal for the PDLC film. The structural analysis by ^{1}H NMR spectroscopy for these samples is shown in figure 4.24. It is observed that the signals of all groups in the liquid crystal are almost identical with the same chemical shifts. This indicates the structural stability of the liquid crystal upon exposure to high irradiation doses.

4.8 Conclusions

Photoinduced polymerization process PIPS has been used to prepare PDLC films with different morphology and has been characterized by POM, DSC and FTIR spectroscopy. The relationship between morphology, composition domains and molecular interactions has been investigated.

Morphology of PDLC films was found to be dependent on the conditions of preparation as the irradiation dose, initiator concentration and liquid crystal concentration in the initial mixture. Alignment of nematic dispersed phase in contact with the polymer network is sensitive to the morphology and branching of the polymer chains, which is related to the condition of preparation of the PDLC films. Morphology and LC distribution in TPGDA was elaborated, where higher reaction rate leads to smaller LC droplets size which accompanied with low molecular weight polymer networks.

FTIR measurement showed changes in the 2EHA/5CB samples based on the curing method, which indicate different condiment behavior of LC between UV and EB curing, based on the spectral bands of alkene at 1637, 1622, 1407 and 810 cm^{-1} during polymerization, notice that no emergence of new bands upon formation of polymer networks.

DSC analysis showed that phase transition can be adjusted over the temperature range between the transition temperatures prepared from acrylate polymer by varying irradiation rate, initiator concentration and the composition of the initial mixture.

Confinement dynamic of liquid crystal in the polymer matrix has been established based on the preparation conditions. Furthermore, stability of liquid crystal phase has been investigated at longtime and high radiation exposure.

4.9 References

[1] F. Roussel, U. Maschke, J.-M. Buisine, X. Coqueret, F. Benmouna, Phys. Rev. E., 62, 2310-2316 (2000).
[2] G. P. Crawford, S. Zumer, Eds, Liquid Crystals In Complex Geometry, Taylor & Francis: London, (1996).
[3] P. J. Wojtowicz, P. Sheng, Plenum Press: New York (1974).
[4] F. D. Bloss, Optical crystallography, Mineralogical Society of America: Washington D. C., (1999).
[5] S. Chandrasekhar, Liquid Crystals, Cambridge Univ. Press: Cambridge (1977).
[6] G. P. Crawford, J. W. Doane, S. Zumer, Oxford University Press: New York, p.347 (1997).
[7] M. Mucha, Prog. Polym. Sci., 28, 837-73 (2003).
[8] L. Bouteiller, P. LeBarny, Liq. Cryst., 21, 157-74 (1996).
[9] Drzaic, P. S. Liquid Crystal Dispersions; World Scientific: Singapore (1995).
[10] F. Roussel, J.M. Buisine, U. Maschke, X. Coqueret, Liq Cryst, 24, 555–61 (1998).
[11] R.T. Pogue, L.V. Natarajan, S.A. Siwecki, V.P. Todiglia, R.L. Sutherland, T.J. Bunning, Polymer, 41, 733–41 (1999).
[12] D. Nwabunma, H. W. Chiu, T. Kyu, Macromolecules, 33, 1416-24 (2000).
[13] K. Amundson, A. Van Blaaderen, P. Wiltzius, Phys. Rev. E., 55, 1646-54. (1997).
[14] A. Benmouna, X. Coqueret, J.M. Buisine, A. Daoudi, F. Benmouna, F. Roussel, U. Maschke, Molec. Cryst., 365, 1243-1251, 2001.
[15] P.W. Voorhees, J. of Statistical Physics, 38, 231 (1985).
[16] F.M. Mirabella, J.S. Barley, J. Polym. Sci., Part B : Polymer Physics, 32, 2187 (1994).
[17] K. R. Amundson, M. Srinivasarao, Phys. Rev. E., 58, R1211-4. (1998).
[18] H. Tanaka, J. Phys.: Condens. Matter, 12, R207-64 (2000).
[19] P. Majewska, M. Rospenk, B. Czarnik-Matusewicz, L. SobczyK, Chemical Physics, 334, 117, (2007).
[20] H. Gunzler, H.U. Gramlich, IR Spectroscopy, Wiley-VCH, (2002).
[21] K. Kamide, S. Matsuda, K. Kowsaka, Polymer Journal, 20, 3, 231, (1988).
[22] L. Frunza, H. Kosslick, U. Bentrup, I. Pitsch, R Fricks, S. Frunza, A. Schonhals, J. of Mol. Struct., 651, 341, (2003).
[23] Z. Chen, R. Nozaki, Physical Review, E 84, 011401 (2011).
[24] F. Roussel, J.M. Buisine, U. Maschke, X. Coqueret, Phys. Rev., 62, 2 (2000).
[25] M. Ballauff, Mol. Cryst. Liq. Cryst. Lett., 4, 15–22 (1986).
[26] M. Vilfan, T. Apih. P.J. Sebastiano, G. Lahajnar, S. Zumer, Phys. Revue E, 5, 1708 (2007).
[27] I. Gnatyuk, G. Puchkovoska, I. Chashechnikova, F. Nozirov, S. Jurga, B Peplinska, Journal of Molecular Structure, 700 183 (2004).
[28] F. Rousel, C. Canlet, B.M. Fung, Phys. Revue E, 65, 2, 1701 (2002).
[29] P. J. Collings, J. S. Patel, Eds., Oxford University Press: New York (1997).
[30] K. Hiltrop, H. Stegemeyer, Ber. Bunsen. Phys. Chem., 85, 582-8 (1981).

[31] M.F. Sharlow, W.M. Gelbart, Liq. Cryst., 11, 25-30 (1992).
[32] F.M. Aliev, V.N. Zgonnik, Eur. Polym. J., 27, 969-73 (1991).
[33] G.W. Smith, Phys. Rev. Lett. 70, 198 (1993).
[34] R.S. Barnum, S.H. Goh, J.W. Barlow, and D.R. Paul, J. Polym.Sci., Polym. Lett. Ed. 23, 395 (1985).
[35] R. Z. Greenley, Polymer Handbook, J. Brandrup, E. H. Immergut, E. A. Grulke, Eds. John Wiley and Sons: New York, II-268 (1999).

5 BRANCHING AND CHAIN TRANSFER IN RADICAL POLYMERIZATION

5.1 Introduction to chain transfer

Chain transfer to polymer during free-radical polymerization can lead to highly branched polymers, with significant consequences on their rheological and mechanical properties. Chain termination occurs when two radical species react to form one or two new molecules. Therefore, Chain transfer occurs when a radical reacts with a non-radical species on the double bond (C=C) of the propagating polymer chain to produce a new radical. The chain end radical usually attacks the weak bond and a monomer transferred to the chain end.

NMR spectroscopy is considered a powerful tool for investigation of polymer molecular structure. NMR can be used to estimate the degree of branching, which may influence the mechanical properties of polymer network. The magnetic relaxation and the dipolar correlation effects can give information about polymer crosslink density [1,2].

In free radical photopolymerization of acrylates under UV irradiation, the weight percent of photoinitiator and the intensity of UV irradiation affect the molecular structure of the polymer network. On the other hand, the intensity of electron beam EB dose plays a major role in determining the molecular structure of the produced polymer. In this work the molecular structure and degree of branching will be investigated, in addition to the study change transfer to liquid crystal during the photopolymerization under different preparation conditions, by varying the irradiation intensity, initiator and liquid crystal concentration in the composite mixture. Furthermore, this study will offer a control mechanism in preparation of PDLC. 2EHA and TPGDA have been used to perform this study with 5CB as a liquid crystal to prepare the composite films.

In free radical polymerization of acrylates, transfer to polymer has a considerable effect on the properties of polymer network. During propagation reaction, transfer to polymer leads to mid-chain radicals and branching which have much lower reactivity than the end chain radicals that result in decreasing the polymerization rate [3,4]. The mid-chain radicals are usually formed by intramolecular transfer to polymer.

Mechanism of branching has been reported in the literature in polyacrylate systems by several research groups. Branching of poly(2EHA) by solution polymerization in cyclohexane solvent was studied and also for the solution polymerization of poly(methyl acrylate) [5,6].

Solution state NMR spectroscopy would give high spectral resolution makes it suitable for wide range of polyacrylate systems which exhibit full solubility during analysis. Whereas, this technique has limitations for the polyacrylates of low solubility or gel fraction. Thus more accurate measurements can be obtained by solid state NMR spectroscopy to overcome the low solubility. However solid state NMR has low sensitivity and resolution compared to solution state NMR specially analysis of crosslinked polymers.

The objective of this chapter is to study branching and chain transfer in photopolymerized systems based on the nature of branching in radical polymerization of 2EHA that was not discussed in the literature despite the importance of solvent-free acrylate polymerization in many commercial applications. In addition, to investigate the intermolecular and intramolecular chain transfer to the polymer and liquid crystal during polymerization.

5.2 Transfer reaction to the polymer

Chain transfer to polymer takes place with existing polymer chain at low monomer concentration in the reactive mixture, usually at the end of a radical polymerization when almost all monomer has been consumed during the photopolymerization. Termination of the growing radicals lead to chain transfer to monomer or chain transfer to solvent during polymerization and generate dead polymers and other radical species. Furthermore, termination may take place by coupling reactions with the radical species. Backbiting and hydrogen abstraction result in the formation of tertiary radicals as shown in figure 5.1. Long chin branches are formed by hydrogen abstraction while backbiting result in short chain radicals.

5.2.1 Intramolecular chain transfer

Intramolecular chain transfer reaction has received growing interest in the research studies in the last few years to describe kinetic of acrylate polymerization. It has been characterized in the polymerization of ethylene in which growing radicals form six membered intermediate rings [7]. Presence of characterization tools like NMR spectroscopy has accelerated these research interests to study the reaction mechanism of acrylate radical polymerization. Chain transfer may occur at low monomer concentration during the propagation reactions in the

polymerization of acrylates [8,9]. Intramolecular transfer to polymer is now recognized as a major reaction in the radical polymerization of acrylates; the transfer proceeds mainly through backbiting leading to short-chain branches.

5.2.2 Intermolecular chain transfer

Intermolecular chain transfer to polymer and random intramolecular transfer to polymer lead to formation of long-chain branches of various lengths. Gel formation is common in polymerization of acrylic monomers, which occur due to intermolecular chain transfer to polymer followed by termination by combination [10]. Short chain branches are obtained by backbiting and are of few monomer units long in terms of polymerization kinetics, while the branches formed by intermolecular transfer result in long chain branches.

Intermolecular chain transfer to polymer increases with polymer concentration and hence with conversion. Low monomer concentration would lead to a higher rate of intermolecular chain transfer to polymer, namely to a higher amount of gel [11]. Mechanism of both intermolecular and intramolecular chain transfer to polymer can be summarized in figure 5.1 as follow:

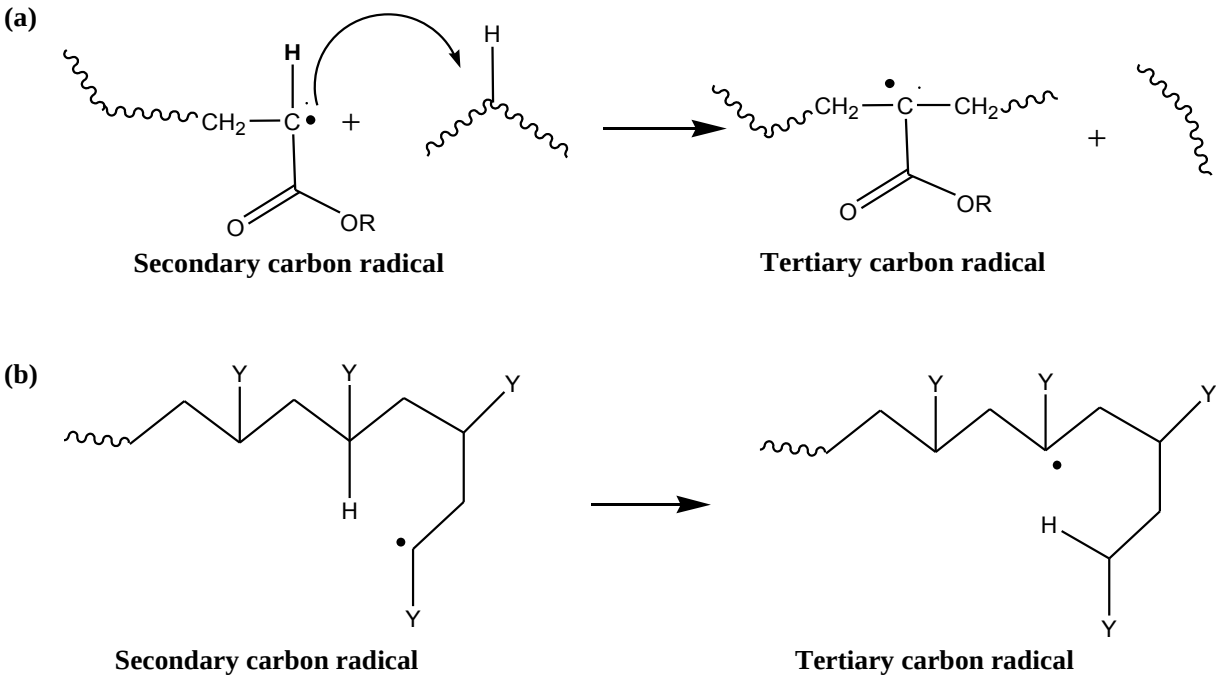

Figure 5.1: The mechanism of the (a) Intermolecular (b) Intramolecular chain transfer in free radical photopolymerization of 2-ethylhexyl acrylate, Y= COOR.

Transfer reactions to polymer were studied by many authors [12,13,14]. It is a complex reaction as radical exists inside the chain not at the chain end. The end chain radical is transferred either to a polymer chain or it is transferred in its own chain by a mechanism involving intramolecular six centers. From this radical that formed in the middle of the chain, there may be several reactions does not lead to a sudden increase of the molar mass.

The simplest mechanism is the addition of a monomer to form a quaternary carbon. While, ß division causes the formation of a secondary radical building at the chain end as shown in figure 5.2. A structural analysis of the polymer appears necessary to confirm or to ignore this type of mechanism; NMR is the ideal tool for this type of analysis.

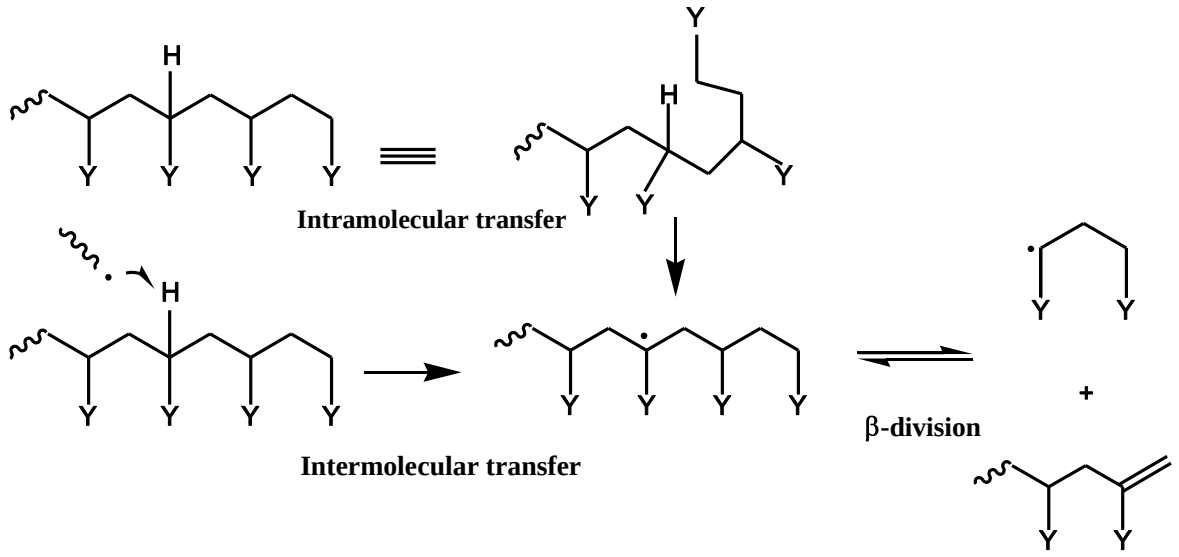

Figure 5.2: The mechanism the formation macromolecules by the transfer to polyacrylates polymer, Y=COOR.

Short chain branching has a significant effect on the melting point, glass-transition temperature and hardness as well as the degree of crystallinity. While, long-chain branching affects rheological properties such as sedimentation behavior, intrinsic viscosity and elasticity of the polymer melt.

Branching and chain transfer was observed using ^{13}C NMR spectrometry in solution polymerization of 2EHA by hydrogen abstraction of tertiary C-H on the polymer backbone, at low monomer conversion where the initial monomer concentration decreased due to the consumption of monomer [15].

5.3 Structural analysis

The molecular structure of the monomer, liquid crystal and polymer system has been performed by ^{1}H and ^{13}C NMR spectroscopy to describe the internal configuration and shape of the liquid crystal and polymer systems.

5.3.1 Structural analysis by ^{1}H NMR spectroscopy

The ^{1}H NMR spectra of the 5CB liquid crystal is shown in Figure 5.3. We observe displacement the protons of the aromatic ring of 5CB between 7 and 8 ppm. In this range, 2EHA has no signals. The aliphatic protons appear at the right hand side of the spectra between 1 and 2 ppm and the $CDCl_3$ signal appears at 7.2 ppm.

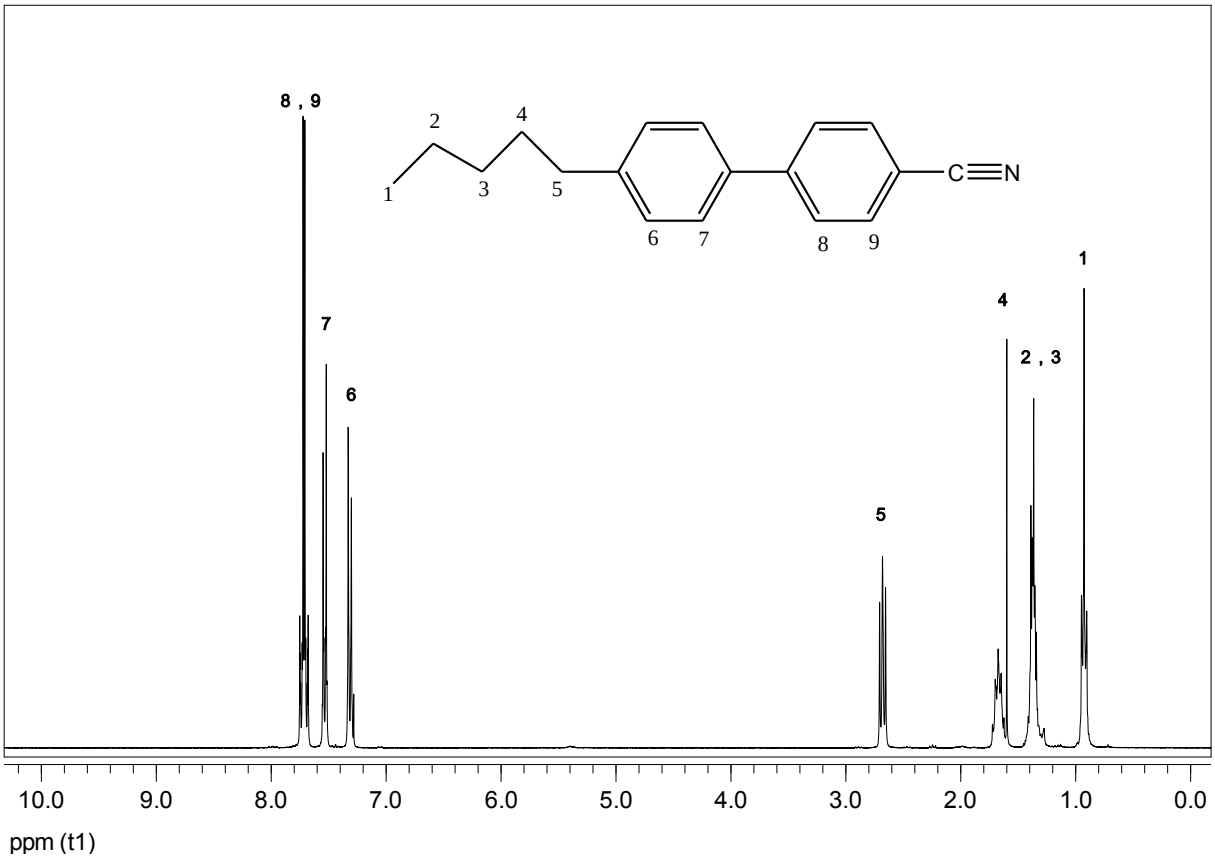

Figure 5.3: ^{1}H NMR spectra of pure the liquid crystal 5CB.

^{1}H spectra of 2EHA monomer is presented in figure 5.4, protons of C=C bond appears between 5.5 and 6.5 ppm, this signal is expected to disappear after polymerization. The aliphatic protons are located at the right hand side of the spectra between 1 and 2 ppm. The slight shift around this signal represents the 8-cis and 8-trans protons at the end of the monomer chain.

Table 5.1: The ^{1}H NMR spectral assignments for 2EHA monomer.

Peak	Chemical shift (ppm)	Proton
6	4.1	$-OCH_2$
7	6.1	vinyl-tertiary
8 trans	5.9	vinyl- trans
8 cis	6.4	vinyl-cis

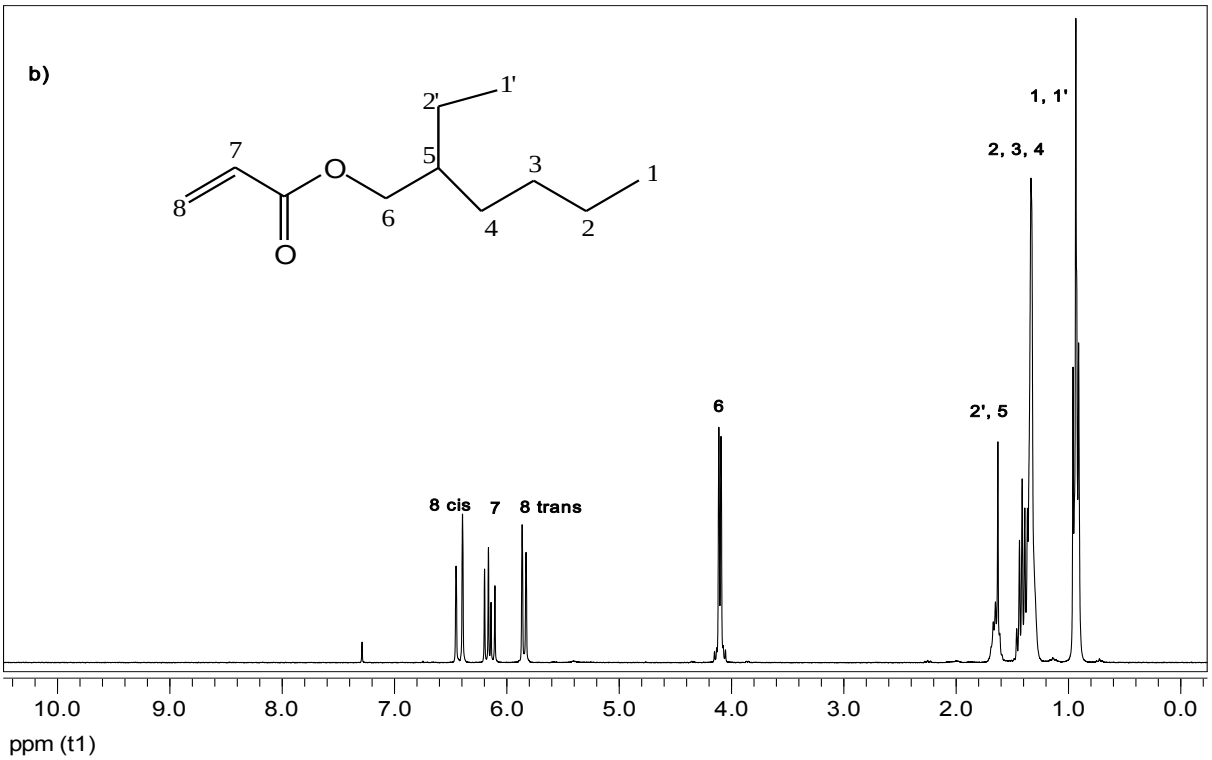

Figure 5.4: ^{1}H NMR spectra of 2-ethylhexyl acrylate (2EHA) pure monomer.

In figure 5.5 presented the ^{1}H NMR spectra of poly(2EHA). We clearly observe the disappearance of C=C signals located between 5.5 and 6.5 ppm after complete polymerization. On the other hand, the signals for the secondary and tertiary carbons of the backbone appear at 1.9 and 2.3 ppm respectively. Furthermore a small shift of the C-3 of the polymer chain from 4.1 to 3.9 is observed in the spectra.

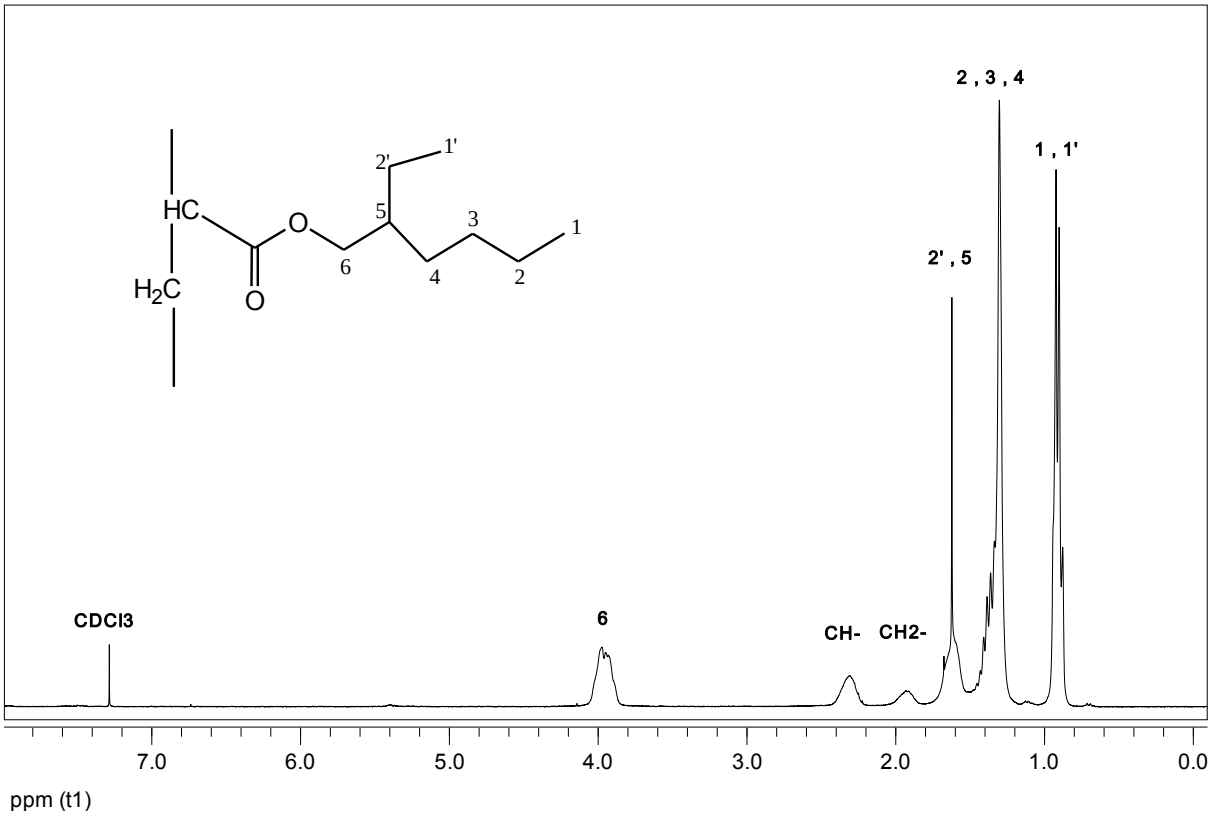

Figure 5.5: ^{1}H NMR spectra of poly 2-ethylhexyl acrylate polymer.

^{1}H NMR spectra of pure TPGDA is given in figure 5.6. The C=C double bond protons appear at the left hand side of the spectra and have a chemical shift between 5.5 and 6.5 ppm. The slight shift around the double bond signal represents the 1-cis and 1-trans protons at the end of the monomer chain. The aliphatic protons are at the right hand side of the spectra at a chemical shift between 1 and 2 ppm. The $CDCl_3$signal appears at 7.2 ppm. The other signals represent the chemical shift of the other protons in TPGDA monomer, the location of these protons are labeled with numbers in the spectra.

Table 5.2: The ^{1}H NMR spectral assignments for 2EHA polymer.

Peak	Chemical shift (ppm)	Proton
6	4.1	$-OCH_2$
CH-	2.1	Backbone-tertiary
CH_2	1.9	Backbone- secondary

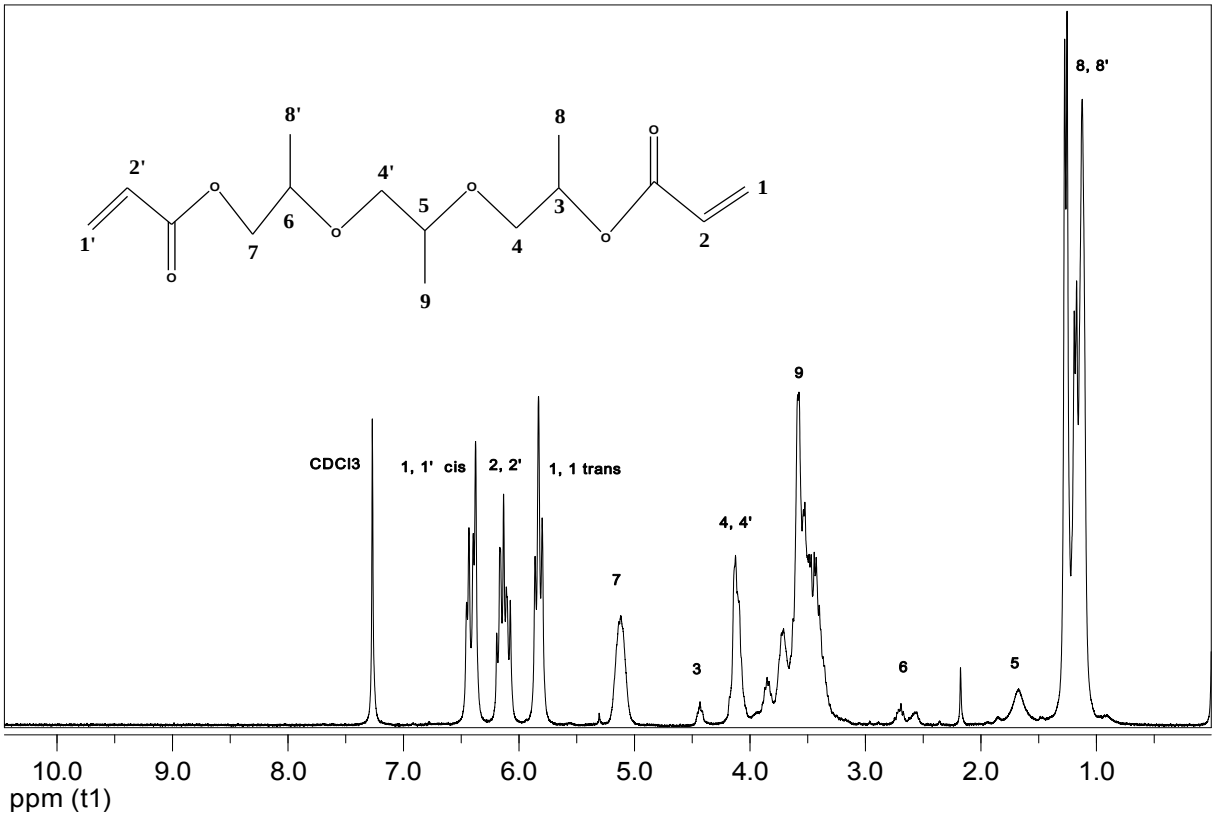

Figure 5.6: ^{1}H NMR spectra of pure tripropylene glycol diacrylate (TPGDA) monomer.

Radical polymerization of TPGDA results in the formation of crosslinked polymer due to the presence of two functional groups in the monomer chain. Solubility of crosslinked polymers in $CDCl_3$ is low compared to the monofunctional acrylates. Liquid state ^{1}H NMR spectroscopy of TPGDA polymer is shown in figure 5.7. Disappearance of double bond peaks are clearly observed in the spectra. In addition, signal of the methylene protons appears at about 3.7 ppm while the aliphatic protons at the right hand side of the spectra. The solid state NMR spectroscopy has considerable limitations to determine clear chemical shift of poly(TPGDA). This requires more sophisticated NMR spectroscopy to perform constructive solid state analysis.

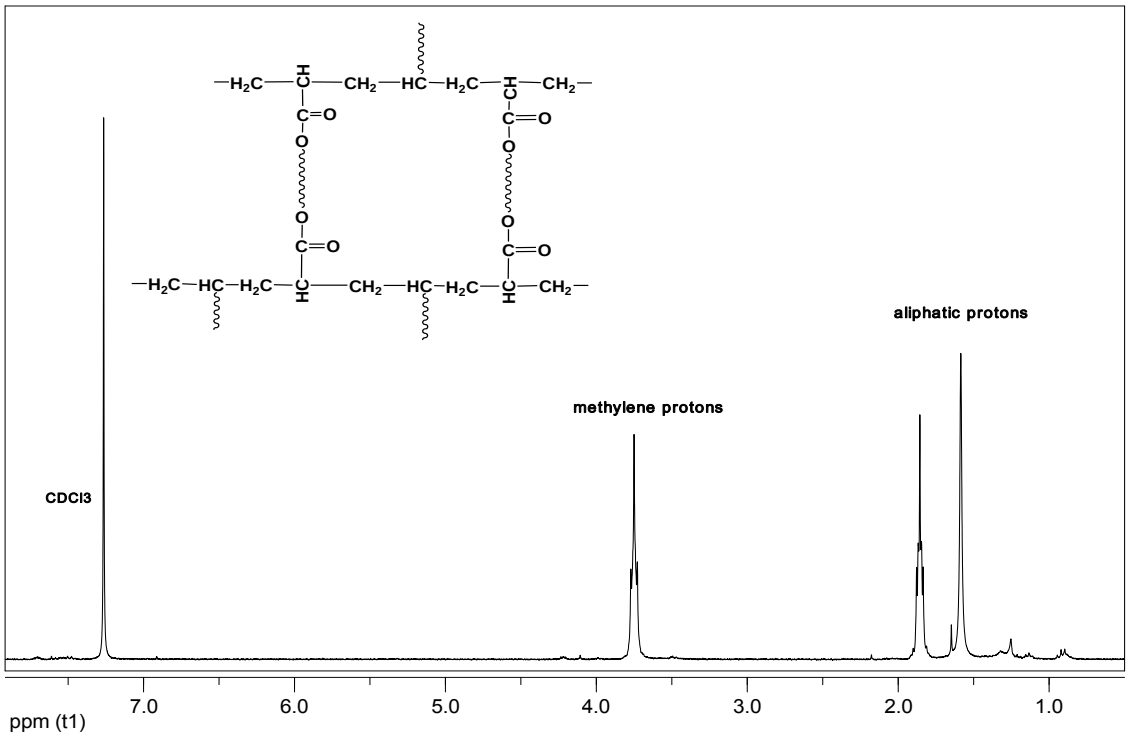

Figure 5.7: ^{1}H NMR spectra of Poly tripropylene glycol diacrylate poly(TPGDA) polymer.

5.3.2 Structural analysis by ^{13}C NMR spectroscopy

^{13}C NMR spectroscopy indicates number of carbon atoms occupying specified environments in the molecule. By comparing chemical shifts of signals in the spectrum, we may be able to infer the structural environments of carbon atoms in the molecule. ^{13}C NMP spectrum of 2EHA monomer is presented in figure 5.8, assignments of the peaks are given in table 5.3. Chemical shifts were referenced to the solvent $CDCL_3$ resonance which lies at 77 ppm. Additionally, terminal methyl group of 2EHA monomer unit was observed at 11 ppm.

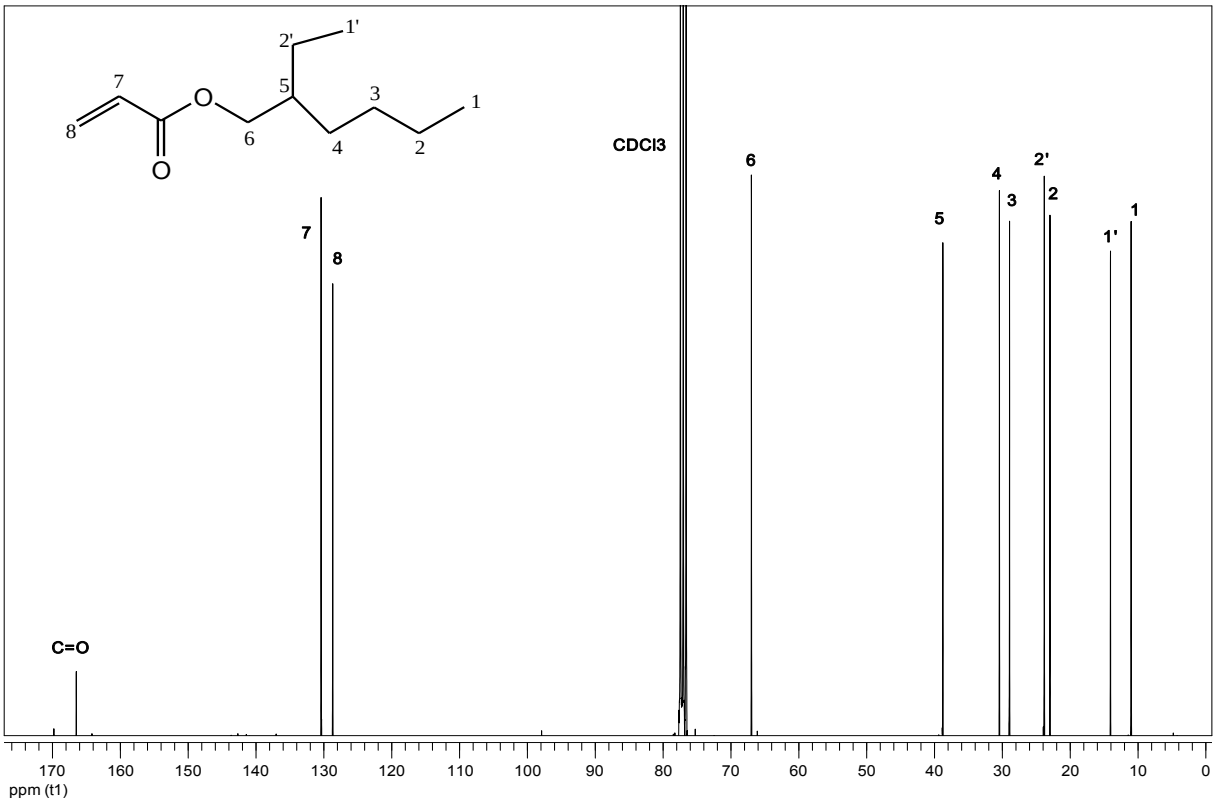

Figure 5.8: ^{13}C NMR spectra of poly 2-ethylhexyl acrylate PEHA polymer.

Table 5.3: ^{13}C Shift assignments of 2EHA monomer

Chemical shift (ppm)	**Carbon**
10.3	1-CH_3
13.4	1'-CH_3
22.6	2-CH_2
23.5	2'-CH_2
28.6	3-CH_2
30.1	4-CH_2
38.5	5-CH
66.0	6-CH_2
128.5	8-CH_2=
130.5	7-CH=
168.5	C=O

Figure 5.9 presents the ^{13}C spectra of pure 5CB, the chemical shift of aromatic ring carbons is observed between 128 and 132 ppm. The carbons of the aliphatic group are located at the right hand side of the spectra between 10 and 32 ppm. Chemical shift of the carbon of benzyl group is found at about 36 ppm. Displacement of $CDCl_3$ is located at 77 ppm.

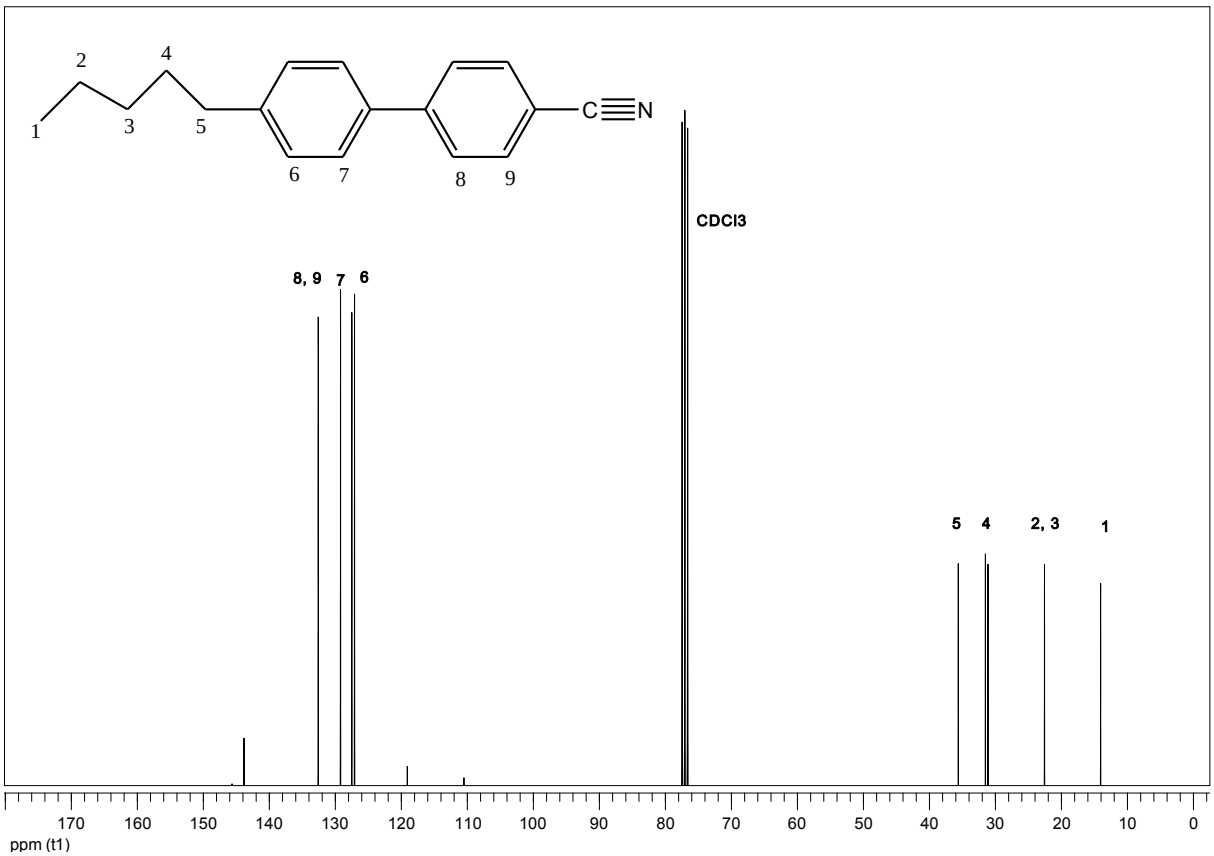

Figure 5.9: ^{13}C NMR spectra of pure liquid crystal 5CB.

In figure 5.10, ^{13}C chemical shifts for P2EHA systems have previously been reported as: 48, 41 and 35 ppm for the quaternary carbon C_q, tertiary carbons CH_t and CH_2 sites respectively. Chemical shifts for P2EHA are given in table 5.4.

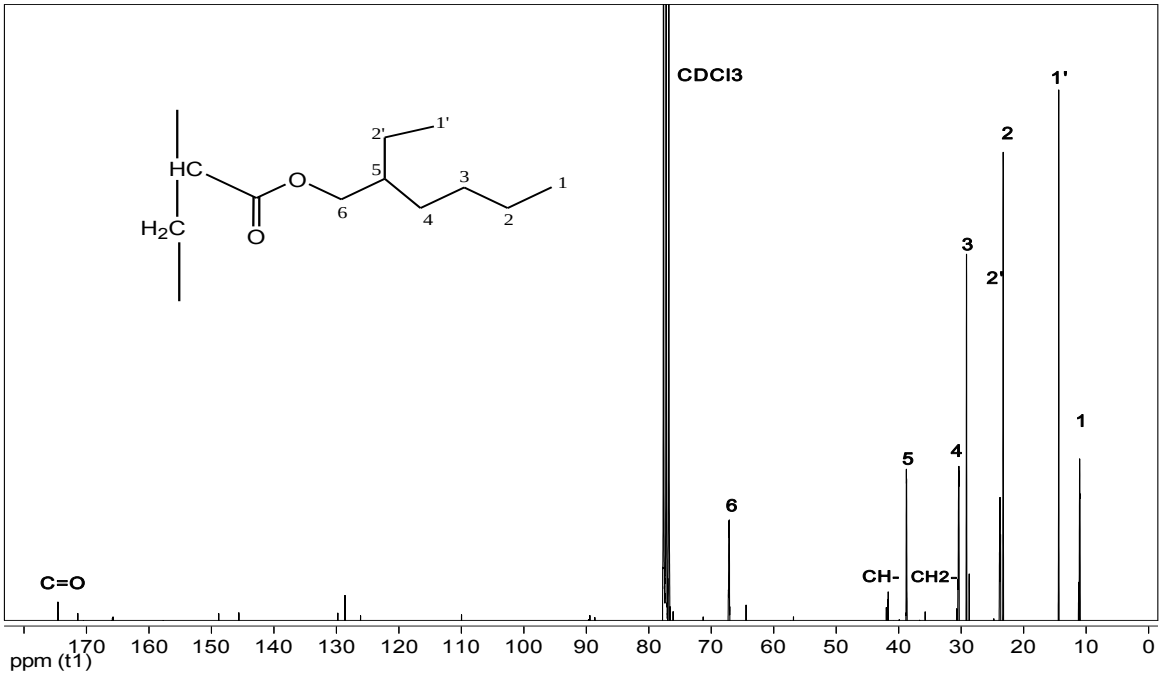

Figure 5.10: ^{13}C NMR spectrum of poly(2-ethylhexyl acrylate) in $CDCl_3$ solvent. The assignments of the labeled peaks are given in Table 5.2.

Table 5.4: The ^{13}C Shift Assignments of poly(2-ethylhexyl acrylate) system.

Chemical shift (ppm)	**Carbon**
10.3	1-CH_3
13.4	1'-CH_3
22.6	2-CH_2
23.5	2'-CH_2
28.6	3-CH_2
30.1	4-CH_2
34.8-35.6	Backbone-secondary CH_2-
38.5	5-CH
41.2	Backbone-tertiary CH-
48.0	Branch quaternary C_q
66.0	6-CH_2
77	Solvent $CDCl_3$
171.2	branch or terminal C=O
173.5	2EHA C=O

5.4 Degree of branching

Degree of branching can be defined as the ratio of the branched to non-branched units. During photopolymerization process, one can distinguish between three types of polymer chains based on the type of carbon atom in the polymer chain, which are secondary carbon CH_s, tertiary carbon CH_t and C_q representing linear and branched polymer chains as shown in figure 5.11. Degree of branching may be generally quantified based on the areas of the branched quaternary site $A(C_q)$ and of the non-branched tertiary carbon site $A(CH_t)$ [16].

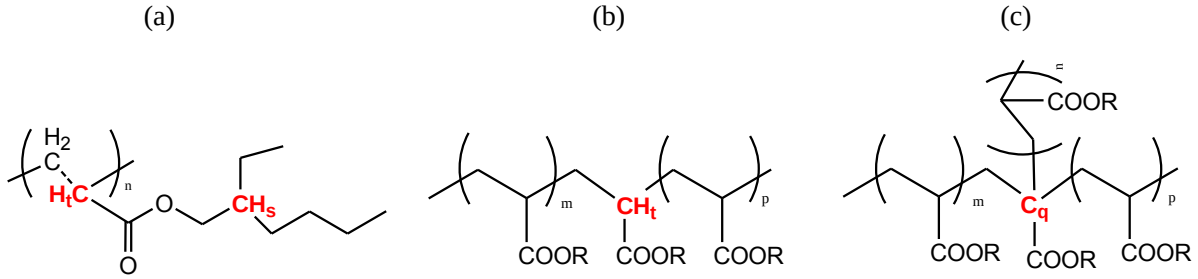

Figure 5.11: Chemical structure of the (a) 2EHA monomer unit, (b) linear poly(2EHA) and (c) branched polymer.

Secondary radicals are usually obtained in propagation reactions, while the tertiary radicals result from chain transfer to polymer by backbiting. The tertiary radicals are less reactive than the secondary radicals that result in domination of backbiting that reduce propagation rate during polymerization [17].

Distortionless enhancement by polarization transfer (DEPT) experiment is highly sensitive and can fully separate the carbon signals. DEPT technique was used to determine the multiplicity of the peaks, i.e., whether a given carbon was primary, secondary, tertiary or quaternary. The mole percent of branched units in the P2EHA samples can be calculated as follows:

$$\%\ Branch = \frac{A(C_q)}{A(C_q) + \frac{A(CH_t + CH_2)}{2}} * 100 \qquad (5.1)$$

where $A(C_q)$ is the peak area corresponding to the quaternary carbon and $A(CH_t)$ and $A(CH_2)$ area under peaks corresponding to CH- and CH_2 of the backbone as shown in figure 5.11-(c).

Since the peak corresponding to quaternary carbon not clearly identified in the ^{13}C NMR spectra which shows formation of quaternary carbon can be neglected in studying the configuration and branching of polymer networks. Further analysis of polymer matrix will be basically based on formation of terminal double bond carbon at the end of the polymer chains and the extent of tertiary and secondary backbone carbons.

Quantification of branching can be estimated based on peaks area of the CH- and CH_2- of the backbone as shown in figure 5.12 using equations 5.2 and 5.3:

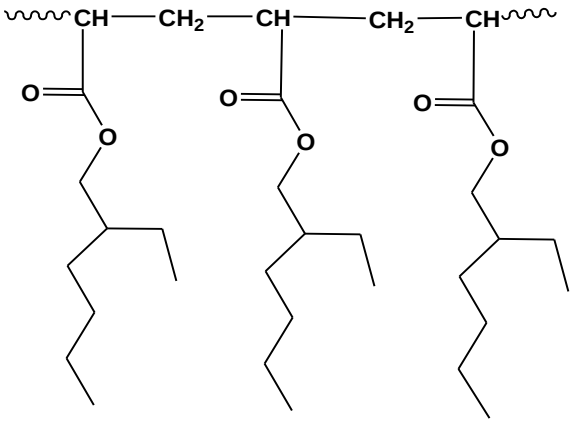

Figure 5.12: The chemical structure of P2EHA.

$$\%\ Branch = \frac{\frac{1}{3}A(-CH + CH_2-)}{A(All\ backbone\ carbons)} * 100 \qquad (5.2)$$

$$\%\ Branch = \frac{A(CH-)}{A(CH-) + A(CH_2-)} * 100 \qquad (5.3)$$

Percent of terminal double bonds can be calculated based on presence of unsaturated double bond in the polymer network in the ^{13}C NMR spectra using the following equation:

$$\%\ Terminal\ group = \frac{A\ (C=O)_t}{A(C=O)} * 100 \qquad (5.4)$$

where, $A\ (C=O)_t$ is the peak area of C=O next to a terminal double bond and $A(C=O)$ is the peak area of all C=O in the chain.

Furthermore, percent of terminal double bonds can be calculated based on the presence of unsaturated double bond in the polymer network by ^{1}H NMR spectra based on the following equation:

$$\%\ Terminal\ group = \frac{A\ (=CH_2)_t}{A(-OCH_2)} * 100 \qquad (5.5)$$

where, $A\ (=CH_2)_t$ is the peak area of $=CH_2$ of the terminal double bond and $A(-OCH_2)$ is the peak area of all hydrogen in the polymer chain.

Configuration of terminal double bond of the polymer chain is given in figure 5.13.

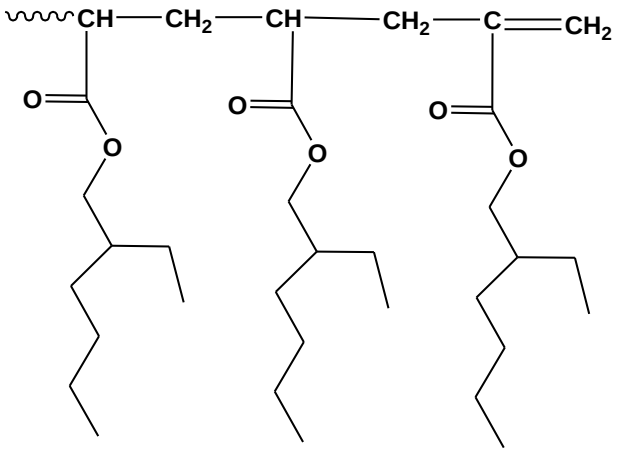

Figure 5.13: The terminal double bond of P2EHA.

In figure 5.14, chemical shifts of terminal double bond of P2EHA are assigned using ^{1}H NMR spectroscopy. Chemical shift of the vinyl chain end $=CH_2$ is found at 5.5 and 6.7 ppm due to presence of different cis and trans environment of the two hydrogen atoms. The peak at 1.9 ppm represents protons of CH_2- next to the quaternary carbon of the end group. Protons of the backbone carbon CH- appear at 2.3 ppm.

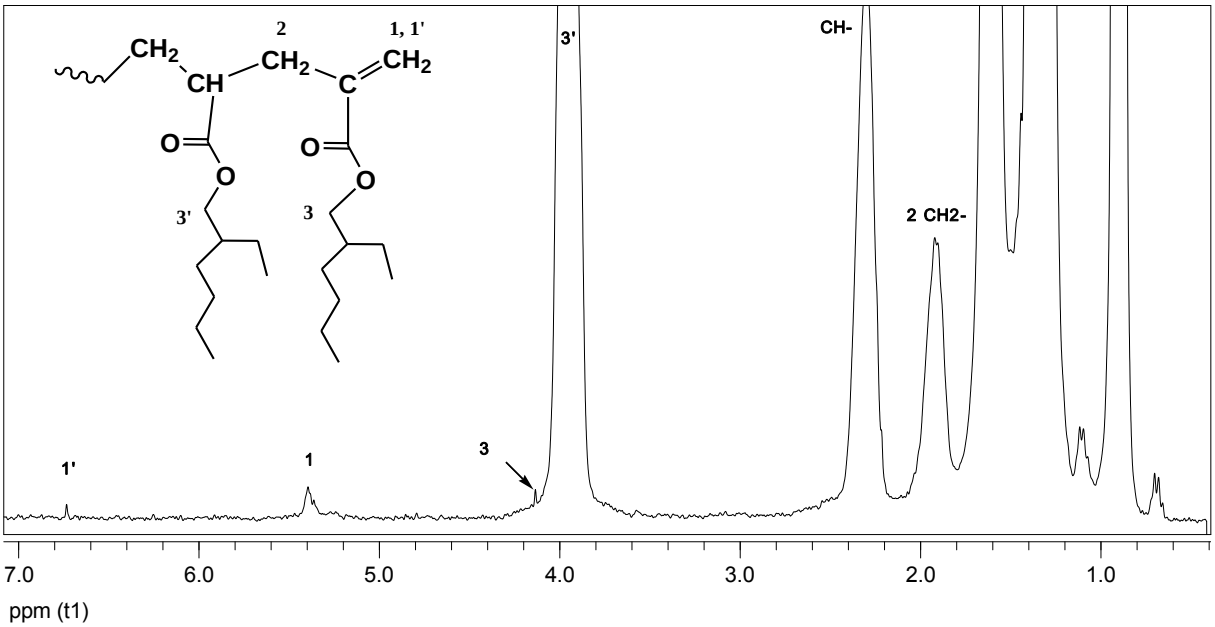

Figure 5.14: ^{1}H NMR spectra of P2EHA in $CDCl_3$ solvent.

Presence of terminal double bond carbon can be confirmed by ^{13}C NMR spectroscopy; the same sample shown in figure 5.14 has been analyzed by ^{13}C NMR spectroscopy and presented in figure 5.15.

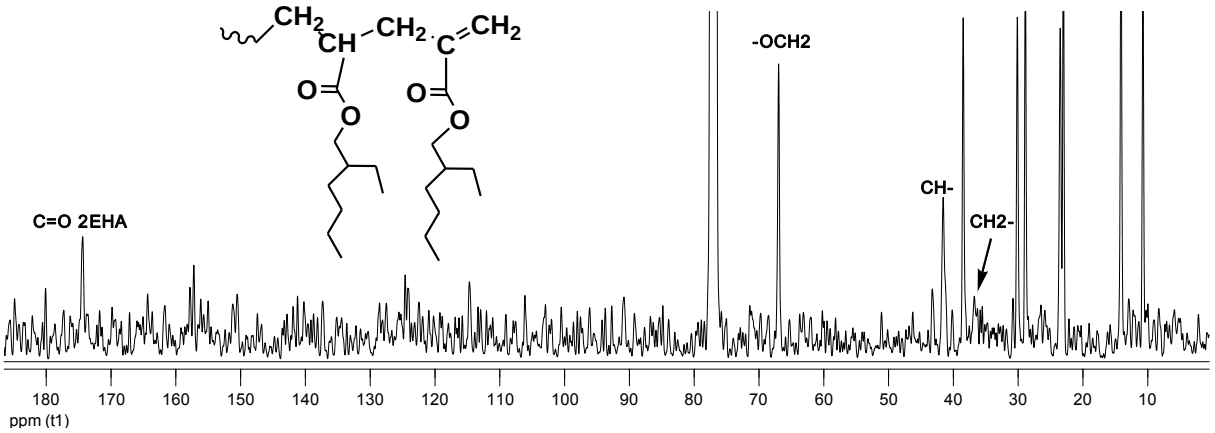

Figure 5.15: ^{13}C NMR spectra of P2EHA in $CDCl_3$ solvent.

In the ^{13}C spectra of P2EHA, terminal C=O group resonance is not clear compared to the ^{1}H spectra in figure 5.15, ^{1}H spectra will be used for quantification of the terminal double bond group and compare different samples based on the preparation condition and composition of the reactive mixture.

5.5 Qualitative analysis of degree of branching

In radical photopolymerization, composition of the reactive mixture and preparation conditions are the key factors that determine reaction rate and reaction mechanism. Accordingly, type of radical species that are formed and the rate of initiation and propagation steps will affect the degree of branching in the polymer chains. In this part, degree of branching will studied as a function of initiator concentration, LC concentration under UV/EB irradiation.

Chain transfer to polymer may occur either at the unsaturation terminal end group by building on the polymer chain end, or by formation of quaternary radical which have a chemical shift of 48 ppm in the ^{13}C NMR spectroscopy. The results obtained by ^{13}C spectroscopy for our polymer composites show no signals attributed to the quaternary carbon at 48 ppm. Which indicate the absence or very low concentration of the quaternary carbon to reflect chemical shift in the ^{13}C spectra, thus, reaction seems to be negligible in radical polymerization of monoacrylates. In solution polymerization of acrylates, formation of quaternary carbon can be observed at lower polymerization rate due to decreasing monomer concentration in the reactive mixture. Transfer reactions usually occur in the polymer by a transfer of radical either by intermolecular or intramolecular chain transfer.

5.5.1 Effect of irradiation rate

Curing parameters have a significant effect on characteristics of the polymer system in radical photopolymerization. Curing efficiency supports optimization of polymer properties within minimum exposure time for the desired industrial applications. This requires good understanding of polymerization kinetics and reaction mechanism, to control the preparation conditions based on the required application. Final objective is to achieve high conversion and composite film with good mechanical and chemical properties [18].

Effect of the UV dose on the extent of $=CH_2$ terminal double bond of P2EHA prepared under different UV irradiation doses is shown in figure 5.16 by ^1H NMR spectroscopy. The $-OCH_2$ chemical shift of the terminal double bond carbon appears at 4.2 ppm adjacent to the $-OCH_2$ protons of the polymer chain, amount of terminal double bond protons at 240 mJ/cm^2 UV dose is clearly much larger than the resonance of that at 400 mJ/cm^2 of UV dose. This is a clear indication of presence of higher amount of terminal double bond at lower irradiation doses. This can be explained by the difference in the reaction rate, at which higher irradiation

dose result in the higher initiating rate and formation of higher amount of radical species that lead to the consumption of more double bonds during the polymerization reaction.

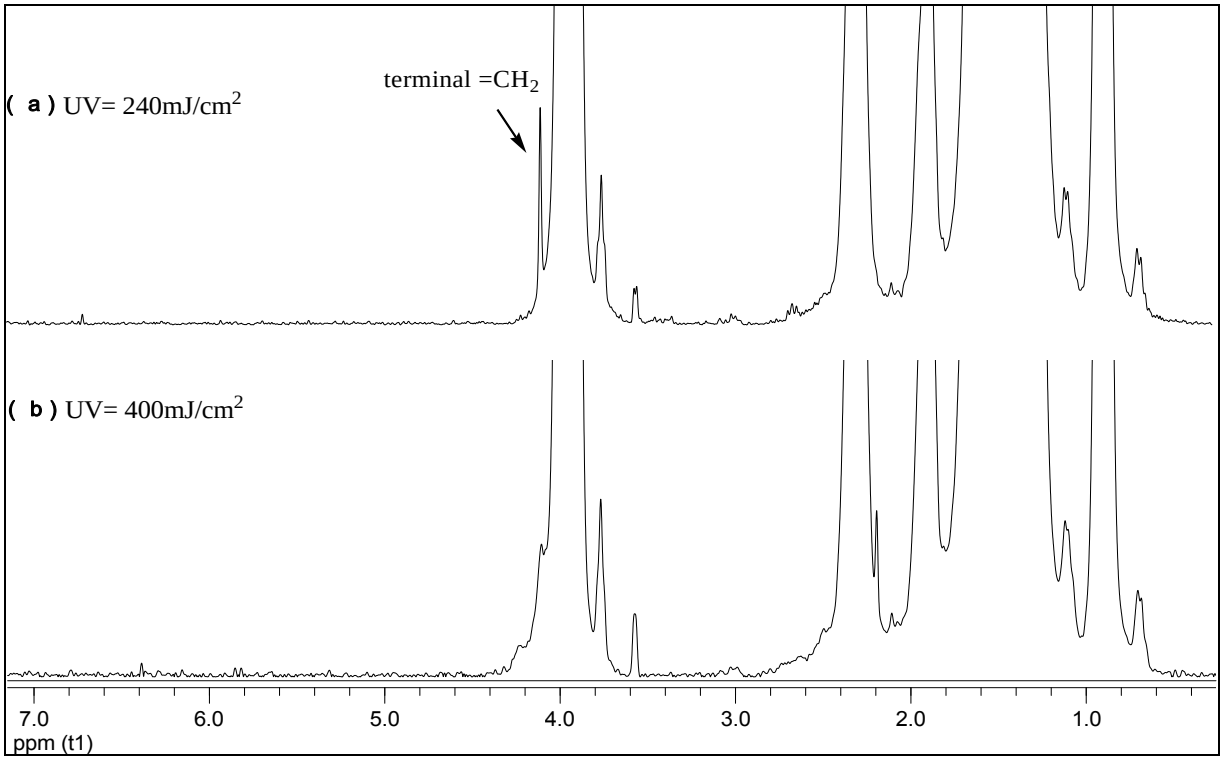

Figure 5.16: The terminal double bond of P2EHA prepared under (a) UV=240 mJ/cm^2 and 400mJ/cm^2 UV dose.

To compare the abundant of the tertiary and secondary backbone carbons at different UV irradiation rates, ^{1}H NMR spectra in 5.16 has been used and applying equation 5.3. No effect of the irradiation rate on the quantity of tertiary and secondary carbons at different irradiation rates is observed. This confirms the previous observations obtained by ^{13}C NMR spectroscopy which show the absence of quaternary carbons in the polymer chains.

Effect of UV irradiation dose on the evolution of terminal double bond and backbone carbons is presented in table 5.5 for a mixture prepared at different irradiation rates. The UV rate has no considerable effect on the ratio of tertiary to secondary backbone carbons in the product matrix. While, increasing UV rate from 120 to 400 mJ/cm^2 leads to a decrease in the terminal double bond ratio from about 8 to 3 ratio percent. This behavior can be explained in terms of polymerization kinetics, where increasing UV rate leads to increase the propagation rate of photopolymerization, which increases potential for formation of more monomer radical

species in the media and chain propagation occurs at the newly formed radical than end double bond termination mechanism.

Table 5.5: Ratio of terminal double bond and backbone carbons as a function of UV irradiation rate.

UV rate (mJ/cm^2)	**% ratio (CH-/CH_2-)**	**% ratio (CH_2=/-OCH_2)**
120	64,10	7,62
240	64,52	2,88
400	63,69	2,75

Evolution of tertiary to secondary carbons and the terminal double bond ratio is presented in table 5.6. A smooth decrease on the tertiary to secondary backbone carbons ratio is observed by increasing EB rate. On the other hand, a significant drop of the terminal double ratio is observed by increasing the EB rate, where doubling the EB rate from 5.8 to 11.5 kGy corresponds to drop in the terminal double bond from about 18.4 to 10.9%. At low EB rate, less radical species are formed in the reactive mixture which reduce the propagation rate, thus, propagation rate increase the potential for formation of end group termination than the chains propagation. As clearly observed in the table 5.6, increase the EB rate to 34.6 kGy results in sharp decrease in the terminal double bond group to less than 2% due to the formation of high percent of monomer radical species.

Table 5.6: The ratio of terminal double bond and backbone carbons as a function of EB rate.

EB rate (kGy)	**% ratio (CH-/CH_2-)**	**% ratio (CH_2=/-OCH_2)**
5.8	65,36	18,42
11.5	62,89	10,93
23,00	41,84	6,67
34.6	39,53	1,72

5.5.2 Effect of photoinitiator

Initiator concentration has a considerable effect on the polymerization rate. In chapter 3 of this study, reaction rate has been studied at different weight percents of the photoinitiator starting from low 0.5 wt % to high 6 wt % photoinitiator. It was observed that the initiation and propagation steps increase rabidly with increasing the concentration of initiator in the composite mixture. The behavior of polymerization and structural analysis of polymer networks at different weight percents of the initiator is given in figure 5.17 by ^{1}H NMR spectroscopy.

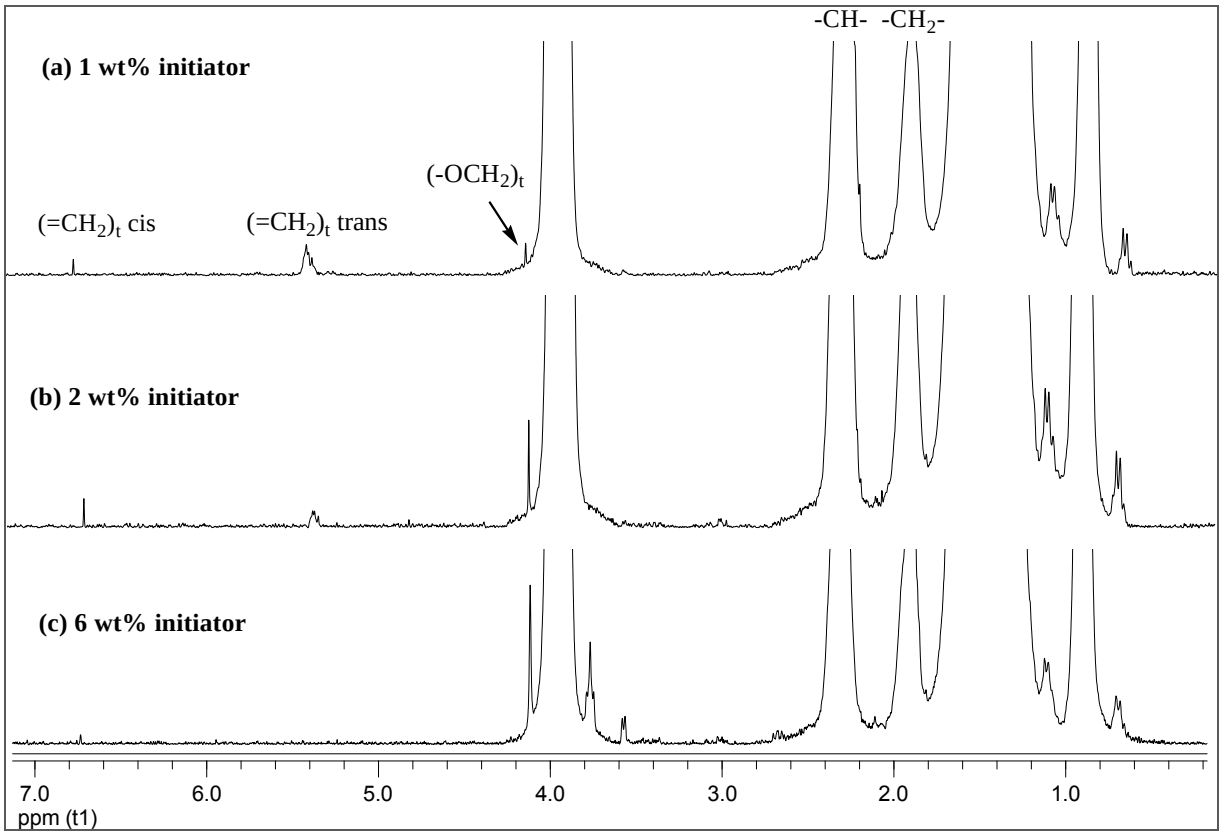

Figure 5.17: Structural analysis of P2EHA prepared by (a) 1 wt % (b) 2 wt % and (c) 6 wt % initiator.

In figure 5.17, absence of the monomer double bond protons between 5 and 6 ppm is a clear indication about the completion of the polymerization reaction in all samples. The protons of terminal double bond appears at 5.5 and 6.7 ppm, protons of the terminal -OCH_2 group appears at 4.1 ppm and the protons of the backbone carbons CH- and CH_2- at 1.9 and 2.1 ppm respectively. We observe the absence or very weak signal of the terminal double bond at higher initiator concentration of 6 wt %, while these signals at 1 and 2 wt % of the initiator

are clearly identified. This can be explained by total consumption of monomer species in the mixture due to presence of high density radical species in the mixture before they can join the polymer chain. Presence of resonances relating to the CH_2= chain end at low initiator concentrations support formation of β-division species and accordingly formation of short chain branches as previously presented for the mechanism of chain transfer reaction in figure 5.2.

Table 5.7: Ratio of terminal double bond and backbone carbons as a function of initiator concentration.

wt % initiator	**% ratio (CH-/CH_2-)**	**% ratio (CH_2=/-OCH_2)**
0.1	65,87	8,83
0,5	65,36	4,12
1	64,52	0,60
2	64,31	0,58

Quantitative comparison of backbone and terminal double bond carbons is given in table 5.7. It can be observed from the obtained data that there is no variation of the ratio between the tertiary and secondary backbone carbon. While, a significant drop of the terminal double bond ratio is observed by increasing the initiator weight percent, at higher concentrations of 2 wt %, only traces of the terminal double bond exist in the polymer mixture. These results support the idea of formation of more radical species and active sites which accelerate consumption of monomer molecules and increasing propagation rate of polymerization at higher initiator concentration.

5.6 Effect of liquid crystal

Polymerization rate increases in less ordered liquid crystal phase based on the monomer structure and liquid crystal properties and concentration. During polymerization, segregation of monomer molecules into the liquid crystal phase results in increasing the local concentration of double bonds and polymerization rate increases. Variation of polymerization rate and degree of segregation play a vital role in preparation of PDLC systems which affect

formation of polymer network structure and accordingly the performance of composite materials in the electronic devices applications. P2EHA/5CB are prepared at different weight percent of the liquid crystal is given in figure 5.18 by ^{1}H NMR spectroscopy.

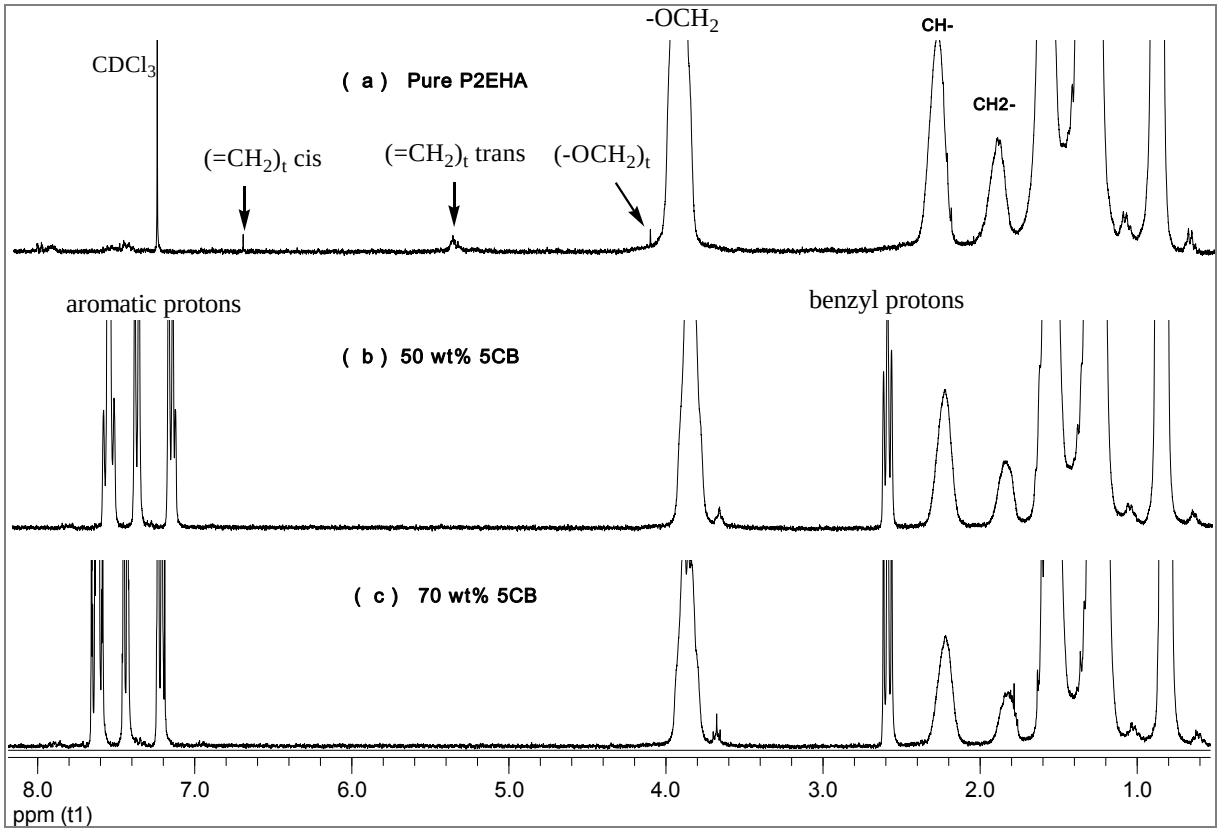

Figure 5.18: Structural analysis of purified P2EHA/5CB composite (a) pure P2EHA (b) 50 wt % 5CB/2EHA and (c) 70 wt% 5CB/2EHA.

The terminal -OCH_2 protons are observed at 4.1 ppm and signals of terminal double bond CH_2= at 5.4 and 6.7 for the trans and cis respectively. It is clearly observed absence of the terminal double bond and terminal –OCH_2 by increasing LC concentration in the reactive mixture. While on the other hand, signals of the benzyl group at 2.6 ppm; and the aromatic group appears between 7 and 8 ppm as shown in figure 5.18 (a) and (b) of the spectra. Absence of terminal double bond group by addition of liquid crystal in the radical polymerization can be explained by increasing local concentration of double bond due to the alignment effect of liquid crystal molecules. This behavior reduces possibility of β-division and toward higher potential of intermolecular chain transfer with long chain branches.

Table 5.8: Ratio of terminal double bond and backbone carbons as a function of LC concentration.

wt % 5CB	%ratio (CH-/CH_2-)	%ratio (CH_2=/-OCH_2)
P2EHA	64,10	7,62
30	60,24	1,56
50	59,52	□□ 1
70	58,82	□□ 1

Effect of 5CB concentration on polymer chain structure is shown in table 5.8. increasing LC concentration in the initial composite has no significant effect on the ratio of tertiary to secondary backbone carbons, whereas a sharp drop of the terminal double bond concentration in the polymer matrix from 30 to 70 wt % of 5CB in the photopolymerized matrix. This behavior is likely as a result of orientation effect of liquid crystal molecules, that increases local density of double bonds and accordingly lead to increase the propagation rate of polymerization. These observations confirm the kinetics behavior of polymerization at different weight percents of liquid crystal in chapter 3.

5.6.1 Transfer reaction to liquid crystal

Liquid crystal may act as chain transfer agent at the weak site of the chemical bond. This may lead to formation of low molecular weight polymers. Chain transfer to liquid crystal can be significant at higher weight percent of the liquid crystal in the initial composite mixture.

To investigate presence of chain transfer to liquid crystal, ^1H NMR spectra of pure P2EHA has been compared with the spectra of purified 70/30 wt% of 5CB/2EHA composite mixture.

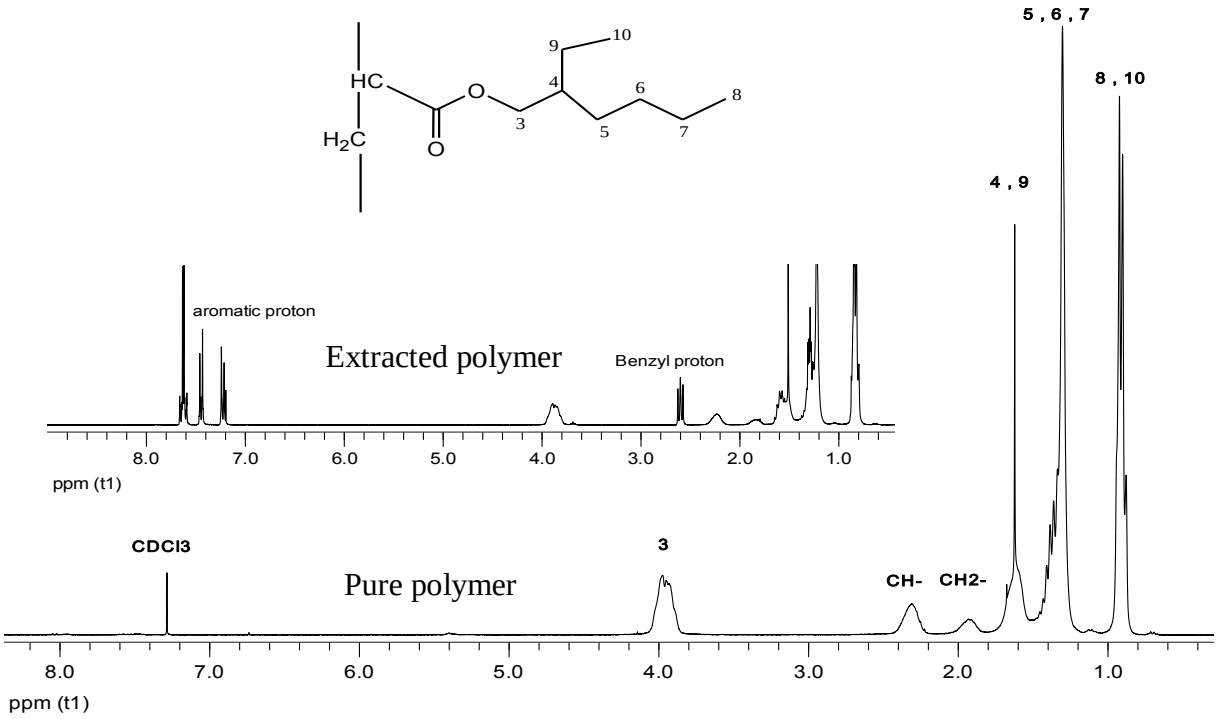

Figure 5.19: ^{1}H spectra of pure 2-ethylhexyl acrylate polymer in chloroform. Inset: ^{1}H spectra of 2EHA polymer extracted from 70 /30 wt % of 5CB/2EHA composite.

As presented in figure 5.19, ^{1}H NMR spectroscopy shows the presence of aromatic hydrogen between 7 and 8 ppm, which indicates presence of certain amount of the aromatic group connected to the polymer matrix. Benzylic hydrogens are known as highly reactive as a result of resonance stabilization of resulting radical by the aromatic ring. 5CB has been washed out five times and dried under vacuum at 60°C. A benzyl group of 5CB increases potential of benzylic hydrogen abstraction that supports abstraction from monomer backbone. Guymon et al., has identified a transfer reaction of radical 5CB in isotropic phase, a bond between the acrylate and 5CB occur on the proton 5 of the liquid crystal which is the most stable intermediate radical. That is the reason of presence of aromatic protons of in the proton NMR spectra. Mechanism of the chain transfer to liquid crystal is illustrated in figure 5.20.

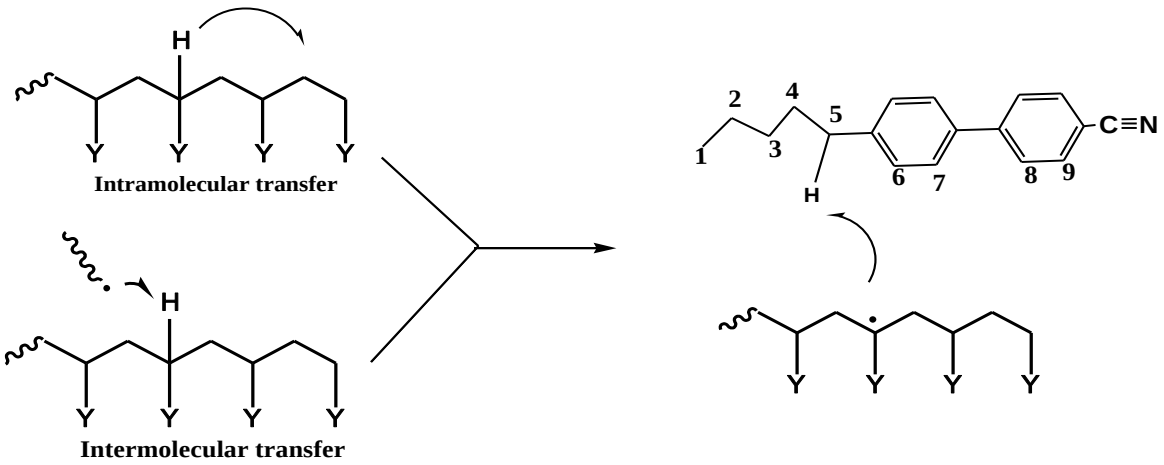

Figure 5.20: Mechanism of chain transfer to liquid crystal

NMR analysis show no chemical bond formed between the acrylate and liquid crystal. Although we did not rule out the hypothesis of influence of transfer reaction, based on the idea that the kinetics of polymerization is related to probability that a growing chain in the middle continues to spread when finding a monomer molecule. This could be explained in terms of the mixture viscosity, where increasing viscosity would limit the diffusion of reactive species and monomer radicals to join the propagating chain, thus, chain transfer occurs to liquid crystal, and can increase at higher liquid crystal concentration. The obtained polymer network by variying the liquid crystal concentration shows considerable impact of the liquid crystal on polymerization process as critical variable in the preparation of PDLC systems.

5.7 Conclusion

Variation of the preparation conditions and composition of polymer/liquid crystal composite allow demonstration of the internal structure of polymer network during radical photopolymerization of monoacrylate systems. More comprehensive understanding of the structural characteristics of the polymer composites has been achieved. The irradiation dose, the initiator concentration and the liquid crystal concentration are the key factors that determine the polymer architecture and the degree of branching in the polymer chains based on the choice and application of these factors during the curing process. The intermolecular and intramolecular chain transfer has a considerable effect on the formation of radical species in terms of short or long chain branching. The formation of secondary and tertiary carbons and terminal double bond has been investigated at different preparation conditions. The terminal double bond has a considerable effect on the degree of branching based on the conversion rate. The effect of the initiator concentration and the irradiation rate on the polymer configuration was presented, at low polymerization rate the reaction kinetics support the formation of β-division species and intramolecular chain transfer dominates toward short chain branches. This may support the understanding that the terminal double bond and β-division are in competition on the formation of branching at high conversion rates.

At higher concentrations of the liquid crystal in the polymerized mixture results in high degree of alignment of the monomer species and hydrogen abstraction dominate that support the intermolecular chain transfer for long chain branches. The chain transfer to liquid crystal has been investigated to understand the interactions between the monomer and the liquid crystal structure and the effect of liquid crystal on the polymerization kinetics. It has been presented that presence of chain transfer to liquid crystal occurs on the benzyl hydrogen of the liquid crystal as a factor to determine the polymer network architecture. The optimization of the irradiation dose, initiator concentration and liquid crystal concentration leads to improve the properties of the polymer network according to the required product applications.

5.8 References

[1] V.M. Litvinov, A. Dias, Macromolecules, 34, 4051 (2001).
[2] M. Garbarczyk, F. Grinberg, N Nestle, W. Kuhn, J. Polym. Sci. B Polym. Phys. 39, 2207 (2001).
[3] A. N. Nikitin, P. Castignolles, B. Charleux, J. P., 24, 13, 778-782, (2003).
[4] P. Castignolles, R. Graf, M. Parkinson, M. Wilhelm, Gaborieau, M. Polymer, 50, 11, 2373-2383 (2009).
[5] C. Plessis, G. Arzamendi, J.M. Alberdi, M. Agnely, J.R. Leiza, J.M. Asua, Macromolecules, 34, 6138 (2001).
[6] N. Ahmad, D. Britton, F. Heatley, P.A. Lovell, Macromol. Symp., 143, 231 (1999).
[7] E. McCord, W. Shaw, R. Hutchinson, Macromolecules, 302, 246-256 (1997).
[8] G.E. Scott, E. Senogles, J. Macromol. Sci. Chem., 8, 4, 753-73 (1974).
[9] C. Quan, PhD thesis, Drexel University (2002).
[10] P. Castignolles, Macromol. Rapid Commun., 30, 1995–2001 (2009).
[11] I. Gonzalez, M. Paulis, J.C. de la Cal, J.M. Asua, Chemical Engineering Journal, 142, 199–208 (2008).
[12] E. Sato, T. Emoto, P. B. Zetterland, B. Yamada, Macromolecules. Chem. Phys., 205, 1892 (2004).
[13] F. Heatley, P.A. Lovell, T. Yamashita, Macromolecules, 34, 7636 (2001).
[14] J. Chiefari, R. Mayadunne, G. Moad, E. Rizzardo, S.H. Thang, Macromolecules, 32, 7700 (1999).
[15] F. Heatley, P. A. Lovell, T. Yamashita, Macromolecules, 34, 7636-7641 (2001).
[16] P. Castignolles, R. Graf, M. Parkinson, M. Wilhelm , M. Gaborieau, Elsvier, Polymer, 50, 2373–2383 (2009).
[17] C. Plessis, G. Arzamendi, J.M. Alberdi, M. Agnely, J.R. Leiza, J.M. Asua, Macromolecules, 34, 6138-6143 (2001).
[18] K. Berchtold, J. Nie, J. Stansbury, B. Lu, E. Beckel, C. Bowman, Macromolecules, 37, 3165-3179 (2004).

6 CHARACTERIZATION THE MORPHOLOGY AND MOLECULAR WEIGHT DISTRIBUTION OF PDLC SYSTEMS

6.1 Introduction

Morphology of PDLCs prepared by UV and electron beam EB curing depends on the LC concentration, the cure temperature, and the preparation conditions [1,2]. The polymer properties in term of glass transition temperature and architecture play the major role in the industrial applications of these products. Properties of the polymer films are also related to molecular weight distribution (MWD) and architecture of polymer chains.

Modification and control of molecular architecture and selectivity of compounds leads to a novel generation of materials with sophisticated properties ready for use in various areas of modern technologies [3,4]. In solution polymerization, polymerization rate was found to increases as the polymerization temperature is decreased into more ordered liquid crystal phases. This behavior can be explained by the monomers segregation in the LC, which leads to increasing the local concentration of double bonds [5].

In radical polymerization of acrylic polymers, MWD and the gel fraction largely determine the final properties of the polymer composites.

The polymer/liquid crystal gels are obtained by polymerization of small amounts of monomer in a liquid crystalline solvent [6]. These gel systems are of particular interest due to a number of interesting properties in the PDLC applications. Gel fraction and MWD can be controlled by adding chain transfer agent or cross-linker [7,8]. 2EHA has a low glass transition temperature (T_g= -80°C) and suffer from chain transfer to polymer which lead to different network structures [9]. Chain transfer reaction in radical polymerization of acrylates involves abstraction of hydrogen atoms from tertiary backbone (C-H), caused formation of insoluble network. These network structures have a major effect on the thermal and electrooptical properties of the PDLC films.

Higher molecular weight polymer is required for good physical and mechanical properties, which can be achieved at low reaction rate using low UV or EB dose. Low reaction rate may lead to reduction the termination rate. In EB initiation, low dose results in reduction of

initiating species concentration leading to higher molecular weight polymer [10]. Polymerization rate in the acrylate systems is proportional to the dose rate [11]. Different techniques have been applied to study these acrylate networks. Polymerization kinetics has been investigated using infrared spectroscopy, while characterization of chain transfer and heterogeneity of polymer matrix have been studied using liquid-state NMR spectroscopy. These techniques offered valuable information on the polymer composite system as previously discussed in chapter 3 and 5 of this study, however, they do not allow the complete chemical characterization of network structures.

The anisotropic reaction in the presence of liquid crystal may widely alter the polymerization kinetics. The change in the polymerization reaction may affect the evolution of polymer matrix structure and modify the final polymer morphology and network alignments. Consequently, the interactions between composition species will change toward different PDLC films [12].

The main intention in this chapter is to gain more insight on the network structures by studying the morphology of PDLC films. A comparison between the UV and EB curing will be investigated by varying the preparation conditions. To characterize the polymers formed by radical polymerization, relation between the chemical composition, structure and final network properties must be elucidated. Therefore, better understanding of polymerization is essential to describe effects of polymerization conditions on the performance of PDLC's.

MWD of polymer chains analysis was conducted by gel permission chromatography (GPC) to describe the internal morphology of the polymer matrix in an attempt to improve the final properties of the polymer blends. Degradation and stability of the polymer matrix, such as physical or mechanical properties referred to as thermal analysis. The dynamic mechanical properties of the UV and EB curable films were conducted using Rheometrics dynamic mechanical analyzer. The viscoelastic properties such extension storage moduli E' =3G' or shear storage moduli G', extension loss moduli E" =3G" or shear loss moduli G", and dynamic loss tangent tanδ were measured as a function of the temperature. Furthermore, glass transition measurements and the phase transitions were performed using DSC technique to describe the variation of the phase behavior and the morphology of the polymer composites. The use of these techniques gives information about physical properties, morphology and MWD of the polymer networks.

6.2 The thermal analysis of acrylate networks

6.2.1 Thermal stability

Thermal stability of acrylate networks was studied by DSC and TGA techniques. Thermogravimetric analysis is well known technique to evaluate thermal stability of polymer blends. Figure 6.1 shows the thermal degradation of P2EHA samples prepared under different UV irradiation rates.

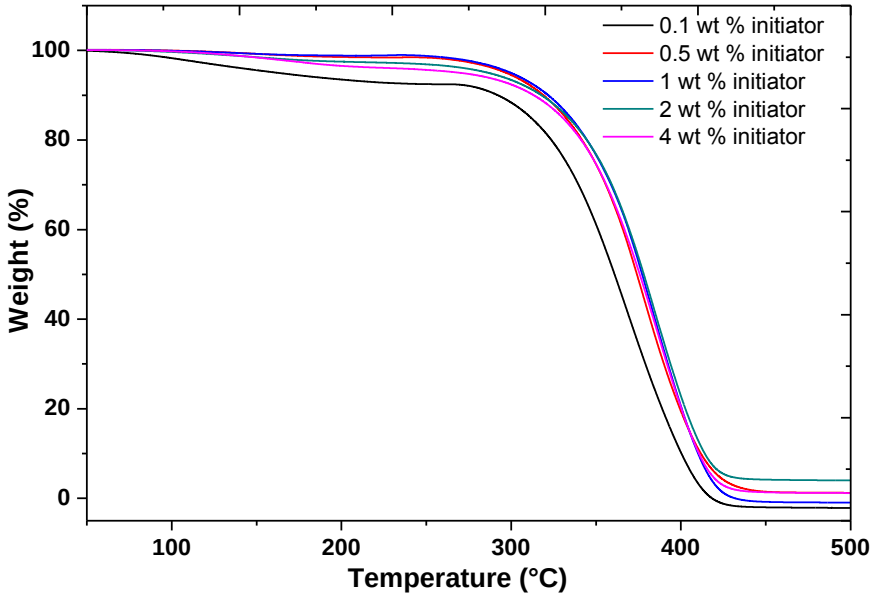

Figure 6.1: TGA thermogram of UV polymerized 2EHA as a function of initiator concentration.

Thermogravimetric analysis shows a first loss of mass of approximately 5 wt % at a 250 °C temperature and a second loss of mass due to degradation in the 320–400 °C temperature range. Comparison between P2EHA prepared with different weight percents of photoinitiator indicates that there is no significant difference in the degradation behavior, except for very low weight percent of initiator which show faster mass loss with of 10 wt % possibly due to the presence of un-reacted monomer imbedded in the polymer matrix.

Thermogravimetric data of EB curing 2EHA is presented in figure 6.2 at different EB irradiation rates. It is observed that about 5 wt % mass loss of polymer prepared at EB rate 23 kGy starts at about 300°C temperature, whereas at higher irradiation rates the first mass loss

occurs at approximately 200°C and shows faster degradation rates. This could be a result of the difference in the chain length between polymer networks or due to the thermal degradation of P2EHA that takes place by a stepwise unzipping mechanism leading to faster degradation. The inset in figure 6.2 shows a comparison between the thermogravimetric data of UV and EB curing. Degradation trends are similar with almost no significant change in loss of mass between the two systems because of the similar molecular structure of polymer. The little lower stability of the UV cured film may be caused by residue of unreacted photoinitiator or the radicals that are trapped in the polymer network.

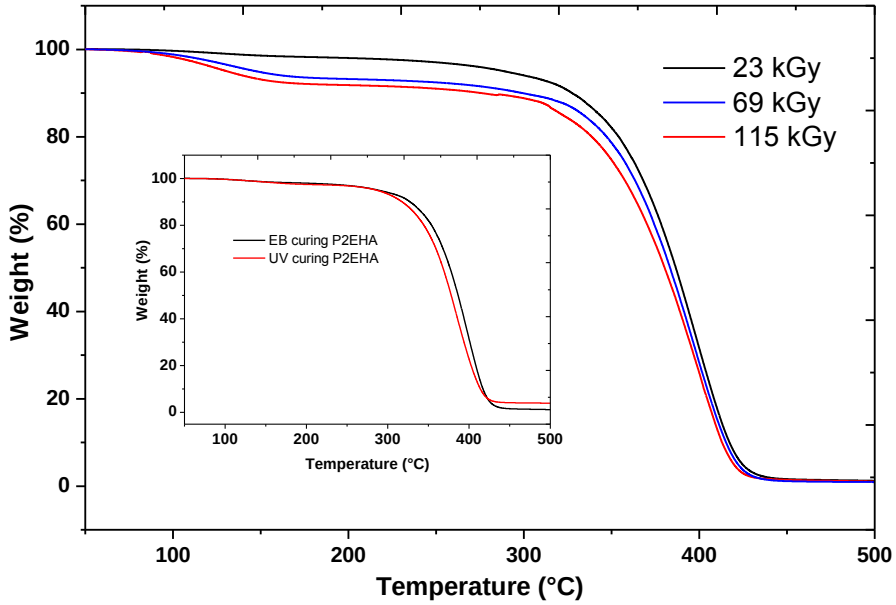

Figure 6.2: TGA thermogram of EB polymerized 2EHA at different irradiation rates. The inset is comparison between UV and EB curing of P2EHA.

It is obvious that EB cured film exhibits relatively higher thermal stability compared with UV cured films. This can be explained by the higher degree of branching and crosslinking of EB cured films due to the high EB irradiation dose. However, all polymer films possess relatively similar networks shown by the same trend of the thermogram. TGA data are summarized in table 6.1. TGA experiments show a smooth thermal decomposition of all acrylate network samples: samples decompose totally at ± 420°C without considerable residue left. This suggests that decomposition of the different acrylate networks follows one main thermal degradation route with the formation of low molecular weight molecules.

Table 6.1: TGA result of different UV and EB cured acrylates.

Sample	*10 % wt loss* (°C)	*50 % wt loss* (°C)	*90 %wt loss* (°C)
wt % initiator			
0.1 wt% initiator	287	360	399
0.5 wt% initiator	319	374	411
1 wt% initiator	321	378	410
2 wt% initiator	318	379	414
4 wt% initiator	312	376	410
EB rate			
23 kGy	327	387	417
69 kGy	297	385	414
115 kGy	272	383	416
UV rate			
55 mJ/cm^2	327	379	413
140 mJ/cm^2	329	380	413
240 mJ/cm^2	318	378	414
400 mJ/cm^2	**333**	**387**	**416**

6.2.2 Thermomechanical properties

A polymer can be characterized by its T_g. Knowledge of influence of the initial mixture composition and the curing conditions on the chemical network structure is important for designing polymer materials suitable for technological applications. Therefore, characterization of polymer network structure is essential to prepare highly functional polymer composites. Inclusion of side component is usually accompanied by change in the glass transition temperature and curing conditions. DSC experiments show one endothermic peak for all the acrylate polymer represent the glass transition temperature , with different LC/monomer ratios, the endothermic peak is caused by the acrylate network and the liquid crystal. An increase in liquid crystal concentration leads to decreases the glass transition temperature.

Chemistry of photoinitiators is critical to achieve efficient polymerization and to improve the mechanical and physical properties of polymer. Figure 6.3, shows DSC thermogram for UV polymerized P2EHA at 2 and 4 wt % photoinitiator. Polymer samples have been analyzed in the temperature range between -72°C and 100°C and found a glass transition T_g lower than -60°C. The T_g was reported as the midpoint of the change in heat capacity during the first heat ramp. A sufficient initiator concentration has been used to insure complete polymerization to arrive at normalized conditions for comparison purposes. All DSC measurements have been

performed at a maximum double bond conversion. Dependence of glass transition temperature on the initiator concentration is clearly indicated, where increasing the amount of photoinitiator in the initial mixture from 2 to 4 wt % lead to drop of T_g with about 2°C.

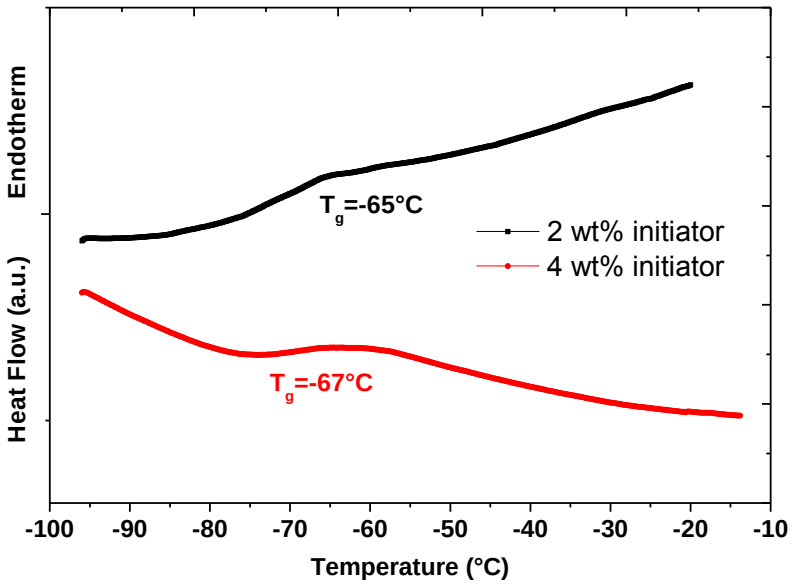

Figure 6.3: DSC curve of P2EHA polymer as a function of photoinitiator concentration.

Thermodynamic behavior is important to understand the effect of the initiator concentration on the polymerization reaction. The double bond conversion in the monomer is exothermic from the thermodynamic point of view. From the DSC thermogram of figure 6.3, it is observed that the enthalpy has higher value for higher initiator concentrations, which indicates higher polymerization rate.

Photoinitiator can absorb light directly to generate a reactive free radical and initiates polymerization. Increasing the amount of photoinitiator likely increases final degree of conversion. Effect of initiator concentration can be explained as follows, assuming that the initiator is equally distributed within the component mixture. At very low initiator concentration, photoinduced polymerization is initiated at each point where radicals are formed; the active radical species initiate further polymerization until the reaction is terminated. Based on the polymerization kinetics, each initiator molecule absorbs UV light and dissociates into two free radicals. Thus, a small amount of initiator leads to large structural units within the material, whereas a large amount will lead to smaller structural units [13]. Furthermore, higher initiator concentration may lead to denser material structure

with many polymer chains. On the other hand, low initiator concentration will lead to low number of polymer chains at high chain length.

Effect of irradiation doses on the behavior and characteristics of acrylic polymer matrix had been studied by comparing the mechanical properties of polymer film prepared at different irradiation rates. Variation of T_g as a function of the curing rate can be elaborated also using the DSC analysis. Figure 6.4 shows the thermogram for P2EHA prepared at different irradiation rates. T_g of P2EHA was lower than -60°C, which decreases gradually by increasing the UV irradiation rate. At low UV rate of 55 mJ/cm^2, the T_g was -62°C and decreased to about -64°C by doubling the UV dose to 120 mJ/cm^2. A further increase in the UV rate to 240 mJ/cm^2 shows a drop of the T_g to about -67°C. This behavior can be explained by formation of more radical species at higher irradiation dose which accelerate the formation of more polymer chins with low molar mass compared to the case of low irradiation rates, where relatively low amount of radical species are formed with large structural polymer units.

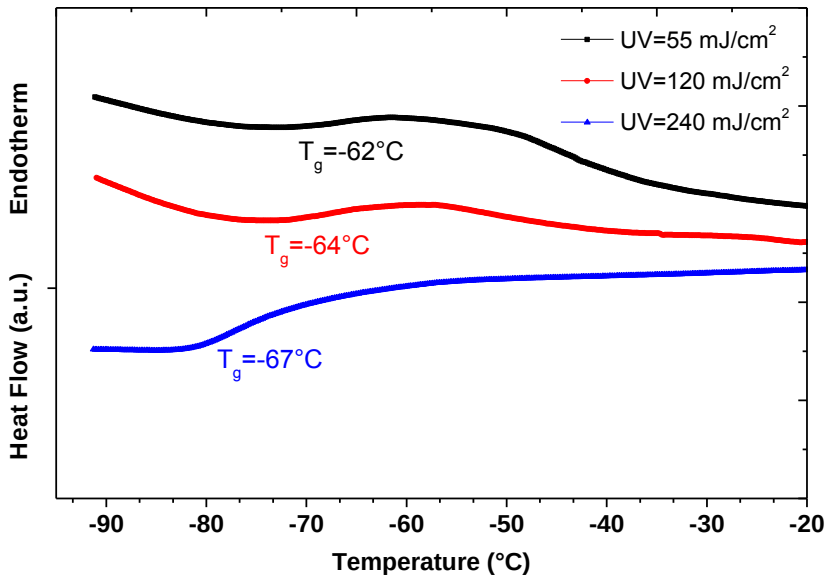

Figure 6.4: DSC curve of P2EHA polymer as a function of UV irradiation rate.

A comparison between the UV and EB cured films is given in figure 6.5. DSC thermogram shows the T_g of UV and EB samples; it is observed that EB polymerized film has lower T_g than UV cured one. The significant drop in the T_g of the EB cured P2EHA can be explained by the major difference in the polymerization kinetics between the two polymerization methods. In EB polymerization, relatively high irradiation dose results in formation of large amount of radical species upon exposure to the EB irradiation, which leads to growing of high

amount of propagation chains radical with low structural chains. In general, difference in the glass transition between both methods is relatively high, which support the hypothesis of different molecular structures between UV and EB films. The drop in the glass transition temperature can be explained by formation of lower molecular weight polymer chains which have more mobility segment than higher molecular weight chains.

A summary of DSC thermogram results for UV and EB P2EHA are presented in table 6.2.

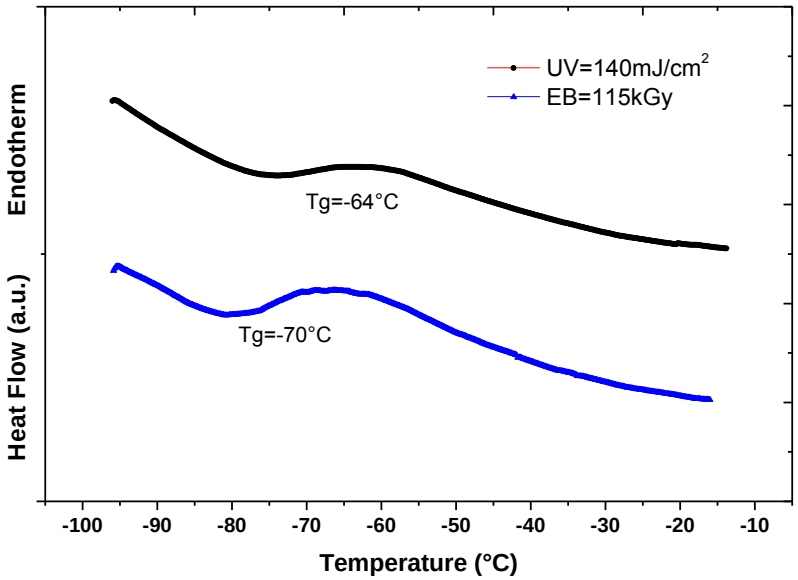

Figure 6.5: DSC curve of P2EHA polymer as a function of UV irradiation rate.

Table 6.2: DSC results of different UV and EB cured acrylate systems

Sample	***Glass transition Tg* (°C)**
initiator (wt %)	
0.5	-64
2	-65
4	-67
EB rate (kGy)	
23	-65
69	-67
115	-70
UV rate (mJ/cm^2)	
55	-62
140	-64
240	-67

6.3 The thermal analysis of difunctional acrylates

Polymerization of difunctional acrylates results in highly crosslinked polymer because each monomer molecule has two vinyl active sites. Mechanical properties can be described by degree of crosslinking as a key factor that determines the mechanical properties of the polymer matrix. TPGDA monomer has a glass transition temperature T_g of about -40°C, that would exceeds 45°C by polymerization and may vary based on the preparation conditions. In figure 6.6, shown DSC thermogram of poly(TPGDA) samples prepared at different initiator concentrations and UV dose 240 mJ/cm^2. It is observed from the thermogram that the T_g deceases slowly with increasing the the initiator concentration in the initial polymerized mixture. This may occurs due to formation of short crosslinking network by increasing the amount of initiator, whereas a longer crosslinked network is obtained at lower initiator concentrations.

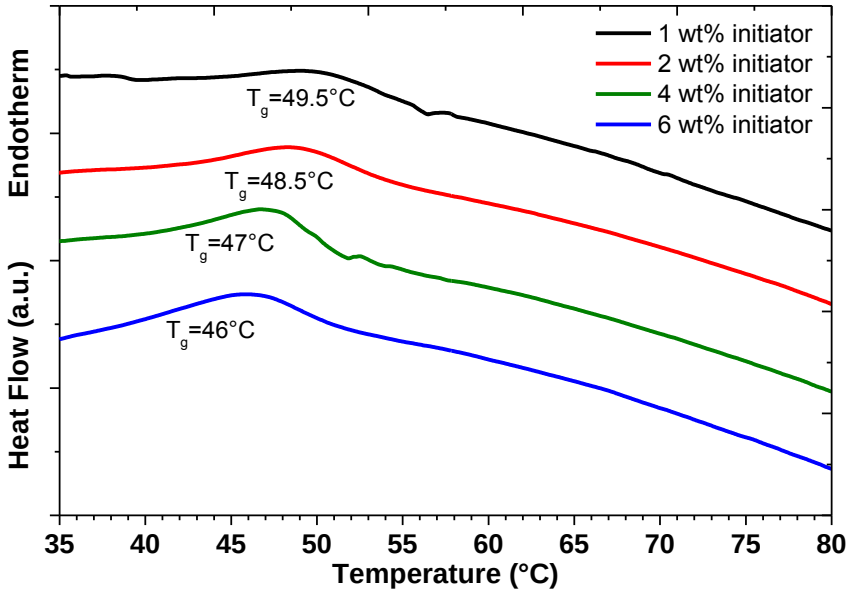

Figure 6.6: DSC curve of poly(TPGDA) polymer as a function of initiator concentration.

To study effect of EB irradiation curing on the mechanical properties of EB polymerized TPGDA. Polymerization has been performed by varying the EB rate. The DSC thermogram of polymer samples as a function of EB rate is presented in figure 6.7. The results indicate that a small change of the glass transition temperature is observed with increasing EB doses. The little variation of T_g is not clear to verify the exact behavior of poly(TPGDA) as a function of irradiation rates. However, high irradiation dose may lead to more chain scissions rather than crosslinking of the polymer chains especially at higher EB rates. In the UV curing,

efficient crosslinking can be achieved and chain scission reaction can be neglected due to relatively low UV irradiation rate compared to the EB one [14]. Thus, a compromise should be made between degree of crosslinking and the EB dose to improve the mechanical properties of the polymer matrix.

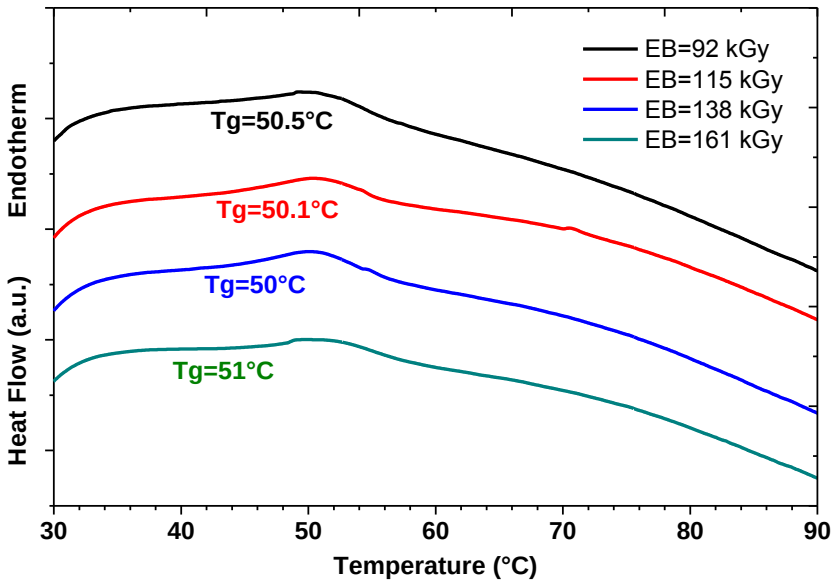

Figure 6.7: DSC curve of poly(TPGDA) polymer as a function of EB rate.

MWD of polymer chains is the key factor that determines the mechanical properties of the polymer blends. The kinetic of chain length of free radical polymerization of is defined as the average number of monomer molecules consumed per initiating radical species. Therefore, broad molecular weight distribution of polymer chains makes it difficult to detect clear glass transition temperature T_g by DSC technique especially in the highly branched polymer material. A further morphology elaboration and polymer network structure is required to understand the mechanical properties of polymer. Determination MWD by gel permeation chromatography GPC is considered highly effective to analyze the polymer internal structure and morphology.

6.4 The gel fraction

During polymerization, highly branched polymers are formed usually characterized by their degree of solubility in a given solvent. Insoluble fraction of these polymers is known as gel [15]. Gel effect usually occurs during free radical polymerization of acrylate monomers and related to the polymerization rate. Mechanism for the formation of gel can be described by the

intramolecular and intermolecular chain transfer to polymer followed by termination by combination [16].

P2EHA cured samples were weighed and dissolved in tetrahydrofuran THF for 48 hours at room temperature, and then filtered and dried at 60°C to constant weight. The gel fraction of the polymer samples were calculated using the following equation:

$$\%\ Gel\ fraction = \frac{W_t}{W_0} * 100 \qquad (6.1)$$

where W_0 and W_t are the sample weight before and after dissolved in THF.

In Figure 6.8, shown the gel content of P2EHA by varying UV dose at 55, 120, 240, 400 mJ/cm^2. By increasing the UV irradiation rate, gel contents of all samples were about 8% at UV dose 55 mJ/cm^2 and increased to 16% at UV dose of 400 mJ/cm^2.

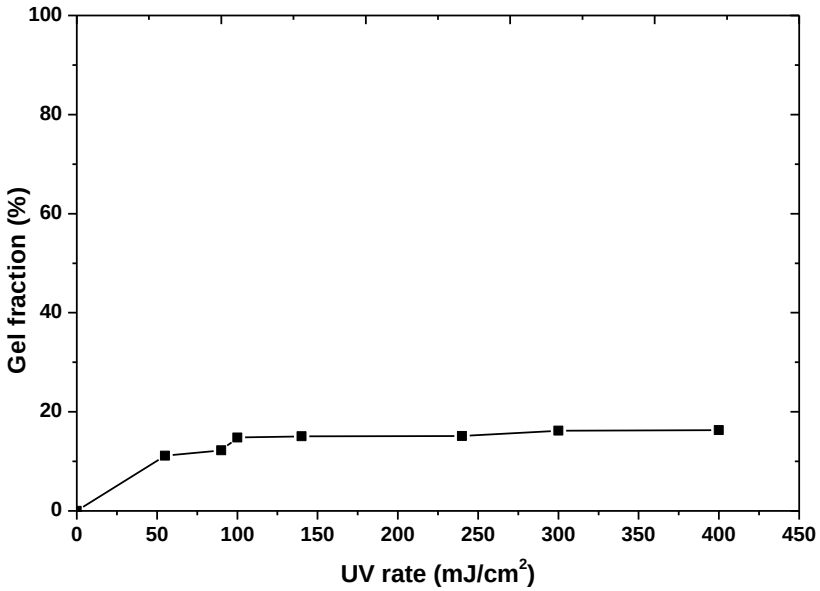

Figure 6.8: Change in gel content in P2EHA with varying UV dose.

Effect of EB irradiation rate on gel contents of P2EHA polymer films is shown in figure 6.9. In this work, the gel contents of the polymer films have been determined at a maximum double bond conversion, and these films have been exposed to further irradiation dose equivalent to the initial dose, the gel contents of the extra irradiated polymer films have been evaluated and compared with the original polymer films. It is observed that the gel contents increase with increasing irradiation rates, where the gel content of the polymer film at 11 kGy

was about 26% and reached to 40 % at EB dose 115 kGy. In the second series of samples with extra irradiation doses, a further increase of the gel contents is observed with about 10% compared with the original samples to reach about 50% gel content. Explanation for this interesting behavior could be due to the degradation effect of the high EB dose, which leads to degradation of the large structural polymer units into smaller units with high degree of branching and accordingly more gel contents.

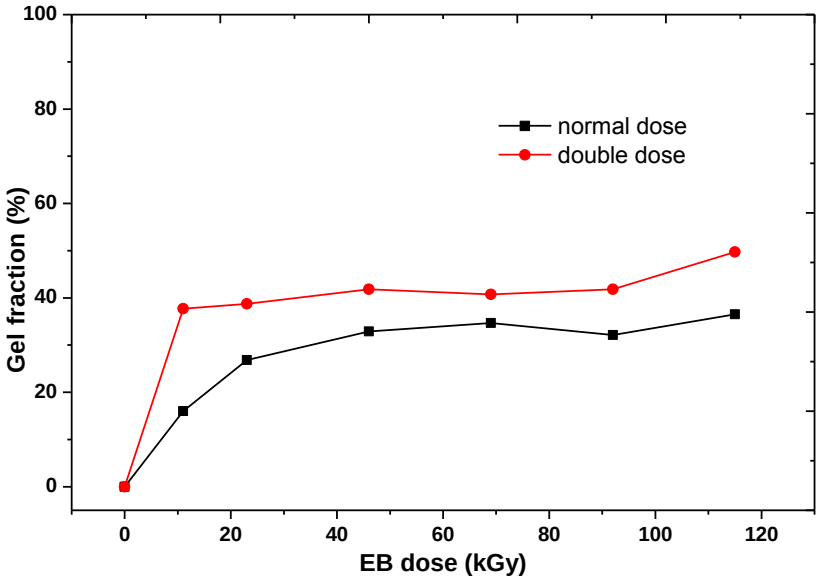

Figure 6.9: Change in gel content in P2EHA with varying EB dose.

The effect of photoinitiator concentration on gel content would give similar behavior as the effect of UV irradiation rate on the gel content, where, the polymerization rate increases with increasing the photoinitiator concentration and smaller polymer chains are formed which may leads to higher percents of gel in the polymer material.

6.5 Molecular weight distribution analysis

Analysis of MWD produced during polymerization of acrylic esters can be used to understand the reaction kinetics. Chain transfer including chain transfer to monomer and possible intramolecular chain transfer has a considerable effect on reaction rate measurements. Molecular weight can be controlled by several techniques. Low polymer molecular weight can be achieved by increasing the concentration of photoinitiator relative to monomer. Variation the irradiation dose can also be used to control the MWD of polymer chains. Another method to control the molecular weight of polymer is based on using chain transfer

agents to the reactive mixture. In addition, molecular weight can be controlled by conducting polymerization at high temperatures, which have drawback regarding energy consumption, the volatility of reactive molecules and can be more applicable in solution polymerization.

Evolution of MWD of P2EHA polymer and a polymerized mixture of 70/30 wt % of 2EHA/5CB is shown in figure 6.10 using the GPC chromatogram. 5CB signal appeared at 21 min at the right hand side of the chromatogram. The small peaks after 22 min are equivalent to the THF solvent. The retention time of P2EHA is observed at 12 min while that of polymer/liquid crystal composite is detected at about 13 min, which indicates formation of higher molecular weight polymer chains than in the polymer/5CB composite.

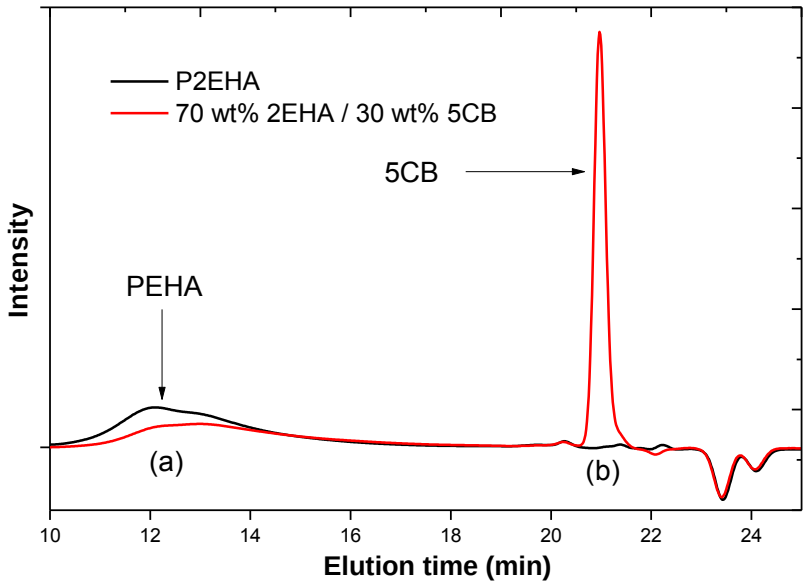

Figure 6.10: Overlay of chromatogram of P2EHA and 70 wt% 2EHA/30 wt% 5CB obtained by GPC analysis.

6.5.1 Variation of MWD with LC concentration

A series of samples with a monomer concentration ranging from 100 wt % monomer (no LC) to 30 wt % (70 wt % LC in the monomer/LC mixture) were exposed to the UV light. The obtained polymer/liquid crystal films were analyzed by GPC measurements.

Addition of liquid crystal to the initial mixture may result in variation of phase structure based on the LC concentration in the composite mixture. Effect of LC on the MWD of polymeric chains has been determined by GPC and presented in figure 6.11. Typically, higher amount of 5CB in the reactive composite leads to decreasing molar mass of polymer chains. The signal

of P2EHA appears at 12 min while that of 70 wt % 5CB the retention time requires about 15 min to appear in the chromatogram. This can be explained by the distribution of liquid crystal in the monomeric domain that accelerates formation of smaller polymer units, where the propagating polymer chains are hindered by the liquid phase during polymerization.

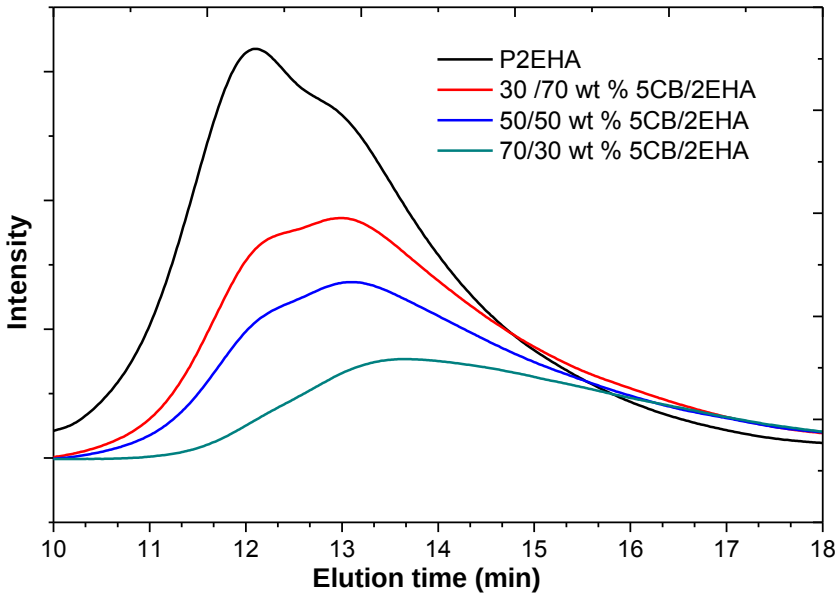

Figure 6.11: GPC chromatogram for P2EHA at different LC concentrations.

We could measure the variation of polymer molar mass in terms of the LC concentration using GPC as shown in Figure 6.12. Weight and number averaged molar masses M_w and M_n exhibit a considerable drop when LC concentration increases. This result means that as the precursor system is more dilute with the addition of LC, chain growth stop at a smaller mass of the polymer, since the probability of contact between two reacting species decreases.

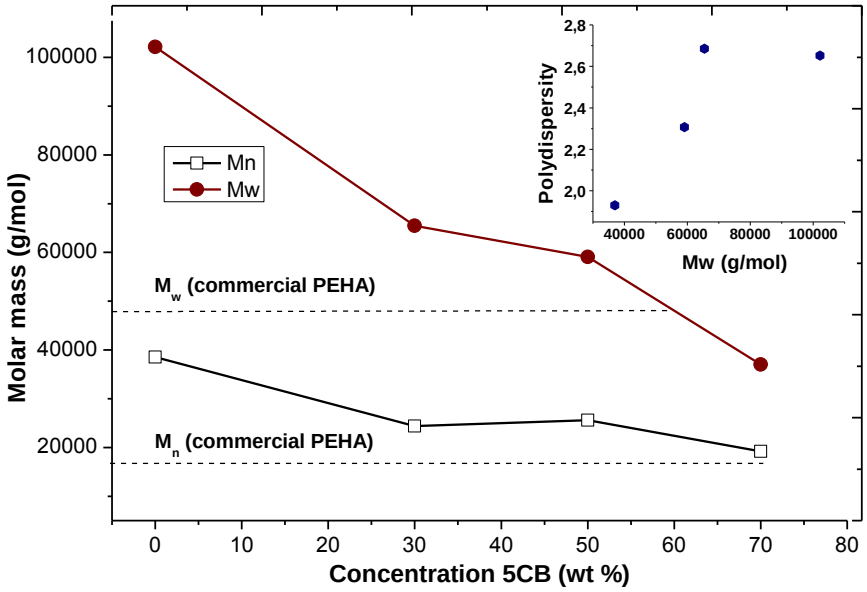

Figure 6.12 :The change of the molar mass of PEHA as a function of 5CB concentration for the PEHA/5CB system under UV curing. *Inset***:** Variation of the polydispersity M_w/M_n with the molar mass of polymer

M_w and M_n values are averages of two measurements made on samples prepared under the same polymerization conditions. The dashed lines in Figure 6.12 present M_w and M_n of the commercial PEHA. These values intercept with those of the polymer in the systems in the vicinity of 65 wt % 5CB. Below this concentration, the samples have higher molar masses compared to those of the commercial polymer, it can be realized that at low concentration of reacting monomers the polymerization rate is low, which results in lower molecular weight of polymer.

The inset in figure 6.12 shows that for UV cured systems, variation of the polydispersity exhibit a trend opposite to those of the molar mass curves. Polydispersity increases remarkably at higher molar masses of the polymers, this agrees with those results obtained in figure 6.12 that the presence of 5CB prevent the formation of high molar mass polymer which results in lower polydispersity.

6.5.2 MWD of electron beam cured system

Polymerization rate has a profound effect on the MWD of the produced polymer. EB irradiation is characterized by relatively high irradiation dose. That result in high polymerization rates compared with other curing techniques. Furthermore, incorporation of

liquid crystal allows the reactive species to participate in the propagation step at different rates based on the mixture composition. This would leads to formation of different molar mass polymers with broad MWD depending on the dynamics of reaction. Figure 6.13 show GPC chromatogram of P2EHA prepared at different EB irradiation rates. GPC signals of EB cured system show broad bimodal curves, which indicate wide distribution of the MWD of polymer chains. The first peak corresponds to curing rate at 11 kGy represents higher molecular weight, while the second peak of 58 kGy corresponds to lower MWD of polymer. Interesting behavior of MWD during EB curing is observed that each peak is composed of a combination of two peaks. The first part that appears at low molecular weight at about 12 min retention time, and the second part with higher molecular weight at 10 min retention time. This phenomena can be explained by the polymerization kinetics, where the part of the peak of low molecular weight represents the polymer chains that formed at the first stage of the reaction, while the part of the peak with high molecular weight polymer represent the polymer chains that formed during the propagation step of the reaction.

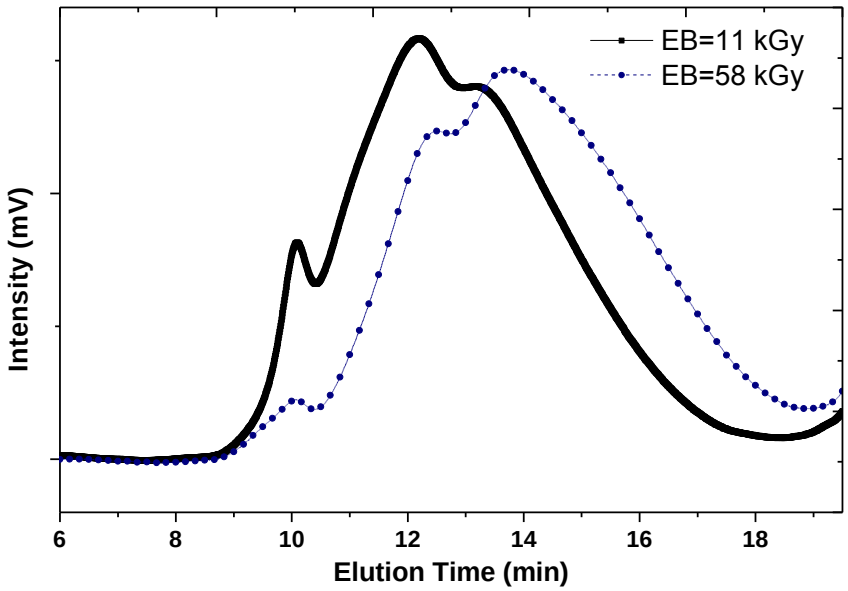

Figure 6.13: GPC chromatogram for EB cured 2EHA with variety at EB rates.

MWD of polymer chains obtained by EB or UV curing can be widely different. Figure 6.14 shows a comparison of the chromatograms for P2EHA prepared by EB and UV curing. It can be observed the totally different behavior of the formation of polymer chains between both methods. In the UV curing polymer, a relatively sharp monomodal curve is obtained, that indicates the formation of similar population of polymer with monomodal distribution of molar mass, whereas, the EB cured sample (dashed line) show different behavior in which a

bimodal distribution of polymer chains are obtained, indicates formation of wide distribution of polymer with different molar mass. Similar behavior of both UV and EB methods is observed at 10 min retention times, which correspond to formation of high molar mass polymer at the propagation step of polymerization. Furthermore, it is clearly observed high MWD of polymer obtained by UV curing than the EB case.

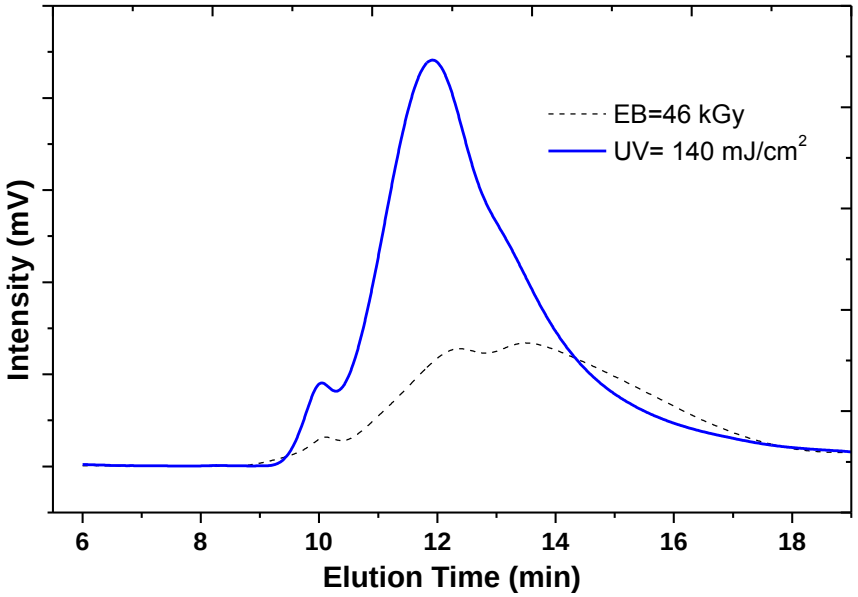

Figure 6.14: GPC chromatogram for P2EHA prepared by EB and UV curing

Effect of liquid crystal concentration on the mechanism of MWD of polymer during the polymerization reaction is shown in figure 6.15. The continuous line shows that a monomodal distribution of molar which support the idea of narrow MWD of 2EHA under UV irradiation. Sharp drop of MWD is observed upon increasing the amount of liquid crystal, where the signal of P2EHA appears at 12 min while that of 70 wt % 5CB appears at 13.5 min. The dashed line in the chromatogram shows another behavior in which broad molecular weight of polymer chains are obtained. Interestingly, the small signal at 10 min retention time does not appear by incorporation of high amount of 5CB in the initial mixture. That can be explained by the diffusion limitation due to presence of liquid crystal molecules in the media which reduce mobility of radical species. Thus, high molar mass of polymer chains are not observed at 70 wt % of 5CB with broad MWD.

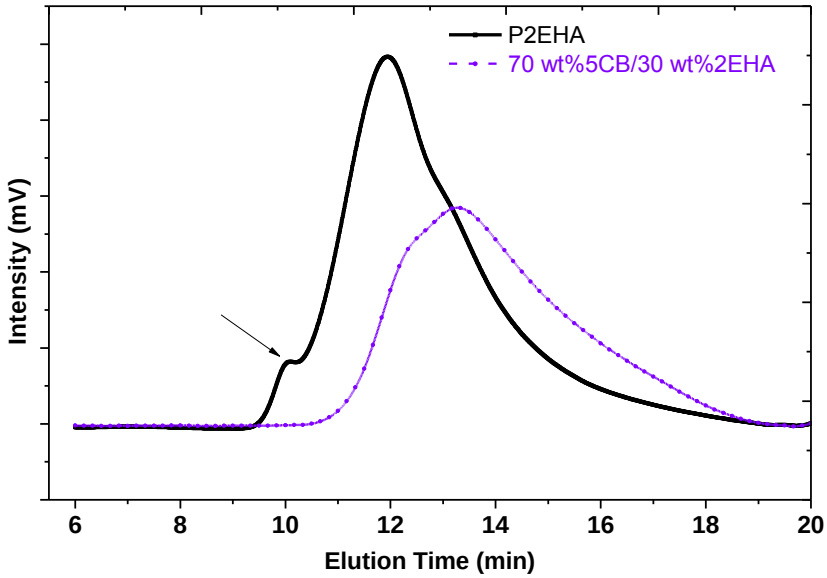

Figure 6.15: GPC chromatogram for P2EHA and 70/30 5CB to monomer ratio prepared by UV curing.

Variation of MWD of P2EHA/5CB composites is shown in figure 6.16. Samples have been prepared at normalized conditions with fixed UV rate of 240 mJ/cm^2 and 2 wt % photoinitiator. M_n and M_w show a gradual decrease with increasing the amount of 5CB in the initial mixture.

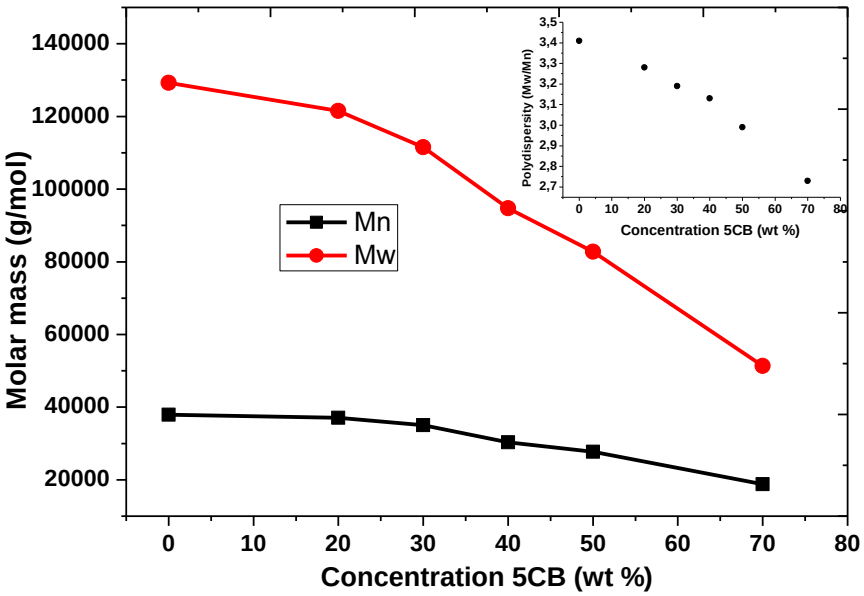

Figure 6.16 : The MWD of P2EHA as a function of 5CB concentration under EB curing.

Inset: the polydispersity as a function of 5CB concentration.

MWD of UV cured films as a function of the liquid crystal concentration is being controlled by two factors: first variable is the curing rate of UV irradiation which favor the formation low molar mass units, the second one related to presence of liquid crystal molecules in the polymerized mixture which also enhance formation of low molar mass polymer units and finally a significant drop of the MWD is observed where M_w drops from 129×10^3 g/mol to about 51×10^3 g/mol at 70 wt % of LC. Polydispersity is consequently decreases with increasing the amount of liquid crystal, which is another indication for formation of lower molar mass distribution at higher concentrations of LC. A summary of the GPC results are given in table 6.3.

Table 6.3: The molar mass and polydispersity as a function of 5CB concentration.

LC/2EHA (wt %)	***M_n (g/mol)***	***M_w (g/mol)***	***M_w/M_n***
no LC	37923	129280	3,41
20/80	37094	121511	3,28
30/70	35003	111541	3,19
40/60	30305	94728	3,13
50/50	27694	82788	2,99
70/30	18821	51341	2,73

High EB dose lead to different reaction kinetics during polymerization process compared with UV curing technology. This reaction mechanism would affect the molar mass of polymer chains. Effect of EB irradiation rate on the MWD of polymer films prepared by EB curing is given in figure 6.17 between 11.5 – 92 kGy irradiation rates. The MWD of EB cured polymer films show continuous decrease with increasing the ED irradiation rates, where M_w drops from 114×10^3g/mol at 11.5kGy to reach about 57×10^3 g/mol at 69 kGy of EB rate. On the other hand, polydispersity increases with increasing irradiation rate to reach about 3.5 at 69 kGy. This can be explained by formation of wide molar distribution of polymer units at higher irradiation rates, in which EB high intensity accelerate formation of increasing amounts of radical species at the initiation step of the polymerization reaction, that result in propagation of more polymer chains during the reaction. The GPC results of MWD as a function of the EB rate is presented in table 6.4.

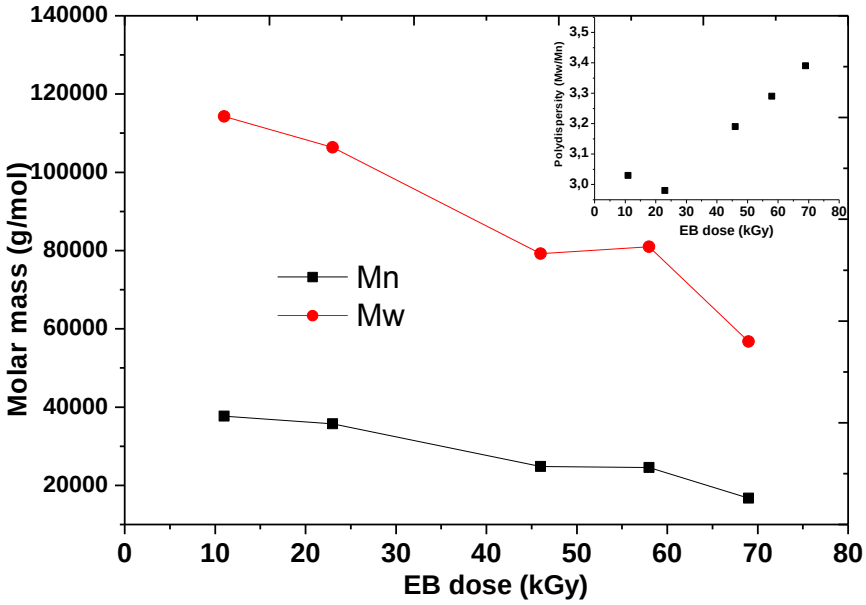

Figure 6.17: The MWD of EB cured P2EHA as a function of EB irradiation rate. Inset: the polydispersity as a function of EB rate.

Table 6.4 : The molar mass and polydispersity as a function of EB irradiation rate.

EB dose (kGy)	M_n *(g/mol)*	M_w *(g/mol)*	M_w/M_n
11	37678	114242	3.03
23	35724	106349	2.98
46	24823	79216	3.19
58	24584	80989	3.29
69	16732	56729	3.39

6.5.3 MWD of UV cured system

Polymerizations of 2EHA have been carried out at variety of UV irradiation rates to evaluate the relation between the UV rate and the MWD of polymer chains. UV rates have been varied between 55 – 400 mJ/cm^2. In figure 6.18, GPC chromatogram results are presented in terms of M_w and M_n molecular weights. It can be observed from the GPC results that significant drop of the molar mass is observed by increasing UV rate.

M_w dropped from 386×10^3 g/mol at 55 mJ/cm^2 dose to about 152×10^3 g/mol at 400 mJ/cm^2 UV dose. Furthermore, polydispersity show a continuous decrease with increasing UV dose from 3.4 to 2.4 by decreasing the UV rate from 55 to 400 mJ/cm^2. These observations can be explained by change of polymerization kinetics as function of UV dose.

At low UV doses, dissociation of photoinitiator molecules are relatively low which results in formation of small amount of radical species, that shift toward formation of larger polymer units. While, higher irradiation doses result in formation of much higher amount of the radical species which accelerate formation of lowed molar mass. Details of the GPC results are presented in table 6.5.

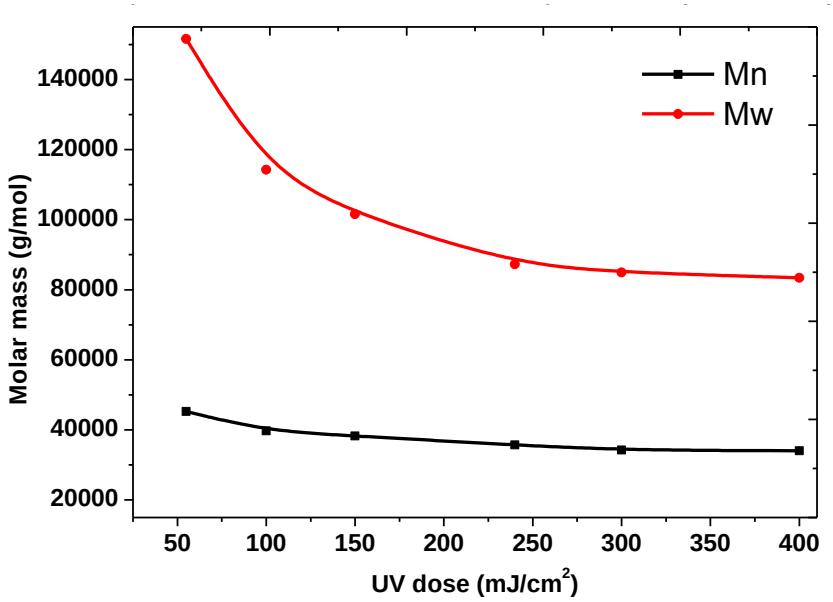

Figure 6.18: The MWD of P2EHA as a function of UV irradiation rate.

Table 6.5: The molar mass and polydispersity as a function of UV irradiation rate.

UV dose (mJ/cm²)	*M_n (g/mol)*	*M_w (g/mol)*	*M_w/M_n*
55	45237	151537	3.35
100	39750	114240	2.87
150	38285	101528	2.65
240	35673	87290	2.48
300	34233	84938	2.45
400	34049	83379	2.45

6.5.4 Effect of initiator concentration on the MWD

Photoinitiator concentration has a major effect on the polymerization kinetics during UV curing. Polymerization rate increases rapidly by increasing the amount of initiator in the initial mixture as discussed in chapter 3 of this study [17]. Therefore, this would affect morphology of produced polymer network and hence the MWD of polymer chains. In this

section, GPC was used to study the effect of initiator concentration on MWD of polymer starting from very low to relatively high concentrations. Figure 6.19 shows GPC chromatogram for P2EHA prepared at different initiator concentrations (Darocur 1173) at fixed UV rate of 120 mJ/cm^2 until maximum double bond conversion.

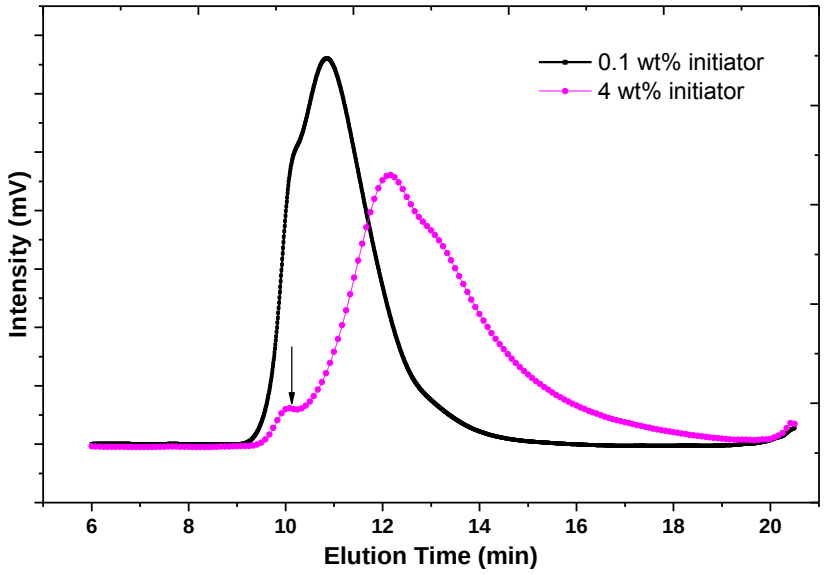

Figure 6.19: GPC chromatogram for P2EHA and as a function of initiator concentration.

GPC signal of low initiator concentration (0.1 wt %) appears at about 11 min while that of high initiator concentration appears at about 13 min. In addition, a narrow MDW is observed at low initiator concentration compared to broad MWD at high amount of initiator concentration. We also observe the small signal that appears at 10 min retention time at high initiator concentration, which corresponds to formation of certain amount of polymer chains at the beginning of the polymerization reaction. This signal is almost disappeared in the sample of low initiator concentration. This phenomenon can be explained by the difference in the polymerization kinetics based on the initiator concentration. At very low initiator concentrations, this leads to initiation of small amount of radical species in the photopolymerized reaction which enhance the propagation of chains with large molar mass. On the other hand, higher initiator concentrations would lead to initiation of much more radical species in the media, which lead to propagation reaction on many active sites and lower molar mass units are formed.

GPC chromatogram results in terms of M_n and M_w are presented in figure 6.20. It can be observed from the GPC results that significant drop of molar mass by increasing the initiator concentration in the initial mixture. M_w has dropped from 386×10^3g/mol at 0.1 wt %

initiator and sharply decreased to about 104×10^3 g/mol at 6 wt % initiator concentration. Furthermore, polydispersity show a continuous decrease with increasing the initiator concentration from 1.9 at 0.1 wt % initiator and dropped to 4 at 6 wt % initiator concentration. Details of the GPC results are presented in table 6.6.

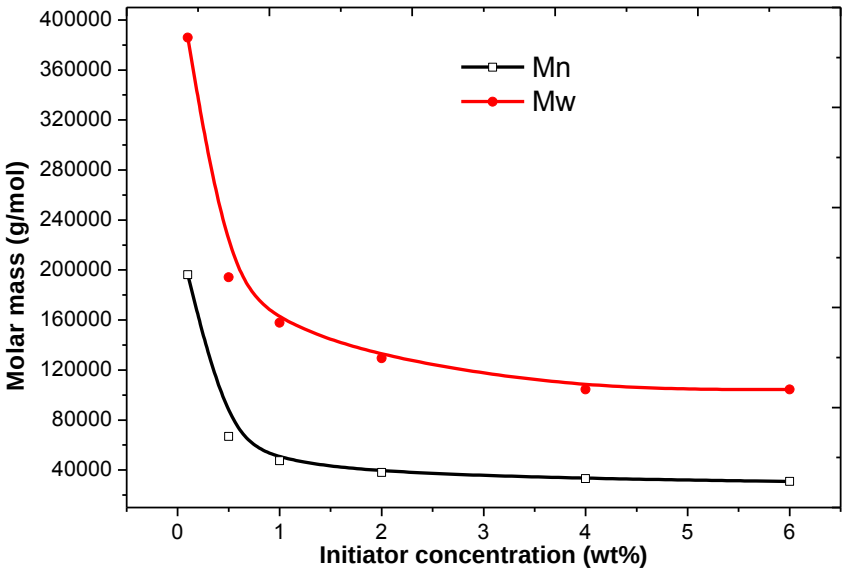

Figure 6.20 : MWD of EB cured P2EHA as a function of initiator concentration.

Table 6.6 : The molar mass and polydispersity as a function of the initiator concentration.

Initiator conc. (wt %)	M_n *(g/mol)*	M_w *(g/mol)*	M_w/M_n
0.1	196247	385806	1.97
0.5	66759	194072	2.91
1	47505	157753	3.32
2	37923	129280	3.41
4	33149	104411	3.15
6	30931	104387	4.02

6.6 Crosslinking and scission reactions under EB irradiation

High EB dose may lead to certain degree of degradation reactions in the polymer chains, which leads to reduction of crosslinking or curing efficiency. As a result, average molecular weight of the polymer will decreases because of chain scission or would increase the molecular weight by crosslinking as shown in figure 6.21.

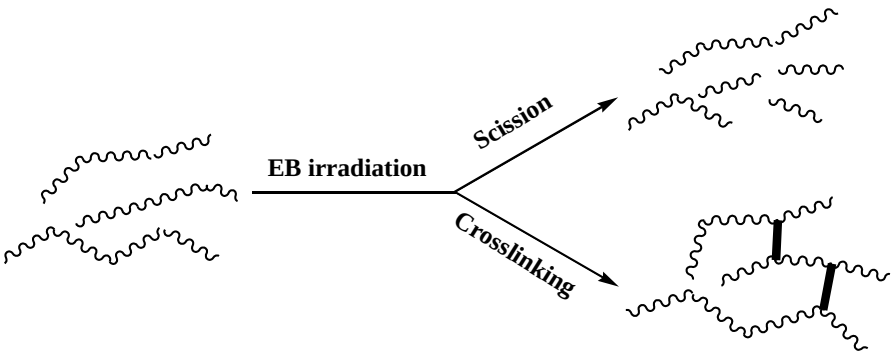

Figure 6.21: Scission and crosslinking in electron beam curing.

In EB curing, high doses may lead to both crosslinking and scission reactions with more chain scissions rather than crosslinking of the polymer chains [18]. Tertiary hydrogen of chain backbone would be the most possible hydrogen atom towards radical attack. Abstraction of this hydrogen gives rise to tertiary radical which lead to scission reactions.

In this section, we study effect of high EB irradiation doses on the MWD of polymer chain of P2EHA by comparing the molar mass of polymer unit at relatively intermediate dose of between 11 – 92 kGy, and exposing the same polymer samples with 4 times to the same EB after maximum conversion. GPC results are shown in figure 6.22 in terms of weight average molecular weight. It is clearly observed sharp decrease of the weight average molecular weight M_w by exposing the samples to extra irradiation doses. This directly indicates the scission reactions under high EB doses on the polymer chains that resulted in significant drop of the MWD of the polymer chain. Detailed GPC results are summarized in table 6.7 representing normal and extra BB doses.

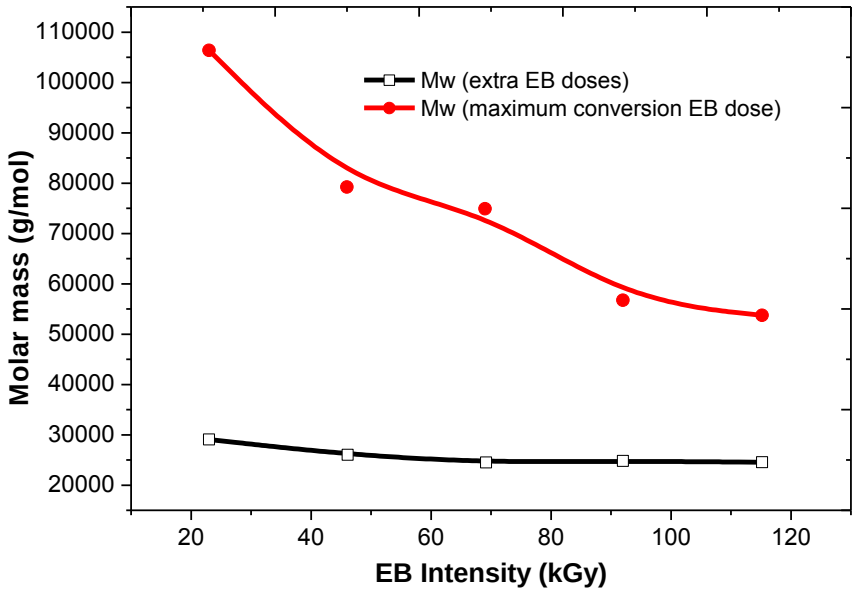

Figure 6.22 : MWD of EB cured P2EHA as a function of EB dose at maximum conversion and 4 times extra EB dose.

Table 6.7 : Effect of extra EB irradiation dose on the weight average molecular weight Mw and polydispersity. The symbols (l) and (h) indicate the normal and extra EB irradiation doses respectively.

EB dose. (kGy)	***Mw (l) (g/mol)***	***M_w/M_n (l)***	***M_w (h) (g/mol)***	***M_w/M_n (h)***
23	106349	2.98	29047	1.84
46	79216	3.19	25990	1.84
69	74878	3.51	24508	1.98
92	56729	3.39	24792	2.08
115	53729	3.40	24526	2.13

GPC results show that high EB doses enhance chain scission, which results in further decrease of the polydispersity by the formation of more uniform chain length at higher irradiation doses. Furthermore, relatively high polydispersity at normal EB dose support the hypothesis that the formation of high amount of radical species leads to broadening of the MWD, this may occur as a result of slow propagation of polymer chains due to low mobility of radical species at higher doses, where many propagating radicals are formed.

6.7 The dynamic mechanical properties of P2EHA

High molecular weight polymer is required for good physical and mechanical properties, which can be achieved by low reaction rate using UV initiation or low EB rate. Low reaction rate may lead to reduction of termination rate. In EB initiation, low dose results in reduction in concentration of initiating species leading to higher molecular weight polymer [19]. Polymerization rate in the acrylate systems is proportional to the dose rate. Several UV curing techniques have been applied to crosslink these acrylic monomers to improve their mechanical and physical stability [20]. The acrylic polymers are usually linear with a low degree of crosslinking, which plays major role in controlling the mechanical properties of these polymers.

Properties of the acrylic polymers were investigated by the dynamic mechanical properties. The viscoelastic properties of the material can be described by the storage shear modulus *G'* and the loss shear modulus *G"*. The change of the viscoelastic properties and the glass transition temperature can be used to characterize the MWD of polymer chain. Low radiation rate and initiator concentration lead to low concentration of the imitating radicals that result in higher molecular weight polymer chains.

In this section, we study effect of the preparation conditions on the mechanical behavior of acrylate polymers and describe the internal morphology of polymer blend in an attempt to improve the final properties of the polymer matrix.

Dynamic mechanical properties of the UV and EB curable films were conducted using Rheometrics dynamic mechanical analyzer. The temperature dependence of the viscoelastic properties such extension storage moduli E' =3G' or shear storage moduli G', extension loss moduli E" =3G" or shear loss moduli G", and dynamic loss tangent tanδ were measured at 1 Hz and 5°C/min heating rate. An amount of 0.5 g polymer sample was used to perform the analysis. The relationship between the initiator concentration and the dynamic mechanical properties such as viscosity η, storage moduli G' dynamic loss tangent tanδ are shown in figure 6.23.

Dynamic viscosity η, storage moduli G' and the loss moduli G" are deceasing by increasing the temperature. While tanδ temperature curve shift to higher temperature range for UV curing of 2EHA with remarkable decrease with increasing the initiator concentration.

For the UV cured system, by increasing the initiator concentration in the reactive mixture we clearly observe increase of the viscoelastic properties of the polymer film, which can be explained by decreasing molecular weight of the polymer chains by UV irradiation. At 25°C, G' value for 0.1 wt % initiator is about 17×10^3 Pa and decreases to about 10^3 Pa at 4 wt % initiator. A dramatic drop is also observed for η from 3×10^3 Pa.s at 0.1 wt % initiator to less than 500 Pa.s at 4 wt % initiator. In table 6.8, given the dynamic mechanical properties of several P2EHA films as a function of initiator concentration, with its equivalent molar mass and polydispersity of each film at room temperature.

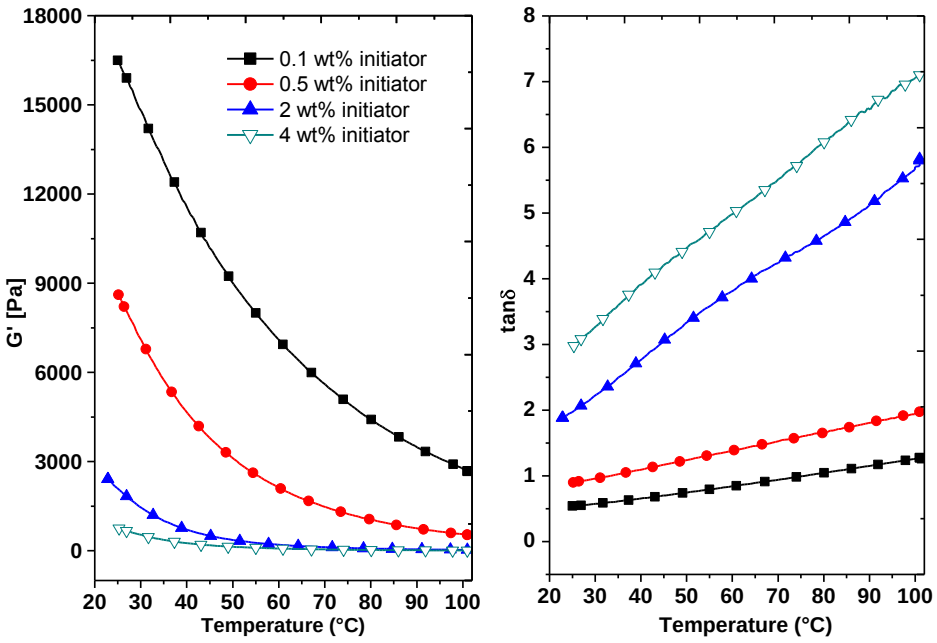

Figure 6.23 : Storage modulus G' and dynamic loss tangent tan δ vs. temperature as a function of initiator concentration at 1 Hz.

Table 6.8 : The dynamic mechanical properties with Mw and polydispersity at 25°C.

Sample	*G' (Pa)*	*Viscosity η (Pa.s)*	*tan δ*	*M_w (g/mol)*	*M_w/M_n*
0.1 wt% initiator	17×10^3	3×10^3	0.54	386×10^3	1.97
0.5 wt% initiator	9×10^3	1.8×10^3	0.90	194×10^3	2.91
2 wt% initiator	3×10^3	0.9×10^3	1.98	158×10^3	3.32
4 wt% initiator	10^3	0.4×10^3	2.97	104×10^3	3.15

Effect of UV rate on the dynamic mehanical properties is presented in figure 6.24, it is observed that the viscoelastic properties of the polymer films decease with increasing UV irradiation rate. The value of storage modulus show a considerable drop from 2.4×10^3 Pa at UV dose 90 mJ/cm^2 to about 2×10^3 at dose of 400 mJ/cm^2. These results support the previous MWD results, which indicate decease of MWD of polymer units by increasing UV irradiation rate. Dynamic mechanical properties of several P2EHA films as a function of UV dose, with its equivalent molar mass and polydispersity of each film are given in table 6.9.

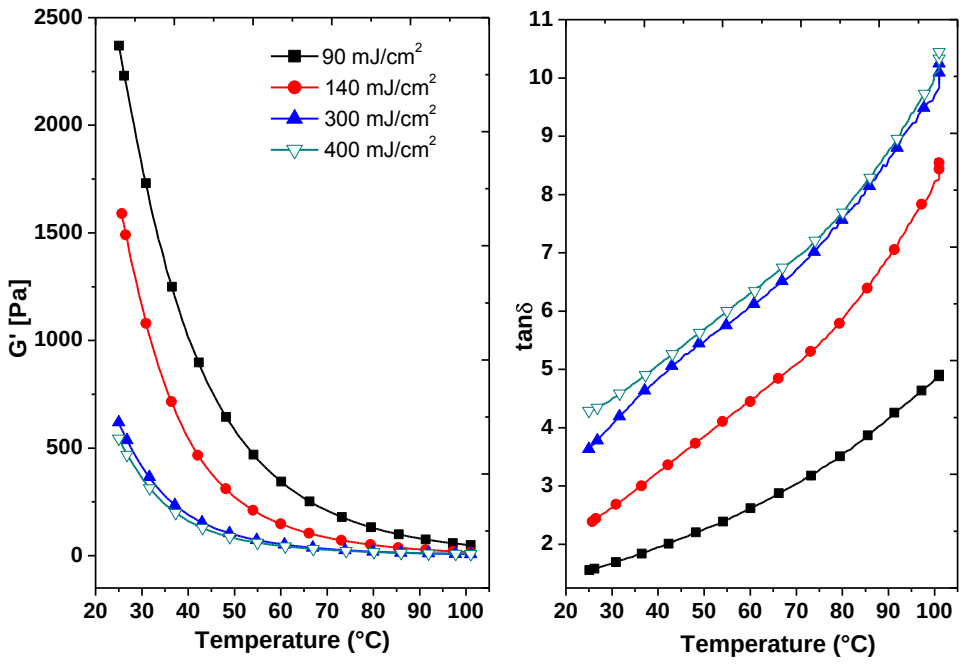

Figure 6.24 : Storage modulus G' and dynamic loss tangent tan vs. temperature as a function of UV dose at 1Hz.

Table 6.9 : The dynamic mechanical properties with Mw and polydispersity at 25°C.

Sample	*G' (Pa)*	*Viscosity η (Pa.s)*	*tan δ*	*M_w (g/mol)*	*M_w/M_n*
90 mJ/cm^2	2.40×10^3	0.70×10^3	1.55	114×10^3	2.87
140 mJ/cm^2	1.60×10^3	0.66×10^3	2.38	101×10^3	2.65
300 mJ/cm^2	0.62×10^3	0.37×10^3	3.63	85×10^3	2.45
400 mJ/cm^2	0.51×10^3	0.33×10^3	4.29	83×10^3	2.45

The behavior of EB cured 2EHA is presented in figure 6.25. In contrast to UV curing, it shows that the viscoelastic properties of polymer films increase with increasing EB irradiation rate. The storage modulus increases from 0.9×10^3 Pa at EB rate of 23 kGy to about 3.6×10^3 Pa at 92 kGy irradiation rate. Furthermore, a considerable increase of viscosity is observed by increasing EB irradiation rate from 200 Pa.s at 23 kGy to about 660 Pa.s at 92kGy of EB irradiation rate. Dynamic mechanical properties of several P2EHA films as a function of EB rate, with the equivalent molar mass and polydispersity of each film are given in table 6.10.

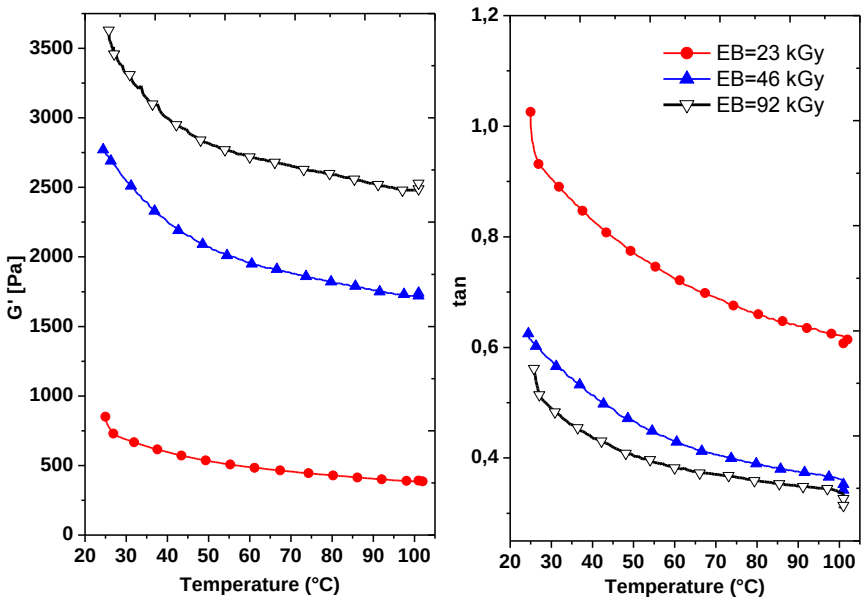

Figure 6.25 : Storage modulus G' and dynamic loss tangent tan vs. temperature as a function of EB irradiation dose at 1Hz.

Table 6.10: The dynamic mechanical properties with Mw and polydispersity as a function of EB dose at 25°C.

Sample	*G' (Pa)*	*Viscosity η (Pa.s)*	*tan δ*	M_w *(g/mol)*	M_n/M_w
23 kGy	0.85×10^3	0.19×10^3	1.02	106×10^3	2.98
46 kGy	2.77×10^3	0.52×10^3	0.62	79×10^3	3.19
92 kGy	3.63×10^3	0.66×10^3	0.56	56×10^3	3.39

Dynamic loss tangent tanδ which represents the material damping for the EB curing shows a different behavior from UV curing. In EB curing, tanδ decreases with increasing temperature in contrast to UV curing, which shows increase of tanδ with increasing temperature. In addition, tanδ have lower values ranging between 0.5 and 2 in average while that of UV curing is located between 2 and 10. This can be explained in terms of MDW of polymer chains, where highly branched polymer chains are formed in the EB curing film compared to low degree of branching and higher molar mass polymer in the UV systems.

In summary, it is hard to compare directly the properties of the EB and UV films. However, a remarkable drop of the viscoelastic properties is observed between the polymer films prepared by EB curing compared to the EB curing polymer. This behavior can be explained by considerable difference of MWD of polymers prepared by UV and EB irradiation. In general, UV curing mechanism allows higher molecular weight distribution during the propagation step, while EB mechanism accelerates termination and combination step that lead to lower molecular weight polymers. It is expected that the differences in the viscoelastic properties and glass transition temperatures of the polymers have direct correlation with the internal structure of polymer chains in terms of its MWD.

6.8 Conclusion

Morphology PDLC of systems that were prepared by UV and EB curing are found to be dependent on both liquid crystal concentration and the cure method under different preparation conditions. In particular, low MWD is observed at high liquid crystal

concentrations, and high polymer molar mass network are observed at low liquid crystal concentrations.

GPC revealed a set of parameters that can contribute to improve understanding the processes of phase separation. There is also a strong relationship between the kinetics of polymerization and phase separation that explains probability that radical species encounter a monomer molecule. Behavior of MWD in the composites could be explained by considering the interactions between the monomer and LC to produce phase separation. Higher LC concentrations lead to reduce molecular mobility in the polymerized mixture, where a lower molecular mobility causes a decrease in the polymerization rate and consequently low molecular weight chains are formed. Furthermore, amount of LC dissolved in the polymer has a considerable impact on its thermophysical parameters, which by consequences affect the overall properties of polymer/LC composite material.

Higher polymerization rates may lead to broadening of MWD and increase polydispersity. Therefore, MWD can be adjusted by an appropriate choice of the preparation condition. A compromise between the reaction condition variable may lead to optimization and control the finalmorphology of polymer matrix.

The viscoelastic properties of acrylic polymer (P2EHA) were investigated. The dynamic viscosity η, storage moduli G' and the loss moduli G'' are decreasing dramatically with temperature. The value of material damping tanδ is increasing with temperature in the UV curing polymer, while tanδ deceases gradually in EB curing systems. The glass transition temperature of polymer films has been determined for the UV and EB curing polymer films. Glass transition temperature was found to decrease with increasing the irradiation rate for both EB and UV curing and decreases with increasing initiator concentration.

UV and EB irradiation rate and the weight percent of the photoinitiator have a considerable influence on the mechanical and physical properties of the polymer films. Change of mechanical and physical properties can be explained by change in MWD of polymer chains.

6.9 References

[1] I. Dierking, L. L. Kosbar, A. C. Lowe, G. A. Held, Liq. Cryst. 24, 387 (1998).

[2] L. Lucchetti, F. Simoni, J. Appl. Phys. 88, 3934 (2000).

[3] F. Benmouna, A. Daoudi, F. Roussel, J.-M. Buisine, X. Coqueret, U. Maschke, J. Polym. Sci., Part B: Polym. Phys., 37, 1841 (1999).

[4] U. Maschke, X. Coqueret, M. Benmouna, Macromol. Rapid Commun., 23, 159-170 (2002)

[5] Guymon, C. A.; Bowman, C. N. Macromolecules, 30, 1594 (1997).

[6] R. A. Hikmet, H. M. Boots, J. Phys. Rev. E, 51, 5824 (1995).

[7]C. Plessis, G.Arzamendi, J. M.Alberdi, M.Agnely, J. R. Leiza, J. M. Asua, Macromolecules, 34, 6138–6143 (2001).

[8] J. Chauvet, J. R.Leiza, J. M. Asua, Polymer, 46, 9555–9561 (2005) .

[9] F. Heatley, P. A. Lovell, T. Yamashita, Macromolecules, 34, 7636–7641 (2001).

[10] H. Kudoh, M. Celina, G. Malone, R. Kaye, K. Gillen, R. Clough, Radiat. Phys. Chem., 48, 555 (1996).

[11] B. Defoort, G. Larnac, X. Coqueret, Radiat. Phys. Chem., 62, 47 (2001).

[12] C. Guymon, L. Dougan, P. Martens,N. Clark, D. Walba, C. Bowman, Chem. Mater., Vol. 10, No. 9, 2379 (1998).

[13] W.S. Kim, R. Houbertz, T.H. Lee, B.S. Bae, Journal of Polymer Science: Part B: Polymer Physics, Vol. 42, 1979–1986 (2004).

[14] B. Likozar, M. Krajnc, Journal of Applied Polymer Science, 110: 183–195 (2008).

[15] C. Plessis, G. Arzamendi, J. R. Leiza, H. A. S. Schoonbrood, D. Charmot, J. M. Asua, Macromolecules, 33, 4 (2000).

[16] S. Zhu, Y. Tian, A.E. Hamielec, Macromolecules, 23:1144–1150 (1990).

[17] A. Elqidrea, R. Meziane, U. Maschke, Molecular Crystals and Liquid Crystals 547 pp. 128-134 (2011).

[18] J Lal, J. E. McGrath, R. D. Board, J. Polym. Sci., A. 1. 6 821 (1968).

[19]H. Kudoh, M. Celina, G. Malone, R. Kaye, K. Gillen, R. Clough, Radiat. Phys. Chem., 48, 555 (1996).

[20] D. Satas, Handbook of pressure sensitive adhesive technology. New York: Satas & Associates, (1999).

7 GENERAL CONCLUSION AND FUTURE WORK

Radiation curing of acrylates is widely used technique for polymerization of acrylates in preparation of many materials ranging from simple adhesives and coatings to highly sophisticated materials as PDLC's used in the electronic devices.

The work presented in this thesis involves synthesis of polymer composites of 2EHA and 5CB as liquid crystal using UV and EB curing. In order to better describe this system, a polymer films were prepared and fully investigated and then the liquid crystal was incorporated into the matrix to evaluate the effect of liquid crystal and interactions between molecules on the properties of the PDLC film. This work has lead to better understanding the properties and structure of the polymer matrix and polymer/LC composites prepared under different preparation conditions.

The reaction rate and kinetics of polymer composites were investigated using FTIR spectroscopy. Effect of UV or EB irradiation doses, initiator concentration and liquid crystal contents on the polymerization rate have been studied. The conversion rate was found to increase with increasing UV or EB doses and the initiator concentration, and decreases with increasing the liquid crystal concentration in the reactive mixture. Maximum conversion was achieved within very short exposure time in EB curing compared to the UV curing one.

Relationship between morphology, composition domains and molecular interactions between the polymer and liquid crystal has been investigated using POM and DSC.

The morphology of PDLC films was found to be dependent on the preparation conditions and liquid crystal concentration. Alignment of nematic dispersed phase in contact with the polymer network was found to be sensitive to the morphology and branching of polymer chains. Confinement dynamic of liquid crystal in the polymer matrix has been established. The stability of liquid crystal phase has been investigated at longtime and high irradiation rate.

Chain transfer reactions during polymerization of 2EHA have been investigated using ^{1}H and ^{13}C NMR spectroscopy for different composite mixtures and curing rates. This allows demonstration the evolution of internal structure of the polymer network during radical polymerization. A more comprehensive understanding of the structural characteristics of the polymer composites has been achieved. Formation of intermolecular and intramolecular chain transfer has been well defined in terms of short or long chain branching during

polymerization. Effect of initiator concentration and the irradiation rate on the polymer configuration was presented. At tow polymerization rate, reaction kinetics support formation of β-division species and intramolecular chain transfer dominates toward short chain branches, while, at higher conversion rates formation of terminal double bond enhances the formation of higher degree of branching in the polymer matrix. Furthermore, effect of liquid crystal content on degree of branching and the chain transfer to liquid crystal was studied, higher liquid crystal concentration was found to enhance formation of long chain branches, the chain transfer may occur on the benzyl hydrogen of liquid crystal.

MWD of polymer matrix was studied and characterized using gel permeation chromatography. This revealed a set of parameters that can contribute to improve understanding the processes of phase separation. A strong relationship between kinetics of polymerization and phase separation was observed which was used to explain MWD during polymerization. The behavior of MWD in the composites has been explained by considering the interactions between monomer and LC to produce phase separation. Higher LC concentrations lead to reduce molecular mobility in the polymerized mixture, where a lower molecular mobility causes a decrease in the polymerization rate and consequently low molecular weight chains are formed. Furthermore, amount of LC dissolved in the polymer has a considerable impact on its thermophysical parameters, which by consequences affect the overall properties of the polymer/LC composite material.

The viscoelastic properties of P2EHA were investigated using dynamic mechanical analysis technique DMA. The dynamic viscosity η, storage moduli G' and the loss moduli G'' are decreasing dramatically with temperature. The value of the material damping tanδ was found to increase with temperature in UV curing polymerization, while tanδ decreases gradually with temperature in EB curing systems. The glass transition temperature of the polymer films has been determined for the UV and EB curing polymer films. The glass transition temperature was found to decrease with increasing irradiation rate for both EB and UV curing, and decreases with increasing the initiator concentration.

Detailed description and characterization of P2EAH and 5CB composites enabled the optimization of the irradiation dose, initiator concentration and liquid crystal concentration which leads to enhance preparation of polymer networks according to the required product applications.

This work can be further improved by using and comparing different monomers and liquid crystal systems to understand the response and behavior of the composite system using different components. Analysis of difunctional polymer system requires further work to understand the system on microscopic level using Scanning Electron microscopy and soils state NMR spectroscopy.

In conclusion, this work fully describe the PDLC composites at different reaction conditions, which lead to offer a model of operating conditions to prepare the film based on the required applications. Explanation of the electro-optical of the polymer matrix can be presented based on the description of morphology and configuration of the matrix, which have been briefly analyzed and discussed in the thesis.

8 PUBLICATIONS AND PRESENTATIONS

1. A. Elqidrea, R. Meziane, U. Maschke, Kinetics and molecular weight characterization of poly (2-ethylhexyl acrylate) and liquid crystal (5CB) composites, **Molecular Crystals and Liquid Crystals 547** pp. 128-134 (2011) [doi: DOI: 10.1080/15421406.2011.572804].

2. A. Elqidrea, U. Maschke, Confinement Dynamic of liquid crystal in poly 2-ethylhexyl acrylate Polymer Matrix in free Radical Polymerization, **24th International Liquid Crystal Conference**, August 19th - 24th 2012, Mainz, Germany.

3. Ammar Elqidrea, Ulrich Maschke, Morphology Control and Mechanical Properties of Polyacrylates Polymers Prepared by UV and Electron Beam Photopolymerization, **Journées Nord Ouest Européennes des Jeunes Chercheurs (JNOEJC)**, 18-19 March 2010, Lille 1 University, Villeneuve D'ascq, France.

4. A. Elqidrea, U. Maschke, Molecular Weight distribution of Polymer/Liquid crystal Composites prepared by UV and EB Curing, **39ème Journées d'Etudes des Polymères (JEPO 39)**, 16 - 21 October 2011, University Lille 1, Lille, France.

5. A. Elqidrea, U. Maschke, Characterization the Effect of UV and Electon beam Irradiation dose on the Formation of Polymer Dispersed Liquid Crystal Systems, **Journées Nord-Ouest Européennes des Jeunes Chercheurs (JNOEJC)**, 14 -15 June, 2011, University of Caen, Caen, France.

6. A. Elqidrea1, R. Meziane2, U. Maschke, Analysis the Formation of Polymer/Liquid crystal Systems Using Ultraviolet and Electron Beam Curing, **German Liquid Crystal Conference**, 30th March to 1st April 2011, University of Hamburg, Hamburg, Germany.

7. A. Elqidrea, U. Maschke, Morphology and mechanical properties of polyacrylates prepared by free-radical UV and electron beam polymerization, **PolyRay**, 28 - 29 March 2012, Technology Transfer Center, Le Mans, France.

8. Monomer Chan Length Controlling the Morphology of Liquid Crystal/Polymer Network systems, Y. Derouiche, A. Elqidrea, U. Maschke, F. Dubois, R. Douali and M. Azzaz, **38th Topical Meeting on Liquid Crystals, March**, 10 – 12 March 2010, Mainz University, Mainz, Germany.

9. Ammar Elqidrea, Rachid Meziane, Ulrich Maschke, Study of the radical polymerization of 2-ethylhexylacrylate and the effect of liquid crystals on the properties of the obtained polymers, **23rd International Liquid Crystal Conference**, July 11th – 16th 2010, The Jagiellonian University, Kraków, Poland.

10. Ammar Elqidrea, Ulrich Maschke, Study of the radical polymerization of 2-ethylhexylacrylate and the effect of liquid crystals on the properties of the obtained polymers, **Journées Nord Ouest Européennes des Jeunes Chercheurs (JNOEJC)**, 18-19 March 2010, Lille 1 University, Villeneuve D'ascq, France.

11. Ammar Elqidrea, Ulrich Maschke, The effect of UV irradiation dose on Chain transfer during photopolymerization of Mono acrylates in isotropic phase, **European Symposium of Photopolymer Science**, November 28th - December 1st 2010, Mulhouse, France.